# Development of human skin models for the study of anti-bacterial adherence treatments


The University Of Sheffield.

**Thesis submitted for the degree of Doctor of Philosophy**


## Nathan Wong

Supervisors: Prof Peter Monk, Prof Sheila MacNeil, Dr Lynda Partridge, and Dr John Common

Department of Infection, Immunity and Cardiovascular Disease
Faculty of Medicine, Dentistry and Health
University of Sheffield, United Kingdom


**April 2023**

# Declaration

The work presented in this thesis is the work of the candidate, with the following exceptions:

- Cytometric bead array assays were performed by the core facility of flow cytometry at the University of Sheffield

- Flow cytometry was assisted, with reagents provided, by Dr Baptiste Janela and Ms Toh Yingxiu

- Histology slides were scanned by Ms Sarah Zulkifli of the A*STAR Microscopy Platform

- Gram-staining was performed as a service by the histopathology facility at A*STAR

**PhD funded by the University of Sheffield and A*STAR, Singapore under the A*STAR Research Attachment Programme (ARAP)**

# Acknowledgements

First, I would like to thank my supervisors: Prof Peter Monk, Prof Sheila MacNeil, Dr Lynda Partridge, and Dr John Common, for their guidance, knowledge, and limitless patience throughout this PhD. Thanks to them, I have survived the past 4 years with my willingness to pursue a career in academic research intact. I would also like to thank the staff that keep the lab running, without whom nothing would get done: Katie Cooke, Vanessa Singleton, and Jon Kilby, you're the backbone of this university. My thanks also go to Dr Anthony Bullock and Dr Rahaf Issa for their advice and support from the very beginning.

I would also like to thank the men and women that form the John Common and Birgit Lane labs in A*STAR, Singapore, it has been the experience of a lifetime to learn from, and work alongside you all.

Additional thanks also go to my friends: Seetanshu, Bea, Nadia, Elisabeth, Jason, Pablo, Kathryn, Euan and Joanna for their unwavering support, encouragement and for reminding me to go outside from time to time. Special thanks go to Emma and Natalia for coming all the way to Singapore to visit me. Our trip to Vietnam has prompted me to drink less.

Finally, I thank my family, because of whom, I will always work hard and never give up.

"Oh, if life were made of moments even now and then a bad one! But if life were only moments, then you'd never know you had one."

Stephen Sondheim, *Into the Woods*

# Table of Contents:

# Abstract:

CD9 is a tetraspanin exploited by *Staphylococcus aureus* (*S. aureus*) in order to infect host cells. Thus, it has been identified as a target for anti-adhesion therapeutics that reduce contact between a pathogen and the host and thereby reduce infection. Furthermore, as anti-adhesion agents are not bactericidal, pathogenic resistance is less likely to occur in comparison to antibiotics. We have previously designed peptides targeting CD9 for anti-adhesion therapy and have successfully shown them to be effective in reducing *S. aureus* adherence to keratinocytes in 2D assays and 3D human skin models. However, the effects these peptides may have on immune cell function is currently unknown. The hypothesis of this study is that these peptides will be effective in reducing *S. aureus* infection in human skin without compromising immune cell function.

Using a variety of models from 2D *in vitro* assays to 3D explants of human skin and to mouse models, we demonstrate that pre-treatment with CD9-derived peptides reduces *S. aureus* adherence to keratinocytes as shown by colony forming unit (CFU) counting, histology and flow cytometry. In addition, phagocytosis assays were performed with immune cells in isolation to show that peptide treatment did not negatively affect phagocytosis.

In conclusion, we found that *S. aureus* infection is significantly reduced in skin models pre-treated with CD9 peptides in comparison to controls, and that immune cells pre-treated with peptides phagocytose the same amount of *S. aureus* as non-treated controls.

# List of figures:

## Chapter 1



## Chapter 2



## Chapter 3



## Chapter 4

## Chapter 5



# List of tables

# Abbreviations

α-MEM: Alpha Minimum Essential Medium
AIP: Autoinducing Peptide
AgrC: Accessory gene regulator C
ALI: Air-Liquid Interface
AMPs: Antimicrobial Peptides
APCs: Antigen-Presenting Cells
Atl: Autolysin
BSA: Bovine Serum Albumin
cDC1s: conventional Dendritic Cells type 1
cDC2s: conventional Dendritic Cell type 2
CBA: Cytometry Bead Array
CFU: Colony Forming Unit
CHIP: Chemotaxis Inhibitory Protein
DAMPs: Damage-Associated Molecular Patterns
DAB: 3,3'-Diaminobenzidine
DAPI: 4′,6-diamidino-2-phenylindole
DCs: Dendritic Cells
DED: De-epidermidised dermis
dLNs: draining Lymph Nodes
DMEM: Dulbecco's Modified Eagle Medium
DNA: Deoxyribonucleic Acid
EC: Extracellular loop
ECM: Extracellular Matrix
EGF: Epidermal Growth Factor
ELISA: Enzyme-Linked Immunosorbent Assay
EPS: Extracellular Polymeric Substances
FACS: Fluorescence-assisted Cell Sorting
FBS: Foetal Bovine Serum
FnBP: Fibronectin Binding Protein
FcR: Fc Receptors
G-CSF: Granulocyte Colony-Stimulating Factor
GM-CSF: Granulocyte-Macrophage Colony-Stimulating Factor
HBSS: Hank’s Balanced Salt Solution
H&E: Haematoxylin and Eosin
HRP: Horseradish Peroxidase
IL: Interleukin
ILC: Innate Lymphoid Cell
iSALT: induced Skin-Associated Lymphoid Tissue
LB: Lysogeny Broth
LCs: Langerhans Cells

LDH: Lactate Dehydrogenase
LTA: Lipoteichoic Acid
MCP-1: Monocyte Chemoattractant Protein 1
MOI: Multiplicity of Infection
MRSA: Methicillin-Resistance *S. aureus*
MSCRAMMs: Microbial Surface Components Recognizing Adhesive Matrix Molecules
NS: non-significance
NADPH: Nicotinamide Adenine Dinucleotide Phosphate
NETs: Neutrophil Extracellular Traps
OCT: Optimal Cutting Temperature
PAMPs: Pathogen-Associated Molecular Patterns
PBMCs: Peripheral Blood Mononuclear Cells
PBS: Phosphate Buffer Saline
PIA: Polysaccharide Intercellular Adhesin
PMA: Phorbol 12-myristate 13-acetate
PPP: Platelet Poor Plasma
PRP: Platelet Rich Plasma
PRRs: Pattern Recognition Receptors
ROS: Reactive Oxygen Species
RPMI: Roswell Park Memorial Institute
*S. aureus: Staphylococcus aureus*
SarA: *Staphylococcus* accessory regulator A
SCC: Squamous Cell Carcinomas
SPF: Specific-Pathogen-Free
SraP: Serine-rich adhesion for Platelets
SSTI: Skin and Soft Tissue Infections
TEM: Tetraspanin-Enriched Microdomain
TGF-β: Tumour Growth Factor-β
TLRs: Toll-Like Receptors
$T_H1$: T Helper 1 cell
$T_{regs}$: Regulatory T cells
T/T: Triiodo-L-thyronine/apo-Transferrin

# Chapter 1 Introduction

## 1.1 Skin

The skin is the largest organ of the human body. As the barrier between the body and the external environment (Salmon et al., 1994), it is an essential part of the innate immune response and is the first line of defence against pathogenic invasion, whilst still allowing the passage of water and ions. Whilst the skin is predominantly a barrier, it can also produce antimicrobial peptides such as defensins, and secrete cytokines and chemokines to recruit other immune cells to mount an immune response to infection (Chu, 2012; Smeekens et al., 2014). The skin also plays host to a wide variety of microorganisms, both commensal and opportunistic (Muszer et al., 2015), which will be discussed in more detail later in section 1.3.

### 1.1.1 Epidermis

Skin is made of multiple layers (Figure 1.1). The keratinocyte is the primary cell type that proliferates and differentiates to form the epidermis. The uppermost layer of the epidermis is the stratum corneum, which is made up of dead cells without nuclei and hard protein envelopes that form a barrier (Losquadro, 2017). It is a waterproof layer due to lipid build up and close cell junctions. Beyond this layer is the stratum granulosum, the layer where keratinocytes lose their nuclei and flatten to form the hard envelope. Below the stratum granulosum is the stratum spinosum, a thicker layer of partly differentiated cells with oval nuclei and a build-up of keratin, resulting in a spiny phenotype due to protruding cellular processes. The stratum basale forms the base of the epidermis, made up of actively dividing keratinocytes and melanocytes (Yousef and Sharma, 2017). As newer cells are produced, the older cells migrate upwards towards the surface as they differentiate and lose their nuclei. As they move towards the surface, they undergo cell death and form the desiccated stratum corneum (Haake et al., 2001; Yousef and Sharma, 2017). These layers of dead keratinocytes and intercellular lipids create a dehydrated milieu that discourages the growth of certain

microbes that require moisture such as *P. aeruginosa* (Eyerich et al., 2018). In some parts of the body, namely the hands and feet, there is the stratum lucidum, a thin layer of dead keratinocytes specifically found in areas with thicker skin. The stratum lucidum can be found between the stratum corneum and the stratum granulosum.

### 1.1.2 Dermis

Between the epidermis and dermis is the epidermal-dermal junction that connects the stratum basale of epidermis to the papillary layer of the dermis. The function of the epidermal-dermal junction is to provide a zone for the exchange of fluids and nutrients between the keratinocytes in the epidermis and the cells in the dermis (Fenner and Clark, 2016). The dermis is a series of connective tissues that forms a protective layer for internal structures. The dermis is composed of two regions, the top region is the papillary region, and the lower region is the reticular dermis. The papillary region contains lymphatic capillaries and Meissner Corpuscles that are receptors for pressure. Underneath the papillary region is the reticular region, which is made up of elastin and collagen. The reticular dermis provides structure to the skin and supports hair follicles, sweat glands and nail beds. The cells that constitute the dermis are the fibroblasts that secrete extracellular matrix (ECM) proteins, supply nutrients to the epidermis and to regulate temperature (Malissen et al., 2014).

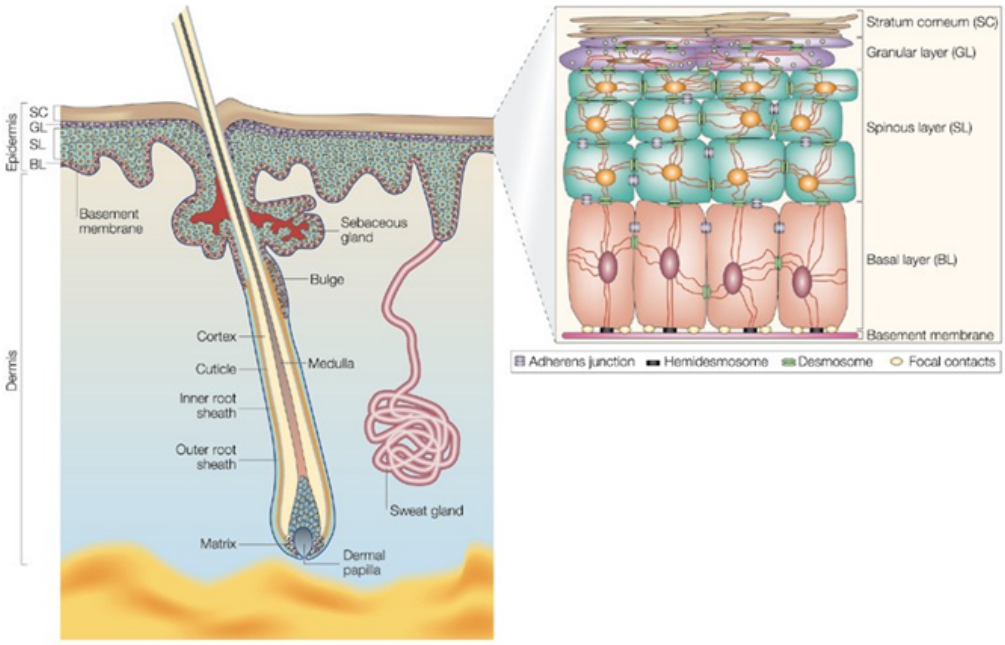


**Figure 1.1 Layers of the skin**

The epidermis is composed of keratinocytes in varying states of differentiation. The dermis is a mixture of immune cells, connective tissues, sweat glands and hair follicles. Reproduced with permission from Fuchs & Raghavan, 2002. Licence number 5183240378495

## 1.2 Skin Immunology

Skin infections can occur if the epidermis is compromised as further discussed in section 1.3.1. This is usually through physical mechanisms that remove or bypass the epidermis, such as burns or cuts, or if the skin has been weakened in diseases like atopic dermatitis or psoriasis (Cogen et al., 2008). However, the skin can typically mount a response to infection using the resident immune cells (Figure 1.2). In the epidermis there are Langerhans cells (LCs), residential dendritic cells (DCs) of the skin which are predominantly found in the stratum spinosum. The dermis contains mast cells, macrophages, DCs and B and T cells (Nestle et al., 2009). Additionally, neutrophils and monocytes circulate in the bloodstream but can be quickly recruited to sites of infection.

Host cells have pattern recognition receptors (PRRs) such as Toll-like Receptors (TLRs) on their cell surface that recognise pathogen associated molecular patterns (PAMPs) like endotoxins or damage associated molecular patterns (DAMPs) like ATP. This recognition triggers a cascade resulting in the production of proinflammatory cytokines and chemokines to recruit other immune cells to the site of infection (Krishna and Miller, 2012a, 2012b). These cytokines are proinflammatory, increasing vascular permeability which increases the recruitment of immune cells to the wound site.

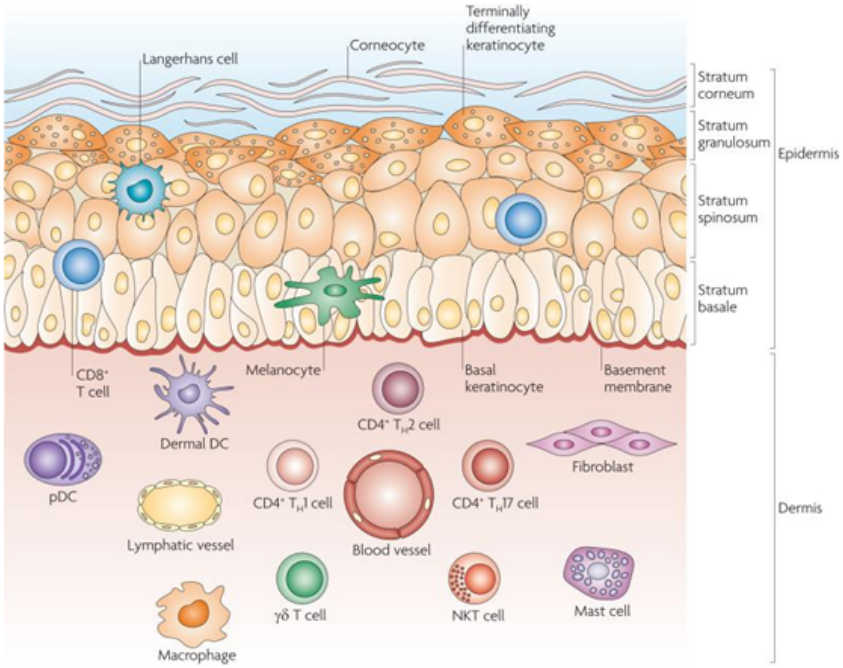


**Figure 1.2 Pathogens trigger an immune response to eradicate infection**

PAMPs are recognised by keratinocytes, which secrete cytokines to activate DCs, which migrate to prime and activate T and B cells. These T and B cells secrete cytokines to recruit more immune cells and clear infection. Reproduced with permission from Nestle et al, 2009. Licence number 5183240713932

### 1.2.1 Antimicrobial Peptides

Following skin exposure to PAMPs or DAMPs, cell signalling pathways within keratinocytes activate and induce an inflammatory response (Figure 1.3). One such response is the secretion of AMPs that protect against microbes by inducing cell lysis

or interfering with a microbe's ability to synthesise deoxyribonucleic acid (DNA) (Nguyen et al., 2011). To bind to bacteria, AMPs carry an overall positive charge from basic residues and bind to negatively charged polysaccharides and phospholipids on the cell membrane of bacteria. The AMPs, human β-defensins and cathelicidin, also induce the production of cytokines to further increase immune activity (Alcayaga-Miranda et al., 2017).

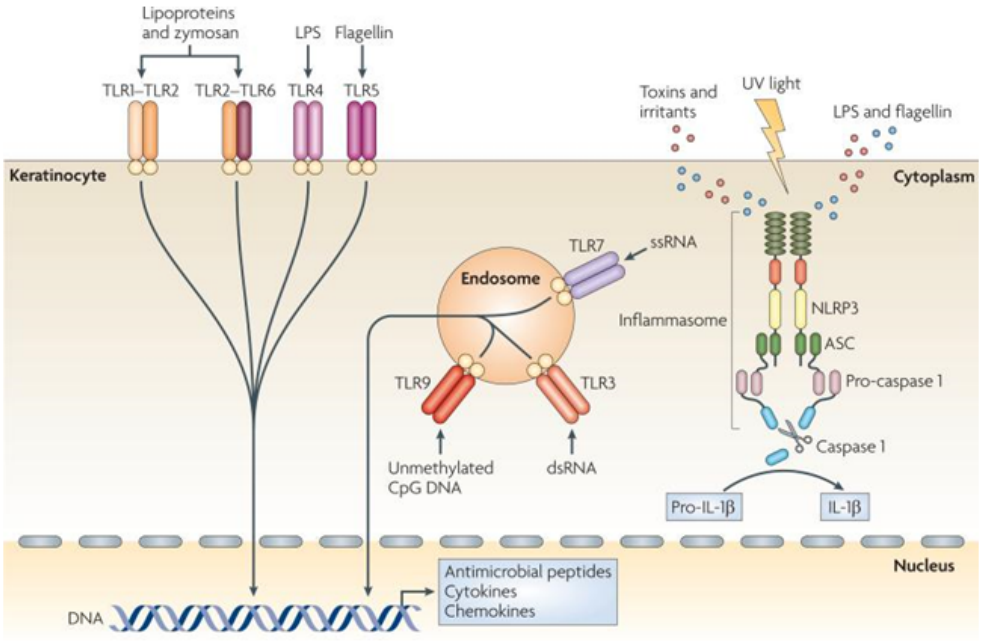


**Figure 1.3 Toll-like receptors on keratinocytes alert them to Pathogen-Associated Molecular Patterns or Damage-Associated Molecular Patterns**

TLR recognition results in keratinocytes secreting AMPs and cytokines to activate downstream immune responses. TLRs are receptors that recognise PAMPs. Reproduced with permission from Nestle et al, 2009. Licence number 5183240713932

### 1.2.2 Conventional Dendritic Cells

Dendritic cells are professional pathogen-sensing antigen-presenting cells (APCs) important in initialising immune responses. Dendritic cells are critical for priming the adaptive immune response by migrating from a site of infection to the lymph nodes whilst transporting foreign antigens to present to immature T cells in the lymph nodes. In the skin, there are two subsets: conventional type 1 dendritic cells (cDC1s) and conventional type 2 dendritic cells (cDC2s). cDC1s are identified by their expression

of XCR1 and cDC2s are identified by CD11b (Janela et al., 2019). Whereas Langerhans cells are the DCs of the epidermis, conventional DCs reside in the dermis.

cDC1s are a rare DC subset, noted for excellent cross-presentation of extracellular antigens compared to other DC subsets. cDC1s can effectively prime $CD8^+$ T cells against bacteria or viruses. cDC1s exhibit better cross-presentation of antigens derived from necrotic cells due to their expression of the necrotic receptor Clec9a. This receptor and the chemokine receptor, XCR1, are unique markers of this subset. cDC1s recognise intracellular pathogens and start type 1 immune responses including Innate Lymphoid Cell (ILC) type 1, Natural Killer cell and T Helper 1 ($T_H1$) cell induction. Moreover, cDC1 efficiently cross-present extracellular antigens to $CD8^+$ T cells and secrete interleukin (IL)-12, making them important for cytotoxic responses to viral infections and tumours (Merad et al., 2013). cDC2 induces different responses, such as the activation of ILC2 and $T_H2$ cells against parasites and during asthma, and the induction of ILC3 and $T_H17$ immune responses to extracellular bacteria (Durai and Murphy, 2016; Kumar et al., 2019).

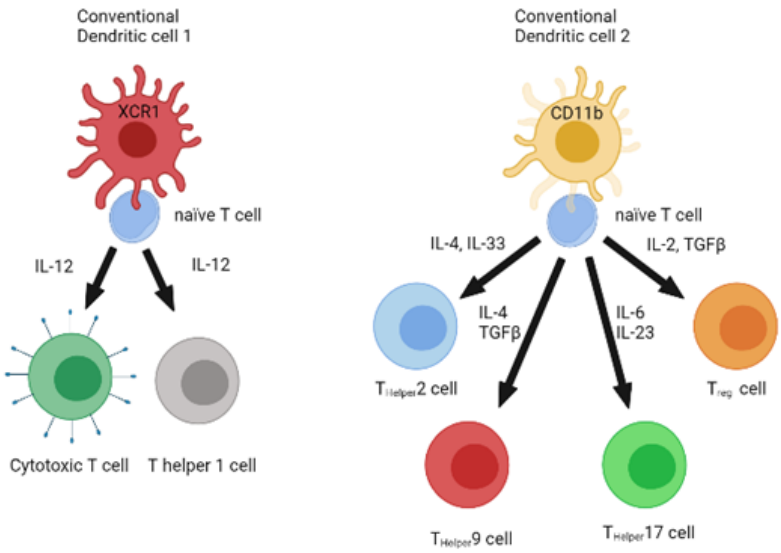


**Figure 1.4 cDC1 versus cDC2 activity**

cDC1s are involved in the differentiation of naïve T cells into cytotoxic T cells and $T_H1$ cells via the secretion of IL-12 **(left)**. cDC2s facilitate T cell development into $T_H2$, $T_H9$, $T_H17$ and $T_{regs}$ with a variety of cytokines **(right)**. Adapted from Kumar et al, 2019 and reproduced with BioRender.

### 1.2.3 Langerhans Cells

Langerhans cells are amongst the first immune cells to respond to infection from pathogens targeting the skin (Pasparakis et al., 2014). LCs are found in the basal and suprabasal layer of the epidermis and will migrate from the skin to the draining lymph nodes (dLNs) during steady state but will migrate faster during inflammation (Rajesh et al., 2019; Stoitzner, 2010).

Langerhans cells act as an APC that can process antigens and migrate from the epidermis to secondary lymphoid tissues to present the antigens to naïve T cells. In steady state, LCs play a role in maintaining tolerance by inducing activation and proliferation of skin resident $T_{regs}$ (Clayton et al., 2017), and suppressing the inappropriate activation of skin resident tissue effector memory cells. $T_{regs}$ are a T cell subtype that suppress inappropriate immune responses to maintain homeostasis and self-tolerance. $T_{regs}$ are able to inhibit T cell proliferation and cytokine production and play a critical role in preventing autoimmunity (Kondělková et al., 2010). Bacteria-primed LCs induce a high percentage of $T_{regs}$ indicating that LCs play a role in maintaining commensal tolerance (van der Aar et al., 2013). During infection, LCs can phagocytose antigens from pathogens for presentation to a T cell. LCs interact with and prime T cells to lead the adaptive response, from promoting recruitment of neutrophils to interacting with B cells, the cells that will become plasma cells and secrete antibodies (Merad et al., 2008).

In recognition of Gram-positive bacteria such as *S. aureus*, LCs express TLR2 however, TLR2 is weakly expressed and so the response to Gram-positive bacteria is impaired (van de Aar et al, 2007). In contrast to dermal DCs, LCs weakly express TLR2 along with TLR4 and TLR5. This poor responsiveness results in low reactivity to bacteria. LCs are also poor in internalising, processing, and presenting antigens of *S. aureus* and mounting a T cell response, as seen in the *in vitro* niche (Okabe and Medzhitov, 2014; West and Bennett, 2018). It is this weak responsiveness that relates to how T cells help maintain tolerance of the commensal skin microbiome. Interestingly, LCs are implicated in *S. aureus*-induced skin inflammation. In mice, it has been shown that in response to *S. aureus*, murine LCs induce $T_H17$ response to contain *S. aureus* infection, but the IL-17 secreted by LCs will also aggravate atopic

dermatitis (van Dalen et al., 2019). LCs also possess the unique C-type Lectin receptor, Langerin, which is a receptor for *S. aureus* on human Langerhans cells.

Despite having clear dendritic functions, LCs are ontologically derived from macrophages (West and Bennett, 2018). Embryonic LCs develop from a common macrophage precursor, this is theorised to be due to macrophage precursors being recruited to tissue-specific sites and differentiating into a cell type that is adapted to that location-specific niche (Okabe and Medzhitov, 2014; West and Bennett, 2018). Adult cells are derived from myeloid cell progenitors which typically derive from the foetal liver (Rajesh et al., 2019). Contrarily, classical DCs are derived from the bone marrow precursors.

Langerhans cells play a role in wound healing. In chronic wounds, LCs have been found in greater numbers in healing chronic diabetic foot ulcers compared to non-healing (Stojadinovic et al., 2013). From this, the authors theorised that LCs played an important role in the outcome of healing versus non-healing chronic wounds. Migration of LCs appears to be crucial in wound healing. Nakamura et al., demonstrated that knockout mice for Monocyte Chemoattractant Protein 1 (MCP-1) could not recruit LCs and consequently displayed delayed wound re-epithelialisation. This suggests that impaired migration of steady-state LCs during re-epithelialisation contributes to wound chronicity (Nakamura et al., 1995).

### 1.2.4 Lymph nodes

Lymph nodes are structures of the lymphatic system and play a key role in the adaptive immune system. Lymph nodes are linked by lymphatic vessels and are the major sites of T and B cells. Antigen presenting cells such as DCs take up antigens and migrate from their original location towards their dLNs. APCs present the antigen to T cells and consequently activate the T cells (Tai et al., 2018).

Some resident immune cells migrate to lymph nodes to induce peripheral tolerance to tissue self-antigens or initiate a response e.g., infection or injury. LCs and cDCs migrate to skin dLNs to induce self-tolerance or induce adaptive immune response and

then T cell responses. Neutrophils can also migrate towards dLNs in response to infection, for example, to prevent the dissemination of *S. aureus* which has survived the phagocytosis process of macrophages (Bogoslowski et al., 2018; Miller and Simon, 2018). Upon stimulation, cDCs enter the afferent lymphatic vessels and migrate to the lymph nodes, carrying antigens from pathogens from the site of infection to the lymph nodes. DCs also carry antigens from commensal or self-antigens to regulate tolerance. In dLNs, DCs present antigens to $CD4^+$ or $CD8^+$ T cells to regulate adaptive immune responses.

Since the 1980s, studies revealed that T cells and DCs interacted under inflammatory conditions in the skin as well as in lymph nodes (Streilein, 1983). Dermal DC clusters around post-capillary venules were found during the elicitation phase of contact hypersensitivity reactions (Natsuaki et al., 2014; Ono and Kabashima, 2015). These clusters are seen in mouse models of contact hypersensitivity; dermal DCs contact effector T cells and activate them. In these events, keratinocytes and macrophages also play a role in this activation. This inducible structure involving macrophages, dermal DCs, and T cells is essential for the activation of effector T cells. In an example of such an experiment, T cells isolated from the dLNs of mice sensitised with haptens were labelled with a fluorophore and transferred to a non-sensitised mouse whose DCs were tagged with another fluorophore. In the steady state, the tagged DCs diffused randomly but, after a topical challenge, DCs formed clusters and interacted with the tagged T cells (Natsuaki et al., 2014).

### 1.2.5 Neutrophils

A neutrophil's primary function is to phagocytose a microbe and to kill pathogens. Neutrophils circulate throughout the body in the blood until they are signalled towards a site of injury or infection. Neutrophils are professional phagocytes that are amongst the first responders to infection. Neutrophils are recruited to a site of skin infection by chemokines and the PRRs on neutrophils recognise PAMPs expressed on pathogens and subsequently initiate the production and secretion of pro-inflammatory cytokines and chemokines (Miller and Cho, 2011).

Neutrophils express a wide range of receptors such as TLRs, complement and Fc receptors that mediate the phagocytosis of opsonised bacteria. The neutrophils can kill the bacteria by phagocytosing the microbes and secreting reactive oxidative species to kill the bacteria. Alternatively, neutrophils can also kill microbes by expelling DNA, coated in AMPs and histones, which can kill pathogens when they come in contact with these extracellular traps. These are known as neutrophil extracellular traps, or NETs (Kaplan & Radic, 2012).

In response to damage or to a pathogen, a variety of cells such as monocytes, macrophages, fibroblasts, and keratinocytes will produce and secrete chemoattractants including IL-8, CXCL6 and Leukotriene B4, which bind to circulating neutrophils. These neutrophil chemoattractants direct neutrophil movement out of intravascular circulation to the site of damage or infection within tissues, resulting in the rapid influx and accumulation of neutrophils (Rigby and DeLeo, 2012). *S. aureus* express surface components such as lipoteichoic acid (LTA) and secrete molecules such as staphylococcus enterotoxin A and B which elicit IL-8 production by epithelial cells and monocytes etc. (Soell et al., 1995).

Neutrophils survey the venules for signs of inflammation or damage, chemoattractants diffuse from the site of infection and into the bloodstream, attracting the neutrophils. Selectins expressed on the surface of endothelial cells and neutrophils interact, resulting in tethering and rolling of neutrophils along the endothelial wall (Ley et al., 2007). Rolling is stopped by integrin-dependent interactions via leukocyte adhesion molecules e.g., LFA-1 and Mac-1 (Ley et al., 2007; Yilmaz and Granger, 2010). Neutrophils become firmly adhered then transmigrate between endothelial cells into tissues. This process, from start to finish, is known as extravasation. Upon entry into the tissue, neutrophils can recognise PAMPs, bacterial surface receptors and secretions e.g., lipoproteins, LTA and flagellin, and attack invading pathogens (Rigby and DeLeo, 2012). This engagement activates pathways in neutrophils to promote the neutrophils' survival, facilitate adhesion and phagocytosis, elicit degranulation and nicotinamide adenine dinucleotide phosphate (NADPH) oxidase-derived ROS and antimicrobial proteins upon fusion with the phagosome.

### 1.2.6 Macrophages

Macrophages are phagocytic cells found in the dermis. They possess both inflammatory and wound healing functions depending on the situation. Macrophages typically phagocytose cellular debris or pathogenic agents as well as secreting inflammatory cytokines such as IL-1β, IL-6 or TNFα. Like neutrophils, macrophages are quick to respond to infection and will migrate towards the site of infection to phagocytose pathogens. As professional APCs, macrophages can also present antigens of phagocytosed pathogens to activate the adaptive immune response (Pidwill et al., 2021).

Macrophages are vital for fighting bacterial infection as shown in animal infection models in which the macrophages have been depleted. In these models, mice lacking macrophages have increased bacterial burden and bacterial sepsis (Surewaard et al., 2016). Upon infection, keratinocytes sense invading pathogens via PRRs which recognise PAMPs such as LPS or endotoxins. This recognition induces epithelial signalling to recruitment phagocytes such as macrophages and neutrophils with pro-inflammatory cytokines and chemokines such as granulocyte-macrophage colony-stimulating factor (GM-CSF), granulocyte colony-stimulating factor (G-CSF) and MCP-1 (Pidwill et al., 2021).

Macrophage response and function is dependent on their polarisation, which in turn is dependent on the stimuli present in their immediate environment. In steady state conditions, macrophages will be polarised towards a ‘M2’ phenotype that conveys a tissue repair or wound healing functionality to macrophages. In response to danger signals, macrophages can become pro-inflammatory ‘M1’ macrophages and alter their function towards pathogen killing such as increased nitric oxide production (Brann et al., 2019).

Upon encountering *S. aureus*, M1 macrophages will attempt to phagocytose the bacteria. Upon engulfing the pathogen, macrophages would then fuse their phagosome with lysosomes containing ROS and reactive nitrogen species. However, *S. aureus* evolved to survive or evade this interaction and survive macrophage activity. As an example of this, *S. aureus* prevents phagolysosomal formation after being

internalised by macrophages (Tranchemontagne et al., 2015). Biofilms are structures that can protect bacteria from its environment (Thi et al., 2020) (discussed further in section 1.3.5.1). Macrophages can effectively phagocytose single bacteria but are less effective in phagocytosing biofilm-associated bacteria. Co-culture studies with macrophages and biofilms have shown that macrophages only poorly phagocytose biofilm-associated bacteria (Thurlow et al., 2011). *S. aureus* biofilms elicit an M2 phenotype in macrophages (reviewed in Gries and Kielian, 2017), indicating that biofilms can attenuate host pro-inflammatory responses, and this is associated with uncontrolled bacterial spread (Asai et al., 2010). Furthermore, *S. aureus* can induce Protein Kinase B signalling which decreases M1 polarisation (Brann et al., 2019). This is also seen in keratinocytes in which *S. aureus* biofilms elicit a lesser inflammatory response than planktonic bacteria (Secor et al., 2011).

## 1.3 Skin microbiome

The skin provides a habitat for a microbiome that is composed of over 1000 species of bacteria (Grice et al., 2009). The composition of the microbiome varies in different body sites as the skin provides diverse microenvironments that allow some species to thrive better than others. Body sites can vary in terms of pH, temperature, moisture, and light exposure. Parts of the skin can be oily (the face), moist (at the bend of the elbow or groin), or dry (the forearms) (Byrd et al., 2018). These sites are affected by the presence of appendages such as sweat glands or hair follicles. Moist areas are more abundant in sweat glands which acidify the skin, making the conditions unfavourable for the colonisation of some microbes e.g., *Streptococcus pyogenes* (Grice & Segre, 2011). Oily sites such as the face contain more sebaceous glands that secrete sebum, a hydrophobic coating that acts as an antibacterial shield (Byrd, 2018). Consequently, the composition of the skin microbiome can vary greatly. For example, sebaceous sites like the face are predominantly composed of *Propionibacterium* species, whereas bacteria that thrive in humid environments, such as *Staphylococcus* and *Corynebacterium* species, are more abundant in moist areas, such as the bends of the elbows and the feet (Byrd et al., 2018).

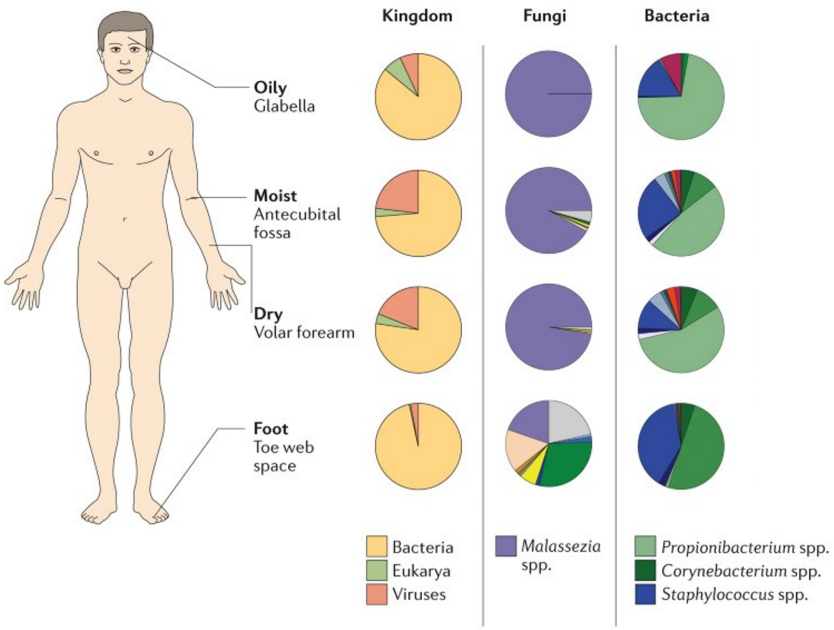


**Figure 1.5 Skin microbiome composition varies with body location**

The skin is divided into four major microenvironments: oily, moist, dry, and foot. The variations in conditions such as humidity, warmth, and acidity results in variations in relative abundance in kingdom, fungi, and bacteria. Pie charts represent consensus relative abundances across healthy adults. Reproduced with permission from Byrd et al., 2018. Licence number 5481991251147

Typically, the bacteria of the microbiome are commensal, and they interact to provide a degree of protection from pathogens (Boxberger et al., 2021). Pathogens are prevented from colonising the skin by competing for resources such as nutrients or space, secreting antimicrobial peptides (AMPs) (Nakatsuji et al., 2017), or free fatty acids that act on other microbes to inhibit pathogenic invasion and prime the immune system (Baldwin et al., 2017; Williams et al., 2019) by inducing the generation of regulatory T ($T_{regs}$) cells by directly sensing the microbial products (Brown et al., 2012; Ong et al., 2002).

A notable example of a commensal bacteria of the skin microbiome that plays a protective role is *Staphylococcus epidermidis*. *S. epidermidis* confers direct protection against *S. aureus* through bacterial effectors, namely phenol-soluble modulins (PSMs). PSMs can protect against pathogenic bacteria such as *S. pyogenes* and *S. aureus* by causing lipid vesicle leakage (Cogen et al., 2010). *S. epidermidis* provides

further protection to the skin by diminishing inflammation post-injury (Lai et al., 2009) and enhancing T cell development (Laborel-Préneron et al., 2015; Naik et al., 2012).

However, resident microbes can cause infections and enter the bloodstream, potentially leading to fatal infections, especially in the case of immunosuppressed patients (Cogen et al., 2008). An example of a commensal species that can cause dangerous infections is *S. aureus*, a serious threat to the body if it invades the bloodstream, to cause bacteraemia (Tong et al., 2015). However, *S. aureus* is also a commensal bacteria found in the skin microflora of roughly 30% of the human population. Gram-positive bacterial genera e.g., *Staphylococci* represent an important population of the commensal microbes that colonise the skin of healthy people but can become opportunistic and pathogenic should the area of skin it colonises become wounded (Chiller et al., 2001). This is because the opportunistic bacteria can now colonise a new area without competition for nutrients.

### 1.3.1 Bacterial skin pathogens

Some of the bacteria in the skin microbiome are opportunistic, capable of changing from commensal to pathogenic once the bacteria are able to gain access into the tissue, pass the epidermis and cause infection. Bacterial skin infections have a wide range of clinical manifestations, ranging from impetigo, to folliculitis, to necrotising fasciitis (Sukumaran, 2016).

#### 1.3.1.1 *Staphylococcus aureus*

*Staphylococcus aureus* is a species of Gram-positive cocci that typically colonises tissues such as the skin and nasal epithelium. It is one of the leading causes of skin infections and is a leading causative agent of cellulitis and impetigo (Tong et al., 2015). *S. aureus* can enter the skin via breaks or weaknesses in the epidermis and it has a wide range of adhesins to interact with fibronectin presented on cells. *S. aureus* can invade deeper into the skin and enter the bloodstream from which it can spread systemically and cause more severe infections, potentially leading to multiple organ failure (Thomer et al., 2016).

*Staphylococcus aureus* is an important cause of skin and soft tissue infections (SSTI) and is associated with atopic dermatitis, which affects roughly 20% of children and 3% of adults globally. It is an opportunistic bacterial species that can reside commensally on the skin of 30% of adults but can become invasive should the epidermis of the host be breached, or the skin microbiome is disrupted. *S. aureus* also represents a global issue as overuse of antibiotics has led to the rise of antibiotic resistant strains of *S. aureus*, notably methicillin-resistance *S. aureus* (MRSA).

Of the bacteria species mentioned in sections 1.3, this thesis is focused on *S. aureus* as it is a well-characterised pathogen and a common model choice for studying bacterial skin infections. Furthermore, it is a skin pathogen of significant clinical importance, causing skin infections globally with symptoms varying from impetigo to necrotising fasciitis (Del Guidice, 2020).

#### 1.3.1.2 *Streptococcus pyogenes*

*Streptococcus pyogenes* is a species of Gram-positive cocci that, whilst infrequent, are a clinically important human pathogen. The most severe *S. pyogenes* infection can manifest as Streptococcal Toxic Shock Syndrome (STSS) or necrotising fasciitis (Johansson et al., 2010). There are nearly two million new cases of *S. pyogenes* infection each year (Avire et al., 2021, WHO, 2005). The throat and skin are reservoirs for *S. pyogenes*, and it can be transmitted through respiratory droplets, or skin contact with broken skin that has secretions from infected sores (Walker et al., 2014). *S. pyogenes* uses a variety of cell surface proteins to adhere to human cells. For example, Protein M on the bacteria cell surface binds directly to components of the ECM e.g., fibronectin (Cue et al., 2001).

#### 1.3.1.3 *Cutibacterium acnes*

*Cutibacterium acnes* is a Gram-positive bacterial species that colonises human skin. It can contribute to the human body by digesting sebum, resulting in the secreting of free fatty acids. This produces an overall acidic pH to skin, inhibiting pathogenic

bacteria from spreading (Elston et al, 2019). However, *C. acnes* has also been associated with a variety of diseases such as acne vulgaris and infections post implant surgery (Fischer et al, 2020). Whilst it has not been fully characterised, it has been described that *C. acnes* possesses adhesins to glycosaminoglycans (GAGS) and dermatan sulphate (Martin et al, 2022).

#### 1.3.1.4 *Pseudomonas aeruginosa*

*Pseudomonas aeruginosa* is a gram-negative opportunistic pathogen that is commonly associated with burn wounds. *P. aeruginosa* is also a pathogen of clinical interest as it is a common cause of hospital-acquired infections and is a pathogen capable of forming biofilm (further discussed in section 1.3.5.1). These biofilms are capable of forming on medical equipment such as catheters or implants, making it a pathogen of significant clinical concern (Khatoon et al, 2018*). P. aeruginosa* possesses two lectins, LecA and LecB, which binds to carbohydrate ligands on host cells to promote *P. aeruginosa* adhesion to host cells (Wilhelm et al., 2019)

### 1.3.2 Pathogen entry

Bacteria can gain entry into the skin by adhering to exposed matrix factors and cell surface receptors that are normally inaccessible. Bacteria interact with host cell receptors to adhere to the cells, allowing them to target specific environments in a host which are viable for them to proliferate (Ribet and Cossart, 2015). Once bacteria have adhered, they can survive extracellularly as biofilms or internalise into a host cell and eventually reach the bloodstream after transcytosis, causing systemic damage. In the UK alone, approximately 130,000 people will visit the hospital with burn wounds with 10,000 of those patients being severe enough to warrant admittance to the hospital with infection being a major complication of burn injury (Young, 2013). The cause of most burns in the UK is simply due to carelessness or inattentiveness, resulting in an accident during cooking or scalding oneself with a hot drink. Besides the physical or psychological effects of burn wounds, infections occur due to the disruption in the

skin's mechanical integrity resulting in an impaired defence against pathogens or opportunistic bacteria such as *S. aureus*.

### 1.3.3 *Staphylococcus aureus* adhesion

*Staphylococcus aureus* has a wide range of adhesins e.g., microbial surface components recognizing adhesive matrix molecules (MSCRAMMs) like fibronectin binding protein (FnBP) A and B. As its name suggests, FnBP adheres to fibronectin on target epithelial cells (Joh et al., 1999). *S. aureus* can simultaneously bind to human cells by binding to fibronectin, as eukaryotic cells also have surface receptors to fibronectin (Figure 1.6).

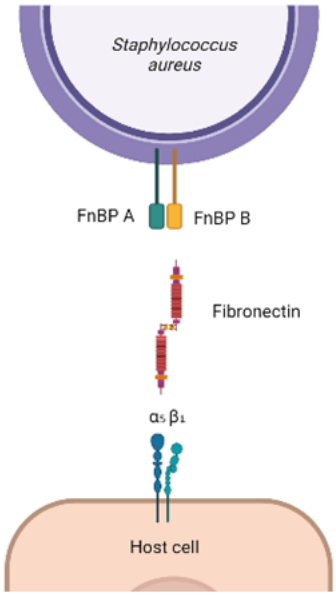


**Figure 1.6 Fibronectin Binding Protein binds to α5β1**

Simplified diagram describing how FnBP expressed by *S. aureus* binds to $\alpha_5\beta_1$ expressed by eukaryotic cells. Adapted with permission from Sinha et al, 1999 and reproduced with BioRender. Licence number 5183250034813.

Sinha et al. showed that fibronectin acts as a molecular bridge by connecting FnBP-expressed *S. aureus* with integrin α5β1 expressed on human cells. This host-pathogen interaction anchors *S. aureus* to a host cell, as well as encouraging the internalisation of bacteria by epithelial and endothelial cells (Sinha et al., 1999).

Another group of proteins utilised by S. aureus to adhere and gain entry into host cells are the heparan sulphate proteoglycans (HSPGs), specifically syndecan-1 (SDC-1). SDC-1 is associated with *S. aureus* adherence to epithelial cells, with SDC-1 KO mice displaying greater resistance to corneal infection by *S. aureus* (Hayashida et al., 2011). Recently, Green et al. proposed a novel model in which CD9 organises tetraspanin-enriched microdomains containing SDC-1 or α5β1, leading to the recruitment and organisation of fibronectin fibrils on the cell surface for bacterial adhesion (Green et al., 2023)

### 1.3.4 Additional adhesion mechanisms by other skin bacterial pathogens

#### 1.3.4.1 Flagella

Other adhesion mechanisms and targets exist for bacterial species that can colonise the skin. *P. aeruginosa,* possess flagella which are vital for motility and adhesion (Bucior et al., 2012; Garcia et al., 2018). The flagellum is utilised by multiple bacterial species for adhesion as well as invasion, however many of the receptors targeted by the flagella have not been determined. In the case of *P. aeruginosa*, multiple target cells and proteins have been identified, such as HSPGs and mucin (Haiko and Westerlund-Wikström, 2013).

#### 1.3.4.2 Lipoteichoic acid

It is proposed that *S. pyogenes* adheres to epithelial cells by first overcoming electrostatic repulsion between the bacterium and host cell. This is mediated by lipoteichoic acid (LTA). The fatty acid moiety of LTA allows for initially weak interactions between *S. pyogenes* and the fatty-acid binding domains of the host cell membranes. *S. pyogenes* can then adhere more strongly to host cells with adhesins such as protein F that binds to fibronectin (Courtney et al., 2002).

#### 1.3.4.3 Hydrophobic attachment

Both bacterial and host cells have overall negative charges and therefore repel each other. Bacteria must overcome the repulsion caused by the charge, some bacteria can also present positively charged or hydrophobic molecules to overcome the initial repulsion and allow weak association; this facilitates the formation of stronger bonds and avoids clearance (Krasowska and Sigler, 2014). Medical equipment such as filters and catheters are made from hydrophobic materials making it relatively simple for bacteria to adhere and create problems with biofilms (Francolini and Donelli, 2010). *S. aureus* can colonise and form biofilms on medical equipment and are more resistant to removal (Zheng et al., 2018).

### 1.3.5 *Staphylococcus aureus* evasion of immunity

Whilst some bacterial species have evolved to be tolerated by the immune system, they also possess mechanisms to actively evade the host immune response. For example, *S. pyogenes* can secrete a variety of proteins that can target complement components or antibodies for degradation or interfere with Fc recognition by phagocytes. In both cases, this interference by *S. pyogenes* impairs phagocytosis (Laabei and Ermert, 2019). Another skin bacteria, *C. acnes*, produces the antioxidant, catalase, which is essential for *C. acnes to* survive phagocytosis by macrophages (Fischer et al., 2013, Yamamoto et al., 2019).

*Staphylococcus aureus* possesses a wide variety of factors to evade the host immune system. For example, *S. aureus* produces Protein A, which binds to the Fc region of IgG making it inaccessible to FcγR thus preventing IgG-dependent phagocytosis, this also hinders the classical complement pathway ultimately preventing C3b from being deposited on the surface of the bacteria, inhibiting opsonisation (Goldmann and Medina, 2017, Iwatsuki et al., 2006).

To evade phagocytosis, *S. aureus* can produce leukotoxins that are cytolytic to neutrophils, macrophages, and monocytes (Kaneko and Kamio, 2004). In addition to this, *S. aureus* can also produce chemotaxis inhibitory protein (CHIP) to bind

complement protein C5a to further inhibit phagocytosis and Map (an extracellular adherence protein) that inhibits neutrophil recruitment (Bestebroer et al., 2010; de Haas et al., 2004). *S. aureus* has adapted ways in which to evade the innate immune system, but it has also gained the ability to manipulate the adaptive immune response. *S. aureus* can be internalised inside host cells in order to avoid immune responses and to further spread throughout the system and cause infection. This depends on FnBPs and the host integrin α5β1 which are found on endothelial cells, epithelial cells, and keratinocytes (Kintarak et al., 2004).

*Staphylococcus aureus* has also developed resistance with the RexAB protein, which can repair damage caused by an oxidative burst from a neutrophil. The increase in DNA repair and damage to telomerase, combined with low fidelity in checking the repaired DNA, promotes the chance of resistance being developed (Painter et al., 2015). DNA repair promotes the emergence of small colony variants and resistance, promoting survival, gene diversity and host adaptation. These small colony variants are resistant to the oxidative burst, surviving the immune response and resulting in a persistent infection (Painter et al., 2017). Bacterial resistance to non-lactam antibiotics such as vancomycin or daptomycin is increasing, and alternative treatments need to be explored and developed.

Some studies have noted the ability of *S. aureus* to specifically evade the skin immune system. Kwiecinski et al. identified the ArlRS-MgrA cascade as a critical regulatory system used by *S. aureus* to adhere to host endothelial cells, this cascade alters the expression of Ebh and SraP which otherwise interferes with *S. aureus* binding to fibroblasts (Kwiecinski et al., 2019). This research was later expanded in a study that concluded that *S. aureus* used the ArlRS-MgrA cascade to evade the immune system during skin infection, in which the authors demonstrated that ArlRS-MgrA was essential for *S. aureus* to evade neutrophils *in vivo* (Kwiecinski et al. 2021).

Studies indicate that *S. aureus* can localise and survive inside the lysosomes of macrophages to evade the immune system (Surewaard et al., 2016). *S. aureus* are able to also internalise inside keratinocytes; in a recent study, the authors demonstrated that clinical isolates of *S. aureus* from patients with atopic dermatitis

were capable of localising to, and surviving in, the lysosomes of HaCaT keratinocytes, whereas lab strains of *S. aureus* and *S. epidermidis* were unable to do so (Moriwaki et al., 2019). As strains of *S. aureus* can survive in the lysosome, keratinocytes may serve as a reservoir that allow *S. aureus* to evade immune cells. *S. aureus* internalisation by keratinocytes was also shown to aid *S. aureus* resistance against antibiotic killing (Marbach et al., 2018, Al Kindi et al., 2019).

Interestingly, Bitschar et al., showed that skin inflammation induced neutrophil recruitment that in turn enhanced *S. aureus* colonisation, due to keratinocyte interaction with neutrophil NETs. The authors suggest that soluble factors secreted by infected keratinocytes induced the neutrophils to release NETs ultimately increasing *S. aureus* colonisation. The authors were able to demonstrate that released DNA was responsible for the increase in *S. aureus* colonisation. However, the authors were unable to determine why this was the case (Bitschar et al., 2020).

Finally, a study using skin explants demonstrated that, upon contact with skin, *S. aureus* upregulated the expression of proteases such as staphopain and aurelysin that cleave and inactivate antimicrobial peptides (Burian et al., 2019).

#### 1.3.5.1 Biofilms

Biofilms are aggregated microbial communities that are attached to a surface and encased by an ECM (Costerton, 1978). The biofilm matrix is composed primarily of proteins, polysaccharides, and extracellular DNA. Biofilm formation protects the bacteria from its environment i.e., altered pH, nutrient scarcity, and mechanical force, but also from host immune responses and antibiotics (Fux et al, 2005, Stewart et al., 2001). Bacteria can infect in their planktonic form or by creating a biofilm that offers protection and makes infections harder to treat.

There are generally 4 stages to biofilm development: adhesion, aggregation, maturation, and dispersal. In the adhesion stage, bacteria can adhere to a surface or host cell via weak non-specific charges, this is due to the overall charge and hydrophobicity of the host and pathogen (Krackler and Orth, 2013). This is followed by stronger adhesion, mediated by specific interactions between bacterial surface

molecules and host cell receptors. Planktonic bacteria utilise a variety of factors and mechanisms to adhere to a host cell or surface, examples include MSCRAMMS, FnBPs, clumping factors (ClfA and ClfB), and serine-aspartate repeat family proteins (SdrC, SdrC and SdrE) (Peng et al., 2022).

After adhering to the surface, the bacteria undergo changes in gene expression to upregulate the production and secretion of the components needed to form the biofilm (Garrett et al., 2008). The bacteria begin to proliferate to form microcolonies and secrete polymeric molecules to form the biofilm matrix. During the aggregation stage, signalling molecules known as autoinducers are secreted by bacteria for cell-to-cell communication. This communication is known as 'quorum sensing', the communication mechanism between bacterial cells whereby autoinducers stimulates gene expression (Schulze et al., 2021). Bacteria detects the changes in bacteria density in the surrounding environment based on the changes in concentration of autoinducers. Once the autoinducer reaches a certain threshold, the expression of relevant gene in bacteria is initiated to adapt to the changes in the environment (Lu et al., 2019). The bacteria secrete extracellular polymeric substances (EPS), such as polysaccharide intercellular adhesion (PIA), which interact to form stronger bonds between cells. EPS is the scaffold that allows biofilms to mature into 3D mushroom-like structures, with channels within the structure for water and nutrient transport for the bacteria deep within the biofilm structure (Flemming and Wingender, 2010). Quorum sensing in *S. aureus* is regulated by the accessory gene regulator (agr) system, to prompt genetic adaptions for bacterial communication. The agr system responds to bacterial cell density and, in the case of gram-positive bacteria such as *S. aureus,* use an autoinducing peptide (AIP) as the signal molecule of cell density (Rutherford and Bassler, 2012). Once the biofilm has matured, an oversaturation of bacteria is observed and the agr system increases the expression of degradative proteases and decreases the expression of colonisation factors. This results in the biofilm breaking down, dispersing the bacteria (Le and Otto, 2015).

Biofilms act as an immune evasive mechanism as biofilms create a favourable environment that increases antibiotic resistance and impairs host immunity (Ricciardi et al., 2018) (as discussed in section 1.2.6). Biofilms secrete a variety of proteins such as PSMs or leukocidins to lyse neutrophils (Bhattacharya et al., 2018). In addition to

this, biofilms can also skew macrophage responses towards the M2 anti-inflammatory state, which is inefficient for phagocytosing bacteria within the biofilm (Gries et al., 2017). Physically, the complex structure of biofilms of multiple microcolonies can render them more resistant to antibiotics as the EPS and other proteins present in the biofilm make it difficult for antibiotics to penetrate to the bacteria within. The amount of antibiotics needed to kill bacteria within a biofilm may be 100 to 1000 times higher than planktonic bacteria (Olson, 2015).

### 1.3.6 Antibiotic resistance

Over the years there has been a rise in antibiotic resistance to the extent it has become one of the leading public health threats of the 21st century. Resistance is now seen in nearly all antibiotics leading to the need for new antibiotics or alternate therapeutics (Ventola, 2015).

This rise in drug resistance has arisen due to the misuse of antibiotics (neglecting to complete a course of antibiotic treatment or not using the prescribed dosage), along with extensive agricultural use. The abuse of antibiotics creates a selective pressure on the bacterial population that kills drug-sensitive bacteria but allows resistant bacteria to survive and flourish with less competition. Furthermore, resistant genes and mechanisms can be transferred between bacterial species (Read et al., 2014).

#### 1.3.6.1 Methicillin-resistant *Staphylococcus aureus*

Methicillin-resistant *Staphylococcus aureus* is a form of *S. aureus* that is resistant to β-lactam antibiotics, such as methicillin and oxacillin, which work by inhibiting essential bacterial metabolic processes e.g., cell wall or fatty acid synthesis. It can either be hospital-acquired or community-acquired, depending on the source of infection. Prior to antibiotics, *S. aureus* infections had a mortality rate of 80%, this plummeted with the introduction of the natural penicillin G in the 1940s however, *S. aureus* became resistant within the same decade. In 1959, methicillin was introduced to treat penicillin-resistant *S. aureus*, but resistant strains were discovered in the UK a mere two years later and eventually spread across the world (Peacock and Paterson, 2015). Annually

in the EU, MRSA infections have been estimated to result in one million additional days of hospitalisation and hospital costs of €380 million (Gould et al., 2010).

## 1.4 Current treatments for *Staphylococcus aureus* infection

Bacterial infections are typically treated with antibiotics delivered systemically either by oral or intravenous administration. MRSA is typically treated with vancomycin, but resistance is increasingly spreading. The misuse of antibiotics, either by needlessly using them or not completing a course of antibiotics, imposes a selective pressure on the bacterial population. By killing sensitive bacteria but allowing the resistant mutants to survive, the mutated strains can proliferate with less competition for resources e.g., food and space, and pass on the resistance genes to other microbes by horizontal or vertical gene transmission (von Wintersdorff et al., 2016). This has resulted in the rise of MRSA which has made treatment with antibiotics far more difficult (Davies and Davies, 2010; Martin et al., 2019).

### 1.4.1 Tetraspanins and their exploitation by *Staphylococcus aureus*

Tetraspanins are a superfamily of membrane proteins expressed in eukaryotes (Hemler, 2003). Tetraspanins interact with other tetraspanins as well as proteins, such as integrins, and lipids to form tetraspanin-enriched microdomains (TEMs). TEMs are cell membrane structures which serve as molecular organisers whose functions are implicated in a wide variety of cellular activities such as cell adherence, signalling and fusion (Hemler, 2003; Parthasarathy et al., 2009). Tetraspanins also play a role in the development of skin. For example, CD151 is a tetraspanin found on endothelial, epithelial and DCs and interacts with integrins α3β1 and α6β4 in skin and forms laminin-binding complexes to modulate their function (Li et al., 2013). Whilst few tetraspanins have distinct phenotypes, CD151 is clearly essential in skin development as a deletion or deficit of CD151 results in the disruption of the basement membrane of skin. Deletion of CD151 in mice also results in the disruption of the glomerular basement membrane leading to kidney failure (Sachs et al., 2006; Crew et al., 2004).

Structurally, tetraspanins have four transmembrane domains, a shorter extracellular loop (EC1), a longer extracellular loop (EC2) and two intracellular termini and the EC2 contains a conserved CCG motif in EC2 (Boucheix and Rubinstein, 2001) (Figure 1.7). Bacteria can exploit host cell membrane structures, TEMs, to use as adherence platforms. Tetraspanins are exploited by pathogens as gateways into cells; previous research has shown that an overexpression of CD9 increases susceptibility to *Corynebacterium diphtheria* toxin by increasing cells sensitivity to the toxin (Nakamura et al., 2000). Pathogens can exploit TEMs to enter a host cell. More commonly, bacterial adhesion requires an indirect interaction with tetraspanins, through receptors embedded in TEM which the bacteria directly interact with (Green et al., 2011; Monk & Partridge, 2012).

Tetraspanins are being considered as a possible avenue of study for novel therapeutics as they are implicated in pathogen entry, as well as showing a degree of redundancy, meaning it is possible to target specific tetraspanins without severely disrupting host function (Hassuna et al., 2009). Tetraspanin knockout mice remain viable and typically display mild defects that indicates a capacity for tetraspanins to compensate for each other. For example, the deletion of CD9 in mice results in the disruption of sperm-egg fusion (Boucheix, 2000). However, injecting CD81 mRNA into the CD9-deficient eggs helps to partially restore fusion rates. Huang et al. believes this could be due to the similarity in primary structure between CD9 and CD81 (Huang et al., 2005).

Tetraspanins show potential as useful targets for novel treatments, especially if TEM function can be disrupted, this is because it is likely to result in the disorganisation of multiple receptor proteins that are potential targets for bacterial adhesion (Ventress et al., 2016). Together, this research suggested that peptides derived from tetraspanins could affect the ability of bacteria to adhere *in vivo*, the Monk laboratory have shown that peptides based on the EC2 domain of CD9 could inhibit *S. aureus* adhesion to keratinocytes with no effect on keratinocyte viability or migration (Ventress et al., 2016).

A small number of studies suggest a role for tetraspanins in skin immunity. An early study by Mantegazza et al. demonstrated that a variety of tetraspanins were expressed

on the surface of immature DCs, with the authors speculating that the tetraspanins may have an important role in downmodulating DC migration given that antibody treatment against the tetraspanins reduced DC migration. In addition, the authors specifically noted that CD63 was internalised and translocated towards MHCII-enriched compartments after simulation, leading the authors to propose the possibility that CD63 is involved in antigen capture and processing (Mantegazza et al., 2004). Another tetraspanin linked to dendritic cell function is CD37, which was shown to promote dendritic cell migration as CD37 knockout mice displayed impaired dendritic cell migration from the skin to draining lymph nodes (Gartlan et al., 2013).

In a more skin-specific context, a recent study defined Langerhans cell subsets into specific populations. The two main subsets, LC1 and LC2, were predominantly defined by their expression of langerin amongst other markers, with LC2 being enriched for CD63. Whilst no specific function was attributed to CD63 in LC2 Langerhans cells, the authors observed LC2 Langerhans cells playing a more immunoregulatory role that CD63 may contribute to (Liu et al., 2021). Rindler et al., performed single-cell and proteomic profiling on melanocytes from patients suffering from atopic dermatitis and the authors observed that CD81 was noticeably upregulated in melanocytes in AD skin. The authors noted that CD81 facilitated TGF-β signalling in melanocytes along with CD9 and speculated that this increased CD81 would influence melanocyte growth and melanin production. However, the authors also add that they did not notice overt clinical dyspigmentation in the AD patients (Rindler et al., 2021). An important study linking tetraspanins with skin immunity is a study highlighting the importance of CD9 to cutaneous wound healing. In that study, the authors reported a significant delay in wound healing in CD9 knockout mice, demonstrating that re-epithelialisation was adversely affected due to impaired migration of the epidermis (Zhang et al., 2012).

In a review on keratinocyte-secreted extracellular vesicles by Nasiri et al., the authors highlight a group of extracellular vesicles known as exosomes, as defined by their size and that they express tetraspanins on their surface. As keratinocytes are the first skin cells to encounter an environmental allergen or pathogen, keratinocytes can operate as modulators for the migration of inflammatory immune cells which in turn can be mediated by exosomes (Nasiri et al, 2020). Secreted exosomes from keratinocytes can function as immunomodulators and interact with APCs, an example of this was

demonstrated by Kotzerke et al., in which murine keratinocyte-secreted exosomes were readily taken up by dendritic cells (Kotzerke et al., 2013). A similar study was later performed which showed that, upon pathogen detection, keratinocytes could secrete extracellular vesicles that modulated the innate immune response. However, it should be noted that this was only seen *in vitro* (Papayannakos et al., 2021).

Several studies have provided evidence of the importance of tetraspanins as molecular partners and organisers. In a review by Rocha and Perugini, the authors highlighted the relevance of tetraspanins in APCs for their role in antigen recognition and presentation. This is through the organisation of PRRs and their downstream signalling and regulation of antigen trafficking (Rocha-Perugini et al., 2016). In their review, the authors cited the work of Peng et al., who reported that CD9 and CD81 are molecular partners for the trimeric form of FcεRI, the high-affinity receptor for IgE, on APCs (Peng et al., 2011). As FcεRI plays an important role in antigen uptake and is highly expressed in the monocytes and epidermal DCs of AD patients (Shin and Greer, 2015), Peng et al. sought to understand the link between the role of tetraspanins and FcεRI. Using flow cytometry, the authors reported that epidermal DCs had higher expressions of multiple tetraspanins including CD9 and CD81 in the lesional skin of AD patients compared to healthy controls. Analysis in AD patients also revealed that $FcεRI^+$ monocytes strongly expressed CD9 and CD81 whereas the $FcεRI^-$ population only showed moderate expression, indicating a concomitant upregulation of CD9 and CD81 on $FcεRI^+$ APCs. Furthermore, the authors were able to show that CD9 and CD81 co-localised with FcεRI and were tightly associated, concluding the CD8 and CD81 were molecular partners for FcεRI on monocytes.

This study is in line with an earlier study by Jockers and Novak, who reported that the expression of tetraspanins was noticeably distinct between patients with atopic dermatitis and psoriasis compared to healthy controls (Jockers and Novak, 2006). Atopic dermatitis and psoriasis are two of the most common chronic inflammatory skin diseases, whilst they have significant differing features, e.g., clinical pathology and immunological mechanisms, they both share common features such as the high

recruitment of proinflammatory cells from the blood into the skin (Chovatiya and Silverberg, 2019). This recruitment requires multiple proteins such as selectins, integrins and tetraspanins. To investigate the differences in expression, the authors used flow cytometry to evaluate the expression of adhesion molecules and tetraspanins of monocytes of patients with atopic dermatitis, psoriasis, or healthy controls. The authors found increased expression of tetraspanins CD9 and CD53 on monocytes from patients with psoriasis compared to normal patients, expression of CD63 was increased but CD81 was decreased in both patients with AD and psoriasis, compared to healthy controls. In addition to this, the authors also reported upregulation in the expression of β-integrins on the surface of monocytes in AD patients. As tetraspanins interact with β-integrins, the increased tetraspanin expression could result in enhanced affinity and avidity of monocytes from AD patients, thus enhancing the adhesion of monocytes to endothelial cells. Ultimately, the authors concluded that a distinct expression pattern of adhesion molecules and tetraspanins on the monocytes of patients with chronic skin inflammation may influence the recruitment of inflammatory cells to the skin, identifying these recruitment molecules as potential targets for anti-inflammatory skin therapeutics.

As FcεRI expression is increased in Langerhans cells and DCs in AD patients, Novak et al., had also investigated the effects of FcεRI engagement in Langerhans and DCs and how these effects contributed to atopic dermatitis (Novak et al., 2004). By developing an *in vitro* model that generated DCs that were phenotypically similar to Langerhans cells and inflammatory dendritic epidermal cells present in AD patients, which both display increased FcεRI compared to healthy patients, the authors noticed a distinct pattern of cytokine and chemokine release upon activating these cells with IgE. Specifically, the authors saw FcεRI activation with IgE result in an increased release of proinflammatory cytokines by the Langerhans-like dendritic cells, implying that Langerhans cells may play a role in the recruitment of monocytes and T cells into the skin lesions of AD patients.

Interestingly, Novak et al., observed that FcεRI ligation in their *in vitro* model resulted in increased IL-16 production, a chemoattractant for $CD4^+$ T cells. A study by Qi et al., hypothesised that tetraspanins were a component of the alternate IL-16 receptor on the surface of mast cells. Whilst CD4 is the primary receptor for IL-16, PBMCs and Langerhans cells from CD4-null mice were still responsive to IL-16 indicating the presence of an alternative receptor. Using the MHC-1 cell line, a mast cell line which lacks CD4, the authors were able to report that CD9 participated in the IL-16 mediated chemotaxis and activation of human and mouse mast cells, and that CD9 was the primary IL-16 receptor on the surface of HMC-1 cells (Qi et al., 2006). In the review by Halova and Draber, the authors also cite an article by Kraft et al., in which the authors investigated the role of tetraspanin CD63 in mast cell degranulation using knockout mice (Kraft et al., 2013). In CD63 -/- mice, mast cell numbers and tissue distribution were unaffected by the absence of CD63, however FcεRI-induced degranulation was significantly diminished. The authors also calculated the granular contents of the mast cells and found no differences between the CD63 -/- and CD63+/+ mice, indicating that CD63 deficiency hadn't caused any defects in the production, storage, or distribution of granules, but had altered its release, thus CD63 expression was required for efficient mast cell degranulation via IgE and FcεRI. The authors further demonstrated the role of CD63 in mast cell mediated allergic responses by using mast cell deficient mice. By transferring mast cells from CD63 -/- and CD63 +/+ mice into each ear, the authors induced anaphylaxis with IgE and found that the CD63-/- mouse had less extravasation and no prominent mast cell degranulation.

Together, these studies highlight a role for tetraspanins, their interactions with FcεRI and how they can affect immune cell recruitment and its potential impact on the pathology of AD, thus identifying tetraspanins as a potential therapeutic target for inflammatory skin diseases.

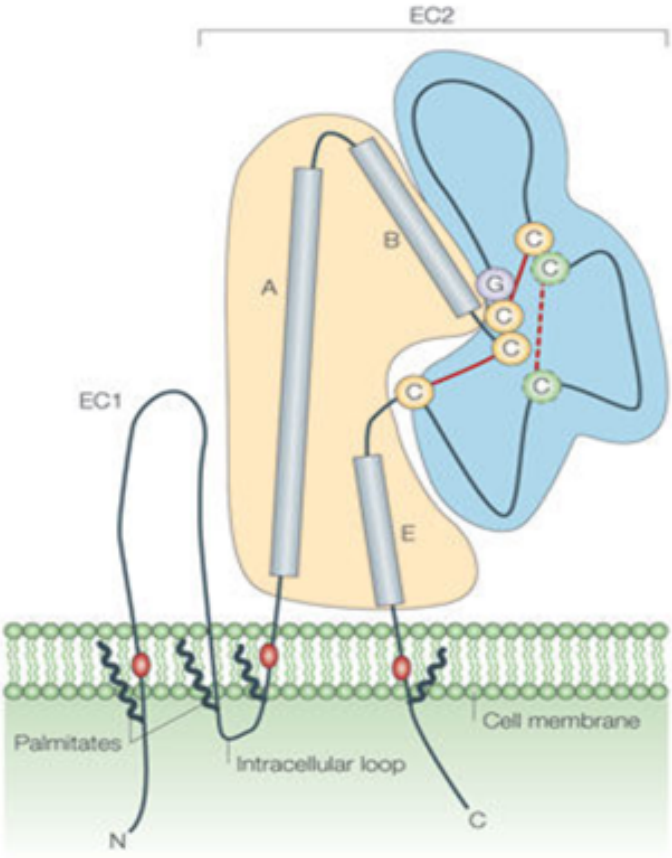


**Figure 1.7 Structural features of tetraspanins**

Tetraspanins have four domains, two extracellular domains, EC1 and EC2 and two intracellular termini. Reproduced with permission from Hemler, 2005. License number 5183300943822

## 1.4.2 Anti-adherence therapy

A new area of research is anti-adherence therapy because this exerts a weaker selective pressure than conventional antibiotics meaning that there is less chance of developing resistance. By reducing adhesion, which can be host-specific or bacteria-specific, pathogens cannot infect host cells (Krachler & Orth, 2013). Anti-adherence therapy works by altering the expression of host cell receptors or interfering with host receptor function, to prevent bacteria from adhering to host cells (Asadi et al., 2019; Hassuna et al., 2009).

The potential of anti-adhesion therapy has been demonstrated by the Monk Lab for a number of pathogenic bacteria. Hassuna et al. have shown that antibodies against tetraspanins and recombinant EC2 domains can disrupt the adherence of multiple bacterial species such as *S. aureus* and *N. meningitidis* (Hassuna, 2009). Later, Green et al. demonstrated that blockade of tetraspanins with either antibodies or recombinant peptides could inhibit adherence of a variety of bacterial species such as *S. pneumoniae*, *N. lactamica* and *N. meningtidis* to epithelial cells (Green, 2011). This was further developed when Ventress et al. showed that peptides derived from CD9 strongly reduced *S. aureus* adhesion to human skin models (Ventress et al, 2016). These studies demonstrated that tetraspanins are molecular organisers that interact with membrane proteins to form TEMs that are exploited as adhesion platforms for bacteria, treatments targeting tetraspanins would disrupt TEM formation, resulting in integrin disorganisation and consequently bacterial adhesion to host cells) (Barreiro et al., 2005; Yáñez-Mó et al., 2009).

Tetraspanins display varying degrees of functional redundancy; aside from several highly specialised tetraspanins such as the bladder-specific uroplakin, few tetraspanins have distinct phenotypes. For example, the deletion of TSPAN32 only results in minor upregulation of T cell proliferation. Relevant to this study, the deletion of CD9 in mice results in no noticeable phenotype. However as mentioned in 1.4.1, sperm-egg fusion is disrupted. Sperm-egg fusion can be restored with an injection of CD81 mRNA which is structurally similar to CD9. This demonstrates that tetraspanins have a functional redundancy, where if one tetraspanin is functionally affected, another can partly compensate. This feature makes tetraspanins a potentially safe target for anti-adhesion therapy but may also indicate that tetraspanin therapies can only ever be partly effective (Huang et al., 2005).

## 1.5 Skin in research

There is a clear need for new treatments for bacteria that cause skin infections, combined with a need for further research into skin diseases in general, such as atopic dermatitis or psoriasis. A promising area of research is the use of human skin models derived from donor skin, this has the advantage of providing a more accurate indication

of a human response to treatment in comparison to an animal model (Moniz et al., 2020). For example, there are major differences in the skin (Mestas and Hughes, 2004); mouse skin has a much thinner epidermis, far more hair follicles, contains dermal T cells which are not found in humans, and the major T cell type appears to be γδ T cells in comparison to our conventional αβ T cells (Salgado et al., 2017). These differences alone can result in different responses between mice and humans, leading to non-translatable study results.

### 1.5.1 Skin models

The use of human skin models may provide a more accurate representation of what a human response would be compared to an animal model. Additionally, an advantage of using human skin models is that they could potentially contribute to the 3Rs (Replacement, Reduction and Refinement) and lead to more humane animal research. Animal testing has brought about a moral debate about subjecting animals to dangerous chemicals and drugs for side effects and toxicity levels. Human skin models experiments could justify the necessity of bringing forward a potential therapeutic for animal experimentation to the Home Office for licence approval. As the skin samples come from cosmetic surgeries such as breast reductions or abdominal surgery, there are significantly fewer concerns about experiments as patients can give informed consent for their skin to be used for research. In addition, for skin research in the UK, all human tissue must be taken with informed consent under protocols approved by an NHS Ethical Committee and stored appropriately often via a Human Tissue Research Bank approved by the Human Tissue Authority, a public body of the Department of Health and Social Care in the UK. There are also concerns of passing on viral diseases such as Hepatitis A that must be considered for the user. Human skin models have potential in drug discovery because they can give more representative results of human responses to a drug as the skin model can be constructed to recreate specific conditions, e.g., skin models can be constructed to replicate psoriasis or atopic dermatitis, allowing the study of cytokine-induced gene expression (Pouliot-Bérubé et al., 2016). However, skin models still need improvement as the use of skin models for drug testing is associated with issues such as low sensitivity to the drug of interest.

This study focuses on 3 kinds of skin models: tissue-engineered skin, collagen-based organotypics and surgical explants (Figure 1.8).

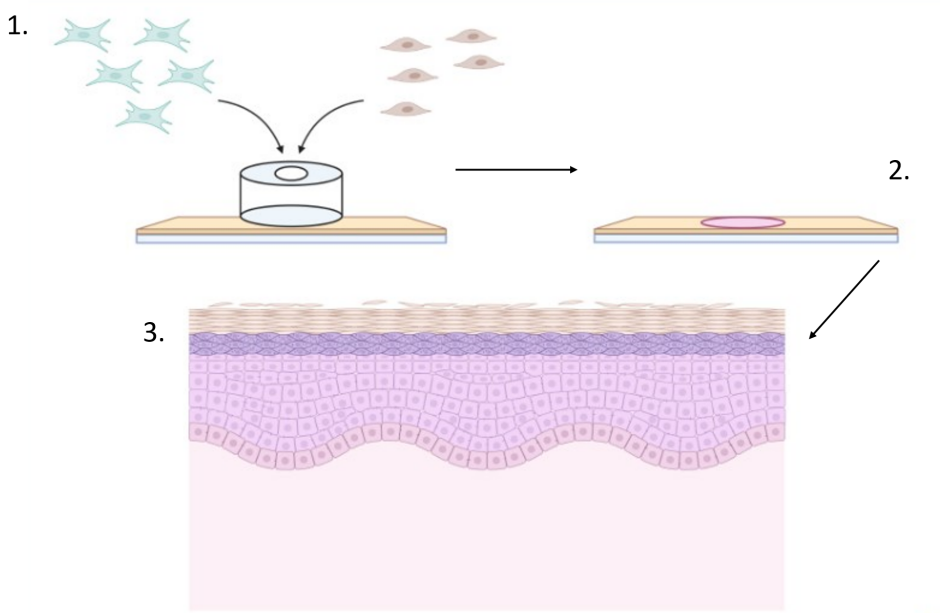


**Figure 1.8 Construction of tissue-engineered skin models**

**1.** A stainless steel ring is placed onto an acellular de-epidermidised dermis, cell suspensions of keratinocytes and fibroblasts are then pipetted into the ring. **2.** The dermis with cell suspension is incubated overnight for the cells to adhere to the surface of the dermis. **3.** The steel ring is then removed, and the dermis is then raised to an air-liquid interface and left to differentiate for 2 weeks to form an epidermis. Figured produced with BioRender.

The MacNeil laboratory has published an extensive range of 3D skin models (MacNeil, 2007). Of these models, the most relevant to this study is the one reported by Shepherd (Shepherd et al., 2009). This model used primary keratinocytes and fibroblasts isolated and derived from patient skin (either breast reductions or abdominoplasties) which were seeded onto a de-cellularised dermal scaffold (or onto cadaver skin purchased from the Euro Tissue Bank depending on availability). The keratinocytes and fibroblasts were seeded onto the scaffold in between two metal rings and cultured at an air-liquid interface for 1-2 weeks. At this point, the model was ready to be infected with the centre of the metal rings acting as a model wound site. The epithelium was then deliberately damaged and then infected. The tissue-engineered

skin model used in this study was similar to the model described by Shepherd et al., with the key difference in methodology being the use of one metal ring rather than two.

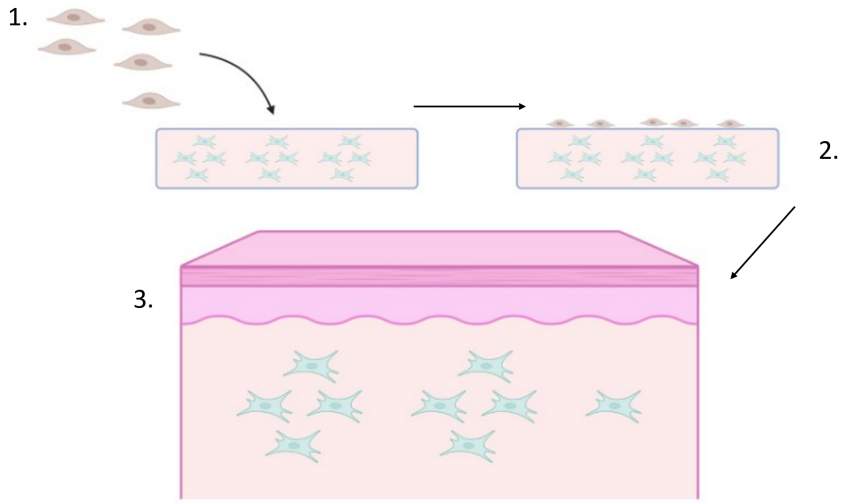


**Figure 1.9 Construction of collagen-based organotypic skin models**

**1.** Fibroblasts are mixed into a collagen suspension and left to set, after which keratinocytes are pipetted onto the surface of the gel. **2.** The keratinocytes adhere onto the gel and proliferate till the cells cover the surface. **3.** The gels are then raised to an air-liquid interface to allow the organotypics to form an epidermis. Figured produced with BioRender.

The second skin model used are the collagen-based organotypics. This model is useful for labs that have an irregular supply of skin for tissue-engineered models. However, it still provides a 3D, multi-layered environment to study skin responses albeit with an architecture less representative of native skin compared to tissue-engineered skin models. Notably, 3D organotypic models lack rete ridges, making the epidermis less firmly attached to the dermis. Briefly, type 1 collagen gel is populated with fibroblasts then allowed to polymerise. The fibroblast-collagen gel then provides a surface for keratinocytes to be seeded onto before the model is incubated at an air-liquid interface for 1-2 weeks to allow the keratinocytes to differentiate and form an epidermis (Figure 1.9).

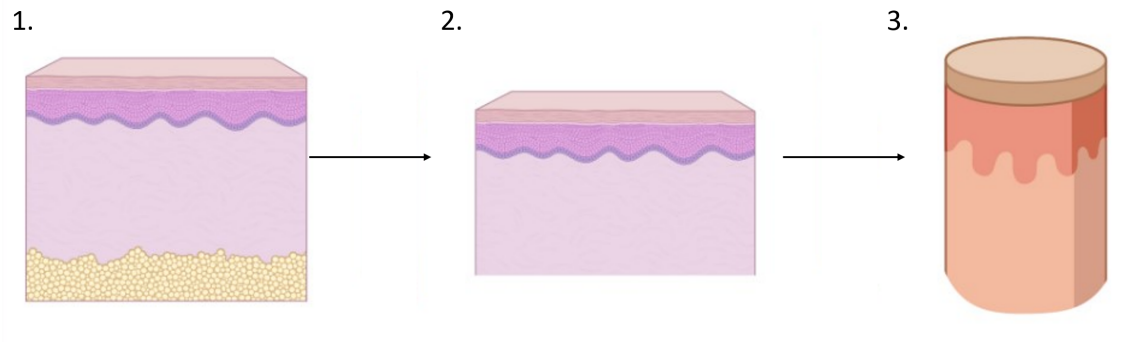


**Figure 1.10 Preparation of surgical explants**

**1.** Surgical explants are received from hospitals and **2.** The hypodermis layer is immediately removed from the dermis. **3.** Biopsy punches are then used to take skin samples of consistent size. Figured produced with BioRender.

The third skin model used in this study are surgical explants. The explant model is considered the 'gold standard' for skin research as it is the most representative model of skin available with the correct architecture and resident immune cells present. Explants are also the easiest to prepare for experiments, needing just the removal of the fat layer and punch biopsies, ensuring the sizes are consistent (Figure 1.10). However, surgical skin is the most susceptible to donor variability and the most difficult of the three models described to acquire reliably, as ideally a collaboration is secured with a surgeon that performs abdominoplasties or breast reduction surgeries on a regular basis. In addition, experiments involving skin explants should be performed as quickly as possible to prevent the resident immune cells dying or migrating out of the explant.

Human skin models can give more representative cellular responses as these models are derived from primary human cells as compared to animals. However, a problem with this model is that it may be difficult to obtain the sufficient skin to establish such models. This may be rectified if a skin model is based on immortalised cell lines, which, in theory, solves the problem of needing a regular skin supply, particularly as primary keratinocytes can only be passaged for a few times before they begin terminally and irreversibly differentiating (Barrandon et al., 2012). However, there are very few skin models based on immortalised cell lines. This is because cell lines do not necessarily

react in the same way a primary cell might, often displaying a subset of the behaviour of the primary cells.

However, human skin models still need to be optimised. Whilst some methodologies can accurately replicate the architecture of human skin, these remain low throughput models lacking a functional immune system or vasculature. Also, culturing the primary cells in preparation for putting a model together requires a significant amount of time.

### 1.5.2 Current immunocompetent skin models

There are currently two methods for creating immunocompetent skin models. Firstly, the immune cells can be integrated into a collagen matrix and simply placed underneath a skin model (Chau et al., 2013; Kühbacher, Henkel, et al., 2017; van den Bogaard et al., 2014). This is performed with T cells that can migrate upwards through the dermis as it is more permeable than the epidermis. Research by van den Bogaard et al. shows that T cells need to be activated before adding to the skin model otherwise T cells do not migrate (van den Bogaard et al., 2014). Secondly, precursor immune cells can be co-seeded together with keratinocytes. This is performed with MUTZ-3 cells, a human cell model for cytokine-inducible DCs, because keratinocytes secrete Tumour Growth Factor-β (TGF-β) and other growth factors that allow the precursors to differentiate into Langerhans-like cells (Bock et al., 2018; Kosten et al., 2015; Laubach et al., 2011).

Whilst there are some models (Table 1.1) that include immune cells, these models currently only include one type of immune cells which is inaccurate given that these immune cells communicate with each other in order to mount a full immune response. The introduction of immune cells remains a major challenge to establishing an immunocompetent skin model (Pupovac et al., 2018).

Currently, researchers have integrated DCs or T cells into human skin models with varying levels of success, with very few attempts to grow skin models using immortalised cell lines which would be an important step forward as this would eliminate the need for skin samples. However, immortalised cells can function

differently compared to the native cells. Jurkat cells, immortalised T cells, display similar T cell receptor signalling events to primary T cells. However, Jurkat cells release significantly fewer cytokines and chemokines upon T cell receptor activation (Bartelt et al., 2009). MUTZ-3-derived Langerhans cells, on the other hand, were able to display phenotypic plasticity that was comparable to primary Langerhans cells making them acceptable substitutes for allergen or irritation assays (Kosten et al., 2015).

Little research has been performed into combining the techniques used for developing more immunocompetent models. For example, it would be interesting to build upon the methodology from Kühbacher et al. for constructing immunocompetent skin models (Kühbacher et al., 2017), as the architecture of the skin model appears to be very similar to real skin, combining this with the MUTZ-3 co-seeding methodology of Bock et al. (Bock et al., 2018) (as the authors' methodology involves our cells of interest). This would be to see if it is possible to engineer a human skin model integrated with other immune cells such as Langerhans-like cells, T cells, neutrophils and mast cells grown entirely from immortalised cell lines. It would be valuable to test these skin models by infecting them with *S. aureus* and treating them with peptides derived from the EC2 domain of tetraspanin CD9. From this we would hope to observe the effects the peptides have on the bacteria's ability to infect the skin models, as well as the effect the peptides have on the integrated immune cell's ability to phagocytose and clear infection.

| Paper | Immune cells added | How the immune cells were added | Skin model origins |
|---|---|---|---|
| **Crosstalk between keratinocytes and T cells in a 3D microenvironment: a model to study inflammatory skin diseases.**<br><br>(van den Bogaard et al., 2014) | CD4+ T cells | T cells added under the insert containing the skin model | Mouse fibroblast cell line 3T3 bought<br><br>Human primary keratinocytes isolated abdominal skin from donors<br><br>CD4+ T cells were purified from blood donations |
| **Development of skin inflammation test model by co-culture of reconstituted 3D skin and RAW264.7 cells.**<br><br>(Chung et al., 2014) | RAW264.7 cells<br><br>(murine macrophage cell line) | Macrophages added under the skin model | Keratinocytes and fibroblasts isolated from human skin donations<br><br>RAW264.7 cells bought |
| **Central Role for Dermal Fibroblasts in Skin Model Protection against Candida albicans.**<br><br>(Kühbacher, Henkel, et al., 2017) | CD4+ T cells | CD4+ T cells were embedded in collagen and placed under the tissue model | Immortalised human fibroblasts (S1F) cell line bought<br><br>Immortalized human keratinocytes (Ker-CT) cell line bought<br><br>Naïve CD4+ T cells isolated from blood |
| **MUTZ-3 derived Langerhans cells in human skin equivalents show differential migration and phenotypic plasticity** | Langerhans-like cells derived from MUTZ-3 cells (human acute myeloid leukemia cell line) | Co-seeding the Langerhan cells with keratinocytes | Fibroblasts and keratinocytes isolated from human skin from patients undergoing breast or abdominal plastic surgery |

| | | | |
|---|---|---|---|
| **after allergen or irritant exposure.**<br><br>(Kosten et al., 2015) | | | MUTZ-3 cells bought |
| **Characterization of reconstructed human skin containing Langerhans cells to monitor molecular events in skin sensitization.**<br><br>(Bock et al., 2018) | Langerhans-like cells derived from MUTZ-3 cell line or from human monocytes | Coseeding the Langerhan cells with keratinocytes | MUTZ-3 cells bought<br><br>keratinocytes and fibroblasts isolated from skin donations<br><br>Human monocytes purified from blood donations |
| **Integration of Langerhans-like cells into a human skin equivalent.**<br><br>(Laubach et al., 2011) | Langerhans-like cells derived from MUTZ-3 cells (human acute myeloid leukemia cell line) | MUTZ-3 cells were differentiated into Langerhans cells then co-seeded with keratinocytes | MUTZ-3 cells bought<br><br>Human primary fibroblasts and keratinocytes isolated from foreskin |
| ***In vitro* micro-physiological immune-competent model of the human skin**.<br><br>(Ramadan & Ting, 2016) | Dendritic cells derived from human leukemic monocyte lymphoma cell line, U937 | Dendritic cells positioned beneath the keratinocyte layer, and the two cell cultures are separated by a porous membrane to allow interactions | Immortalised human keratinocytes (HaCaT) cell line bought,<br><br>U937 cells purchased |
| **The development of a 3D immunocompetent model of human skin**<br><br>(Chau et al., 2013) | Dendritic cells derived from monocytes | Monocytes were differentiated on dendritic cells then incorporated into a gel | Keratinocytes and fibroblasts isolated from human skin donations,<br><br>dendritic cells derived from monocytes from blood donors |

| | | | |
|---|---|---|---|
| **Immune Cell-Supplemented Human Skin Model for Studying Fungal Infections (protocol)**<br><br>(Kühbacher, Sohn, et al., 2017) | Jurkat human T cells | Jurkats in collagen placed under skin model | Immortalised human fibroblasts (S1F cell line)<br><br>Immortalised human keratinocytes (Ker-CT cell line)<br><br>Jurkat human T cell line |

**Table 1.1 List of papers that have integrated immune cells into human skin models.**

### 1.5.3 Animal models for skin research

There is no universal animal model for human skin. Animals are commonly used in skin research for both clinical and commercial drugs. They are used to study drug absorption, wound healing, inflammation, and the like. These kinds of experiments require structural or immunological models that may vary in relevancy depending on the context. Humans are outbred versus lab animals such as mice, which are inbred. Humans have unique genes, upbringing, diets, and environments (Avci et al., 2013; Perlman, 2016). This imposes challenges on appropriate models due to donor variability. Anatomically and immunologically, porcine skin is the closest model to human skin for pre-clinical testing, porcine skin also heals similarly to humans (Summerfield et al., 2015). Whilst pigs are accessible, it is difficult to acquire due to ethical restraints as well as expensive. However, it may be possible to overcome this by using porcine explants if human explants are unavailable.

Mice are usable as models for skin diseases and can be genetically engineered to replicate human skin conditions. For example, Flaky tail mice are mouse models for atopic dermatitis by preventing the mice from expressing functional filaggrin in the epidermis. This results in the mice displaying eczema-like skin lesions that mimic human atopic dermatitis (Jin et al., 2009). Another example of the use of murine

models is the study of skin cancer. Squamous cell carcinomas (SCC) are studied in K14-ER:Ras transgenic mice, which present with epidermal hyperplasia which is associated with impaired differentiation that resembles SCC *in situ* (Ratushny et al., 2012).

To overcome some of the differences between the humans and mice, researchers have also used skin xenografts in an attempt to humanise mice models and better recapitulate human skin physiology (Salgado et al., 2017). Whole human skin xenografts are valuable for studying human skin biology as it maintains the structure of human skin and also contains the immune cells resident in the graft prior to excision. These xenografts can be maintained intact for extended periods of time and do not explicitly damage the architecture of the human skin (Manning et al., 1973). A human biopsy can be secured with sutures around the incision site of the mouse and 4-6 weeks later, the xenograft will have healed and closely resemble normal human skin histologically and still maintain human vasculature with minimal ingrowth of the murine vascular system into the graft bed (Rygaard, 1974; Salgado et al., 2017). Xenografts as described above have been used to study inflammation, melanomas, psoriasis, and other relevant studies concerning human skin immunology. It is a relatively simple technique, but it is restricted by the ethics regarding human sample collection and animal experimentation. Furthermore, the use of human surgical samples is subject to donor variability regarding donor genetics, body site, age, gender etc. Whole human skin xenografts have been used since the 1970s and are still used. Technology has evolved to the extent that sutures are no longer required, and the xenograft can be secured in place with an application of surgical glue (Schulz et al., 2019).

### 1.5.4 Mouse versus human skin

Laboratory mice are by far the most used animal models. Whilst animals such as pigs are considered to be more physiologically similar to humans, mice are typically used because they are easy to house and maintain, economically viable for maintenance and acquisition, and many mouse-specific reagents are available e.g., antibodies (Wong et al., 2011). However, there are multiple differences between mouse skin versus human skin that need to be considered prior to experimentation and how these

differences can affect the interpretation of results. Whilst mice also have skin consisting of three defined layers (the epidermis, dermis, and hypodermis) like humans, each layer has significant differences compared to their human counterparts. Mice have fur which is denser than humans and the murine hair cycle is approximately 3 weeks whereas human hair can last several years, and coverage is variable dependent on the region of the body the hair is found (Wong et al., 2011). There are also differences in the architecture of the skin. Murine skin lacks the sweat glands and rete ridges found in human skin. Mouse skin is also thinner and looser than human skin which is relatively stiffer and adherent to the underlying tissue, this important to consider when researching mechanical factors relating to wound repair. Finally, mice also have an additional subcutaneous muscle layer known as the 'panniculus carnosus' which is found throughout the mice, but only found in the neck region of humans (Sundberg et al., 2012).

Immunologically, there are also differences between mice and humans. In the blood, 50-70% of cells are neutrophils whereas in mice it is 10-25%. Additionally, leukocyte defensins are absent in mice whilst they are present in humans. Laboratory mice are typically raised in sterile environments which are specific-pathogen-free (SPF) (Beura et al., 2016). As such, SPF mice may have immature immune systems compared to wild rodents infected by specific pathogens. This raises the issue that the immune system of SPF mice may be less representative of adult humans (Tao and Reese, 2017).

Despite the differences, mouse models have contributed to our understanding of human skin biology (Mestas and Hughes, 2004). As previously mentioned, the dominant T cell type in mice is γδ whereas in humans it is αβ. The γδ T cells are a subset of T cells capable of recognising antigens without the MHC. γδ T cells are capable of directly attacking pathogens with cytotoxic activity and can activate other immune cells (Bonneville et al., 2010). γδ T cells are typically found in certain anatomical locations e.g., gut and skin (Ribot et al., 2021) where they provide a first line of defence with innate-like responses. These γδ T cells also play an important role in skin immunology, Cho et al. inoculated mice with *S. aureus*, mice lacking γδ T cells developed larger skin lesions with higher bacterial counts compared to wild type mice and mice lacking αβ T cells (Cho et al., 2010). This difference in T cell types may need

to be considered for studies as this difference in T cell populations in mice may lead to a different response to infection or to a drug than in humans.

Mice are not a natural host for human clinical *S. aureus* isolates and the isolate may require genetic adaptation for it to infect mice (Kim et al., 2014). However, mice are still favoured models due to small body size, short gestation, large litter size and less expensive. As reviewed by Kim et al., mice are used to study *S. aureus* regarding issues of clinical interest such as sepsis or skin infection. It has been observed that *S. aureus* can induce a wide spectrum of diseases in mice, like humans. Mice have been used to study contributions of specific skin cells or structures through immune cell deletion with monoclonal antibodies (Kim et al., 2014). C57BL/6 is a good model for mice because it is immunocompetent and would not quickly succumb to infection (Kim et al, 2014., Nippe et al., 2011). However, it is important to note the mouse model used as they may have their own strain-specific responses to infection. For example, C57BL/6 mice generate a $T_H1$ response to infection, whereas BALB/c mice generate a $T_H2$ response (Nippe et al., 2011).

## 1.6 Conclusion

In summary, whilst the skin is well armed as the first barrier between body and pathogens, pathogens have evolved to exploit host cells and become resistant to antibiotics. In researching the interactions between host and pathogens, The Monk lab have identified potential avenues of research in order to inhibit the pathogen's ability to infect host cells whilst minimising any detrimental effects to the host. For better understanding of these interactions, more research should be done using human skin models so that they can give some indication of an immune response to a bacterial challenge such as analysis of the cytokine responses to treatment or infection. In addition, ideally a higher throughput methodology would be an improvement if a useful skin model could be engineered from immortalised cell lines to reduce the dependency on donor skin, as well as eliminating donor variability and improving consistency.

## Aims, objectives and hypothesis.

Based on previous literature, anti-adhesion therapy has been demonstrated to successfully reduce bacterial adhesion to skin, which could consequently reduce the burden of infection. However, our lab has demonstrated this on reconstructed skin models without testing in the presence of immune cells that could be negatively affected by anti-adhesion peptide therapy. Thus, the hypothesis of this thesis is that peptide treatment would be effective in reducing bacterial adhesion to wounded skin without negatively affecting the immune response.

The aims of this thesis are firstly to develop and test different skin models of varying complexity to determine the most suitable model to serve as a platform for bacterial infection; secondly, to test the tetraspanin-derived peptides against bacterial adhesion; thirdly, to test the peptides on immune cells to determine if treatment alters the immune cells' response to bacterial infection, focusing on phagocytosis; fourthly we will combine these test the peptides in an *in vivo* mouse model of infection, to combine a skin infection model with a fully functional immune system.

# Chapter 2 Materials and Methods

## 2.1 Buffers, reagents, solutions, and antibiotics

### 2.1.1 Solutions

**Phosphate Buffered Saline (PBS)**

PBS was made using 5 PBS tablets (Thermofisher) in 1 L of distilled water and was autoclaved at 121$^{o}$C for 15 mins.

**Fluorescence-assisted cell sorting (FACS) buffer**

FACS buffer was composed of 4% foetal bovine serum (FBS), 2 mM EDTA and 0.05% Sodium Azide in 1x PBS

**4′,6-diamidino-2-phenylindole (DAPI) Solution**

10 mg of DAPI stock (Sigma) was dissolved in 2 mL of dH20 for a final concentration of 5 mg/mL and stored at 4°C.

**Lysogeny Broth (LB)**

10 g of LB powder (Sigma-Aldrich) was dissolved in 500 mL of distilled water, autoclaved at 120°C and stored at room temperature.

**LB Agar**

10 g of LB powder was combined with 7.5 g of Agar powder (Sigma-Aldrich) and then dissolved in 500 mL of distilled water and then autoclaved at 120°C. Once cooled, 10 µg/mL chloramphenicol was added. LB agar was used in 10 cm petri dishes.

### 2.1.2 Reagents

**Trypsin-versene**

50 mL of trypsin-versene (Lonza) was added to 450 mL of HBSS and stored at 4$^{o}$C.

**Bovine Serum Albumin (BSA)**

BSA (Sigma-Aldrich) and is fatty acid-free. 1 g was diluted in 20 mL of PBS to make 5% BSA.

**Liberase**

5 mg of Liberase (Sigma-Aldrich) was reconstituted in 400 µL sterile molecular grade water then added to 19.6 mL of Dulbecco's Modified Eagle Medium (DMEM), making a final concentration of 250 mg/mL. Aliquots were stored at -20$^{o}$C.

**Dispase**

0.6 g of Dispase powder (Sigma-Aldrich) was reconstituted in 10 mL of PBS, for a final concentration of 60 mg/mL. Aliquots were stored at -20$^{o}$C.

**Collagenase IV**

200 mg of Collagenase powder (Sigma-Aldrich) was reconstituted in 100 mL of RPMI, for a final concentration of 2 mg/mL. Aliquots were stored at -20$^{o}$C.

**DNAse**

50 mg of DNAse powder (Roche) was reconstituted in 5 mL of glycerol and 5 mL of NaCl solution, for a final concentration of 5 mg/mL. Aliquots were stored at -20$^{o}$C.

### 2.1.3 Antibiotics

**Chloramphenicol**

Chloramphenicol (Sigma-Aldrich) was dissolved in 100% ethanol to a final concentration of 50 mg/ml, then aliquoted and stored at -20$^{o}$C.

**Penicillin-Streptomycin**

Penicillin-Streptomycin (Sigma-Aldrich) was diluted in house as 10 mg/mL stock solutions, aliquoted and stored at -20$^{o}$C.

**Gentamicin**

Gentamicin (Sigma-Aldrich) was used to tissue culture media (DMEM, Green’s media or RPMI depending on the experiment) at a concentration of 20 µL/mL.

## 2.2 Peptides

Peptides derived from the EC2 region (Figure 2.1) of CD9 were generated by GenScript. Scrambled peptides were randomly produced from the CD9 sequence to act as controls. The stapled peptides were generated by the addition of a covalent link between two amino acid side chains of the 800-Cap peptide, forming the staple.

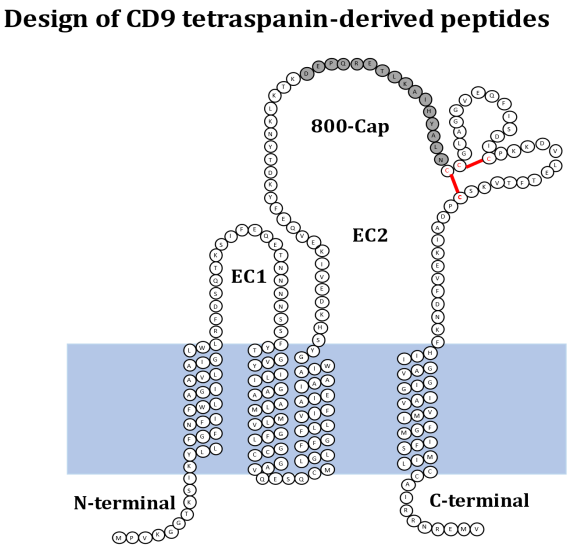


**Figure 2.1 Structure of 800-Cap**

Locations of the EC2 domain of tetraspanin CD9. 800-Cap corresponds to part of the EC2 sub loop created by disulphide bridge formation and is capped with Asp. Red lines represent the disulphide bridges. Patent reference EP4114850A1 (Monk et al., 2021).

| **Peptide** | **Sequence** |
|---|---|
| 800-Cap | DEPQRETLKAIHYALN |
| 800-Cap Scrambled Control | QEALKYNRAETPLDIH |
| 800-Cap Stapled 1 (800i) | DE{i}QRE{ii}LKAIHYALN * |
| 800-Cap Stapled 2 (800ii) | DEPQRETLK{i}IHY{ii}ALN * |
| Mouse 800-Cap | DEPQRETKLAIHMALD |
| Mouse 800-Cap Scrambled Control | QEALKMNRAETPLDIH |
| * {i} and {ii} show the position of staple residues | |

**Table 2.1 List of peptide sequences**

## 2.3 Media and supplements

### 2.3.1 Media

Green's media was made as described by Rheinwald and Green, (Rheinwald & Green, 1975). 108 mL Nutrient Mixture Ham's F-12 containing L-glutamine (Sigma), 330 mL DMEM (Sigma), 5 mL L-glutamine, 5 mL Penicillin-Streptomycin, 1.25 mL Amphotericin B, 50 mL Foetal Bovine Serum (FBS), 2 mL Adenine (46 mM), 2.5 mL Insulin (recombinant human; 1 mg/mL), 0.5 mL T/T (consisting of 1.36 µg/mL 3,3,5, triiodo-L-thyronine 1.36 ng/mL and 5 mg/mL apo-Transferrin), 0.08 mL Hydrocortisone (25 mg/mL), 0.025 mL Epidermal Growth Factor (EGF; recombinant human; 200 µg/mL), 0.5 mL Cholera toxin (from Vibrio cholerae; 847 µg/mL)

### 2.3.2 Supplements

**Foetal Bovine Serum (FBS)**

FBS (Biosera) was heat-inactivated by incubation at 56$^{o}$C for 20 minutes before being aliquoted into 50 mL falcon tubes, frozen and stored at -20°C.

**L-Glutamine**

L-Glutamine (Thermofisher) was aliquoted and stored at -20$^{o}$C.

## 2.4 Cell culture

**THP-1 and U937**

THP-1 (ATCC) and U937 (ATCC) cell lines were cultured in Roswell Park Memorial Institute media (RPMI) (Lonza) supplemented with 10% FBS, 1% L-Glutamine and 1% Penicillin-Streptomycin and incubated at 37$^{o}$C and 5% $CO_2$.

Both THP-1 and U937 cells are immortalised cell lines used as models for human monocytes. Both cell lines were grown in suspension in T-75 flasks and split after roughly 72 hours. Both cell lines are seeded at 2x10$^{5}$/mL. Whilst U937s can be passaged well into their 20s, THP-1s should not exceed passage 20.

**5637 cells**

5637 (DSMZ) cells were cultured in Roswell Park Memorial Institute media (RPMI; Lonza) supplemented with 10% FBS, 1% L-Glutamine and 1% Penicillin-Streptomycin and incubated at 37°C and 5% $CO_2$.

Culturing 5637 cells conditions the media which is necessary for the growth of MUTZ-3 cells. 5637 cells were bought from DSMZ, and 2-3 million cells were seeded into T-175. After incubating the cells in 5% $CO^2$ at 37°C for 72 hours, the media was replaced and reincubated for a further 72 hours. At this point the media was then collected and spun at 200 g for 5 mins then sterile filtered and stored at -20°C for later use.

**HaCaT**

HaCaT cells (Cell Line Services GmbH) were cultured in DMEM (Thermofisher) supplemented with 10% FBS.

HaCaT cells are an immortalised cell line of human keratinocytes that can be cultured without a feeder layer. The cells are cultured in a T-75 flask. To passage the cells, the cells need to be washed twice with PBS before 5 mL of trypsin-versene is added then incubated in 5% $CO_2$ at 37°C for at least 12 minutes. The cells were then spun at 400 g for 5 minutes and then resuspended for a cell count and seeding at $4x10^5$ per flask.

**MUTZ-3**

MUTZ-3 cells (DSMZ) were cultured in 60% Alpha Minimum Essential Medium (α-MEM) (Gibco) containing 20% FBS and 20% 5637-conditioned media. MUTZ-3 cells were cultured in a 24-well plate at a concentration of $0.5\text{-}1x10^6$/ml. MUTZ-3 cells were incubated 5% $CO_2$ at 37°C for approximately 72 hours before media was exchanged by carefully removing 0.5 mL of media without disturbing the cell suspension and cells were passaged every 6 days by centrifuging at 200 g for 5 minutes then resuspending the pellet in fresh media and then the cells were split at a ratio of 1:2.

### 2.4.1 Differentiation of MUTZ-3

The methodology used to differentiate MUTZ-3 cells was described by Kosten et al., 2015; Masterson et al., 2002. MUTZ-3 cells were differentiated into Langerhans-like cells by culturing at $2x10^5$ cells/mL in α-MEM containing 20% FBS, 1% Penicillin-

Streptomycin, 2 mM L-glutamine, 50 μM 2-β mercaptoethanol, 100 ng/mL recombinant human GM-CSF, 10 ng/mL TGF-β and 2.5 ng/mL TNF-α over a period of 7 days. All cytokines were sourced from Miltenyi Biotec. The extent of differentiation was determined by flow cytometry. Cells were harvested and washed, before being stained for CCR6, CD1a and Langerin (antibodies in Table 2.5). Stained cells were analysed with a LSR II (Becton-Dickinson)

## 2.5 Bacterial strain and infections

### 2.5.1 SH1000 strain

The SH1000 strain of *Staphylococcus aureus* contains a plasmid that confers resistance to chloramphenicol and also expresses GFP. The culturing of SH1000 prior to infecting the cells was done with 10 μg/mL chloramphenicol. *S. aureus* was grown in LB Agar and kept at 4$^{o}$C. For use in infection assays, an overnight culture was prepared by using a loop to add 1 colony to 5 mL of LB with 1 μL of chloramphenicol and incubated on a shaker at 5% $CO_2$ at 37$^{o}$C overnight.

### 2.5.2 Infections

For the infection of THP-1s, U937s and neutrophils, the overnight culture was spun at 9000 g for 5 mins and washed with PBS twice. The bacteria were then pelleted and resuspended in RPMI and the $OD_{600}$ was measured using a spectrophotometer. The suspension was then diluted with RPMI until an $OD_{600}$ of 1.0 was found to achieve a colony forming unit (CFU)/mL of ~3 x $10^8$. The multiplicity of infection (MOI) was prepared from this suspension.

For the infection of HaCaT cells, the overnight culture was resuspended in LB and diluted for a $OD_{600}$ of 1.0. The suspension was then aliquoted into 1 mL Eppendorf tubes, spun at 9000 g for 5 mins and washed with PBS twice before being resuspended in DMEM.

## 2.6 Tissue-engineered skin

### 2.6.1 Ethics approval

All work, such as isolation and culturing, using human keratinocytes and fibroblasts used samples that came from abdominoplasty and breast reduction, obtained with prior patient consent under approval by the local ethics committee Sheffield NHS Trust, Sheffield, UK. Tissues and cells were stored under NHS ethics number 15/YH/0177.

Use of human skin explants in Singapore were approved under DSRB 2018/00945 and DSRB 2017/0024 after permission from the Institutional Review Board (IRB).

### 2.6.2 Isolation of keratinocytes

A scalpel sterilised with 70% industrial methylated spirit was used to cut skin pieces into roughly 0.5 $cm^2$ pieces. These were then transferred into 10 mL of 0.1% Difco-Trypsin (Difco, Belgium) and incubated at 4°C overnight. The skin pieces were then added to Green's media and the epidermis was then peeled off with sterilised forceps and the underside of the epidermis and papillary of the dermis gently scraped with a sterile scalpel to remove the keratinocytes in the basal layer. The media containing the keratinocytes was then centrifuged for 5 minutes at 200 g and then resuspended in 4 mL of Green's media. 1 mL of cell suspension was added to a T-75 tissue culture flask containing a feeder layer of i3T3 fibroblasts (communal stocks cultured in-house), all in 15 mL of Green's media at 37°C and 5% $CO_2$. These cells were used between passage 0 to 2.

### 2.6.3 Isolation of fibroblasts

The dermis was minced with a sterile scalpel and then transferred into a petri dish containing 10 mL of 0.5% Collagenase A (Sigma-Aldrich, UK), and incubated at 37°C and 5% $CO_2$ overnight. A cell strainer filtered the larger pieces of dermis that hadn't been broken down by the Collagenase A and the suspension was centrifuged for 10 minutes at 1500 RPM. The cell pellet was then re-suspended in 10 mL of 10%

DMEM medium and cultured in a T-25 tissue culture flask at 37°C in 5% $CO_2$ until the cells became confluent and the cells were transferred to a T-75 with DMEM supplemented with 10% FBS, 1% Penicillin-Streptomycin, 1% L-Glutamine and 0.25% Amphotericin B (250 µg/mL, Thermofisher). These cells were used for experiments between passage 4 and 9.

### 2.6.4 Isolation of de-epidermised dermis (DED)

Explant skin was collected after surgery. Explant skin was then processed in a designated tissue-culture safety cabinet where it was harvested with a Cobbett dermatome (Swann-Morton, UK) to evenly cut the skin to a thickness of approximately 500 µm, resulting in split-thickness skin, which is skin composed of the epidermis and a portion of the dermis. Harvested skin were then placed at 4°C overnight in PBS with 1% Penicillin-Streptomycin and 0.25% fungizone to ensure samples were sterile and microbe-free. DED was obtained by incubating the harvested skin for 24 hours in an excess of PBS before incubating again in 1M NaCl solution. Forceps were used to remove the epidermis. Dermis was stored at 4°C in Green's media.

Alternatively, Euroskin could be used as a source of DED. The MacNeil group has previously published that successful tissue engineered skin can be generated using Euroskin (Deshpande et al., 2013). Plain (unmeshed), glycerol preserved Euroskin was purchased from the Eurobank which preserves human skin for clinical use. Euroskin is donated skin used for the treatment of burns and chronic wounds. Donor skin acts as a 'biological dressing' that temporarily covers wounds until they have healed. Donor skin protects against dehydration and infection and helps relieve pain. Glycerol preservation kills living cells and bacteria, whilst leaving the structure intact, enabling suitability as a DED. Euroskin was washed three times in PBS and incubated at 37°C in 5% $CO_2$ for 72 hours. After incubation, the epidermis was then removed with forceps and the dermis was stored in Green's media at 4°C.

### 2.6.5 Construction and culturing of tissue-engineered skin models

Pieces of DED (1.5 $cm^2$) were sectioned with a sterile scalpel and then placed into a 6-well plate, and a 10mm diameter stainless steel ring with a chamfered edge was pressed on top to create an airtight seal. Keratinocytes (between passages 1 and 3) were pipetted into the centre of the ring at a density of $3x10^5$ cells per composite, and fibroblasts (passages 4 and 9) were seeded at a density of $1x10^5$ cells (Figure 2.2). Green's media was added to the wells outside of the ring and the composites are cultured overnight at 37°C in 5% $CO_2$. The next day, the media inside the ring and the ring itself were removed. The next day, the composites were raised onto stainless girds, so that the underside of the composites was in contact with the media and the top layer exposed to air (air-liquid interface (ALI)). Composites were cultured for 2 weeks at ALI before experimenting. For work requiring the skin to be infected, Green's media was replaced with an antibiotic-free version at least 3 days before infection.

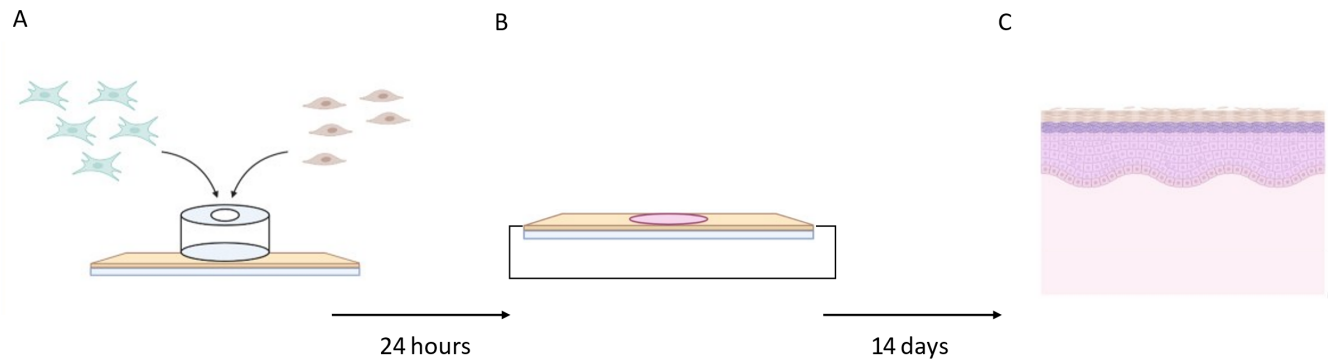


**Figure 2.2 Construction of tissue-engineered skin**

**A)** A steel ring was placed on top of a piece of DED and fibroblasts and keratinocytes were co-seeded inside the ring. **B)** After 24 hours the cells had adhered to the dermis and the ring was removed. The dermis was then raised to an ALI. **C)** After 14 days of culture, the dermis had formed a fully differentiated epidermis. Figured produced with BioRender.

### 2.6.6 Construction and culturing of collagen-based organotypics

Collagen-based organotypic models follow the protocol as performed by Arnette et al., 2016 (Figure 2.3). This methodology used $7.5x10^5$ fibroblasts and $1x10^6$ keratinocytes per model. Briefly, fibroblasts were resuspended in 2 mL of 10X reconstitution buffer (1.1 g NaHCO3, 2.3 g HEPES re-suspended in 50 mL of 0.05 N NaOH and sterile filtered). 2 mL of 10X DMEM was added along with high concentration Type 1 rat tail collagen (~8-10 mg/mL) was added to the fibroblasts until the collagen is at a final concentration of 4 mg/mL. Sterile water is then added for a final volume resulting in the batch being 2 mL of fibroblast-collagen suspension per model. 1 M NaOH is added drop by drop to the suspension until the pH is roughly neutral (suspension would be light pink/red in colour). 2 mL of the neutralised fibroblast-collagen suspension into transwell inserts (Corning), inserts were then added to a 6-well deep plate (Corning) and incubated at 37$^o$C for 30 minutes until the collagen polymerised.

Once the collagen had set, 2 mL of DMEM (with 10% FBS and 1% Penicillin-Streptomycin) was added on top of the model inside the transwell and 13 mL of DMEM (with 10% FBS and 1% Penicillin-Streptomycin) was added to the deep well outside the insert. Models were incubated for 24 hours before keratinocytes were added to the surface.

After 24 hours, keratinocytes were trypsinised and resuspended in Green's media with 10 mM Y-27632 (ToCris) at a concentration of $0.5x10^6$/mL. DMEM was removed from the transwell insert and the deep plate, 2 mL of the resuspended keratinocytes ($1x10^6$ keratinocytes in total) was added on top of the collagen model inside the transwell insert, 13 mL of Green's media was added to the deep well around the insert, models were then incubated for a further 24 hours. After 24 hours, the Green's media in the transwell insert was removed to raise the model to air-liquid interface, the Green's media outside the insert was removed and replaced with Green's media without Y-27632 or EGF. Models were cultured for 14 days with the media being replaced every 48 hours.

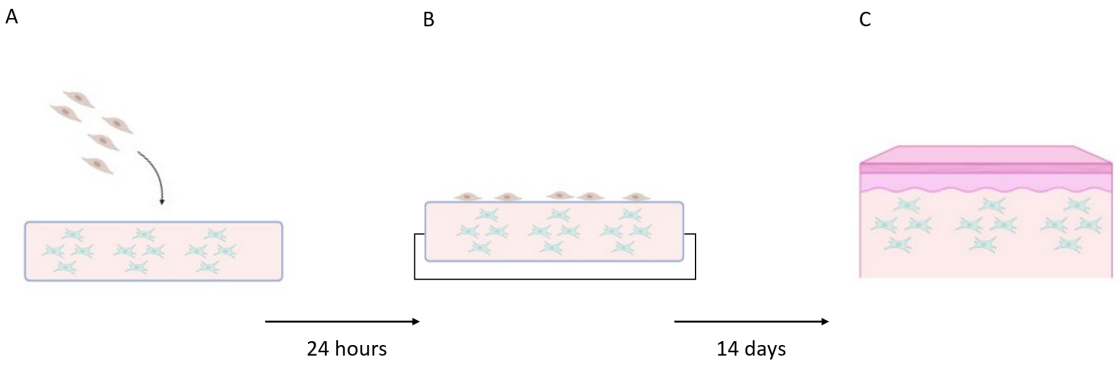


**Figure 2.3 Construction of collagen-based organotypics**

**A)** Fibroblasts were embedded in a collagen matrix then allowed to set, once the gel was set keratinocytes were seeded on top. **B)** The next day the model was raised to an ALI to allow the keratinocytes to differentiate. **C)** After 14 days in culture, the keratinocytes had formed a fully differentiated epidermis. Figure produced with BioRender.

## 2.7 Histology

For histological analysis, tissue samples were fixed in formalin overnight and then embedded in Optimal Cutting Temperature (OCT) embedding medium (Thermofisher, UK) and snap frozen with liquid nitrogen. The samples were then sectioned into 10 µm sections using a Leica Cryostat.

### 2.7.1 Haematoxylin and Eosin (H&E) stain

- 1 min in distilled water
- 90 seconds in haematoxylin to stain the nuclei
- Washed with running water for 5 minutes
- 5 minutes in eosin to stain the cytoplasm
- 2 dips in tap water
- 1 dip in 70% ethanol.
- 30 seconds in 100% ethanol
- 2 dips in 100% xylene.

A coverslip was then placed on the slides with mounting media and the slides were left to dry for 2-3 hours before imaging.

Some samples were analysed as paraffin-embedded samples instead of OCT-embedded. These samples were:

- 3 mins in 100% Xylene to dewax (repeated 3 times)
- 3 mins in 100% ethanol (repeated 3 times)
- 3 mins in decreasing percentages of ethanol (90% to 80% to 70%)
- 3 mins in water
- 5 mins in haematoxylin to stain the nuclei
- 1 min in running water
- 15 seconds in 1% acid-alcohol to differentiate the nuclear staining
- 1 min in running water
- 2 mins to blue in Scott's water
- 1 min in running water
- 45 seconds in eosin to stain the cytoplasm
- 10 seconds in increasing percentages of ethanol (70 to 80 to 90%)
- 3 mins in 100% ethanol (repeated 3 times)
- 3 mins in 100% xylene (repeated 3 times)

A coverslip was then placed on the slides with mounting media and the slides were left to dry for 2-3 hours before imaging with a light microscope.

### 2.7.2 Immunohistochemistry

- 3 mins in 100% Xylene (repeated 3 times)
- 3 mins in 100% ethanol (repeated 3 times)
- 3 mins in decreasing percentages of ethanol (90% to 80% to 70%)
- 3 mins in water
- Heat expose epitopes with antigen exposing solution (Dako) in a pressure cooker
- Allow to cool then rinse for 5 mins in water, rinse in PBS-Tween (89.95% dH2O,10% 10x PBS, 0.05% Tween (Sigma))
- 30 mins blocking with 10% goat serum (in PBS)

- Pour off serum block and add primary antibody for 60 mins (primary antibody diluted with 10% goat serum)
- 10 mins in running tap water
- 5 mins rinse in PBS-Tween
- Secondary antibody (Horseradish peroxidase (HRP) polymer anti-rabbit Envision system, Dako) added for 30 mins
- 10 mins wash in running tap water
- 5 mins rinse in PBS-Tween
- Drop of Envision 3,3'-Diaminobenzidine (DAB) substrate added to sections (1 drop of chromogen with 1 mL of substrate solution)
- Rinse in water to stop DAB reaction
- 30 seconds counterstain with haematoxylin
- 3 mins to dehydrate with ascending percentages of ethanol (70% to 80% to 90%),
- 3 mins in 100 % ethanol (repeated 3 times)
- 3 mins dehydrating with 100% xylene (repeated 3 times)

A coverslip was then placed on the slides with mounting media and the slides were left to dry for 2-3 hours before imaging. For immunohistochemistry, antigen retrieval was performed using a buffer and a 2100 Antigen Retriever (Aptum Biologics, UK) heated to 90$^{o}$C for 10 mins.

For CD68 staining, sections were heat exposed with pH 6.0 sodium citrate buffer (Sigma-Aldrich), Envision DAB substrate was left on the sections to develop for 2 mins.

For Ly6G staining, sections were heat exposed with pH 8.5 EDTA buffer (Sigma-Aldrich), Envision DAB substrate was left on the sections to develop for 3 mins.

Two controls were used for immunohistochemistry: IgG control and no primary control. For the no primary antibody control, 10% goat serum was left on rather than replaced with the primary antibody. For the IgG control, a rabbit IgG isotype control was added instead of the primary antibody.

### 2.7.3 Slide Scanning

Immunohistochemistry slides were scanned with a Zeiss AxioImager Z2 and analysed with MetaViewer; automatic counting was done with Fiji.

## 2.8 Neutrophil isolation

Neutrophils were provided by the Prince Lab, University of Sheffield. Primary cells were isolated from blood taken from human volunteers after obtaining written permission; this was done in accordance with an approved protocol by the South Yorkshire Local Research Ethics Committee (REC reference: 05/Q2305/4).

Human neutrophils were isolated from donated blood using Plasma-Percoll density gradient centrifugation. This procedure was performed in a Microflow class II microbiology safety cabinet in order to prevent neutrophil activation or contamination.

4.4 mL of 3.8% (w/v) tri-sodium citrate (Martindale Pharmaceuticals, UK) was slowly added down the side of the tube to 35.4 mL of blood and gently inverted to avoid bubbles. Blood with 3.8% tri-sodium citrate was centrifuged at 200 g for 20 minutes at room temperature. After centrifugation, the upper phase (platelet rich plasma (PRP)) was transferred into a new 50 mL Falcon tube. For platelet poor plasma (PPP), the PRP was centrifuged at 400 g for 20 minutes to remove the platelets. PPP was transferred to a new Falcon tube and the pelleted platelets were discarded.

The remaining lower phase of cells contained a mixture of red and white blood cells. These cells were mixed with 6 mL of 6% (w/v) dextran 500 (Sigma-Aldrich, UK) (3 g of dextran added to 50 mL of saline). The solution was inverted to mix and avoid bubbles. Any bubbles that may have formed were removed but not popped before solution was left for 20-30 mins to allow the red blood cells to sediment. The upper phase that contained white blood cells was transferred to a new 50 mL Falcon tube using sterile Pasteur pipettes and spun at 200 g for 6 minutes. Upon centrifugation, the white blood cells pellet was resuspended in 2 mL of the previously prepared PPP. White blood cells were further separated by cell density via discontinuous Percoll (GE Healthcare, USA) gradient centrifugation in a 15 mL polypropylene Falcon tube.

Two gradient layers of Percoll mixed with PPP solution were prepared in separate tubes. For the upper phase, 0.84 mL of 90% Percoll was mixed with 1.16 mL PPP making a final ratio of 42:58. The lower phase was made with 1.02 mL of Percoll mixed with 0.98 mL PPP to make a final ratio 51:49. The upper phage mixture was carefully laid onto the lower phase mixture in 15 mL Falcon tubes to generate the discontinuous gradient. Following this, the resuspended pellet of white blood cells was transferred carefully onto the upper layer of Percoll, with care to avoid mixing the layers. The gradient was then spun at 200 g for 11 minutes. This step yields three distinct layers of cells; the top peripheral blood mononuclear cell layer (PBMCs) made up of monocytes and lymphocytes, the middle layer containing granulocytes (neutrophils, eosinophils, and basophils) and the bottom layer made up of red blood cells.

The PBMCs layer was removed by pipetting, the granulocyte layer was then carefully removed with a Pasteur pipette and transferred into a new 50 mL tube with 10 mL of PPP and topped up to 40 mL with HBSS without $Ca^{2+}$ and $Mg^{2+}$ (Lonza). The suspension was then centrifuged at 400 g for 6 mins and each granulocyte pellet was resuspended. For neutrophils, the pellet was resuspended in 2 mL of RPMI supplemented with L-glutamine and 10% FBS and 1% Penicillin-Streptomycin at a concentration of $1x10^6$ cells/mL.

## 2.9 Determining Multiplicity Of Infection (MOI)

For experiments involving HaCaT cells, a 96-well, flat-bottomed plate was seeded with 10,000 HaCaT cells per well and incubated at 37°C in 5% $CO_2$ for 18-21 hours. The media was then removed, and the cells were washed once with HBSS before being incubated for 1 hour in 150 µL of 5% BSA. The BSA was washed with 200 µL of HBSS twice before being infected with 50 µL of bacterial suspension with a MOI of 10, 50, 100, 150 and 200 CFU for 1 hour. After 3 washes with 150 µL of PBS, 50 µL of 2% (w/v) saponin (Sigma-Aldrich) which had been dissolved in PBS and sterile filtered was added to each well. The saponin lysed the cells and released the internalised bacteria. The plate was incubated for 20 minutes, 50 µL of PBS was then added to each well and the wells were scraped and pipetted thoroughly before the suspension was serially diluted from neat to $10^{-5}$ and plated onto LB agar plates for CFU counting.

For THP-1s and U937s, both cell lines needed to be differentiated into macrophages. For this, the cells were seeded onto a 24-well plate at a concentration of $4x10^5$ cells in 1 mL of media containing 2 µg/mL of phorbol 12-myristate 13-acetate (PMA) (Sigma-Aldrich) to differentiate the cells. The cells were incubated for 72 hours in 5% $CO_2$ at 37ºC, then the media was changed to PMA-free media for 24 hours before experimentation.

THP-1 derived macrophages were washed once with HBSS before being infected with a 250 µL bacterial suspension at MOI 0.5,1, 5, 10 and 50. The plate was then placed on ice for 30 minutes before being incubated for 2 hours in 5% $CO_2$ at 37ºC. After incubation, the cells were then washed twice in HBSS before being treated for 1 hour with 2 mL of 20 µL/mL of gentamicin (Sigma-Aldrich) to kill any external bacteria that had not been phagocytosed by the macrophages. The cells were washed three times with HBSS and then reincubated for 15 minutes with 1 mL of 2% (w/v) saponin. Each cell was then scraped with a pipette to lyse any remaining macrophages and the suspension was pipetted up and down thoroughly before the lysate was serially diluted from neat to $10^{-5}$ and plated onto LB agar plates.

For all cell types, the LB agar plates were left to dry in the air in a Microflow class II microbiology safety cabinet before being incubated for 18 hours at 37°C with 5% $CO_2$. The average number of bacteria was determined by taking the average of the 3 drops where the suspension was pipetted onto the plate, then calculating an estimated total number of bacteria/mL (CFU/mL):

$$\text{CFU/mL} = \text{average number of colonies X } \frac{1}{0.001\ mL} \text{ X dilution factor}$$

### 2.9.1 Lactate Dehydrogenase (LDH) assay for THP-1s

After the 2-hour incubation described in 2.9.1, the supernatant from each well to a fresh Eppendorf, then centrifuge at 9000 g for 5 mins to pellet any bacteria. 150 µL of the supernatant was then transferred to a fresh Eppendorf to be stored at -80ºC for the Lactate Dehydrogenase (LDH) Assay the next day. An LDH assay was used to

determine cytotoxicity. LDH is a compound found in living cells, with increasing cytotoxicity, the level of LDH release also increases, and this output was measured with a plate reader. The next day, the supernatants and assay reagents had been warmed to room temperature and 50 µl of the supernatants were transferred to a 96-well plate along with 4 wells as a media only control. With the lights of the safety cabinet turned off, 50 µl of assay reagent was added to each well and mixed. The plate was then covered in foil and left for 30 minutes. 50 µl of stop reagent was then added and the plate was analysed with a plate reader at 490 nm.

### 2.9.2 Adhesion assay

Once the MOI was decided, the protocol for the phagocytosis assay is repeated as described in section 2.9.1. However, in addition to the steps described in 2.9.1, the experiments performed in 96-well plates (HaCaT cells and neutrophils) were treated with 100 µL of the 200 nM CD9-derived peptides for 1 hour before the peptides were replaced with a 100 µL bacterial suspension at a MOI of 50 for HaCaTs and a MOI of 5 for neutrophils. The cells were treated with peptide 800-Cap, its scrambled peptide control and 800i as well as media as an infection only control. For experiments performed in 24-well plates (THP-1s and U937s), the cells were treated with 250 µL of the 200 nM CD9-derived peptides for 45 mins before being removed and being infected with 250 µL of bacterial suspension at a MOI of 5.

To determine bacterial adhesion, two plates of cells were used. One plate was treated with gentamicin at a concentration of 20 µL/mL to kill any external bacteria, and one plate was not. This gave the total number of bacteria and the internal number of bacteria. The internal count was removed from the total count to give the external number of bacteria that had adhered to the cells.

For experiments with primary neutrophils, neutrophils were resuspended in RPMI with 10% FBS as a concentration of $2.5x10^6$/mL. 90 µL of this neutrophil suspension (~225,000 neutrophils) was pipetted into a 96-well tissue culture plate and incubated for 20 mins to allow the cells to settle. After 20 mins, the plate was centrifuged at 6000 g for 3 minutes to pellet the neutrophils. The media was removed, and the neutrophils

were resuspended with 100 µL RPMI containing the CD9-derived peptides at a concentration of 200nM. The plate was then reincubated for 45 minutes. After incubation, the plate was centrifuged again to pellet the neutrophils. The media and peptides were removed, and the neutrophils were resuspended in RPMI containing SH1000 at an MOI of 5. The plate was reincubated for 30 minutes. After 30 minutes of co-incubation, the plate was centrifuged, and the media was replaced with 20 mg/mL gentamicin. The plate was incubated for 20 minutes before the plate was once again centrifuged and the pellet resuspended with 2% saponin. The plate was incubated for 15 minutes and then the wells were scraped and pipetted up and down before being serially diluted and plated onto a LB agar plate for CFU counts.

## 2.10 Phagocytosis assay

After determination of the correct MOI, the protocol for the phagocytosis assay is the same as sections 2.9.1 and 2.9.2 without the LDH assay described in 2.9.1 nor the second plate of cells that is not treated with gentamicin as described in 2.9.2. To summarise briefly, the cells were pre-treated with peptides, or the media only control then infected with a bacterial suspension of the appropriate MOI. The bacterial suspension is then removed, and the cells are washed before being treated with gentamicin to kill any extracellular bacteria. The cells are then lysed with saponin, and the lysate is serially diluted and plated onto LB agar and incubated for colony counting.

## 2.11 Integration of neutrophils into skin

### 2.11.1 Scalpel wounds onto split-thickness skin

Split-thickness skin was cut into 2x2 $cm^2$ pieces and was wounded with a scalpel in a '#' pattern to score the epidermis. The neutrophils were resuspended to a concentration of $1x10^6$/mL and pipetted onto a 2x2 $cm^2$ piece of filter paper placed in a 6-well plate. The wounded skin was then placed on top of the blotting paper and 100 µl of *S. aureus* bacterial suspension ($OD_{600}$=1) was pipetted onto the wound. The skin was then incubated overnight in 5% $CO_2$ at 37°C, then processed for imaging with H&E *(see 2.8.1 Haematoxylin and Eosin stain).*

### 2.11.2 Addition of C5a to burn-wounded skin.

DED was cut into 1.5x1.5 $cm^2$ pieces, then wounded by applying a 2.4 mm diameter soldering iron heated to 150$^oC$ to each composite for 2 seconds. A stainless-steel ring with a chamfered edge was placed onto the DED surrounding the wound site and 100 µL of 200 nM C5a (Hycult) was pipetted over the wound site then incubated for 2 hours. The DED was then cut with an 8 mm biopsy punch and then placed on top of 0.5 mL of neutrophils at a concentration of $2x10^6$ in a transwell insert then Green's media was added to raise the DED to an ALI. The DED was incubated for 6 hours before processing for histology.

This was repeated with tissue engineered skin grown from Euroskin, as it was hypothesised that the reduced thickness of the model would aid the migration of neutrophils across the dermis.

## 2.12 Infection assay of tissue-engineered skin

### 2.12.1 Infection assay on explant skin

Explant skin was collected from the surgeon within 1 hour of surgery. Explant skin was then processed in a designated tissue-culture biosafety cabinet where it was defatted with surgical scissors. A 10 mm biopsy punch (Fisher-Scientific) was then used to take biopsy samples for experimentation.

The biopsy punched samples were then wounded with a soldering iron at 150 $^oC$ for 2 seconds before being washed in PBS. The samples were then placed in 12-well transwell inserts where 100 µl of 200 uM of peptide (peptide reconstituted in DMEM), or DMEM only as a control, was applied onto the skin for 1 hour. 1 mL Green's media was added to the wells under the transwell inserts. Afterwards the peptide was removed and was replaced with 100 µl of $1x10^7$ CFU of SH1000 bacterial suspension. Skin samples were incubated in 5% $CO_2$ and 37$^oC$ for 5 hours.

Afterwards the skin was washed once in PBS to remove any non-adherent bacteria. The skin was then placed into new transwell inserts with fresh media and re-incubated

for 18 hours. After 18 hours, the skin was removed from the inserts and washed three times in PBS. The skin was then halved, half for histology and half for CFU counting. Skin was weighed and then minced in 11% saponin. The saponin lysate was diluted and plated onto LB agar plates Miles-Misra style.

### 2.12.2 Infection assay on tissue-engineered skin

After 2 weeks of ALI, tissue-engineered human skin models were cut with a 10 mm biopsy punch. The infection methodology then follows 2.12.1. After infection and incubation, the tissue engineered skin was then separated into 2 pieces by cutting the skin in half, through the centre. One half was fixed overnight in formalin for histology. The second half was weighed, minced into 8-16 pieces, and placed in an Eppendorf tube containing 1 mL of 10% Saponin for 12-15 minutes. 20 µL of each suspension was then pipetted into 180 µl of PBS and serially diluted before plating Miles-Misra style. The plates were air-dried then incubated overnight at 37$^{o}$C in 5% $CO_2$ before counting the CFU.

## 2.13 Infection assay mouse model

Animal experiments were approved under Institutional Animal Care and Use Committee (IACUC) 171290. Usage was approved after training under the Biological Research Centre (BRC).

Mice used were C57BL/6 mice purchased from InVivos. Mice were 8-10 weeks of age upon reception and experimentation. Mice were received by BRC vets and housed for 72 hours under observation before experiments began. Mice were shaved with a pet shaver to remove fur from the back and sides of the mouse. Hair remover (Veet) was applied onto the shaved areas to remove any remaining hair and prevent hair regrowth during the experimental timeframe. Veet was applied onto the skin for five minutes before being wiped away and any residue was washed away with water. After shaving, the mice were re-housed for 24 hours.

After 24 hours had passed, the mice were processed in a tissue-culture biosafety cabinet. A bacterial pellet containing $1x10^7$ CFU of SH1000 is resuspended in 100 µL of peptide suspension (peptide reconstituted in PBS). The 100 µL of bacteria-peptide suspension is pipetted on a 1x1 $cm^2$ gauze pad then applied onto the back of the shaved mouse. The non-infected control mice had a gauze pad with PBS only applied onto its back. The gauze pad is then secured onto the back of the mice using a half a piece of Tegaderm film dressing (3M) before being further secured with two layers of MeFix self-adhesive fabric (Molnlycke). Bandaged mice were then rehoused for an additional five days. Afterwards, the mice were sacrificed in a $CO_2$ chamber before being harvested immediately.

The bandages were removed and the area previously in contact with the gauze pad was excised with surgical scissors. The 1x1 $cm^2$ area was then halved for histology and for CFU counting. Skin was weighed and then minced in 11% saponin. The saponin lysate was diluted and plated onto LB agar plates Miles-Misra style. For histology, the skin was fixed for 24 hours with 10% neutral buffered formalin (Sigma), the fixed skin was then processed and embedded into wax blocks for sectioning with a microtome. The sections were then stained for H&E or immunohistochemistry *(see 2.7 Histology).*

## 2.14 Flow cytometry

Some mice were used for flow cytometry. The infected area was excised and minced in an Eppendorf tube containing 500 µL of Liberase (250 mg/mL). The minced suspension was then transferred to a 24-well plate on ice until all samples had been transferred. The plate was then incubated in 5% $CO_2$, 37$^oC$ for 90 minutes. Inguinal lymph nodes were also harvested and underwent a similar digestion but with a dispase, collagenase and DNase cocktail. The lymph nodes were also incubated in 5% $CO_2$, 37$^oC$ for 2 hours. Once the tissues had been digested, they were pipetted up and down with a syringe with an 18G needle to break up the suspension.
The cells were then pipetted through a 40 µm filter into a FACS tube and washed with FACS buffer. The cells were centrifuged at 300 g for 5 minutes, supernatant discarded, then resuspended in 1 mL FACS buffer with 10 µL of each sample taken for cell counting. The cells were then centrifuged again then resuspended in 100 µL of flow

cytometry antibody mixture with 10% rat serum before being stored at 4°C for 30 minutes. The stained cells were then washed once again with FACS buffer, centrifuged, and then resuspended in 100 µL DAPI solution before analysis for flow cytometry (LSRII, Becton Dickinson)

## 2.15 Microscopy

Sections were imaged with a BA210 digital microscope (Motic) or a CX41 upright microscope (Olympus) at various magnifications from x4 to x40. Images taken were processed through ImageJ or Fiji.

## 2.16 Statistical analysis

Statistical analyses were carried out using GraphPad Prism 9, and the statistical test chosen is specified in the appropriate figure legend. Data were analysed for normality using the Shapiro-Wilk normality test then the appropriate multiple comparison test. In all cases, non-significance (ns) is $p \geq 0.05$.

| **Target** | **Fluorophore** | **Dilution** | **Manufacturer** |
|---|---|---|---|
| CD45 | FITC | 1:200 | eBioscience (30F11) |
| CD64 | PE | 1:50 | Biolegend (X54-5/7.1) |
| CD11b | PerCP-Cy5.5 | 1:200 | eBioscience (M1/70) |
| EpCAM | PE-Cy7 | 1:200 | Biolegend (G8.8) |
| CD24 | Pacific Blue | 1:200 | Biolegend (M1/69) |
| Ly6G | APC | 1:200 | Biolegend (1A8) |

| | | | |
|---|---|---|---|
| MHCII (I-A/I-E) | AF700 | 1:200 | Biolegend (M5/114.15.2) |
| Ly6C | APC-Cy7 | 1:200 | Biolegend (HK1.4) |
| Nucleus | DAPI | 5mg/ml | Life tech (D1306) |

**Table 2.2 Antibodies for flow cytometry of murine skin**

| **Target** | **Fluorophore** | **Dilution** | **Manufacturer** |
|---|---|---|---|
| CD45 | FITC | 1:200 | eBioscience (30F11) |
| XCR1 | PE | 1:200 | Biolegend (S15046E) |
| CD11b | PerCP-Cy5.5 | 1:200 | eBioscience (M1/70) |
| CD11c | PE-Cy7 | 1:200 | Biolegend (N418) |
| CD24 | Pacific Blue | 1:200 | Biolegend (M1/69) |
| Ly6G | APC | 1:200 | Biolegend (1A8) |
| Ly6C | APC-Cy7 | 1:200 | Biolegend (HK1.4) |
| MHCII | AF700 | 1:200 | Biolegend (M5/114.15.2) |
| EpCAM | Qdot-605 | 1:200 | BD Biosciences (EBA-1) |
| Nucleus | DAPI | 5mg/ml | Life tech (D1306) |

**Table 2.3 Antibodies for flow cytometry of murine lymph nodes**

| Target | Dilution | Manufacturer |
|---|---|---|
| CD68 | 1:100 | Abcam (Ab125212) |
| Ly6G | 1:2000 | Abcam (Ab238132) |

**Table 2.4 Antibodies for immunohistochemistry**

| Target | Fluorophore | Dilution | Manufacturer |
|---|---|---|---|
| CCR6 | APC | 1:200 | Biolegend (353415) |
| CD1a | FITC | 1:200 | Biolegend (300103) |
| Langerin | PE | 1:200 | Biolegend (144203) |

**Table 2.5 Antibodies for MUTZ-3 flow cytometry**

# Chapter 3 Tetraspanin-derived peptides reduce *Staphylococcus aureus* adherence in human skin models.

## 3.1 Introduction

### 3.1.1 Anti-adhesion therapy

Due to the rise of antibiotic resistance, it has become increasingly vital to develop therapeutics that are capable of fighting bacterial infection whilst minimising the development of resistance (Peacock and Paterson, 2015). A viable class of treatments are host-directed anti-adhesion therapeutics. Anti-adhesion therapeutics function by preventing the initial adherence of a pathogen to the host, this prevents the pathogen from being able to infect the host and thereby reduce the burden of infection (Krachler and Orth, 2013). By targeting host proteins rather than bacterial adhesins, this makes it much harder for the bacteria to mutate and develop resistance to the therapeutic. As previously stated in Chapter 1, the Monk Lab have demonstrated anti-adhesion peptides are effective in reducing bacterial adhesion by targeting and interacting with host tetraspanin CD9. Through this, the microdomains involving CD9 are disrupted, disorganising the proteins targeted by *S. aureus* to adhere to cells (Green et al., 2023).

### 3.1.2 *Staphylococcus aureus*

*S. aureus* possesses a variety of adhesins that promote the binding of *S. aureus* to epithelial cells. A notable example is the fibronectin-binding protein (FnBP) on the surface of *S. aureus* that directly interacts with fibronectin on the surface of host cells (Josse et al., 2017). By establishing attachment to host cells, bacteria can overcome the innate cleaning mechanisms of the host body. Furthermore, *S. aureus* can infect cells through the exploitation of tetraspanins such as CD9. Consequently, this makes CD9 a viable target for anti-adhesion therapy.

*Staphylococcus aureus* is the most common cause of skin and soft tissue infections; therefore, this pathogen was chosen to infect models and determine how effective anti-adhesion treatments were at preventing infection. The specific strain used, SH1000, was chosen because it expresses a gene for chloramphenicol resistance, making it useful for colony counting as we could plate bacterial suspensions onto agar plates containing chloramphenicol and select for the SH1000 strain. This is especially useful for the mouse experiments in Chapter 5 as mice cannot be sterilised and we could take advantage of the chloramphenicol resistance of SH1000 to select for it against any bacteria that may exist on the mice as part of their natural skin microbiome.

### 3.1.3 Human skin models

In order to study how *S. aureus* infects the skin and how a potential therapeutic may be effective in its treatment, a suitable model needs to be used that is representative of native human skin. For this thesis, several skin models were compared for their various strengths and weaknesses to select a model that most accurately replicates the structure and function of native human skin and its response to bacterial infection and treatment. A particular requirement is the presence of the main elements of a functioning immune system in the model to allow the evaluation of the effects of CD9-targeting reagents on the immune response to infection. Four models were assessed in this chapter:

1. The simplest skin model would be a 2D *in vitro* model containing only keratinocytes. This would be to represent the epidermal portion of skin and a potential avenue to investigate topical applications onto skin. The keratinocytes used could be primary, but HaCaT cells were chosen as they are an immortalised cell line that would not be subject to donor variability unlike primary keratinocytes (Colombo et al., 2017). Furthermore, HaCaT cells can be cultured in isolation. Primary keratinocytes require a feeder layer to support their growth, this is typically a primary fibroblast cell line ‘3T3s’ that will also need to be irradiated prior to keratinocyte co-culture so as to not proliferate.

2. A 3D tissue engineered model of human skin was also constructed, consisting of primary keratinocytes and dermal fibroblasts grown on a de-epidermised dermis scaffold at air-liquid interface (Chakrabarty et al., 1999). The keratinocytes and fibroblasts communicate to migrate and differentiate into their appropriate locations, forming a dermis, epidermis, and stratum corneum, replicating normal skin structure. The stratified stratum corneum of these models are impermeable to bacteria unless a wound is present that can be exploited. This was previously reported in a similar experiment performed by Shepherd et al. who reported that inoculation of skin without prior injury did not result in bacterial invasion of the tissue (Shepherd, 2009). For experiments, burning was used to simulate a wound to allow opportunistic pathogens to invade the skin. This model provides a relevant and reproducible platform on which to test the peptides in a more complex setting compared to a 2D model.
3. Another 3D model evaluated was a collagen-based organotypic. This model is less representative in structure compared to tissue-engineered models; however, it is less reliant on the supply of surgical waste skin from different patients and so is more reproducible (Roger et al., 2019). Furthermore, this model type is typically used to integrate immune cells or melanoma cells (Hutter et al., 2017; Zoschke et al., 2016).
4. As the culturing and engineering of skin models requires a lot of time and effort, some researchers use the waste explant skin from surgeries such as abdominoplasties and breast reduction surgeries. Once cultured after excision, skin explants are ideal models for human skin as they contain all the resident immune cell types and structures present in native skin and can recapitulate authentic skin diseases, for example, research into type 2 diabetes requires type 2 diabetic tissue. However, skin explants are the most subject to donor variability and lack a vascular system, restricting the opportunity to research cell migration such as when neutrophils migrate into the site of infection from the blood.

Whilst there are a variety of human skin models available, there are multiple pros and cons to each type, as shown in Table 1. Furthermore, the main use of human skin models is for topical applications of drugs and irritants and so optimisation is required to determine which model is most appropriate as a model of bacterial infection on

human skin. We aim to better understand the basics of these skin models, and determine if such models can be characterised, namely if it is possible for these models to be infected with bacteria, and if our peptides can interact and treat these models as the peptides are host-directed therapeutics rather than pathogen-directed. Ultimately, we aim to determine which model provides the most suitable representation of a bacterial infection after wounding in a human skin model that provides a platform for drug testing of appropriate therapeutics.

| Model | Advantage | Disadvantage | Reference |
|---|---|---|---|
| Reconstructed human epidermis | Can be constructed with an immortalised keratinocyte cell line<br><br>Low cost<br><br>Short culture times<br><br>Reproducible | Least representative model of skin<br><br>Lack interactions with dermal cells<br><br>No barrier to infection so infection possible all round the cells, little/no matrix, easily disrupted by cell detachment | (Huet et al., 2018)<br><br>(Frankart et al., 2012) |
| De-epidermised dermis tissue-engineered skin | More morphologically representative than collagen-based organotypics | Dermis is too dense to incorporate immune cells unlike collagen-based organotypics | (Chakrabarty et al., 1999)<br><br>(Xie et al., 2010) |
| Collagen-based organotypic | Easiest to incorporate immune cells<br><br>Easiest to incorporate knockouts | Lack of skin appendages<br><br>Lacks rete ridges so epidermis is more easily detached | (Oh et al., 2013)<br><br>(Roger et al., 2019) |

| | | | |
|---|---|---|---|
| Surgical explants | Most representative architecture of human skin<br><br>Contains residential immune cells<br><br>Best surrogate for *in vivo* human skin | Ethical difficulties<br><br>Most donor variable<br><br>Lack of regular supply and storage issues | (Danso et al., 2015)<br><br>(Neil et al., 2020) |

**Table 3.1 Advantages and disadvantages of various skin models**

### 3.1.4 Tetraspanin-derived peptides

The tetraspanin-derived peptides used in the following experiments, as described in Chapter 2 (Methods and Materials), are derivatives of the peptides used by Ventress et al, 2016.

These peptides function by targeting the host and disorganising the formation of tetraspanin-enriched microdomains (Ventress et al., 2016). These microdomains are involved in the formation of host adhesion platforms used during host cell to cell interactions. These platforms are exploited by bacteria in order to gain access to a cell. This was demonstrated with atomic force microscopy, which showed that the peptide decreased the force required to detach bacteria from the surface of epithelial cells (P. Monk, unpublished data) but not from an abiotic surface, confirming a directed anti-adhesive effect. Peptide treatment of epithelial cells altered the clustering behaviour of CD9 suggesting a direct effect on CD9-dependent adhesion platforms.

The experiments performed in this thesis use peptides that are stapled derivatives 800i and 800ii, designed to be more proteolytically-resistant and efficacious than their precursor, 800-Cap (Monk et al., 2021), itself derived from a published sequence that had modest anti-adhesive activity (Ventress et al., 2016). The stapled peptides displayed the highest levels of alpha-helicity, indicating the stapling stabilised the helical form. The hydrophobic staple also helped to resist proteolytic degradation (Monk et al., 2021). Stapling peptides is a well-known method for improving the stability of peptides (Ali et al., 2019).

The primary aim of this chapter was to establish a skin model as a platform for bacterial infection studies with a secondary aim of testing the stapled peptides against *S. aureus* infections. For this, we constructed multiple skin models to compare and contrast the structure, methodology and materials to determine which model is the most suitable for establishing and supporting a bacterial infection. Next, we tested the peptides on these skin models to observe the efficacy of the peptides against bacterial infection and if the different skin models affect this efficacy.

## 3.2 Results

### 3.2.1 Determining MOI for HaCaT cells

To determine the most appropriate MOI for *S. aureus* infection of HaCaT cells for adhesion assays, HaCaTs were infected with a range of MOIs from 10 to 200 CFU. As Figure 3.1 shows, the number of bacteria adhered to HaCaT cells increased with increasing MOI. Based on previous studies in the Monk Lab, it was determined from dose-response curves that 200nM was the optimal dose to use, with higher doses not being able to further inhibit bacterial adhesion (Ventress et al., 2017).

The most suitable input MOI for use in this assay was determined by titrating the dose of added bacteria against a fixed number of HaCaT cells. The output CFU/mL increased rapidly between MOI 10 to 50 and then tended towards a plateau from ~MOI 100, likely due to the saturation of the high affinity adherence sites on the HaCaT cells. Lower affinity adherence might occur to the abiotic tissue culture plastic, which will not be affected by CD9 peptides. Therefore, an MOI of 50 was determined to be appropriate, with adherence largely to HaCaT cells themselves and leading to an infection with enough bacteria to facilitate counting on an agar plate.

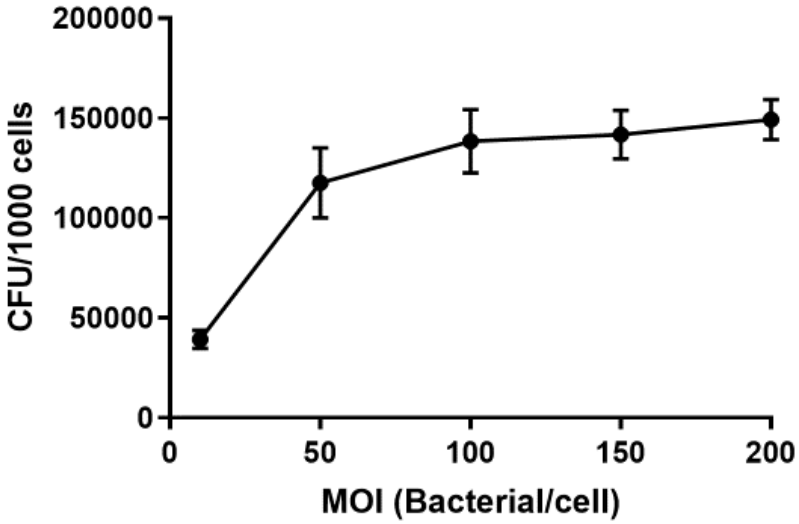


**Figure 3.1 Determination of MOI for *Staphylococcus aureus* infection of HaCaTs**

HaCaT cells were infected with SH1000 at a range of MOIs ranging from 10 to 200 for 1 hour. HaCaTs were then lysed with saponin, and the lysate was plated onto agar plates to quantify the number of adherent bacteria by CFU counting. Experiment was performed with 3 biological replicates each with 3 technical repeats, data represented as mean ± Standard Deviation (SD).

### 3.2.2 CD9-derived peptide treatment reduces *Staphylococcus aureus* adherence to HaCaT cells

HaCaT cells were pre-treated with 200 nM of the peptide derivatives before infection with the SH1000 strain of *S. aureus*. Previous experiments performed by Ventress et al. running similar assays had determined that a dosage of 200 nM would be most appropriate to use for infection assays (Ventress et al., 2017). Pre-treatment with 800-Cap, 800i and 800ii reduced the percentage of cells with adherent bacteria (Figure 3.2), this reduction was not seen in the non-treated control, nor the 800-Cap scrambled sequence control. This indicates that the sequence of the peptides was vital for peptide response rather than just the presence of particular amino acids.

800-Cap, 800i and 800ii were effective in reducing bacterial adhesion by roughly 50% compared to the scrambled control and infection only control. Whilst SH1000 adherence had been reduced, a significant proportion of the bacteria were still able to adhere to the HaCaT cells, indicating that SH1000 is able to use other adherence mechanisms that the peptide treatments did not suppress. As Figure 3.2A only shows limited variability between technical replicates, and Figure 3.2B shows limited variability in the biological replicates, therefore only the mean CFU and percentage of the infection only control data will be shown from this point forward.

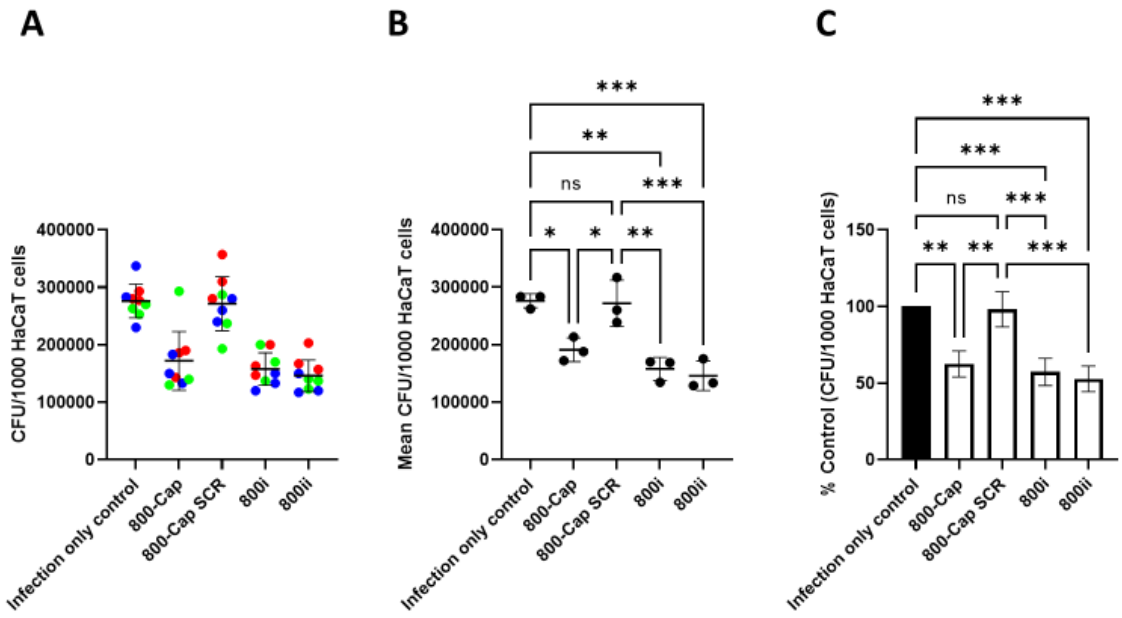


**Figure 3.2 Proteolytically-resistant derivatives of CD9-derived peptides reduce *Staphylococcus aureus* adherence to HaCaT cells**

HaCaT cells were pre-treated with 200 nM CD9-derived peptides, scrambled control, or media only control for 1 hour before the cells were infected with SH1000 at a MOI of 50. Cells were then lysed with saponin then plated onto LB agar plates for CFU counting with the data shown as bacteria per 1000 HaCaT cells. **A)** All replicate bacteria isolated per 1000 cells. Colours represent separate experiments. **B)** Mean CFU/1000 cells. **C)** Data plotted as a percentage of the infection only control. Data are represented as mean ± SD. Data are normally distributed as determined by the Shapiro-Wilk Normality test. 3 biological replicates performed with 3 technical repeats. Data analysed by one-way ANOVA with Sidak's multiple comparisons test * p≤0.05 ** p≤0.01 *** p≤0.001

### 3.2.3 Construction of a 3D tissue-engineered model of human skin

Whilst cell lines are a good model to initially determine the effects of the tetraspanin-derived peptides in a 2D context, they carry multiple limitations as detailed in Table 3.1. Consequently, a 3D tissue engineered skin model was constructed, and optimised as a model to represent *S. aureus* infected wounds in human skin. Tissue engineered skin mimics the architectural structure of native human skin and can be used to analyse the migration and actions of immune cells added to the model. In the future, it can also be used for testing the effectiveness of peptides against bacterial infection.

Figure 3.3A shows a sectioned piece of tissue-engineered skin after 2 weeks in culture ALI stained with haematoxylin and eosin. This model was made of primary keratinocytes and fibroblasts cultured from a human biopsy, seeded onto a DED from the same donor. The cells have migrated and differentiated within the DED scaffold to form a dermis seeded with fibroblasts, an epidermis made up of variously differentiated keratinocytes (granular, basal, and spinous keratinocytes), and a fully stratified stratum corneum.

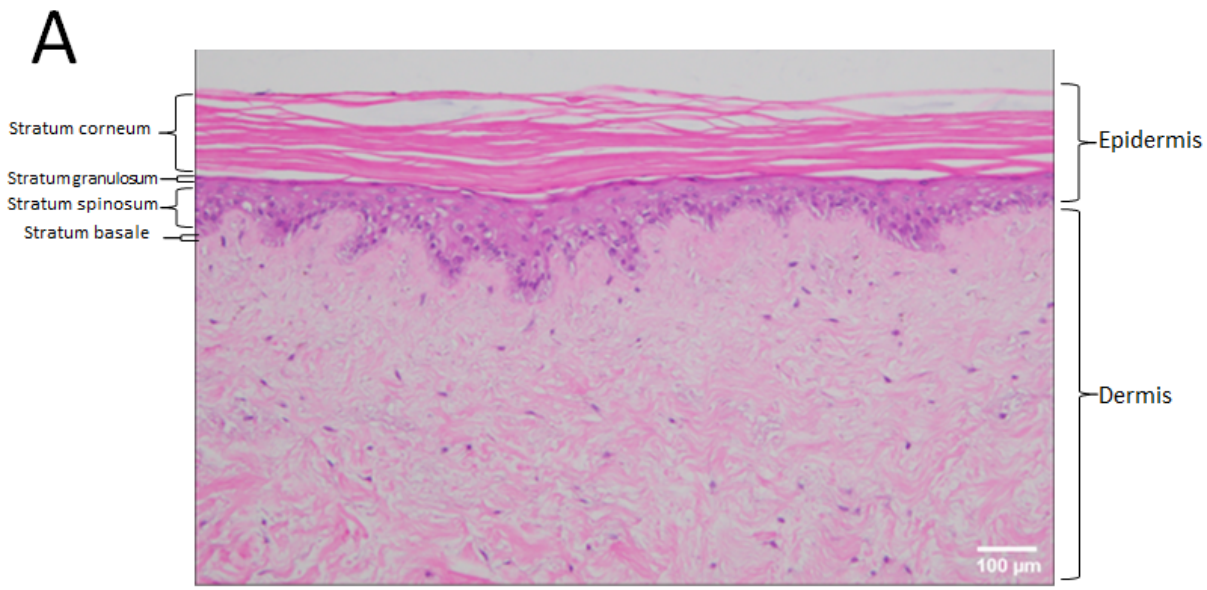

B

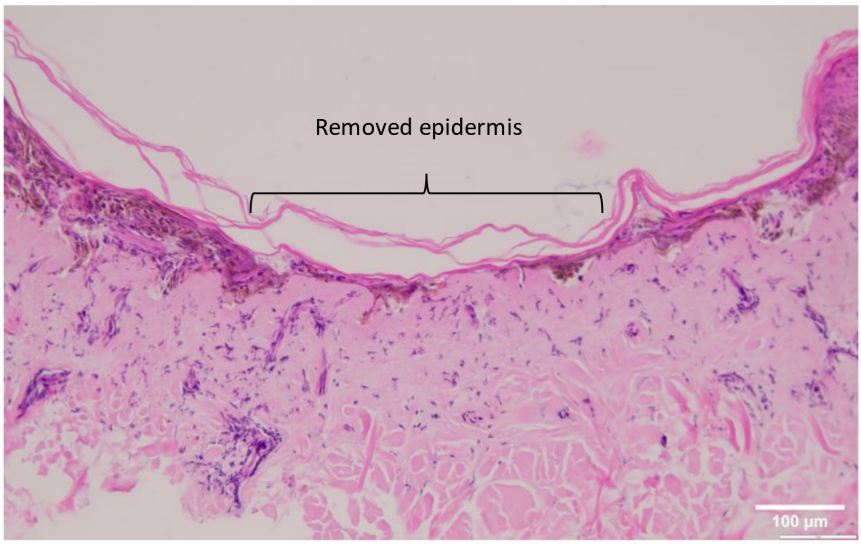


C

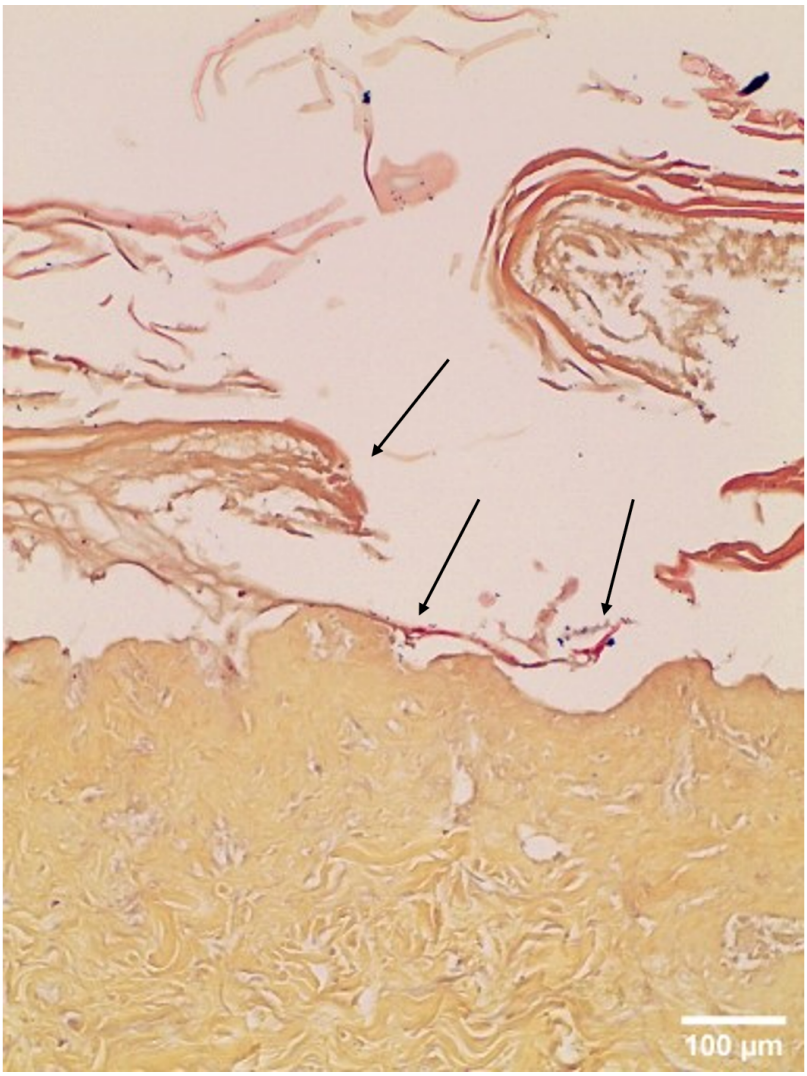

**Figure 3.3 Generation of a 3D tissue-engineered model of human skin for infection assays**

**A)** Tissue-engineered skin was constructed using the methodology published by Chapple et al., 2013. Briefly, primary keratinocytes and fibroblasts were seeded onto a decellularised dermis. The model was then raised to ALI to allow the epidermis to form and differentiate. Formalin-fixed skin sections were prepared and stained with haematoxylin and eosin (H&E) then imaged at x10 magnification. **B)** A tissue-engineered skin model was burned with a soldering iron with a 2 mm diameter tip that was heated to 150 $^{o}$C. The soldering iron made contact with the surface of the model for exactly 2 seconds before contact was removed, along with the epidermis. Formalin-fixed skin sections were prepared and stained with H&E then imaged at x10 magnification. **C)** Burning compromised the epidermis to allow bacterial infection. Formalin-fixed samples were sectioned then Gram-stained to confirm the presence of adherent bacteria. Arrows point to bacterial colonies present on the skin. Sections were imaged at x40 magnification.

As previously reported by Shepherd et al. (Shepherd et al., 2009), it was necessary to breach the epidermis to allow bacterial infection. Tissue-engineered skin was wounded for 2 seconds with a soldering iron heated exactly to 150$^{o}$C. After burning, the skin models were wounded to the extent of the epidermis being breached (Figure 3.3B). The models were pre-treated for 45 mins with 200 nM peptides, and then infected with a bacterial suspension of SH1000. After 5 hours of infection, non-adherent bacteria were washed off, and the adherent bacteria that had survived washing were allowed to further infect for another 18 hours. The skin models were then halved, with half being fixed and sectioned for histology (Figure 3.3A-C) with the rest being processed to release the bacteria for CFU counting (Figure 3.4).

### 3.2.4 Stapled peptides reduce *Staphylococcus aureus* infection in tissue-engineered skin

We were particularly interested in testing the new proteolytic-resistant stapled derivatives as they had never been tested on tissue-engineered skin. We selected the 800i peptide and compared it to the non-treated control as a true scrambled control cannot be designed due to the addition of the staple. As Figure 3.4 shows, stapled peptide ‘800i’ reduced bacterial adherence by roughly 60%.

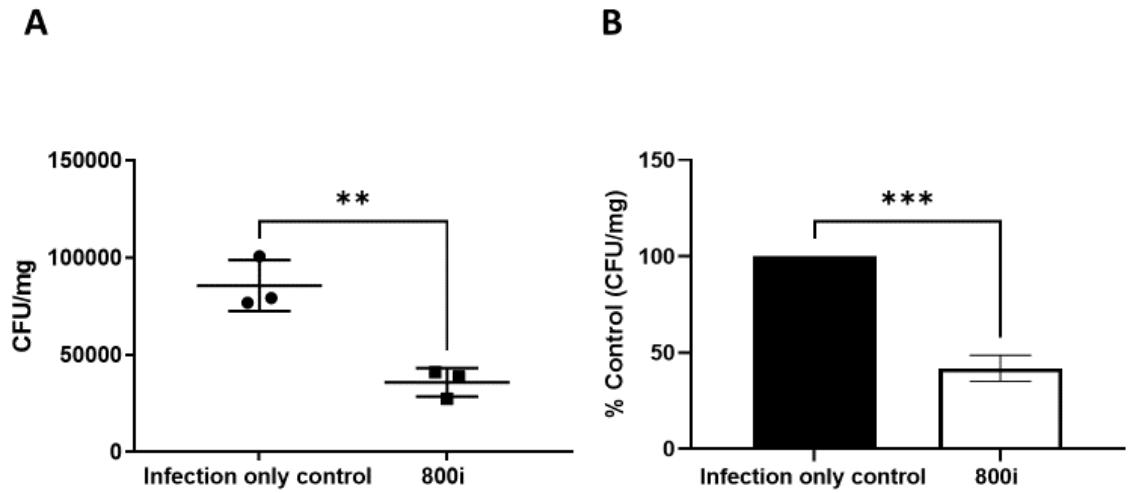


**Figure 3.4 Pre-treatment with stapled peptides reduces *Staphylococcus aureus* adherence in tissue-engineered skin**

Tissue-engineered skin models were treated with 200 nM CD9-derived peptide or the media only, non-peptide control for 45 mins before the models were infected with a bacterial suspension containing $1x10^7$ CFU of SH1000. The models were then minced into saponin, and the lysate was pipetted onto agar plates for CFU counting. **A)** Mean CFU/mg of tissue. **B)** Data plotted as a percentage of infection only control. Data represented as mean ± SD. Data are normally distributed as determined by the Shapiro-Wilk Normality test. 3 biological replicates each performed with 3 technical repeats. Data analysed with unpaired t-test ** $p \leq 0.01$ *** $p \leq 0.001$

This reduction in percentage of bacterial infection indicated that the peptide treatment had reduced the severity of infection of the skin models, likely by reducing the number of bacteria that had initially adhered to the bacteria and consequently lessened the burden of infection. This reduction was not present in non-peptide controls, this suggests that the new peptide derivatives have maintained their efficacy that is still present in 3D models and not just 2D models. This was supportive of the potential role tetraspanin-derived peptides have in anti-adhesion therapy.

### 3.2.5 Pre-treatment with 20 nM peptides reduces bacterial adhesion but with lower efficacy than 200 nM

As we have observed that the peptide is able to interact with the models and can effectively reduce bacterial adherence to skin even in complex 3D contexts, we repeated the previous experiments with a reduced dosage of 20 nM to see if it remained effective. As shown in Figure 3.5, peptide pre-treatment at a concentration of 20 nM is still effective in reducing *S. aureus* adherence to tissue-engineered skin, however its efficacy is reduced compared to a pre-treatment at 200nM. This could likely be due the concentration of the peptide now being too low to saturate the binding sites present at the wound site.

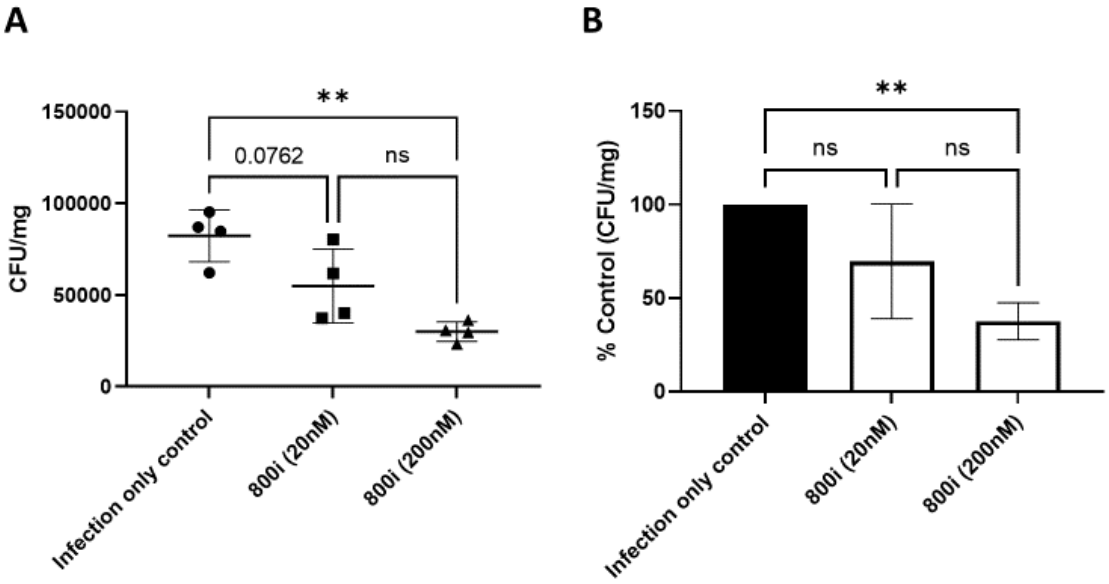


**Figure 3.5 Pre-treatment with stapled peptides reduces *Staphylococcus aureus* adherence in tissue-engineered skin, but efficacy varies with concentration**

Tissue-engineered models were treated with 20 nM or 200 nM CD9-derived peptide or their non-peptide control for 45 mins before the models were infected with bacterial suspension containing $1x10^7$ CFU of SH1000. The models were then minced in saponin. The lysate was then pipetted onto agar plates for CFU counting. **A)** Mean CFU/mg of tissue. **B)** Data plotted as a percentage of infection only control. Data represented as mean ± SD. Data are normally distributed as determined by the Shapiro-Wilk Normality test. 4 biological replicates each performed with 3 technical

repeats. Data analysed by one-way ANOVA with Sidak's multiple comparisons test. ** $p \leq 0.01$

### 3.2.6 Construction of 3D collagen-based organotypic human skin models

A 3D collagen-based human skin model was constructed as a model for *S. aureus* infections of human skin. Collagen-based organotypics can suitably mirror the structure of native human skin and can more easily be modified by the addition of immune cells.

As shown in Figure 3.6A, the keratinocytes have adhered on top of the collagen-fibroblast layer and have formed an epidermis. These models are flat, even in morphology as these models do not possess rete ridges. The H&E staining shows the differentiation of the collagen-based models as the nuclear staining is predominantly at the basal layer and lessens as towards the stratum corneum. This differentiation reflects the differentiation and layering of native skin; however, it is less differentiated in comparison to tissue-engineered skin using a DED (Figure 3.3A).

Upon experimentation, we discovered that these organotypics are too fragile to be burned with the same technique as with the tissue-engineered skin models. The heat from the soldering iron caused the collagen in the model to immediately melt. As such, these models were wounded by carefully cutting the surface of the model with a scalpel (Figure 3.6B) before being infected with *S. aureus* (Figure 3.6C).

A

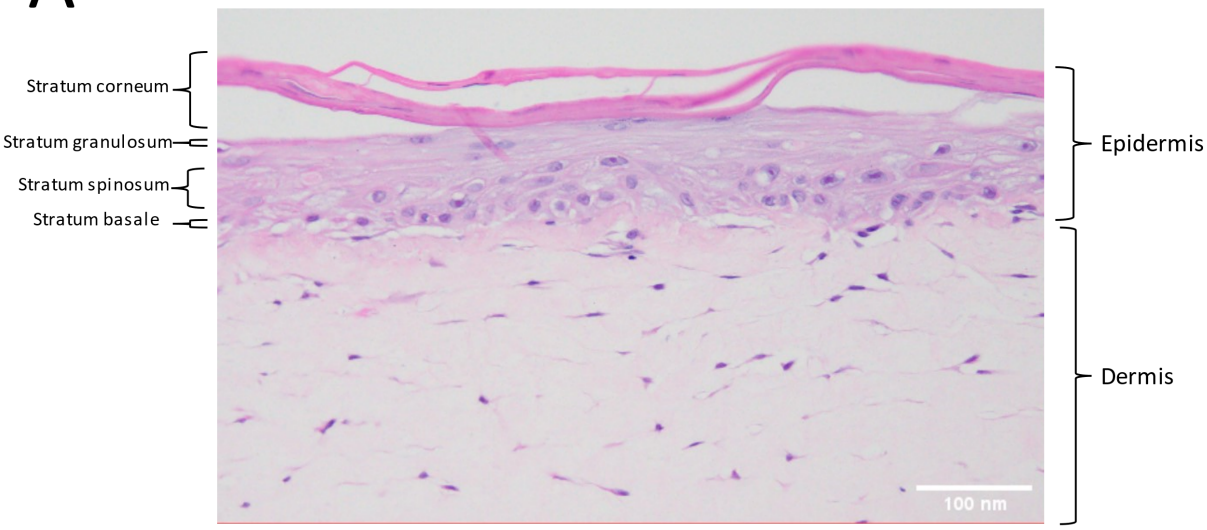
Stratum corneum
Stratum granulosum
Stratum spinosum
Stratum basale
Epidermis
Dermis
100 nm

B

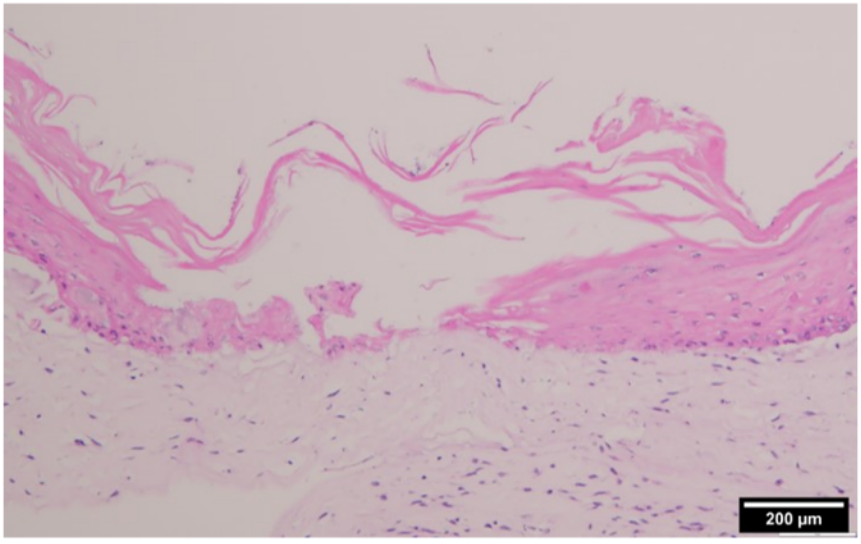
200 µm

C

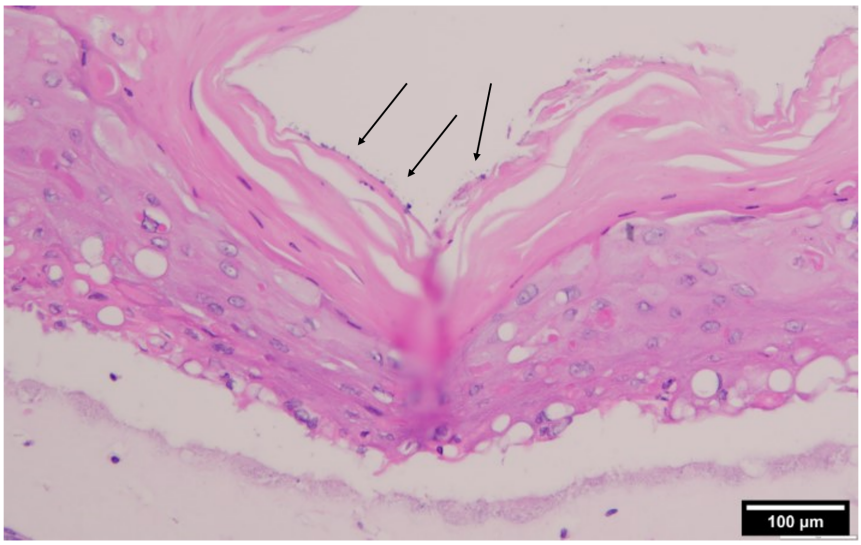


**Figure 3.6 Construction of collagen-based organotypics for infection assays**

**A)** Collagen-based organotypic skin models were constructed using the methodology published by Arnette et al., 2016. Briefly. fibroblasts were mixed into a collagen suspension and left to set to form a gel. Keratinocytes were seeded on top and the models were raised to an ALI to form an epidermis consisting of granular, basal, and spinous keratinocytes, and a fully stratified stratum corneum. Formalin-fixed models were prepared and sectioned, H&E stained and imaged at x10 magnification. **B)** For infection assays, the epidermis was carefully cut with a scalpel to allow for bacterial adhesion. **C)** Bacterial adhesion can be seen adhered to the surface of the model as indicated by the arrows. Panels for Figure 3.6B and 3.6C were imaged at x20 magnification.

### 3.2.7 CD9-derived peptide treatment does not reduce *Staphylococcus aureus* adherence to collagen-based organotypic human skin model

Although tissue-engineered skin models are a good model for human skin that accurately replicates the architecture of skin, they are difficult models to use for the research of immune cells. This is due to the difficulty of introducing the immune cells into the model and for the immune cells to migrate into their correct location within the skin. To this end, we constructed a 3D collagen-based organotypic to determine if it was a suitable model for peptide testing and for infection models involving immune cells. For this, fibroblasts were gelled in a rat tail collagen matrix in transwell inserts to form an artificial dermis. Once the collagen had set, keratinocytes were seeded on top, and an epidermis was allowed to form for 14 days. After which, the organotypics

received the same treatment in Chapter 3, of receiving a 200 nM peptide treatment before an infection with a suspension of SH1000. As shown in Figure 3.7, a trend can be seen in that treatment with 800-Cap and 800i peptide reduced the percentage of adherent bacteria; however, this was statistically non-significant.

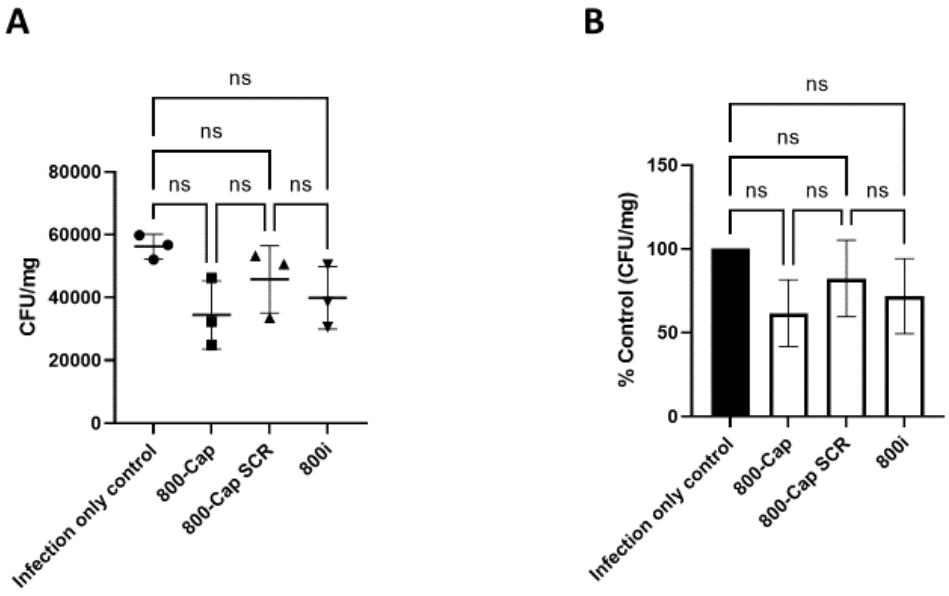


**Figure 3.7 Pre-treatment with CD9-derived peptides on collagen-based organotypic human skin models does not reduce bacterial adherence**

Collagen-based organotypics were wounded by cutting with a scalpel, pre-treated with peptides for 45 mins before infected with $1x10^7$ CFU of SH1000 for 5 hours. The samples were then washed to remove non-adherent bacteria before being minced in saponin. The lysate was then plated onto agar plates for CFU counting. **A)** Mean CFU/mg of tissue. **B)** Data plotted as a percentage of infection only control. Data are represented as mean ± SD. Data are normally distributed as determined by the Shapiro-Wilk Normality test. 3 biological replicates performed with 3 technical repeats. Data was analysed by One-Way ANOVA with a Sidak's multiple comparisons test.

The non-significance of the data in Figure 3.7 could be due to the difficulty in reliably creating a wound that is replicable. Issues were initially found trying to burn wound the collagen-based organotypics so it could be comparable with the tissue-engineered skin data, which was also burn wounded. However, we found that the collagen-based organotypics were significantly more fragile; the models could melt if exposed to the heat from the soldering iron and the dragging motions made when cutting with the

scalpel could disturb and detach the epidermis from the collagen matrix as they use the structures such as rete ridges to provide structural stability. As such the best way to wound the model without detaching the epidermis was to push down the organotypic with a scalpel or one-sided blade however, the trade off from this technique was that it was difficult to determine the depth of the wound made, consequently the size of the wound and how much of the wound was exposed for bacterial adherence and infection.

### 3.2.8 Comparison of commercially available wounded collagen-based organotypics

Whilst the protocols and materials for constructing collagen-based organotypics in-house are available, culturing and generating these organotypics are time-consuming and it is easy for errors to occur throughout the entire process. As such, the construction of organotypics have been commercialised and researchers can now order organotypics which are reproducible and are ready to use in experiments upon delivery. An example of such a company is MatTek, a US-based company that can provide a variety of tissue models such as skin (EpiDerm) and, lungs (EpiAirway) and eyes (EpiOcular). MatTek can provide 3D *in vitro* models of skin, but also models which are pre-wounded either by biopsy punching or by burning. Due to the issues in consistently wounding the in-house generated collagen-based organotypics, we tested the biopsy-wounded and burn-wounded human skin models from MatTek. (Figure 3.7), we tested the MatTek models to determine if these would be more reliable models for infection and drug treatment.

To determine which wound model would be appropriate for infection assays with collagen-based organotypics, the infection assay was repeated on two sets of wound models, a biopsy-punch wounded and a burn wounded set. Following the methodology used with the tissue-engineered models as described in 3.2.7, the biopsy punch pre-wound model is performed with a 2 mm diameter punch to solely remove the epidermis with no noticeable damage to the dermis below. The burn pre-wound model is performed by applying two hot strips of metal to the surface of the model. The temperature of the metal strips and how long the strips were applied onto the epidermis

are currently proprietary. The same infection protocol performed on tissue-engineered skin models as described in 3.2.4 was used on the collagen-based organotypic models to compare how it was as a model for infection.

As Figure 3.8 shows, the biopsy wounded models have the epidermis completely removed, thus allowing greater exposure of the dermis to bacteria. The burn wound models are more irregular and do not necessarily expose the dermis. Furthermore, the 2mm wound site of the biopsy punch model is greater than the wound sites of the burn model meaning there was more opportunity for the bacteria to adhere to the model. This is reflected in Figure 3.9; the effectiveness of peptide pre-treatment is more visible with the biopsy punched model compared to the burn model. The percentage of infection is lower in the biopsy punch wounded models. This is likely due to more of the epidermis being breached in the biopsy wounded models compared to the burn models.

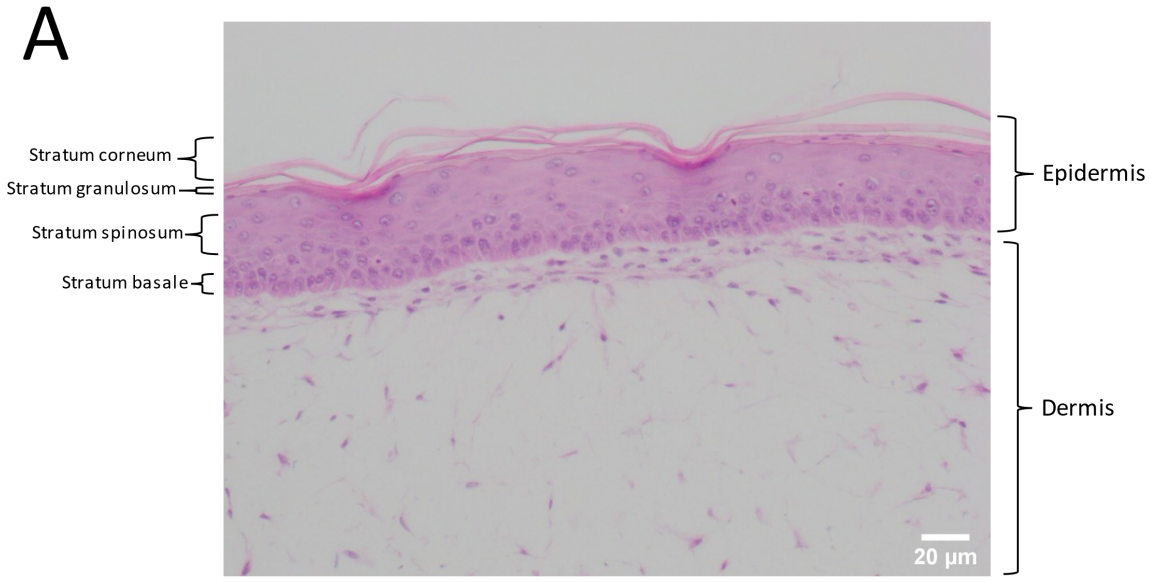

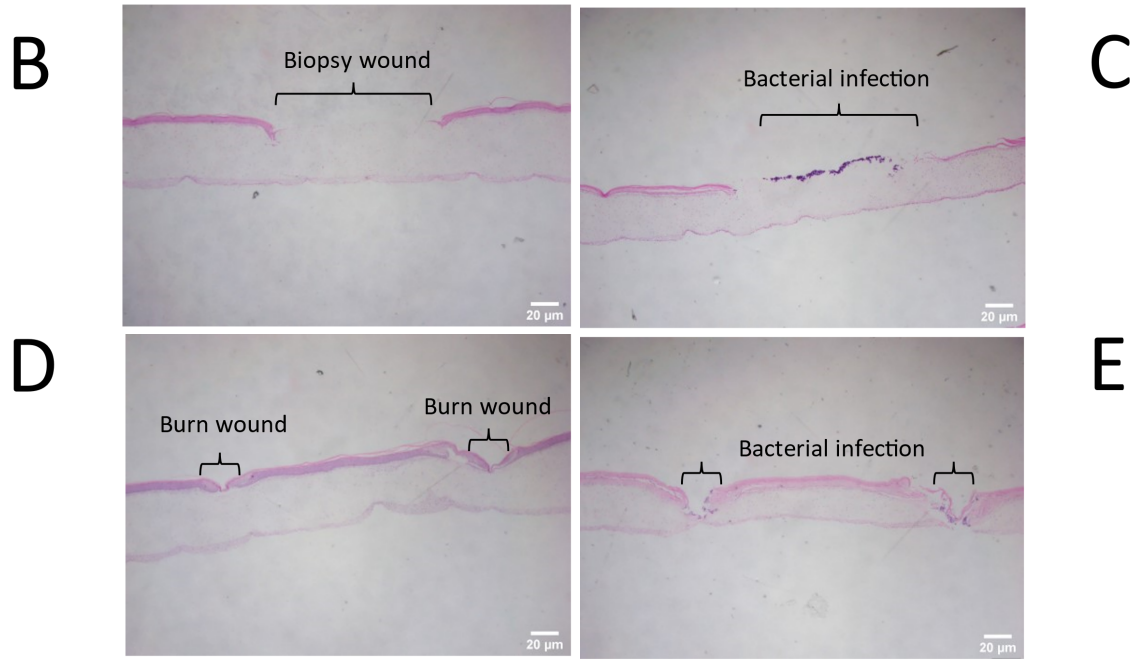


**Figure 3.8 Histology of pre-wounded commercially available models**

H&E-stained cross sections of commercially available collagen-based organotypics after 14 days growth at ALI. Keratinocytes were seeded onto a collagen matrix embedded with fibroblasts, forming an epidermis consisting of granular, basal, and spinous keratinocytes, and a fully stratified stratum corneum. **A)** shows a normal, unwounded section which can be found in both wound models imaged at x10 magnification **B)** is a biopsy wounded organotypic with approximately 2 mm of epidermis having been removed from the model **C)** shows the biopsy wounded model after infection with *S. aureus* occupying the areas not protected by the epidermis **D)** is a burn wounded organotypic with sites where a hot metal strip was applied in order to damage the epidermis **E)** shows the burn wounded model after infection with *S. aureus* occupying the areas not protected by the epidermis. Figures 3.8 B-E were imaged at x1.25 magnification.

As shown in Figures 3.8 and 3.9, the biopsy wounded model is the more appropriate platform for infection assays as the wounding is more regular and reproducible. The burn wound models had burns that were variable in the extent of damage and in size, perhaps due to the use of a matrix as delicate as collagen. Whilst the commercially available collagen-based organotypics display excellent morphology, there are multiple issues compared to in-house construction. This is mainly regarding cost; MatTek models are individually expensive and require a specialised media that is only provided by MatTek at additional cost and whose formulation is proprietary. The experiment involving these models must also be performed within 18 hours after arrival

as the company claims the models cannot last much longer in culture as they were already cultured for 14 days at air-liquid interface prior to arrival. This could be an extremely costly issue should any last-minute issues arise in the lab. However, the greatest issue would be the variability in infection compared to models such as tissue-engineered skin. In the context of a model for infection, the MatTek collagen-based organotypic models were more variable in CFU compared to the tissue-engineered skin models.

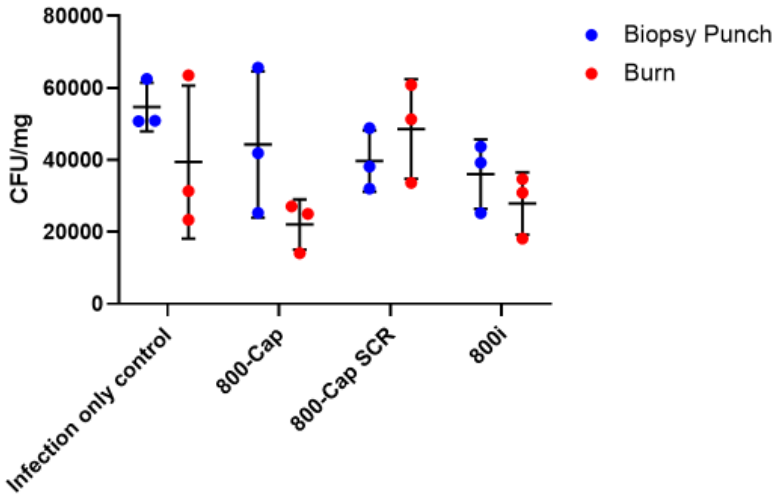


**Figure 3.9 Pre-treatment with CD9-derived peptides on commercially available collagen-based organotypic models against *Staphylococcus aureus* infection**

MatTek organotypic models arrived pre-wounded and were incubated overnight to equilibrate the models after travel. Samples were then pre-treated with peptides for 45 mins before bacterial infection for 5 hours. The samples were then washed to remove non-adherent bacteria before being minced in saponin. The lysate was then plated onto agar plates for CFU counting. Data are shown as CFU/mg of tissue. 1 biological replicate was performed with 3 technical replicates. Data represented as mean ± SD.

### 3.2.9 CD9-derived peptides can reduce *Staphylococcus aureus* adherence to *ex vivo* explant skin

Surgical waste explant skin is regularly available shortly after surgery. Whilst surgical explant skin was gained from circumcisions, breast reductions and abdominoplasties, all samples used in these experiments were taken from abdominoplasties to reduce variability. This is skin that would be the most accurate model for bacterial skin infections as it contains all the structures and cell types found in native skin and, if

quickly added to culture media, could be kept alive for up to 14 days. Whilst it is the most subject to donor variability it was important to test the peptides in this skin to see if the effects were still observable in the most representative context currently available. Upon receiving the skin, it is quickly defatted and then 10mm biopsy punches are taken. These biopsies are subjected to the same burn, pre-treat, and infect methodology as outlined above.

A

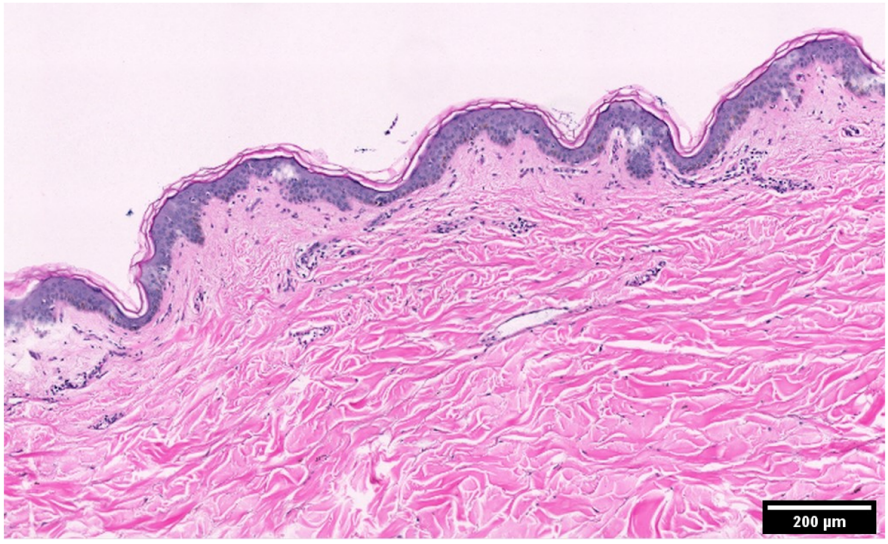

B

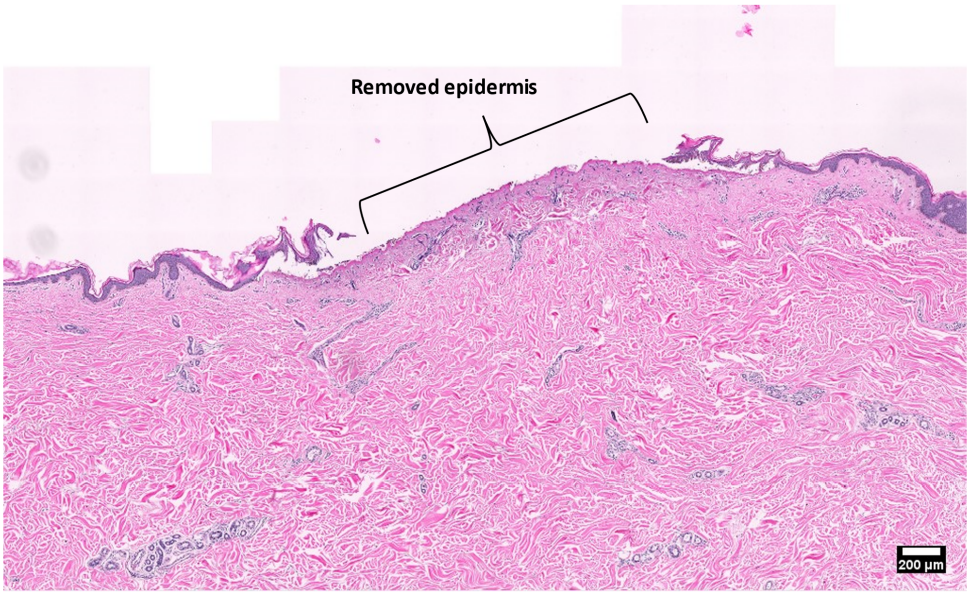


C

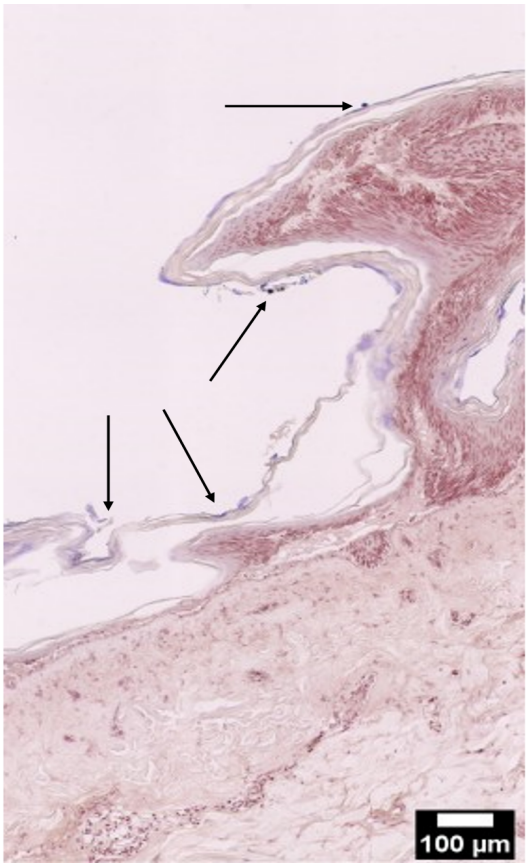

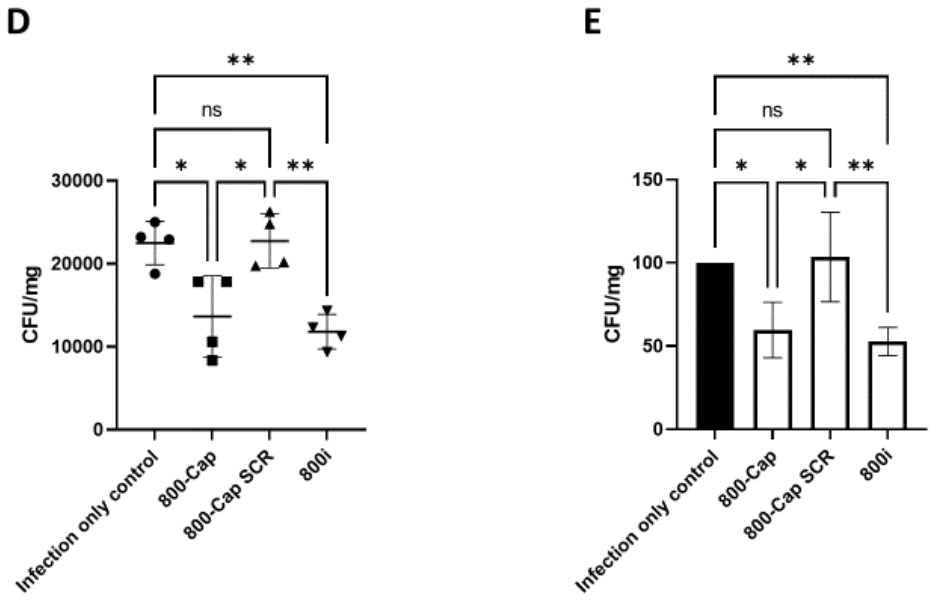


**Figure 3.10 Pre-treatment with CD9-derived peptides reduces *Staphylococcus aureus* adherence on surgical skin explants**

Surgical waste skin was defatted and 10 mm biopsies were taken. **A)** Samples were fixed and sectioned, before being stained with H&E to show structure of native skin at x10 magnification **B)** Biopsies were burned with a soldering iron for 2 seconds**.** Biopsies were then pre-treated with 200 nM CD9-derived peptide or their scrambled control for 45 minutes before the skin was infected with SH1000 for 5 hours. **C)** Arrows indicate presence of bacterial colonies as shown by gram staining. Biopsies were then washed and minced in saponin with the lysate plated onto agar plates for CFU counting. **D)** Data shown as mean CFU/mg of tissue **E)** Data plotted as a percentage of the infection only control. Arrows indicate presence of bacterial colonies as shown by gram staining. Data represented as mean ± SD. Data are normally distributed as determined by the Shapiro-Wilk Normality test. 3 biological replicates performed with 3 technical repeats. Data analysed by One-way ANOVA with Sidak's multiple comparisons test. *p ≤0.05 **p ≤0.01

Much like the infection assays seen with HaCaT cells and tissue-engineered skin models, tetraspanin-derived peptides were still effective in reducing bacterial infection (Figures 3.2 and 3.4). As seen in Figure 3.10, peptides 800-Cap and 800i both reduce the percentage of bacterial infection by roughly 40%, a reduction that is not seen in

the infected control, nor the 800-Cap scrambled control. As the 800-Cap scrambled control had no effect at all on the percentage of bacterial infection, this indicates that the specific amino acid sequences of the peptides found in 800-Cap and 800i are essential for the anti-adhesive effect observed and that this effect can be seen from simple 2D assays up to more complex 3D skin models and up to even more complex native skin biopsies.

## 3.3 Discussion

In this chapter, we compared three types of human skin models: tissue-engineered skin, collagen-based organotypics and surgical explants. All three models have been used extensively throughout the decades for various avenues of skin research. The tissue-engineered skin model first developed by the MacNeil lab in Sheffield in 1999 has been reproduced and adapted by labs as far as Australia (Xie et al., 2010), and is still used in the basis of research over 20 years later (Bolle et al., 2020). Collagen-based organotypics have been used extensively globally with optimisation over time (Arnette et al., 2016; Carlson et al., 2008), and explants have been used the longest (Beaven and Cox, 1965; Neil et al., 2020). For comparing and contrasting the models, we used the following criteria:

### 3.3.1 Accessibility of materials

In comparing these models, we studied the materials and methodology needed to use each model and tried to determine the strengths and weaknesses of each model. Collagen-based organotypics are the easiest to work with in terms of ethics and material acquisition. The most difficult aspects would be acquiring culturing primary keratinocytes and fibroblasts as the reagents and plasticware are commercially available globally. Even then, Kühbacher et al. published a protocol for constructing collagen-based organotypics using commercially available cell lines, Ker-CT keratinocytes and S1F fibroblasts (Kühbacher et al., 2017). Tissue-engineered skin and explant usage is limited due to ethical concerns relating to patient samples and consent. The usage of surgical waste skin requires project approval under the Human

Tissue Act as well as a collaboration with a surgeon for regular supply. Storage of surgical waste skin can also lead to storage issues as surgical waste skin in the UK must be stored in a licensed site that is approved by the Human Tissue Act. The Human Tissue Act dictates the usage of skin and has strict guidelines regarding its collection, handling, and disposal. The licensing to approve a lab for handling and storing skin alone can be prohibitively expensive. In addition, the Human Tissue Act requires researchers handling the skin to be vaccinated against Hepatitis B.

Financially, collagen-based organotypics can be the most expensive of the studied models. This is due to the amount of single use plasticware required (transwell inserts and deep well plates) and the need for high-concentration collagen (8-10 mg/ml). Tissue-engineered skin would be cheaper to construct and is methodically less intensive, however it can also be expensive as it requires custom surgical grade stainless steel rings and grids; however, these are one-off purchases that would last year's assuming they are well maintained. Explants would be the cheapest as they only require the media to sustain them and a biopsy punch to take samples.

### 3.3.2 Structure

In terms of the structure and architecture of the skin, surgical explants are the obvious gold standard as they contain all the structures such as rete ridges, hair follicles and sweat glands. Tissue-engineered skin was ranked second in structure, the epidermis had fully differentiated, and still possessed structures such as rete ridges, however, structures such as hair follicles and sweats had been lost due to a loss of trichogenicity during cell culture (Chan et al., 2015; Higgins et al., 2013; Zhang et al., 2020). Collagen-based organotypics were the least structurally relevant as they did not possess any structures such as sweat glands or hair follicles, and their dermis was solely made of rat tail type-1 collagen. The lack of structures was noticeably important as wounding the collagen-based organotypics could detach the epidermis. Aleemardani et al. discussed the importance of the dermal-epidermal junction and how its anatomical structures, namely rete ridges play a vital role in maintaining structural integrity (Aleemardani et al., 2021).

A lack of rete ridges is seen in the skin disease epidermolysis bullosa, a disease characterised by a loose dermal-epidermal junction that means the epidermis is easily

detached from the dermis and painful blisters can form under minor stress (Bardhan et al., 2020). Various models have been published with the intention of better mimicking and studying the dermal-epidermal junction, with some models being able to succeed in forming rete ridges (Bush and Pins, 2012; Malara et al., 2020; Viswanathan et al., 2016). However, these models all required sophisticated tissue-engineering techniques such as photolithography, electrospinning, and laser structuring. These techniques require specialised equipment which can prevent many labs from reproducing these models, whereas the collagen-based organotypic models described in this study only required relatively accessible lab equipment such as pipettes, centrifuges, and incubators.

Explant skin has the best architecture of skin; however, it is also the most variable due to donor variability, tissue-engineered skin is also subject to donor variability and collagen-based organotypics, whilst the least representative model of the three described, is the most reproducible. Whilst all three models formed a well-differentiated epidermis, this was only qualitatively analysed with H&E histology. This could have been improved using immunohistochemistry to examine the expression of epidermal proteins such as loricrin, K5/K14 or Ki67. This analysis would provide a deeper insight into the structure of the epidermis and the differentiation of the epidermal layers. This would be useful as it could inform us as to the health of the keratinocytes and how many keratinocytes have terminally differentiated. Another staining of interest would have been for CD9 expression. Ventress et al. published evidence showing that CD9 expression correlated with keratinocyte differentiation, specifically that undifferentiated keratinocytes had a higher expression of CD9 compared to differentiated keratinocytes (Ventress et al., 2016). Given that these models were to be used for testing of a CD9-derived peptide, histological staining for CD9 expression would have provided interesting data comparing the CD9 expression in different human skin models could indicate how effective the peptides would be.

### 3.3.3 Methodology

From a technical perspective, all three skin models require different techniques to prepare. Collagen-based organotypics require delicate mixing to ensure the cells are

properly mixed and distributed throughout the suspension without losing too much collagen to the stirrer due to the collagen's viscosity, as well pipetting gently enough to prevent bubbles appearing in the model and affecting the formation of the epidermis. Tissue-engineered skin requires careful handling as it is derived from human tissue and is typically processed with an extremely sharp dermatome. Care must also be taken to ensure the skin is the right way up (papillary region facing upwards); otherwise, the keratinocytes will struggle to adhere to the skin and form a well-differentiated epidermis. The steel ring also used to initially contain the fibroblasts and keratinocytes must also sit properly on the dermis and form a tight seal to prevent the cell suspension from leaking out. Explant skin is the easiest to handle, although care must be taken with the handling of the dermatome (should it be used), the surgical scissors if the explant requires defatting and the biopsy punch to take samples for experimentation. For the tissue culture to grow the epidermis, both tissue-engineered skin and collagen-based organotypics require 14 days of culture at air-liquid interface. Explant skin, which can be kept alive with media for upwards of 3 weeks (Frade et al., 2015; Jacobs et al., 2006) is technically dying tissue and this may need to be considered as possibly affecting the experiment. Regarding cell culture, explant skin requires no cell culture preparation beyond the preparation of media to sustain the explant long enough to last the experiment. Tissue-engineered skin requires careful timing as both the fibroblasts and keratinocytes must be both ready on the same day for construction. Collagen-based organotypics can be more forgiving as the fibroblasts can survive polymerisation inside a collagen gel for at least 1 week before the keratinocytes are ready for use (Salgado, Pers Comms).

### 3.3.4 Wounding and supporting bacterial infection

Regarding skin models in terms of wounding, both tissue-engineered skin and explants were the easiest to wound. Both models were robust enough that they could consistently support a burn wound where the epidermis could be removed with little surrounding damage from the burn site. As described in section 3.2.7, collagen-based organotypics could not be consistently wounded and were more fragile. A dragging motion made with a scalpel could detach the entire epidermis from the model, and the depth of wound could not be controlled and burning the model caused the collagen to

melt. Application of a wound could not be consistently performed on an in-house collagen-based organotypics as the biopsy punch would not pierce the epidermis and consequently crush the dermis below. However, it was possible to purchase such a model from MatTek.

Specialist industrial companies such as MatTek are capable of reliably wounding collagen-based organotypics by using a biopsy punch to remove a specified area of epidermis without compromising the integrity of the dermis below. However, how MatTek can perform such a task reliably and so cleanly is a proprietary secret. In addition, even MatTek are unable to consistently apply a burn wound to their models. The collagen-based organotypics as produced by MatTek may be an industry gold-standard but they are restrictive in that the experiment must be performed roughly 24 hours after delivery and each model can be prohibitively expensive.

Regarding skin models in terms of infection, all 3 models could support a bacterial infection. However, models using a human dermis (tissue-engineered and surgical explant), had higher levels of infection. This is likely due to the human dermis having more adhesion targets for *S. aureus* to bind to. Collagen-based organotypics had lower levels of bacterial infection however, it was notable that the biopsy wounded collagen-organotypic model, which was commercially available from MatTek, had greater levels of infection compared to the burn wounded model. This could be down to the biopsy wounds being consistently made, exposing more of the dermis for bacterial invasion. The burn wounds were inconsistently made, with the wounding sometimes not fully compromising the epidermis. As previously shown by Shepherd et al., a wound was necessary for studying *S. aureus* infection in the model as inoculation of the skin without prior burning of the epidermis did not result in bacterial invasion of the tissue (Shepherd et al., 2009). However, there are skin models which studied *S. aureus* infection without wounding. Reddersen et al. report the use of a collagen-based organotypic skin model whereby a *S. aureus* suspension was topically applied to the surface of epidermis as a tool for evaluating the activity of antiseptics (Reddersen et al., 2019). In this study the authors were able to infect the skin model and described epidermal damage similarly described by Shepherd et al. (Shepherd et al., 2009), and the results described in Figure 3.6. In Figure 3.6B, the epidermis near the wound site is still adhered to the dermis, whereas in Figure 3.6C the infected epidermis had

completely detached from the dermis. Furthermore, the topical application of antiseptics is similar to the topical application of the tetraspanin-derived peptides described in this chapter. This demonstrates that the collagen-based organotypic model may in fact be suitably used without wounding. However, it should also be considered that Reddersen et al. used a significantly higher CFU (skin was infected with 5 µL of $1x10^9$ CFU/mL) and the skin was infected for a longer period of time (24 hours). Additional evidence of a skin model of bacterial infection without the need for wounding is provided by Nakatsuji et al., who investigated the mechanisms behind *S. aureus* invasion into the epidermis. The authors were able to show that *S. aureus* could penetrate the epidermis and were found to be detectable beyond the basement membrane after 48 hours of incubation (Nakatsuji et al., 2016). However, it should also be noted that the collagen-based organotypics used by Nakatsuji et al. were cultured at an ALI for only 7 days. As evidenced by the histological data from Arnette et al., 6 days of ALI gave a well differentiated, but not fully differentiated, epidermis. Whilst the different layers of the epidermis can be observed, the stratum corneum will not have been fully formed, possibly aiding *S. aureus* invasion (Arnette et al., 2016). However, using a shorter ALI culture time could be considered as a possible model for studying bacterial infections given that it may bypass the need to wound the model.

To summarise, we have compared multiple models of human skin as a platform for sustaining a bacterial infection for suitability for peptide testing. Once factoring the materials and technical ability to construct and wound these models, we found that tissue-engineered skin and skin explants were the most suitable models available. This is because these two models supported the most bacterial infection as measured by CFU counts. Furthermore, these two models could be the most consistently wounded allowing for less variation between CFU counts. Between these two, explants would be the preferable choice due to their superior structure, however tissue-engineered skin models could be advantageous if the supply of skin were irregular.

### 3.3.5 Peptide testing

In this chapter it has been shown that the improved peptides, based on the EC2 domain of tetraspanin CD9, can reduce the adherence of *Staphylococcus aureus* to a

variety of human skin models ranging from HaCaT cells in a 2D *in vitro* assay, to tissue-engineered skin models in a 3D context, and finally to fresh *ex vivo* surgical explants. This effect is not seen if the models are not treated with the peptides or with the scrambled control. As the scrambled controls are peptides containing the same amino acids as 800-Cap but in a random sequence, and that the scrambled peptides are manufactured by the same supplier as the peptides of interest (800-Cap, 800i and 800ii), it is suggested that the anti-adhesive effect observed in the skin models are specific to tetraspanin CD9 and is not a nonspecific effect. Impressively, the efficacy of the peptides is maintained across increasingly complex models despite the introduction of various elements to each model. In HaCaTs, tissue-engineered skin and skin explants, the peptides were able to reduce adherence of *S. aureus* by roughly 50%. The only model this effect was not seen was in the collagen-based organotypics, peptide pre-treatment was able to reduce bacterial adhesion however this was only a trend and not significant. This is likely because the collagen-based organotypics were difficult to wound consistently between samples and organotypics contracted irregularly during its development. Commercially available organotypics are available which can overcome these problems. However, even these models have limitations; firstly, these commercial collagen-based organotypics can be prohibitively expensive, which is why the experiment in section 3.2.8 was performed once. Secondly, as seen in the pre-wounded burn models, the wounds were inconsistent, as shown in figures 3.8 D and E, the wounds vary in depth and width.

Whilst a significant effect was seen with the peptide, at least 40-50% of the cells or tissues still had adherent bacteria despite the pre-treatment. This could suggest that some of the bacteria were resistant to the treatment, however as this therapeutic is host-directed, it may be because *S. aureus* relies on multiple mechanisms to adhere to cells, which are CD9-independent. An example of alternative adherence mechanisms are the MSCRAMMs such as autolysin (Atl) or serine-rich adhesion for platelets (SraP) (Josse et al., 2017). The mechanisms involving adhesion with these proteins are independent of fibronectin described in 1.3.2 and it is yet to be determined if the peptides affect the organisation of these MSCRAMMs target proteins. This may indicate that tetraspanin-derived peptides may be best used as part of a wider treatment plan or preventative rather than independently. Whilst peptide treatment can significantly reduce the burden of infection and consequently greatly improve recovery,

it was not observed to completely remove bacteria. It would be worthwhile to evaluate these peptides using the previously described skin models in tandem with other therapeutics to see if bacterial presence could be cleared faster. It is interesting to note that, whilst CD9 expression was high in keratinocytes, it was not seen in dermal fibroblasts. Interestingly, tetraspanins CD63 and CD151 had a high expression on fibroblasts but not on keratinocytes (Ventress et al., 2016). Given that the CD9-derived peptides confer protection to keratinocytes due to their CD9 expression, anti-CD63 or anti-CD151 peptides might be developed to potentially confer protection to fibroblasts.

A 50-60% reduction from untreated/scrambled controls was seen with 800-Cap and 800i against SH1000 at a concentration of 200nM, this effect was reduced when skin models were pre-treated with peptides at a concentration of 20 nM to roughly a 30% reduction of bacterial infection. This was surprising as 2D *in vitro* assays testing the peptide at 20 nM have shown the peptide to still reduce bacterial adherence by 50%. This may be down to the increased complexity and size of the model resulting in not enough peptide interacting with the CD9 binding sites exposed after wounding. 20 nM may be the lower threshold for an effective dosage, and the minimum dosage needed to remove 50% of adherent bacteria may lie somewhere in between 20 nM and 200 nM.

Given that pre-treatment reduces bacterial load, this decreased infection would be easier for the body to control and clear or perhaps easier for a treatment to clear infection. It would be relevant for future work to include additional time points beyond 24 hours to see if this protection is sustained and if a wound model would heal faster with peptide treatment. The mechanism behind the peptides' ability to reduce *S. aureus* adherence has not been fully characterised. However, it has been determined that the peptides are functioning in a similar manner to recombinant CD9 EC2 proteins, which has been shown to decrease the clustering of TEM-associated adhesion proteins as previously described (Green et al., 2011). Future work could include generating skin models with keratinocyte knockouts with individual adhesion proteins being knocked out to see how they relate to TEM clustering and CD9-derived peptide efficacy. This could also be used to observe if it is a protein targeted by pathogens such as *S. aureus* for adherence prior to infection or how it pertains to the development and structure of the epidermis.

The previous generation of peptides were effective against a variety of other pathogens (Ventress et al. 2016). Ventress et al. were successful in demonstrating the CD9-derived peptides could reduce infection of skin models against other strains of *S. aureus* including lab strains and more virulent, clinical strains. It would be clinically relevant to repeat the experiments performed in this chapter to see if this treatment is successful against other strains of bacteria e.g., *E. coli* and *P. aeruginosa* to see the different levels of inhibition.

Surgical skin explants may provide useful information in this regard as it already contains residential immune cells. The cells it lacks for an infection context are the neutrophils that can migrate towards a site of infection. Given that the peptide pre-treatment on the skin explants were able to reduce bacterial adhesion, it is important to determine if the peptides are able to function without affecting the residential immune cells present such as Langerhans cells.

To summarise Chapter 3, we compared and contrasted multiple human skin models to develop as a platform for bacterial infection for the purposes of drug testing. Ultimately, we developed a model for infection and drug treatment demonstrating that pre-treatment with CD9-derived peptides can reduce the adherence of *S. aureus* to host cells. This effect is demonstrated in multiple 2D and 3D models however the effect appears to be limited to roughly 50% reduction, indicating that pathogens such as *S. aureus* may have multiple mechanisms of adhesion and infection, which must also be addressed during treatment. The effects of the peptides are still unknown regarding immune cell function. Therefore, work was carried out in Chapter 4 to determine the safety of the peptides.

# Chapter 4 Towards the development of an immunocompetent skin model

## 4.1 Introduction

### 4.1.1 Tetraspanin peptides and CD9 expression

As mentioned earlier in Chapter 1, the Monk Lab has previously shown that CD9-derived peptides can reduce bacterial adhesion. As these peptides have not been tested on immune cells, it was important to test for any interference with normal immune function by the peptides. This is especially important as CD9 is a ubiquitously expressed protein. CD9 is expressed by all the major leukocyte subsets and also in high levels by endothelial cells (Reyes et al., 2018). CD9 expression has been studied globally due to its involvement with a wide variety of cellular processes such as cell adhesion, motility, membrane fusion and signalling (Andreu and Yáñez-Mó, 2014; Hemler, 2005).

CD9 plays a vital role in multiple immune cells such as the chemotaxis of mast cells and MHC II trafficking in dendritic cells (Brosseau et al., 2018). This reiterates the importance of testing the CD9 peptides on immune cells, at least initially for a function the immune cells tested in this study all share, phagocytosis.

### 4.1.2 Phagocytosis

In the initial response to infection, macrophages and neutrophils will be amongst the first responders to arrive at the site of infection. Commonly, these phagocytes will tackle invading pathogens and necrotic cells via phagocytosis. Phagocytosis is the process by which a cell internalises its target (a particle larger than 0.5 μm) to remove microbes or cellular debris, and to present the antigens to lymphocytes to initiate the adaptive immune response (Uribe-Querol and Rosales, 2020). Initially, a phagocyte will detect a target particle by its surface receptors, which are divided into opsonic and non-opsonic receptors. Opsonic receptors such as Fc receptors (FcR) and complement receptors detect host-derived proteins e.g., antibodies, complement and

fibronectin that have bound to target particles to label them for phagocytosis (Flannagan et al., 2012). Non-opsonic receptors detect PAMPs such as C-type lectins or scavenger receptors. Once a phagocyte has bound to its target, the actin cytoskeleton will remodel itself to engulf the particle. The target is then fused with the phagocyte's lysosome, an organelle containing a variety of enzymes to degrade and lyse the target (Canton, 2014).

### 4.1.3 Phagocytosis of *Staphylococcus aureus*

Epithelial cells such as keratinocytes can sense *S. aureus* via PRRs and detect foreign PAMPs such as LTA, protein A and peptidoglycan. Upon recognition, PRRs begin signalling pathways that result in the production and release of pro-inflammatory cytokines and chemokines e.g., GM-CSF, IL-6 and IL-8 to attract phagocytes to the site of infection (Pidwill et al., 2021). However, *S. aureus* can inhibit this recruitment via the expression of CHIPS which prevent phagocyte binding to *S. aureus* through both the opsonic and non-opsonic receptors (de Haas et al., 2004). As phagocytosis is a major function that contributes to the clearance of a *S. aureus* infection, we sought to investigate how the peptides may affect this action.

### 4.1.4 Langerhans cells

Another APC that resides in the skin is the Langerhans cell. These cells are tissue-resident macrophages that possess DC qualities (West and Bennett, 2018). Despite their macrophage ontogeny, LCs function by taking up and processing foreign antigens and migrate towards the lymph nodes to interact with T cells. A classic cell line used in the research of Langerhans are MUTZ-3 cells. MUTZ-3 cells were isolated from a male diagnosed with acute myelomonocytic leukaemia. Once cultured in a specific cytokine cocktail, MUTZ-3 cells differentiate into Langerhans-like cells that display a similar phenotype to LCs. MUTZ-3 cells have shown themselves to be a human cell line model for the cytokine-induced differentiation of DCs from $CD34^+$ precursors and a useful model for researchers requiring a LC model that does not suffer from donor

variability, nor a lack of access to human skin tissue from which to isolate the Langerhans cells (Masterson et al., 2002).

### 4.1.5 Immunocompetent human skin models

In researching skin for drug testing or for infection models, a commonly used type of model is the collagen-based organotypics. Collagen-based organotypics provides researchers a model to facilitate the study of function and structure of skin that also allows the addition of genetic manipulation and use of patient cells to investigate and validate disease mechanisms and pathways. They also provide an opportunity for researchers to integrate immune cells to observe their function in isolation. Whilst this is difficult and time-consuming, several labs have successfully generated immunocompetent human skin models by integrating immune cell types such as MUTZ-3 Langerhans-like cells to study skin irritation however, it would be useful to also use these models for biofilm studies or infection assays. Human skin models constructed from de-epidermised dermis have been used for immunocompetent models however, this is rarely done as surgical waste skin is often in short supply. Immunocompetent skin models are a limited area of research as there are relatively few publications to lend guidance regarding methodology or potential applications.

The aims of this chapter were to determine if the peptides affected immune function, namely phagocytosis. We hoped to show that the peptides possessed antibacterial properties without preventing immune cells from clearing infection. We also sought to integrate immune cells into human skin models to understand how these immune cells may function in a 3D context and how it may affect the establishment of bacterial infection on human skin models.

## 4.2 Results

### 4.2.1 Determining the MOI of *Staphylococcus aureus* for THP-1s and U937s.

As demonstrated in Chapter 3, the peptides derived from the EC2 domain of CD9 generated by the Monk Lab have shown to be effective in decreasing bacterial adhesion to HaCaT cells. However, it was important to determine if these peptides could inhibit an important element of the immune response in other cell types. Thus, we decided to screen these peptides to see if they had any effect on the ability of THP-1s, U937s and neutrophils to phagocytose bacteria. This was also a good opportunity to compare the two macrophage cell lines, THP-1 and U937, and determine which would be the better model for monocyte-derived macrophages and should be integrated into the 3D tissue-engineered skin model. Firstly, we needed to determine an appropriate MOI to use.

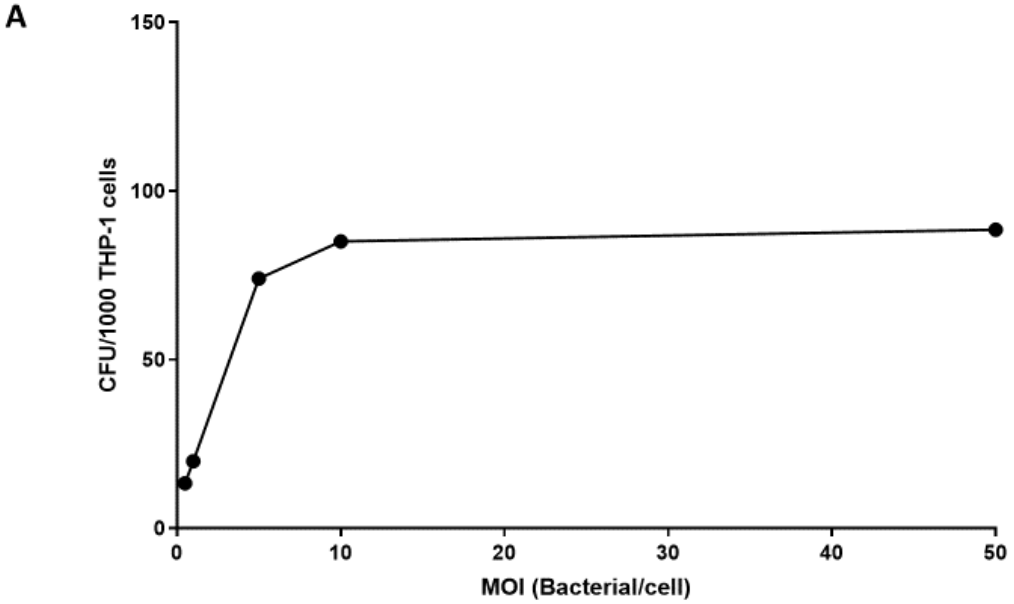

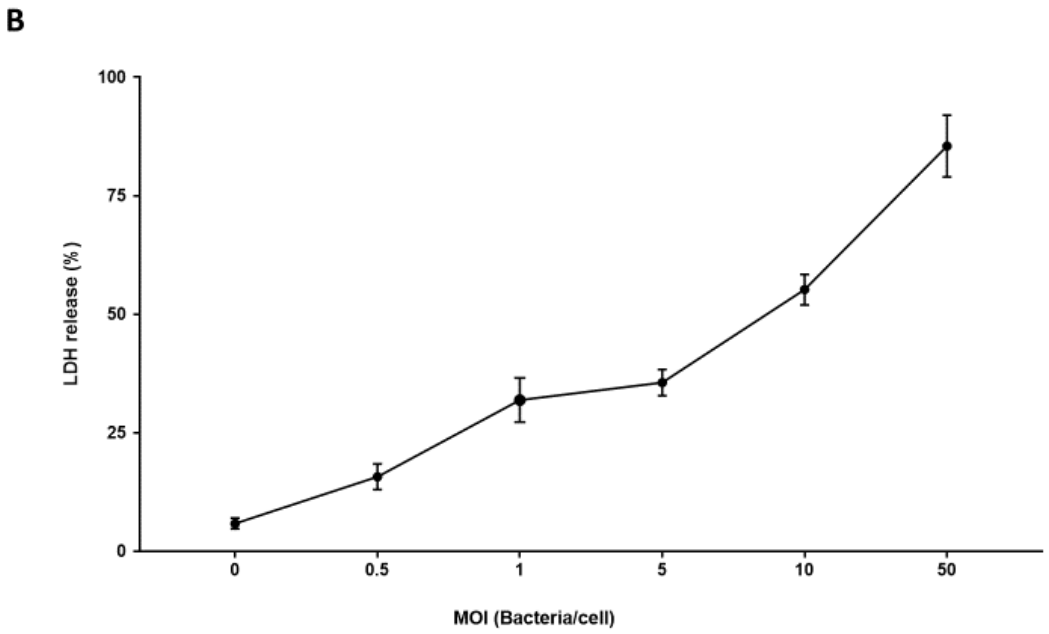


**Figure 4.1 Determining MOI for phagocytosis of *Staphylococcus aureus* by THP-1 cells**

THP-1 cells were infected with SH1000 at MOI 0.5, 1, 5, 10 and 50 for 2 hours. THP-1s were then lysed with saponin and the lysate was then plated onto agar plates for CFU counting to determine bacterial adhesion. **A)** Data shown as CFU/1000 THP-1 cells **B)** Supernatant collected after bacterial infection analysed for LDH released by THP-1s after phagocytosis of *S. aureus*. Data are represented as mean ± SD. 1 biological replicate performed with 3 technical repeats.

Using a phagocytosis assay based on a previous study (Jubrail et al., 2016), THP-1 derived macrophages were infected at MOI 0.5,1, 5, 10 and 50 for 2 hours. From Figure 4.1A, the most suitable MOI would either be 5 or 10 given that the CFU/1000 cells sharply increased from MOI 0.5 to 5, then only marginally increased from 5 to 10 and tended towards a plateau from MOI 10 to 50. This is likely due to saturation of the high affinity adherence sites on THP-1 cells. MOI 5 was chosen because Jubrail et al. reported that THP-1 cells have a finite capacity to phagocytose bacteria that are saturated at MOI 5.

For the LDH assay in Figure 4.1B, we set the limits of LDH release using media only for 0%, and the LDH values for triton for 100% LDH release. Combined with the LDH assay data in Figure 4.1A, we can observe a steady rise in LDH released up to MOI 5 after which LDH release sharply increased. We conclude from this experiment that

increasing the MOI appears to increase the amount of LDH released from the cell. This suggests that during phagocytosis, *S. aureus* causes damage to the cell that increases with MOI. From these experiments, we determined that subsequent experiments should use an MOI of 5.

### 4.2.2 CD9-derived peptides do not affect the ability of THP-1, U937s nor primary neutrophils to phagocytose bacteria.

We wanted to determine if the peptides would negatively affect phagocytosis of *S. aureus* in macrophages and neutrophils. To observe this, THP-1s and U937s were differentiated with PMA into macrophages and primary neutrophils were isolated from blood donors. We pre-treated the cells with 200 nM of the CD9-derived peptides before being infected with the SH1000 bacteria strain. Figure 4.2 shows the number of bacteria phagocytosed by the tested cells as determined with CFU counting. Treatment with 800-Cap or the 800i peptide does not alter the ability to phagocytose bacteria. We also noticed that THP-1 cells were by far the more phagocytic of the two cell lines. We found on average a CFU/1000 THP-1 cells of roughly 1000 bacteria, this equates to 1 THP-1 cell phagocytosing 1 bacterium. This is very low given that macrophages can typically contain dozens of bacteria (Gray et al., 2016) but this low intake may be explained by the low MOI. This CFU/1000 cell is ten times higher compared to U937 cells (Figure 4.2 and 4.3) which on average phagocytosed roughly 0.1 bacteria per cell. Based on these results, THP-1 cells may be a better model of macrophages than U937s and would be preferable for integration into a tissue-engineered skin model using a DED.

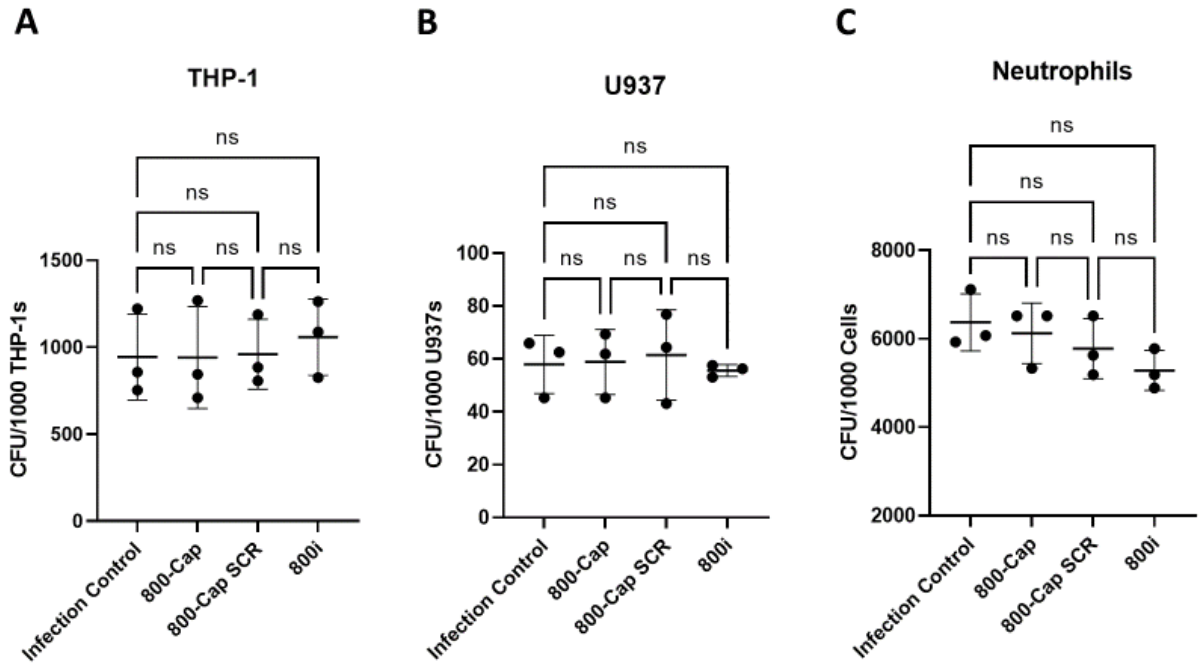


**Figure 4.2 Pre-treatment with CD9-derived peptides does not affect phagocytosis in immune cells**

THP-1s and U937s were differentiated into a macrophage phenotype by incubating with PMA for 72 hours. Primary neutrophils were isolated from patients, plated then incubated for 45 mins to allow them to settle before treatment. All cell types were treated with 200 nM CD9-derived peptides for 45 mins before infection with SH1000 at a MOI of 5. Cells were then treated with gentamicin to kill non-internalised bacteria. The cells were then lysed with saponin, and the lysate was plated onto agar plates for CFU counting. Phagocytosis was determined as the number of internalised bacteria measured with a CFU count. Phagocytosis shown as CFU/1000 **A)** THP-1 cells **B)** U937 cells or **C)** neutrophils. Data was represented as mean ± SD. Data are normally distributed as determined by the Shapiro-Wilk Normality test. 3 biological replicates performed with 3 technical repeats. Data analysed by One-way ANOVA with Šidák's multiple comparisons test.

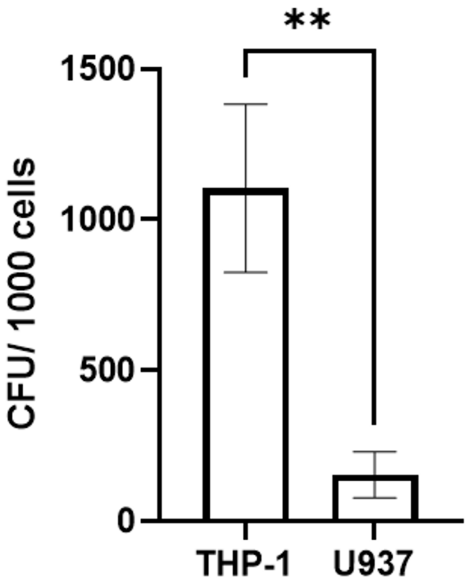


**Figure 4.3 Comparison of bacteria internalised by THP-1 versus U937 cells**

Mean CFU of *S. aureus* phagocytosed by THP-1s versus U937s. Data represented as mean ± SD. 3 biological replicates performed 3 technical repeats. Data analysed by unpaired t-test. **p<0.01

### 4.2.3 CD9-derived peptides do not affect bacterial adhesion to THP-1, U937 nor neutrophils.

As we had previously tested the peptide's ability to reduce adherence of SH1000 against HaCaT cells, we were also curious to see if the same occurred with immune cells. For this, we assessed if 800-Cap and 800i peptides were able to reduce SH1000 adherence to differentiated THP-1, U937s and primary neutrophils, with 800-Cap SCR as a control along with the non-treatment control. Unlike the HaCaT cells, we did not observe any changes in SH1000 adhesion to the immune cells. Figure 4.4 shows the effect of CD9-derived peptides on differentiated THP-1s, U937s and primary neutrophils.

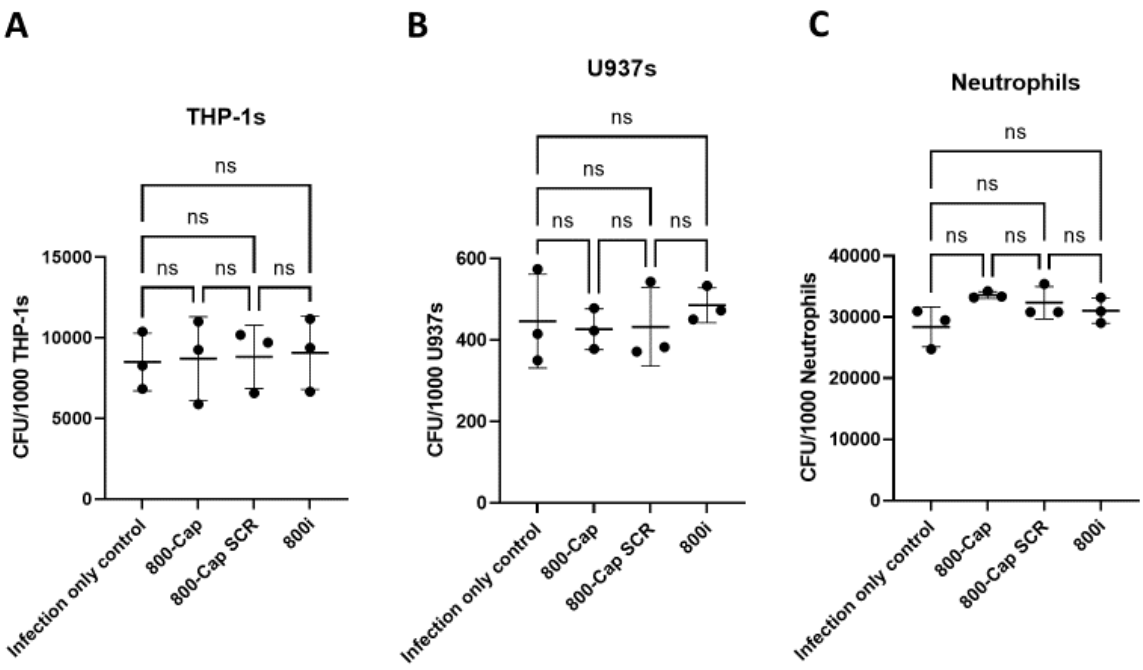


**Figure 4.4 Pre-treatment with CD9-derived peptides does not reduce *Staphylococcus aureus* adherence to immune cells**

2 plates of THP-1s and U937s were differentiated into a macrophage phenotype by incubating with PMA for 72 hours. Primary neutrophils were isolated from patients, plated then incubated in 2 plates for 45 mins to allow them to settle before treatment. All cell types were treated with 200 nM CD9-derived peptides for 45 mins before infection with SH1000 at a MOI of 5. One set of plates were treated with gentamicin to kill non-internalised bacteria, the one set of plates was not. After infection, both sets of plates were treated with saponin to lyse the cells and the lysate was plated onto agar plates for CFU counting. Adhesion was determined as the difference in CFU between the non-gentamicin treated plate (total bacteria) and the gentamicin treated plate (internalised bacteria). Adhesion shown as CFU/1000 **A)** THP-1 cells **B)** U937 cells or **C)** neutrophils. Data are represented as mean ± SD. Data are normally distributed as determined by the Shapiro-Wilk Normality test. 3 biological replicates each performed with 3 technical repeats. Data analysed by One-way ANOVA with Šidák's multiple comparisons test.

Based on Figures 4.2 and 4.4, along with the data from section 3, we found that the peptides had an effect on HaCaT cells but not macrophages or neutrophils. From this, we conclude that the peptides did not negatively affect phagocytosis in macrophages and neutrophils.

### 4.2.4 MUTZ-3 antigen expression changes with differentiation

As part of an attempt to integrate immune cells into collagen-based organotypics, we first needed to differentiate the MUTZ-3 progenitor cells into the Langerhans-like cells for integration into the models. To do this the MUTZ-3 cells need to be cultured in a specified culture medium containing GM-CSF, TGFβ and TNFα. If correctly done the MUTZ-3 cells would increase in expression of CCR6, CD1a and Langerin as performed by Laubach et al, 2011. MUTZ-3 cells needed to be cultured using 5637-conditioned media. 5637 cells are a bladder carcinoma cell line that constitutively secretes cytokines important in the culture of MUTZ-3 cells. The most important of these is GM-CSF, as shown in Figure 4.5, GM-CSF is secreted by 5637 cells and its concentration increases the longer the 5637 cells have to culture. Given that the cells would begin to die after 72 hours in 100% confluency. We decided to harvest the media after 72 hours rather than incubate for longer.

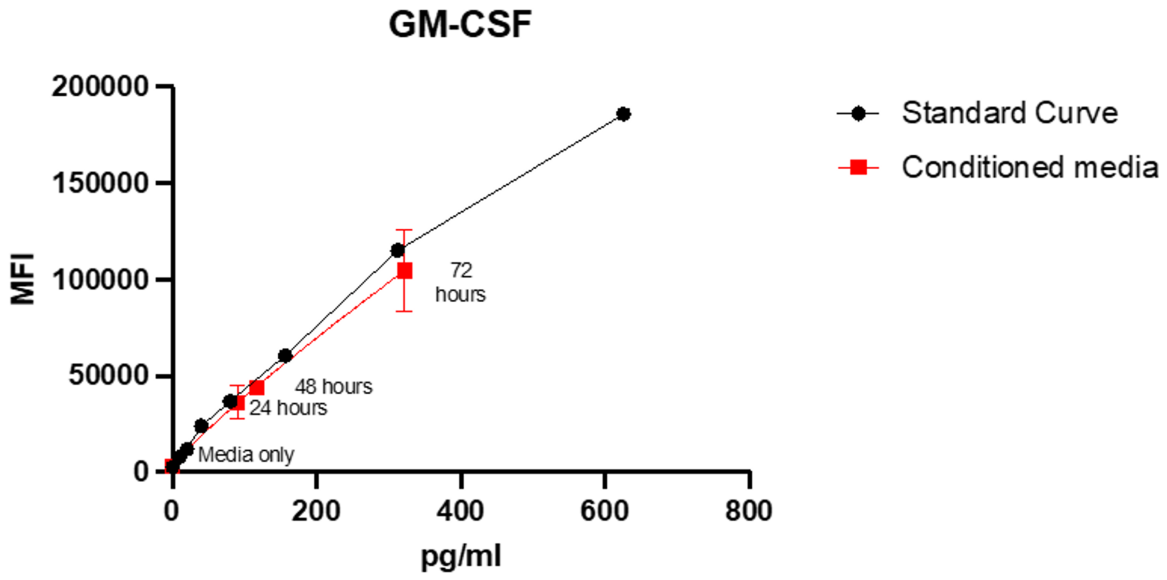


**Figure 4.5 Concentration of GM-CSF in conditioned-5637 media**

$2.5x10^6$ 5637 cells were cultured in a T175 flask and incubated until near confluent. Media was exchanged and the 5637 cells were further incubated for up to 72 hours. Samples of the media were taken and analysed with a CBA assay. Data are represented as mean ± SD. 2 biological replicates performed with 3 technical repeats.

Figure 4.6 shows the expression of CCR6, CD1a and Langerin as measured by flow cytometry. MUTZ-3 cells were cultured for at least 2 weeks before being cultured for a further 10 days in the cytokine cocktail medium as described by Bock et al, 2017. As described in Figure 4.6, we saw an increase in expression of CCR6, CD1a and Langerin in the cells cultured in cytokine cocktail compared to cells in standard media. However, this increase pales in comparison to the data shown by Laubach et al, who saw increases of up to 35% in CD1a and Langerin and 60% in CCR6. Evidently, our attempt to differentiate MUTZ-3 cells was unsuccessful as we only achieved a partial differentiation in a small percentage of MUTZ-3 cells.

Whilst the cytokine cocktail was able to increase expression of CCR6, CD1a and Langerin, it did not increase a sufficient percentage of the MUTZ-3 cells nor was the percentage of expression sufficient as compared to the differentiation done by Laubach et al.

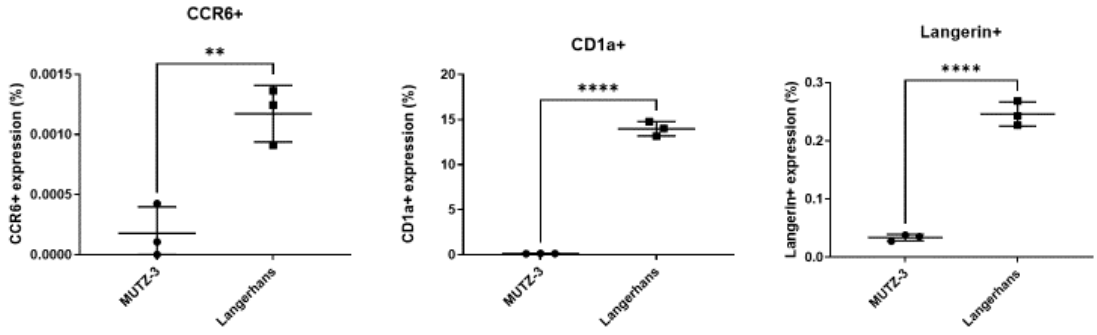


**Figure 4.6 Antigen expression of MUTZ-3 cells changes in presence of cytokines**

MUTZ-3 cells were cultured in a cytokine cocktail before being stained with antibodies for CCR6, CD1a and langerin expression, and assessed with flow cytometry. Data are represented as mean ± SD. Data are normally distributed as determined by the Shapiro-Wilk Normality test. 3 biological replicates performed with 3 technical repeats. Data analysed by unpaired t-test. **p≤0.01 ****p≤0.0001

### 4.2.5 Scalpel wounding on split-thickness skin is unreliable for allowing neutrophil migration

This experiment was to determine if neutrophils would migrate across the dermis and reach the infection site. To see if neutrophils could migrate towards the bacteria rather than the damage caused by burning split-thickness skin was wounded with a scalpel and infected with SH1000, then placed on top of blotting paper holding neutrophils.

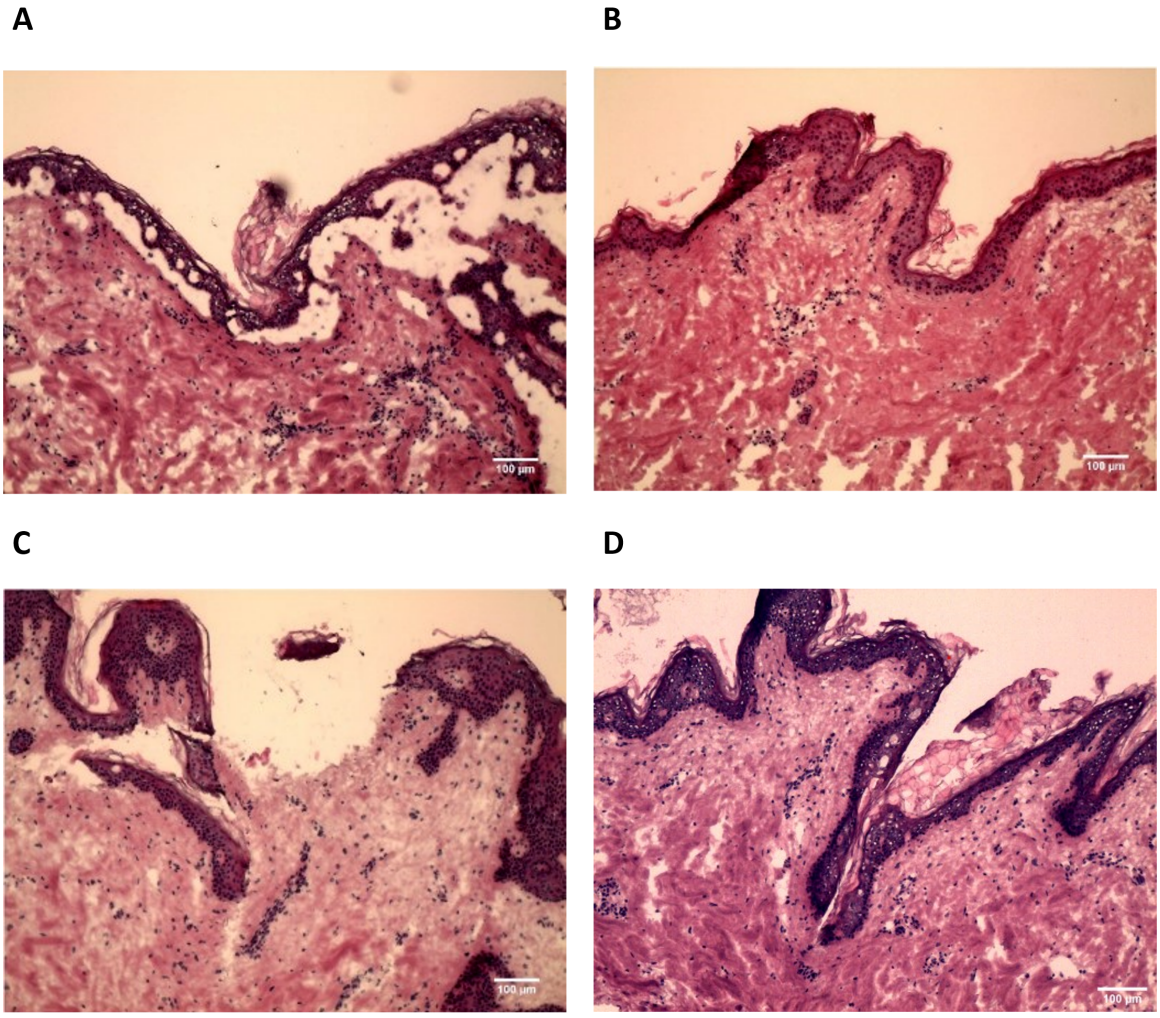


**Figure 4.7 Split-thickness skin wounding and infection**

Skin models were wounded with a scalpel before being infected with a bacterial suspension on top, and neutrophils being added underneath **A)** Skin was wounded then infected **B)** Skin was infected without a wound **C)** Skin was wounded but uninfected. **D)** A skin sample that had been wounded then infected but had displayed no signs of infection as seen by the attached epidermis. All images taken at x20 magnification.

We were able to observe the effects of infection by the detachment of the epidermis from the dermis which is a hallmark of infection by *S. aureus* (Figure 4.7A). We also observed that the epidermis is a competent barrier against infection that prevented *S. aureus* from causing infection when the epidermis was not breached (Figure 4.7B). Whilst the scalpel could generate a wound that removes or bypasses the epidermis (Figure 4.7C), we also saw that a scalpel wound could be ineffective for wounding the skin. The wounds caused by the scalpel were very fine and the skin may quickly close these cuts (Figure 4.7D). Even after a repeat which included stretching the skin after wounding, the skin was able to repair itself. Due to the quick recovery of the skin, we found that some of the controls that should have been infected, were not.

For future experiments, it may be more effective to burn the skin. This would create a more severe wound site that will not recover during the experiment and additionally release more alarmins and DAMPS which may aid the migration of immune cells towards the wound site. We also noticed that $1x10^6$/mL is too low a concentration as the blotting paper cannot contain the suspension. A higher concentration at a lower volume would be needed.

### 4.2.6 C5a can attract neutrophils into the dermis

This experiment was to see if C5a could serve as a better chemoattractant to neutrophils compared to a *S. aureus* infection. This is because C5a is a particularly potent chemoattractant for neutrophils and macrophages (Kew, 2014). To test this, we burnt a piece of DED then incubated it with 200 nM of C5a before incubating it with neutrophils. When the DED was burned with C5a added, we could observe the presence of neutrophils that had migrated into the papillary region of the DED where the soldering iron was applied (Figure 4.8A and 4.8B). As it is DED, there were no keratinocyte structures that could have been stained with H&E. Therefore, all purple structures stained by the haematoxylin are likely to be neutrophils. We do not observe neutrophils migrating into the DED or attraction to the wound site (Figure 4.8C and 4.8D). However, we do observe neutrophil attraction to C5a even without the burn (Figure 4.8E and 4.8F). As we do not see any neutrophil migration into the DED and

only to the surface, a wound site may be needed for the C5a to begin permeating through the DED and thus attract neutrophils into the dermis.

We observed neutrophils in this skin model, which has not been previously documented. However, we cannot easily see the wound site, we also do not see a concentration of neutrophils to a specific site, indicating that the C5a is spread across the skin model. We are able to see the neutrophils in the dermis showing that it is possible for the neutrophils to enter into the tissue. However, judging by the presence of neutrophils in the papillary dermis and absence of neutrophils in the reticular region, with an incubation of 6 hours, it is unlikely that these neutrophils migrated across from underneath the skin. It is more likely that these neutrophils migrated over the skin due to the high volume of the cell suspension. Nonetheless, it is encouraging to see the presence of neutrophils in the skin due to their unique multi-lobular nucleus which can be clearly visualised with H&E.

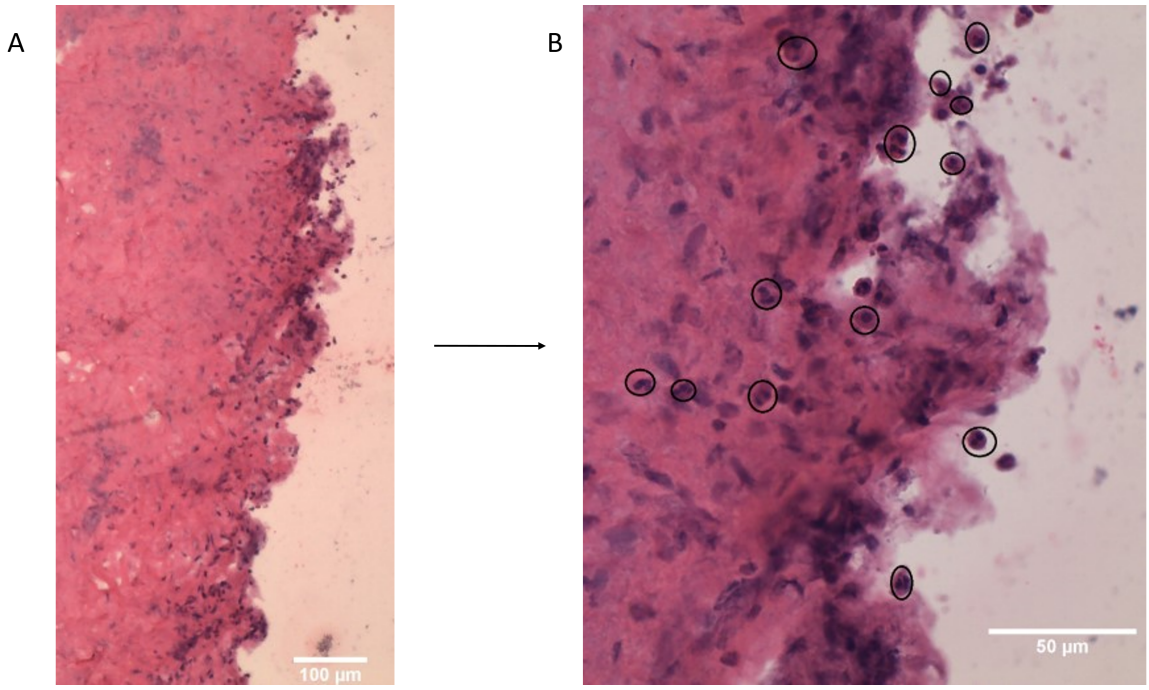

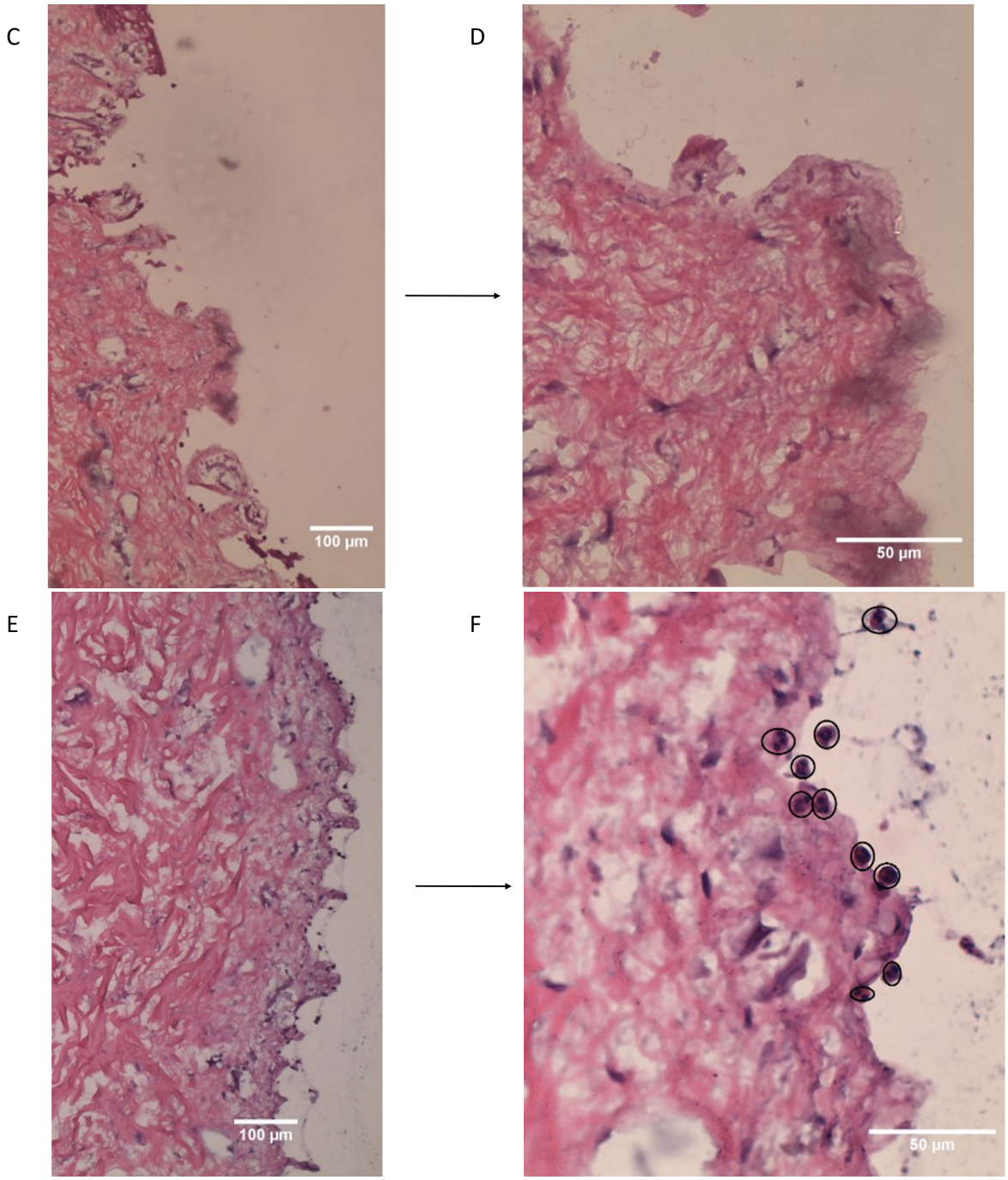


**Figure 4.8 Neutrophil migration across the dermis with C5a treatment**

Dermis was burn wounded before being treated with C5a and having neutrophils added on top. **A)** Burn-wounded dermis treated with C5a at x20 magnification **B)** at x40 magnification **C)** burn-wounded dermis with no C5a at x20 magnification **D)** at x40 magnification **E)** unwounded dermis with C5a at x20 magnification **F)** at x40 magnification. Neutrophils t identified by their nuclear morphology are circled.

### 4.2.7 Euroskin is not suitable for growing tissue engineered skin

The previous experiment was repeated but used DED formed from cadaver skin purchased from the Euro Skin Bank, which has a thinner dermis compared to the engineered skin used in the previous experiment. This was to see if reducing the thickness of the dermis, and therefore reducing the distance required for the neutrophils to migrate, would have any effect on neutrophil influx. Unfortunately, possibly due to how thin the cadaver DED was, the tissue-engineered skin model did not form properly (Figure 4.9). The thinness of the Euroskin made it too delicate and difficult to handle with forceps leading to damage to the dermis, and the epidermis barely formed two layers. This was probably likely because the fibroblasts did not form a sufficient feeder layer for the keratinocytes.

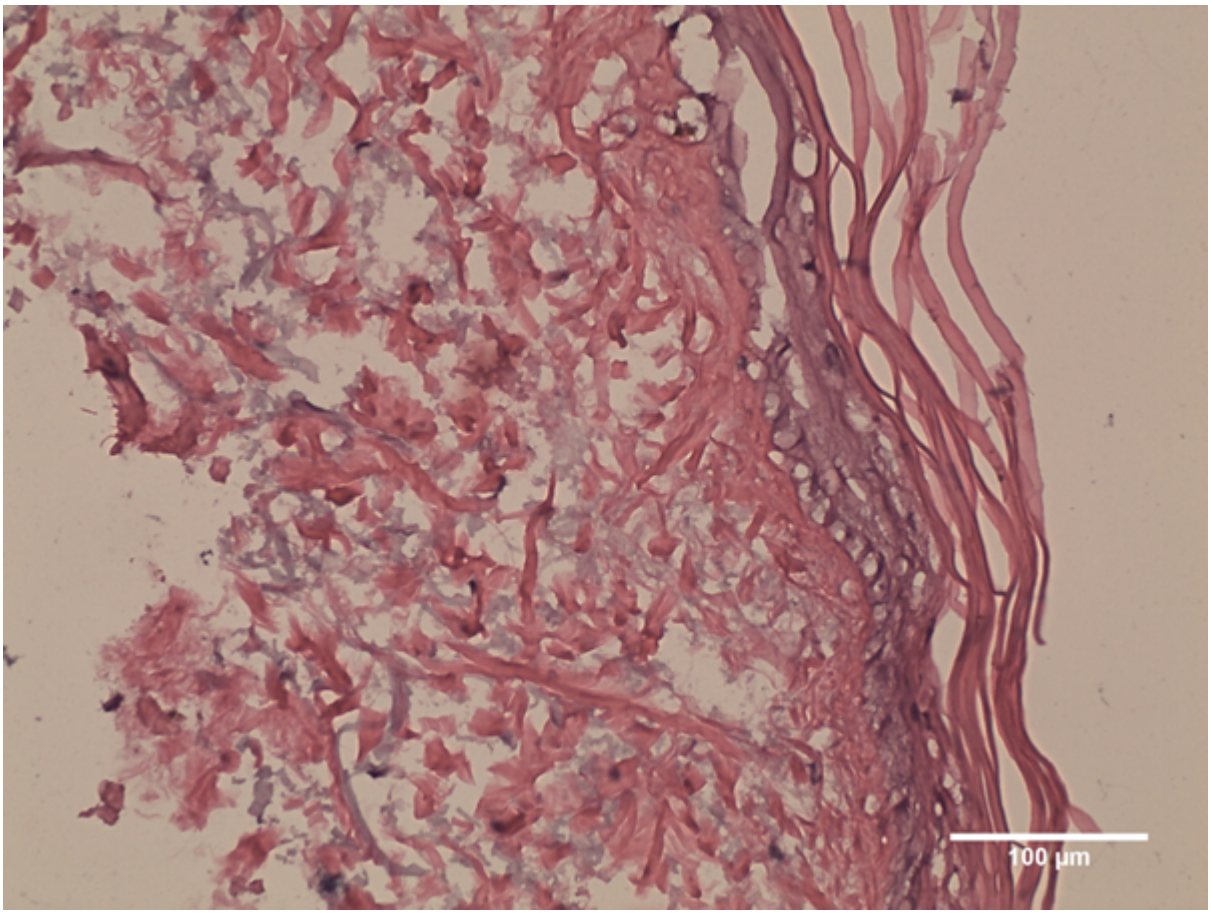


**Figure 4.9 Malformation of the tissue engineered skin**

Euroskin had not properly supported the growth of the fibroblasts or keratinocytes. There is significant damage to the dermis, likely a combination of handling with forceps and 2-3 layers in the epidermis which has separated. This is very different compared

to the tissue engineered skin made with donor DED (Figure 3.3A) image taken at x20 magnification.

## 4.3 Discussion

In this chapter we have shown that the improved peptides do not affect the ability of macrophages and neutrophils to phagocytose bacteria. This was demonstrated in a 2D *in vitro* context that also demonstrated that the peptides did not affect bacterial adherence to these cells. In Chapter 3, we demonstrated that peptide treatment reduced bacterial adherence to human skin models. Combined with the results of Chapter 4, data showing that phagocytosis of SH1000 did not change between peptide treatments, we show that the peptides have an antibacterial effect on keratinocytes without compromising on the ability of immune cells to phagocytose bacteria. This experiment could be improved by performing more assays relating to phagocyte function, such as reactive oxygen species (ROS) and cytokine production. An example of such an assay would be perhaps an enzyme-linked immunosorbent assay (ELISA) which could have measured the concentration of cytokines in the media. Macrophages would have released cytokines in response to the bacteria and released pro-inflammatory cytokines such as TNFα, IL-1 and IL-8 (Arango Duque and Descoteaux, 2014) and it would have better supported our conclusion if we were able to measure the levels of cytokines in the media and if there were any differences between peptide treatments. ROS can be measured using flow cytometric techniques.

CD9 expression is expressed differentially by monocyte subsets with expression being higher in CD16- subsets compared to CD16+ subsets (Tippett et al., 2013). This could be important to consider as peptide treatment could affect monocyte subsets differently. CD9 functionally associates with FcγRs and modifies signals for phagocytosis and inflammatory responses.

As detailed by Kespichayawattana et al., the gram-negative bacteria, *Burkholderia thailandensis*, is capable of surviving in phagocytic and non-phagocytic cells and induce multinucleated giant cell (MNGCs formation, a mechanism that may facilitate cell to cell spread, evasion of the immune system and protect against antibiotics (Kespichayawattana et al., 2004). Sangsri et al. later demonstrated that tetraspanins,

CD9 and CD81, were involved in *B. pseudomallei*-induced MNGC formation. The authors were able to show that pre-treating A549 cells with CD9-EC2 significantly enhanced *B. pseudomallei* internalisation and that CD9-EC2 or anti-CD9 antibodies reduced MNGC formation in mouse macrophages J774.A1 cell line. The authors found that the peptides did not affect adherence, reflecting our data, indicating that perhaps CD9 is not involved in bacterial adhesion in macrophages, as evidenced in THP-1s, U937s and J774A.1s. Additionally, the authors did not observe the CD9-EC2 peptides having an effect on internalisation (Sangsri et al., 2020). Combined with our data, this could indicate that the CD9 peptides could protect macrophages against *Burkholderia* induced MNGC formation, without negatively affecting macrophage phagocytosis. This is similarly shown in the work by Elgawidi et al. Interestingly, Elgawidi et al also showed that an overexpression of CD9 in J774.2 macrophages also showed significant reduction in MNGC formation, and that CD9 KOs enhanced MNGC formation, indicating of a negative regulatory role for CD9 in bacterial-induced fusion (Elgawidi et al., 2020). Based on our data showing CD9 peptides not affecting adhesion in THP-1 and U937 macrophages, CD9, whilst highly expressed on macrophages, may not play a role in bacterial adhesion in phagocytes unlike epithelial cells.

Whilst CD9 expression is low on neutrophils, CD9 expression increases significantly during oral disease, periodontitis, and gingivitis, indicating that CD9 plays a role in neutrophil activation and inflammation resolution (Bisson-Boutelliez et al., 2001). Indeed, Saiz et al, observed decreased neutrophil infiltration in colonic tissue of CD9 KO mice after inducing colitis with dextran sodium sulphate (Saiz et al, 2017). Based on our data, this may indicate a role for CD9 in neutrophil migration and not neutrophil phagocytosis or adhesion.

We found that THP-1 cells have the ability to phagocytose more bacteria compared to U937s at a ratio of 10:1. This is in line with research performed by Mendoza-Coronel et al, 2016 and as detailed by Chanput et al., 2015. However, according to Dintakurti et al, THP-1s and U937s may be differentially inclined towards M1 and M2 phenotypes. Dintakurti found that THP-1s tended towards M1 differentiation and that U937s preferentially differentiated towards the M2 phenotype (Dintakurti et al., 2017). The M1 phenotype is characterised by the production of pro-inflammatory cytokines and phagocytosis and killing of intracellular pathogens, whereas the M2 phenotype is

related to wound healing. This difference in activity could account for the differences in the ability of THP-1s to phagocytose more bacteria compared to U937s. Other researchers have studied the differences between THP-1s and U937s, Mendoza-Coronel and Castañón-Arreola reported that U937s possess less phagocytic capability compared to THP-1s and human monocyte-derived macrophages (Mendoza-Coronel and Castañón-Arreola, 2016) albeit this study was performed using mycobacteria. Madhvi et al, also using mycobacteria, compared THP-1 macrophages to human monocyte-derived macrophages and found that the two cell types were comparable in their ability to phagocytose bacteria, their viability, and their responses to mycobacterial infections. The authors concluded that THP-1 cells were suitable substitutes for human monocyte-derived macrophages for infection experiments (Madhvi et al., 2019). With this published data combined with our results, we also concluded that THP-1s would be the preferred cell line for macrophages to integrate into an immunocompetent human skin model. However, personal communications within the Monk Lab have revealed that the CD9-derived peptides may facilitate wound healing (Monk et al., 2021). It would also be worthwhile to integrate differentiated U937s into a human skin model due to their propensity to adopt a M2 phenotype.

We were unable to test the performance of Langerhans cells, and the possible effects peptide treatment could have on them, in a 3D skin model due to issues differentiating the MUTZ-3 progenitors into Langerhans-like cells. This could be due to a range of factors such as the 5637 cells not secreting enough cytokines into the conditioned media to differentiate the cells. The concentration of GM-CSF measured in the conditioned media did not match the levels of GM-CSF in conditioned media when performed by DSMZ scientists (Steube- Pers Comms). In addition, the antigen expression of the supposedly differentiated MUTZ-3 cells was far below what was achieved by Laubach et al. who published a successful differentiation and integration of MUTZ-3 cells into a collagen-based organotypic human skin model (Laubach et al., 2011). The authors reported that approximately 30-40% of differentiated MUTZ-3 cells expressed CD1a and Langerin, and approximately 50-60% of differentiated MUTZ-3 cells expressed CCR6. This is far higher than we achieved, with Langerin and CCR6 being expressed by less than 1% of differentiated MUTZ-3 cells and CD1a expressed by approximately 15% of cells. The significant increase in CD1a expression indicates that the differentiation was working but perhaps more culture time was required. Other

researchers have published similar methodologies where the MUTZ-3 cells were cultured for upwards of 10 days (Bock et al., 2018; van Dalen et al., 2019). There was difficulty in using MUTZ-3 cells as other researchers recommended using MUTZ-3 cells at passage 20 after thawing to improve consistency between cell responses to cytokines, which meant longer culture periods (van Dalen, Pers-comms). MUTZ-3 derived Langerhans-like cells were reported not surviving much longer than the 2 weeks of ALI after integration into a collagen-based organotypic model (Weindl, Pers-Comms). This discouraged the possibility of long-term infection experiments and may suggest the need for a suitable replacement cell line. Finally, MUTZ-3 cells have been differentiated into Langerhans-like cells for the study of skin sensitisation or response to an irritant, but a more appropriate model may be required for studies involving skin infection, as discussed below.

As *S. aureus* is an opportunistic microbial resident of the skin, it is a frequent cause of skin infections and contributes to the development and progression of inflammatory skin disorders. Therefore, the recognition of *S. aureus* by epidermal Langerhans cells may be important for maintaining skin homeostasis and preventing infection. van Dalen et al. used a humanised mouse model which constitutively expressed human langerin on mouse Langerhans cells. Upon epicutaneous *S. aureus* infection of these transgenic mice, the authors observed high transcript levels for genes relating to a Th17 response. *In vitro* studies in the same study also showed that *S. aureus* triggers Langerhans cells to produce inflammatory cytokines important for the induction of Th17-polarised immune responses (van de Dalen et al, 2019). Combined, these observations indicate that Langerhans cells can detect and respond to *S. aureus* on the skin. The collagen-based organotypic model published by Kosten et al, shows that MUTZ-3 cells can differentiate into Langerhans-like cells, capable of migrating towards the dermis and undergoing a change towards a macrophage-like phenotype upon irritant exposure. Combined, it would have been interesting to use the MUTZ-3-integrated collagen-based organotypic model as a platform for topical *S. aureus* application to see if the MUTZ-3 cells could migrate and differentiate in response to infection. If the MUTZ-3 cells were able to respond to *S. aureus* infection in the collagen-based organotypic model, it would have been very interesting to also use this model for peptide testing to see if the CD9-derived peptides interfered with this process. This is especially important as CD9 is expressed in Langerhans cells and

dendritic cells and is reported to be essential for regulating inflammation (Brosseau et al., 2018), as well as regulating MHC II for antigen presentation to prime $CD4^+$ T cells, which MUTZ-3 cells have been shown to be able to do (Santegoets et al. 2006, Santegoets et al. 2008)

A possible cell line that could be suggested to integrate into skin models are THP-1s. This cell line has also been differentiated into DCs as detailed by Chanput et al, and these DCs have reportedly displayed morphologic, phenotypic, and functional properties of human monocyte derived DCs (Tsuchiya et al., 1980). We had not initially considered using THP-1s as the cell line for DCs as MUTZ-3 cells had been proven to differentiate and integrate successfully into collagen-based organotypics. However, THP-1s could perhaps be considered due to their ease in culturing and relatively long-life span (Plantinga et al., 2015).

Attempts were also made to integrate neutrophils into human skin models. Tissue-engineered skin models were chosen as it was unlikely for primary neutrophils to survive the integration and subsequent 14 days of culture for collagen-based organotypics. We decided to use the dermis alone so the neutrophils would not have to traverse the epidermis and found that the chemoattractant C5a may promote neutrophil migration into the dermis; Figure 4.6 shows the presence of neutrophils in the dermis that had been pre-treated with C5a versus the absence of neutrophils in the dermis without C5a. We tried to take this further by constructing tissue-engineered skin using Euroskin as we hoped that the thinness of the Euroskin would make it easier for the neutrophils to migrate further into the dermis. However, we ultimately found that Euroskin was in fact unsuitable for constructing tissue-engineered skin as there was poor differentiation of the epidermis. We believe this to be a poor batch of skin acquired from the Eurobank and that it was too damaged to allow the keratinocytes to form a sufficient epidermis.

Surgical skin explants are considered the ‘gold standard’ for skin research as they are the best representation of human skin in terms of structure but also because explants also contain resident immune cells such as Langerhans, DCs, and macrophages. However, if cultured on a petri dish, the immune cells could ‘crawl out’ of the explant to migrate towards the nutrients and growth factors in the media (Teunissen et al.,

2012). Surgical explants are some of the best available skin models currently available, but they have drawbacks depending on the desired assay. For example, an assay focusing on DCs in explants may be unfeasible as culturing the explants can lead to DC migrating out onto the tissue culture plate within a few days.

Tissue-engineered skin has been used as an immunocompetent model that can be integrated with T cells (van den Bogaard et al., 2014) and collagen-based organotypics can be integrated with a wider variety of cells such as macrophages (Bechetoille et al., 2011), Langerhans (Kosten et al., 2015) and T cells (Kühbacher, Sohn, et al., 2017). This makes the collagen-based organotypic model an advantageous model as the model could be used to study an immune cell type in isolation in response to a stimulus e.g., allergens or infection, or to understand the relationship between an immune cell, keratinocytes, and fibroblasts. Integration of immune cells into a collagen-based organotypic model depends on which immune cells are used and where these cells normally reside. For example, Langerhans cells are typically located in the epidermis and consequently, Langerhans cells can be integrated by simply pipetting alongside the keratinocytes on top of the dermis, demonstrated by Kosten et al. who observed the response by Langerhans cells in collagen-based organotypic models used to investigate skin sensitisation (Bock et al., 2018; Kosten et al., 2015). For macrophages, the macrophages reside in the dermis, so macrophages are mixed with fibroblasts in the collagen suspension before it has set (Bechetoille et al., 2011). T cell migration into the dermis has been demonstrated in tissue-engineered skin which is more difficult to integrate into skin as the immune cells cannot be simply mixed into the collagen. T cell migration was recapitulated by van den Bogaard et al. who investigated the communication between T cells and keratinocytes in response to inflammation (van den Bogaard et al., 2014) with T cells migrating through the reticular region of the dermis. The authors showed that the T cells needed to be activated to migrate into the dermis. T cell migration was not recapitulated by Kühbacher et al. who integrated T cells into a collagen gel before laying the skin model on top of the T cell-gel suspension. The authors were clearly able to demonstrate T cell communication with fibroblasts in response to *Candida* infection (Kühbacher, Henkel, et al., 2017), revealing that T cells need not need to be in the dermis to communicate with the fibroblasts and affect the immune response to infection.

Whilst these models have been used to understand immune cells in isolation in response to a specific stimulus, they may not provide the full picture as immune cells may perform differently depending on their stimuli. For example, Natsuaki et al. demonstrated that even though inducible lymphoid tissues in the skin were clusters of DCs and T cells, they could not form in the absence of macrophages (Natsuaki et al., 2014).

# Chapter 5 Tetraspanin-derived peptides reduce *Staphylococcus aureus* infection in an *in vivo* murine model.

## 5.1 Introduction

### 5.1.1 Use of animals in drug testing

Clinical trials can demonstrate that a potential new drug is safe and can reach its target site and remain there to deliver its effects. Animal studies are vital to clinical trials as they are used to determine toxicity of the drug and can indicate potential doses for the human trials (Doke and Dhawale, 2015).

Despite differences between animal and human immunology, animals such as mice are still used as models for the reasons outlined in section 1.5.4, namely that they are more economically viable with fewer ethical restraints. For drug testing that eventually reaches human clinical trials, there would almost certainly be animal testing to determine if the drug was effective and to determine toxicity of the drug and possible doses.

### 5.1.2 Animal skin models

A variety of animal species are used to study a wide range of inflammatory and autoimmune skin diseases that are relevant to humans. The use of animals in skin studies have increased with the development of transgenic mice, making the models more relevant to humans as they can more accurately mimic human conditions.

Different animal species are studied depending on the properties of the skin and how it differs to human skin. For example, Rhesus monkeys are similar to humans in terms of absorption, which may be of importance for testing the absorption of a topical drug (Jung and Maibach, 2015). Porcine skin, however, is similar in histology and thickness to human skin (Summerfield et al., 2015). Finally, whilst there are differences in murine

skin as mentioned in section 1.5.4, the use of mouse may be advantageous as there are genetically engineered mouse models to specifically mimic, and study, particular skin diseases such as atopic dermatitis (Avci et al., 2013).

Despite the differences between human and murine skin, we chose to test the experiments on mice as we were unable to construct an immunocompetent skin model. However, this was also an opportunity to use an immunocompetent skin model with a functional vascular system to study if peptide treatment could possibly affect immune cell trafficking.

### 5.1.3 *Staphylococcus aureus* infection in mice

*Staphylococcus aureus* is a human pathogen that can still be used in mouse studies (Liu et al., 2017). Whilst *S. aureus* is typically considered a human pathogen, it has broader significance as *S. aureus* can infect animals as it is also a pathogen that can be harmful to live-stock e.g., sheep, pigs, and cows (Fluit, 2012). The strains capable of infecting farm animals also have the capability to transmit to humans (Spoor et al., 2013).

Mice have been used to study *S. aureus* since the 1880s (Kim et al., 2014; Ogston, 1881), since then, mice have been used as models to study *S. aureus* for wound healing, abscesses, *S. aureus* secreted products such as α-haemolysin and how *S. aureus* interacts with components of the immune system that are conserved and similar in both humans and mice.

The mouse model for *S. aureus* has over time been modified in order to better examine the role of immune cells such as macrophages or neutrophils, and how the structure of the skin relates to bacterial infection, with protocols using specific wounding techniques (tape-stripping or incisions) or infection techniques (topical application or injection).

Mice are also popular choices as a model for *S. aureus* as specific immune cell types can be depleted with monoclonal antibodies. For example, anti-Ly6G can deplete

neutrophils and consequently a lower challenge dose is needed to initiate infection in depleted mice and these mice struggle to contain the infection and result in systemic infection. Experiments such as these can have human relevance as patients with mutations resulting in abnormal immune cell function (e.g., T cells in HIV/AIDS patients) also display an increased susceptibility to *S. aureus* infection (Karauzum and Datta, 2017; Miller et al., 2020). To summarise, human conditions resulting in the depletion or diminished function of certain immune cell types can be recapitulated in mice either transgenically or with antibodies.

The aim of this chapter was to utilise a mouse model of infection by following the methodology used by Liu et al (Liu et al., 2017). We chose this model because the authors had successfully demonstrated that the model could support epicutaneous bacterial infection of the skin for a period of time longer than the 24 hours used in the *in vitro* models (7 days). The longer time period was a more appropriate reflection of a bacterial skin infection and the resultant immune response. This was demonstrated by in a study which showed distinct waves of immune cells passing through bacteria-infected skin which took multiple days to occur (Janela et al., 2019). By ensuring if the mice could sustain an infection of SH1000, we could then proceed with the aim of testing the peptides against SH1000 infection on murine skin. As the model would be using immunocompetent mice with a functional vascular system, we could then examine if the peptides had affected immune cell population or migration.

## 5.2 Results

### 5.2.1 Development of a murine model for cutaneous infection of *Staphylococcus aureus*

The methodology used was based on the protocol described by Liu et al., 2017. The authors used a CFU of $1x10^8$ USA300 to infect mice, and so we decided to test CFU of $1x10^7$, $1x10^8$ and $1x10^9$ to determine which would be best for our strain of *S. aureus*. As shown in Figure 5.1A, we saw that a CFU of $1x10^7$ was optimal because an infection with a CFU of $1x10^8$ and $1x10^9$ had similar CFU counts denoting that by $1x10^8$ the mouse skin can become saturated with bacteria. We decided this would also be useful

because the other infection studies described in chapters 3 and 4 had used a CFU of $1x10^7$ and the data could be comparable.

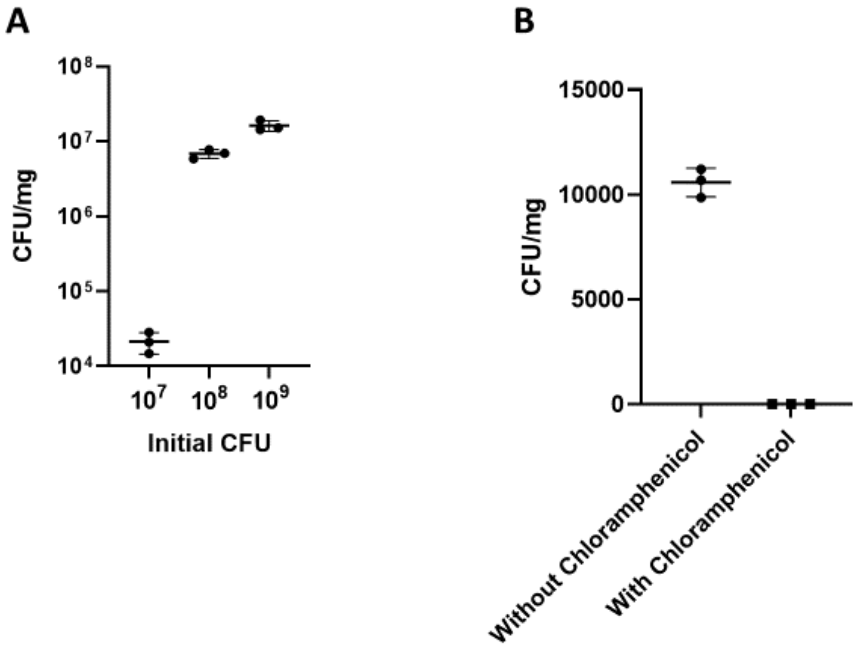


**Figure 5.1 CFU/mg of SH1000 at varying MOI**

As described in 2.13**,** mice were shaved and had a gauze pad with a bacterial suspension ranging from $10^7$ to $10^9$ CFU applied. The mice were bandaged then housed for an additional 5 days. **A)** Mice were then sacrificed to harvest the skin to be lysed for a CFU count shown as CFU/mg **B)** Bacterial suspensions were plated on LB agar plates that either contained chloramphenicol or was antibiotic-free. Data are represented as mean ± SD. 3 biological replicates were performed with 3 technical repeats.

To determine if the normal mice skin microbiome would interfere with the CFU count of SH1000, we topically applied a gauze pad containing PBS onto a mouse for 5 days before harvesting the skin and we plated the bacterial suspension on LB agar plates with or without chloramphenicol.

As shown in Figure 5.1B, we found colonies of various sizes and colours growing on the plates without chloramphenicol whereas we saw no growth on the LB agar plates with chloramphenicol. We decided to only plate the bacterial suspensions onto LB agar

plates with chloramphenicol so any colonies counted would be SH1000 as it carries a resistance to chloramphenicol.

Based on work performed in the Monk Lab, peptides based on murine CD9 had shown to be effective in reducing bacterial adhesion on murine cell lines (Green, 2021). Based on this, we decided to include the murine versions of the peptides on the mouse model as well human 800ii as the stapled version of the murine peptide has not been made.

To determine if the peptides were likely to be effective *in vivo*, we took skin explants from sacrificed mice and repeated the infection assay described in 3.2.4. We decided to test peptides derived from murine CD9 to reflect the differences between human and murine CD9 as well as the human 800ii peptide as we had data to suggest that it was effective on mouse cells (Monk et al., 2021). As shown in Figure 5.2, we found that after 24 hours, the m800-Cap peptide had an effect in reducing the percentage of bacteria adherent to murine skin. Whilst the human 800ii peptide had no effect after 24 hours, there was a trend towards antibacterial activity. We hypothesised that this antibacterial activity would become more apparent given more time and thus decided to continue with the experiment.

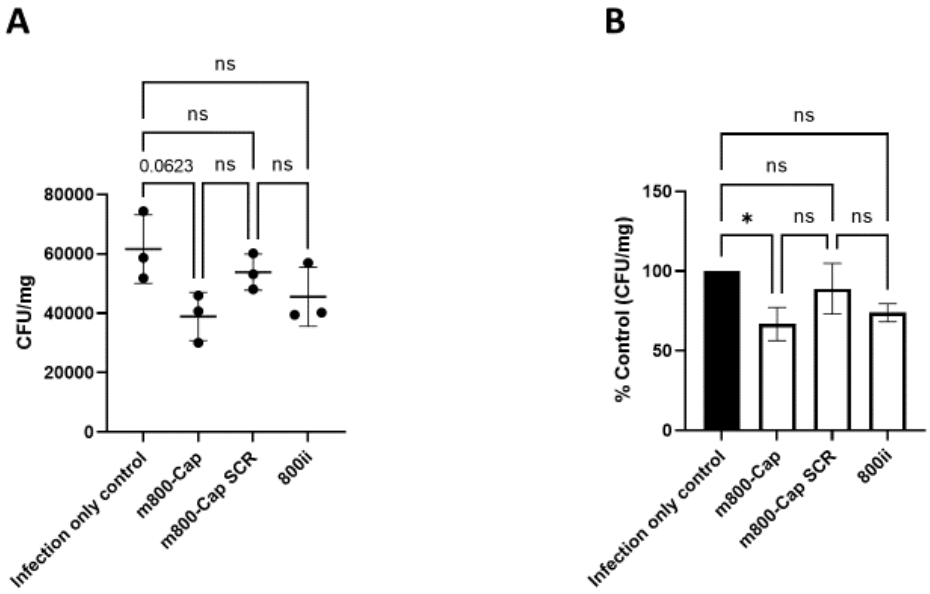


**Figure 5.2 Pre-treatment with CD9-derived peptides reduces *Staphylococcus aureus* adherence to mouse explants**

Mice were shaved and had hair removal cream applied onto the shaved areas. After 24 hours the mice were sacrificed, and the dorsal skin was harvested and burned

before being pre-treated with peptides for 45 mins prior to bacterial infection for 5 hours. **A)** Data shown as mean CFU/mg of tissue **B)** Data plotted as a percentage of the infection only control. Data are represented as mean ± SD. Data are normally distributed as determined by the Shapiro-Wilk Normality test. 3 biological replicates performed with 3 technical repeats. Data analysed by one-way ANOVA with Sidak's multiple comparisons test * $p \leq 0.05$

### 5.2.2 CD9-derived peptide treatment reduces *Staphylococcus aureus* adherence to mice

In Chapter 3, we had concluded that the peptides successfully reduced bacterial adherence and in Chapter 4 we had concluded that the peptides do not affect phagocytosis of *S. aureus* in phagocytes. We then tested the peptides in an animal model as this combines a living skin model with a functional immune system.

Mice were anaesthetised with 5% isoflurane prior to being shaved and then topically applied with Veet, a hair removal cream. This was to prevent hair regrowing during the infection period. A gauze pad containing a co-treatment of peptide and bacterial suspension is applied onto the back of the mouse and the gauze pad is then secured with a piece of Tegaderm dressing. This dressing is then secured with two layers of MeFix bandages. This sufficiently secures the gauze pad across the five-day infection period without need to readjust or reapply the bandages during this period. The dressing and bandages used were chosen for their strong adhesive properties and flexibility allowing them to be tightly bound to the mice without suffocating them.

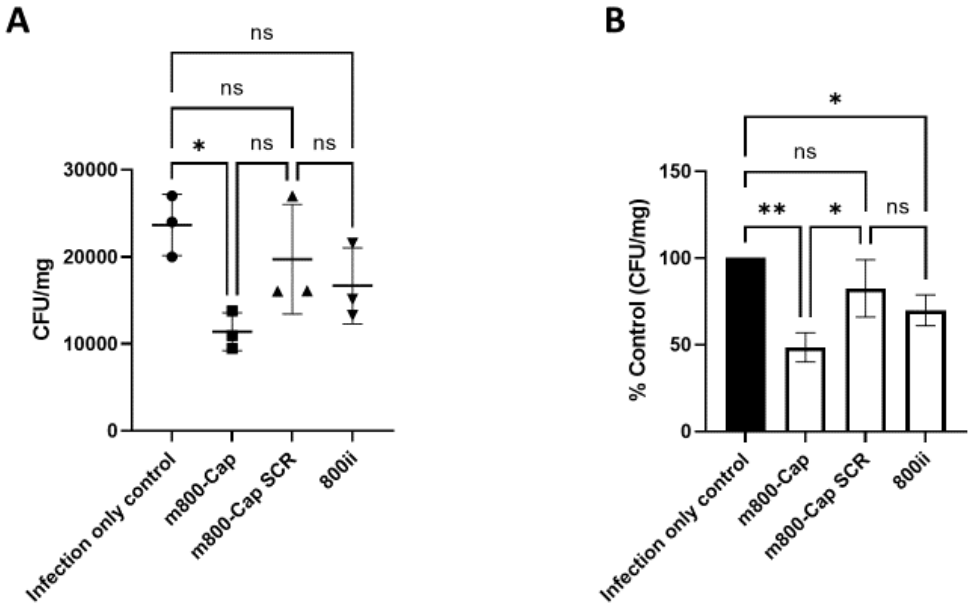


**Figure 5.3 Pre-treatment with CD9-derived peptides reduces *Staphylococcus aureus* adherence to murine skin**

As described in 2.13, mice were shaved and had a gauze pad with a peptide-bacteria co-treatment applied onto their backs. The gauze pad was secured with dressing and bandages to prevent removal and the mice were housed for an additional 5 days. Mice were then sacrificed to harvest the skin for a CFU count. **A)** Mean CFU/mg of tissue **B)** Data plotted as a percentage of the infection only control. Data are represented as mean ± SD. Data are normally distributed as determined by the Shapiro-Wilk Normality test. 3 biological replicates performed with 3 technical repeats. Data analysed with One-way ANOVA with Sidak's multiple comparison test. *p≤0.05 **p≤0.01

We observed a significant decrease in bacterial infection on murine skin co-treated with m800-Cap compared to the untreated infected control and the scrambled control (Figure 5.3). We also saw a significant decrease in bacterial infection in mice co-treated with 800ii albeit to a lesser extent compared to treatment with m800-Cap. From this, we determined that co-treatment with CD9-derived peptides had effectively reduced *S. aureus* adherence to the skin with a greater effect with m800-Cap (~50% reduction) than with 800ii (~25%). We believe that this difference in efficacy is due to m800-Cap peptides being derived from murine CD9 whilst 800ii was derived from human CD9. Importantly, the peptide derived from human CD9, 800ii, was able to

affect murine CD9 and significantly decrease the percentage of bacterial adherence to murine skin.

### 5.2.3 Neither peptide treatment nor infection affect gross skin morphology

Skin harvested from infected mice were fixed for histology and the slides were imaged with light microscopy, scanned, and then analysed with Metaviewer. We were interested to see if the peptide co-treatment had in any way altered the structure of the infected skin. The thickness of skin increases with infection and inflammation and so we were interested if we could observe a relationship between peptide treatment, infection, and skin thickness. As shown in Figure 5.4, we saw no significant difference in the thickness of the skin, either as both the epidermis and dermis, or the epidermis alone (as this is where the bacteria and peptides made contact with the skin). Visual examination of the skin upon removing the bandage also did not reveal obvious damage, inflammation, or necrotic tissue. From this, we concluded that murine skin would not have an adverse reaction to peptide treatment.

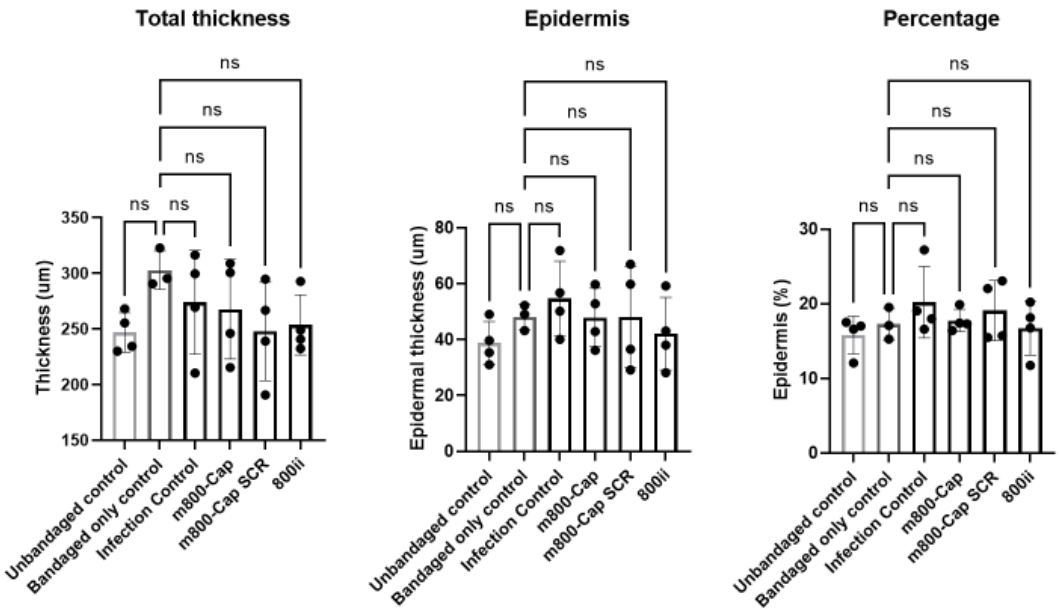


**Figure 5.4 Measurement of the thickness of murine skin**

Murine skin was excised from sacrificed mice and processed for histology. Histological sections of skin were prepared on slides and scanned for analysis with MetaViewer software to measure the epidermis and total thickness of the skin. Data are

represented as mean ± SD. Data are normally distributed as determined by the Shapiro-Wilk Normality test. 4 biological replicates were performed each with 3 technical repeats. Data analysed with One-way ANOVA with Sidak's multiple comparison test.

We also performed immunohistochemistry on the histology sections to specifically count the number of macrophages and neutrophils in a section. As shown in Figure 5.5A, we counted the number of macrophages using CD68 as a macrophage marker. We saw that treatment with the 800ii peptide reduced the number of macrophages compared to the non-treated infection control. This decrease could be because 800ii treatment was shown to reduce bacterial infection (shown in Figure 5.3). A decrease in bacterial infection could result in reduced inflammation and consequently fewer proinflammatory cytokines to attract macrophages. However, we did not see this with m800-Cap, which had a greater effect on reducing bacterial infection. With Ly6G+ used as a marker for neutrophils, we observed no significant difference in the absolute number of neutrophils between peptide treatments, albeit we did observe a trend whereby the absolute number of neutrophils decreased with peptide treatment compared to the non-peptide treatment control and the scrambled peptide control. Figures 5.5 C and D shows that macrophages were distributed throughout the skin, predominantly in the dermis and hypodermis, but were not seen in the epidermis. Figures 5.5 E and F revealed that neutrophils were predominantly distributed in the hypodermis and the epidermis, predominantly at the site of infection.

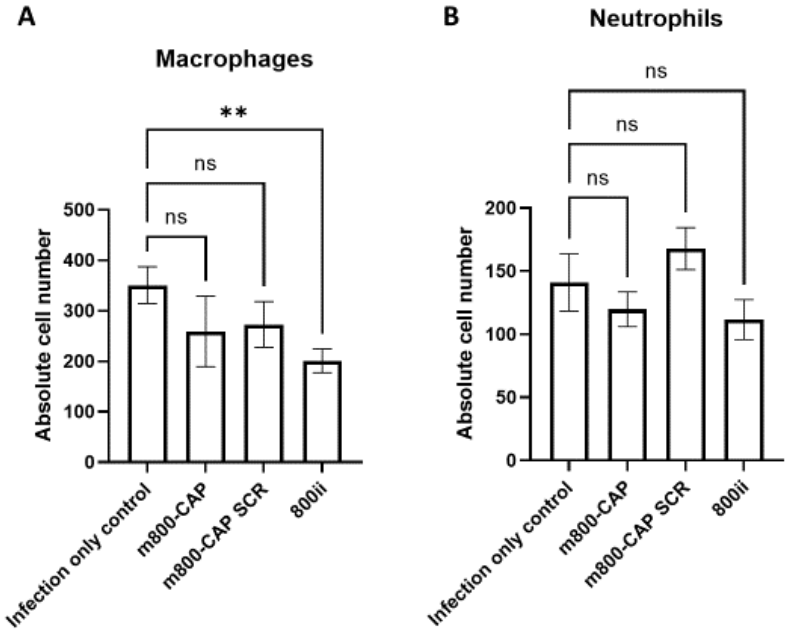

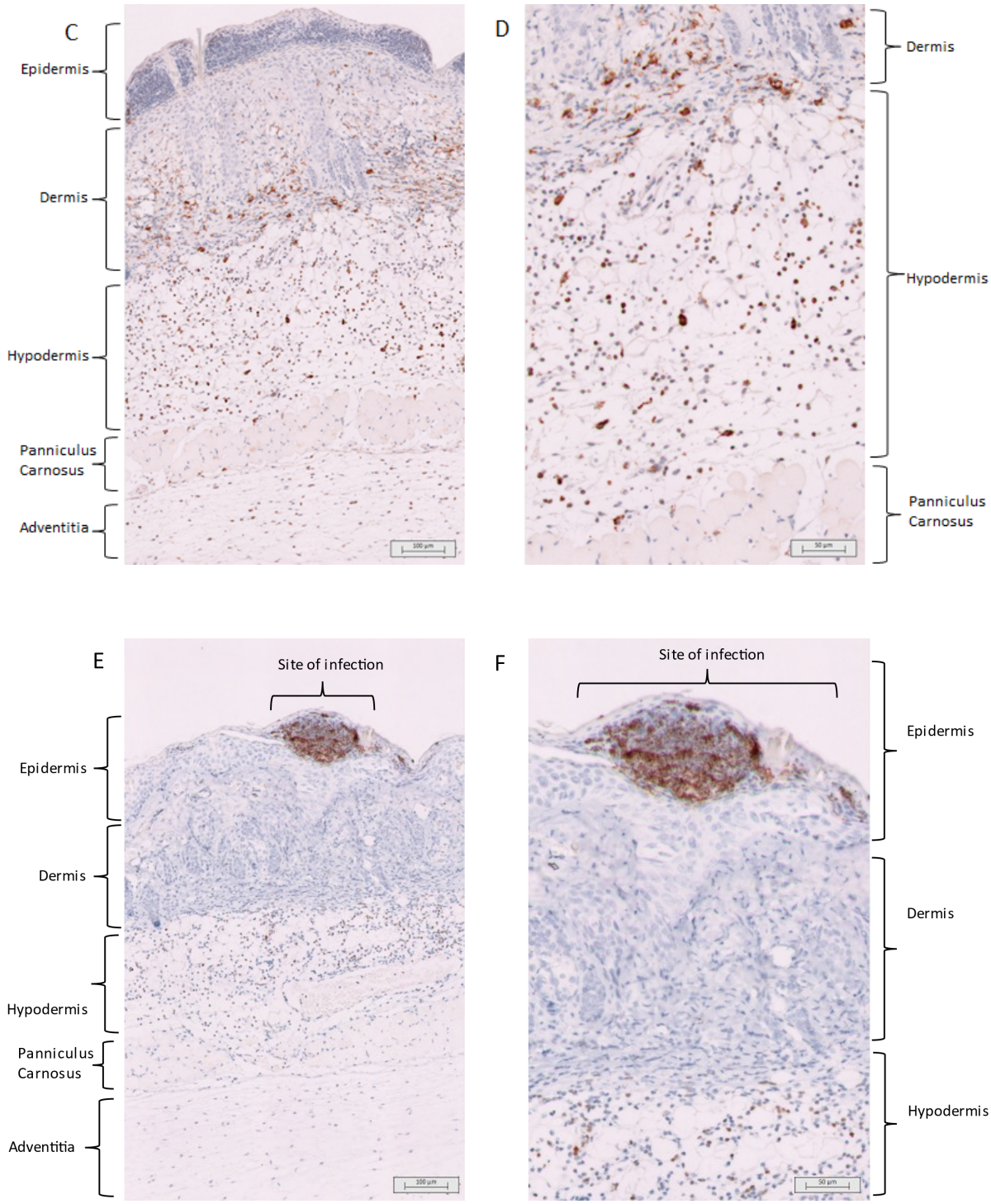


**Figure 5.5 Immunohistochemistry staining for neutrophils and macrophages on histology sections**

Histology sections of murine skin were processed for immunohistochemistry and stained for CD68 or Ly6G. Images were analysed and $CD68^+$ or $Ly6G^+$ cells were automatically counted using Fiji. **A)** Absolute cell number of CD68+ cells as determined by immunohistochemistry. **B)** of $Ly6G^+$ cells **C)** Immunohistochemistry staining for $CD68^+$ cells at x5 magnification **D)** at x10 magnification. **E)** Immunohistochemistry staining for Ly6G+ cells at x5 magnification **F)** at x10 magnification. Data are

represented as mean ± SD. Data are normally distributed as determined by the Shapiro-Wilk Normality test. 4 biological replicates each performed with 3 technical repeats. Data analysed with One-way ANOVA with Šídák's multiple comparison test. **p≤0.01

### 5.2.4 CD9-derived peptide treatment does not affect immune cell populations in skin

To determine if the peptide co-treatment had effects on immune cell populations or migration, we isolated skin from the site of infection where the gauze pad containing SH1000, and the peptide co-treatment was placed. The harvested skin was enzymatically broken down into a single-cell suspension with Liberase and then stained for analysis with flow cytometry, gating the cells for specific populations (Figure 5.6 and Table 5.1). Cells were first gated to remove cellular debris, then for living cells and then singlets before immune populations were determined by if the cells were MHC II positive or negative.

From the flow cytometry data of the immune cells present in the skin (Figure 5.7), we saw a trend indicating that the absolute number of neutrophils increased with infection. This could be expected as neutrophils are recruited from the bloodstream to the site of skin infection.

There was, interestingly, no change in the number of macrophages and monocytes with infection. This was unexpected as we initially expected the macrophages and monocytes to increase in the same trend we saw with the neutrophils and monocytes. There was also no noticeable difference with the absolute number of Langerhans and cDC1s and there was a significant decrease in the absolute number of cDC2s with infection. This could be related to cDC2s reacting to the bandaging as cDC2s have been linked to hypersensitivity studies (Honda et al., 2019), or perhaps due to the bacteria (Kinnebrew et al., 2012; Zhang et al., 2018).

Across all cell types, we saw no significant differences in absolute cell numbers between treatments, which indicates that the peptide treatment had not affected immune cell numbers and their migration.

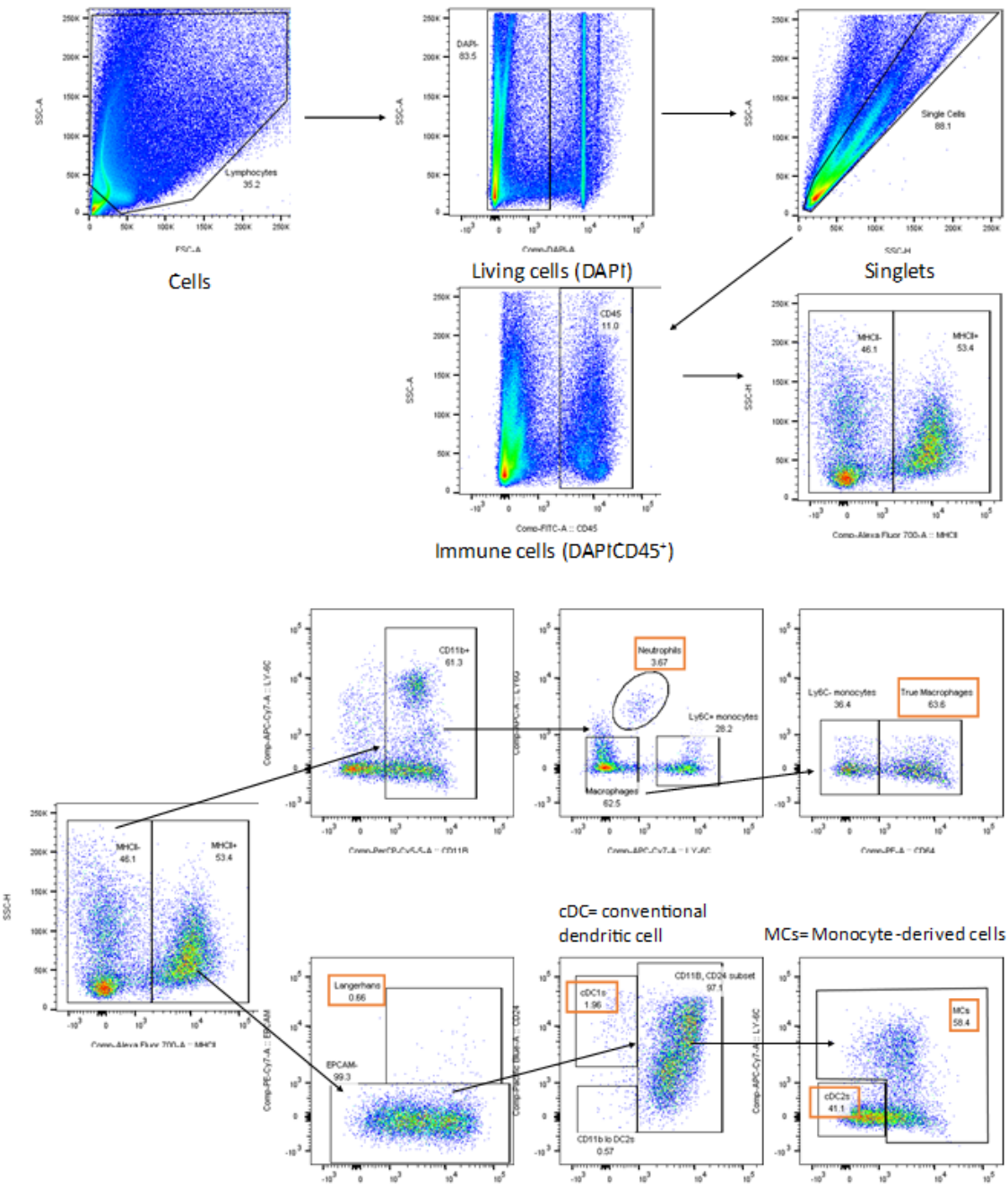


**Figure 5.6 Gating strategy for murine immune cells in the skin**

Murine skin was excised from sacrificed mice and digested with Liberase to release immune cells. Cells were stained with antibodies and analysed with FACS.

| Immune cell | Gating | | | | | | | |
|---|---|---|---|---|---|---|---|---|
| **Neutrophils** | DAPI$^-$ | CD45$^+$ | MHCII$^-$ | CD11b$^+$ | Ly6G$^+$ | Ly6C$^+$ | | |
| **Macrophages** | DAPI$^-$ | CD45$^+$ | MHCII$^-$ | CD11b$^+$ | Ly6G$^-$ | Ly6C$^-$ | CD64$^+$ | |
| **Langerhans** | DAPI$^-$ | CD45$^+$ | MHCII$^+$ | EPCAM$^+$ | CD24$^+$ | | | |
| **cDC1s** | DAPI$^-$ | CD45$^+$ | MHCII$^+$ | EPCAM$^-$ | CD24$^+$ | CD11b$^+$ | | |
| **cDC2s** | DAPI$^-$ | CD45$^+$ | MHCII$^+$ | EPCAM$^-$ | CD24$^+$ | CD11b$^+$ | Ly6C$^-$ | CD64$^-$ |
| **MCs** | DAPI$^-$ | CD45$^+$ | MHCII$^+$ | EPCAM$^-$ | CD24$^+$ | CD11b$^+$ | Ly6C$^+$ | CD64$^+$ |

**Table 5.1 Flow cytometry gating strategy for murine immune cells in skin**

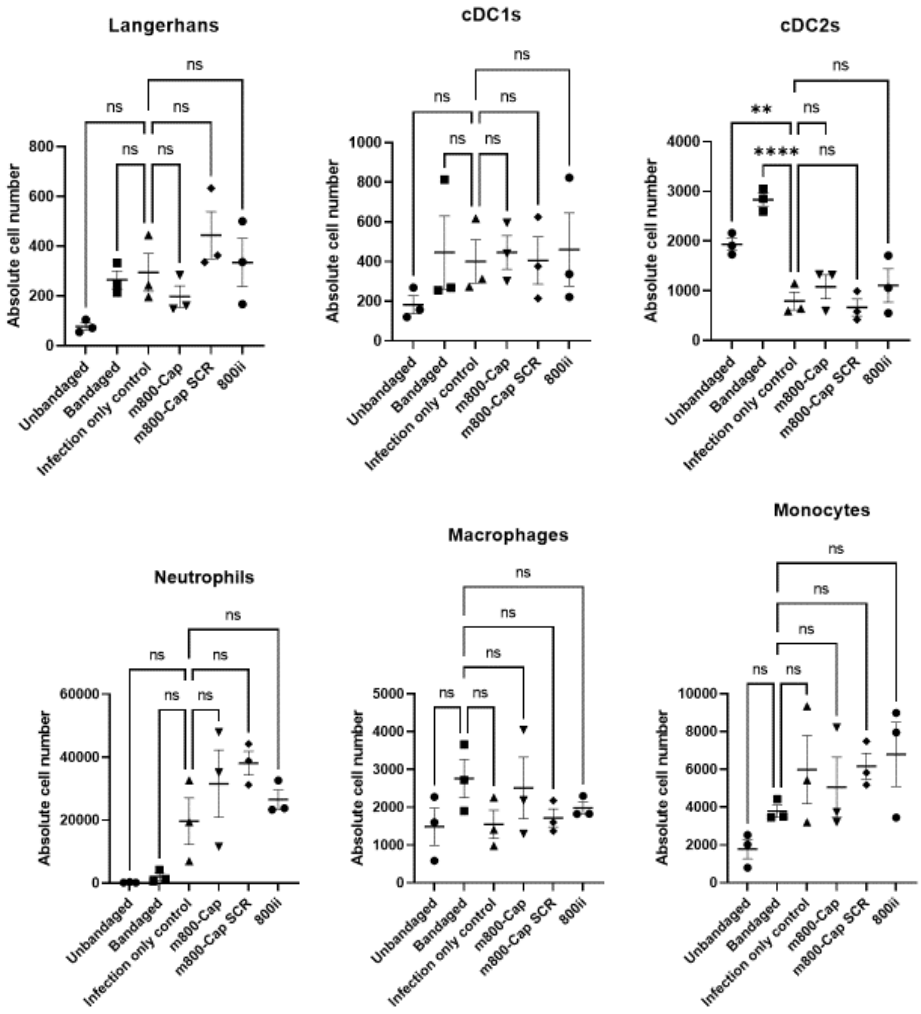


**Figure 5.7 Cell count of immune cells isolated from murine skin post-infection**

Absolute numbers of the main immune cell types in murine skin after the 5 days following cutaneous application of SH1000. Mouse skin was harvested after infection and broken down into a single-cell suspension for analysis with flow cytometry. Data are represented as mean ± SD. Data are normally distributed as determined by the Shapiro-Wilk Normality test. 3 biological replicates performed with 3 technical repeats. Data analysed with One-way ANOVA with Šídák's multiple comparison test.

**p≤0.01 ****p≤0.0001

### 5.2.5 CD9-derived peptide treatment does not affect immune cell populations in lymph nodes

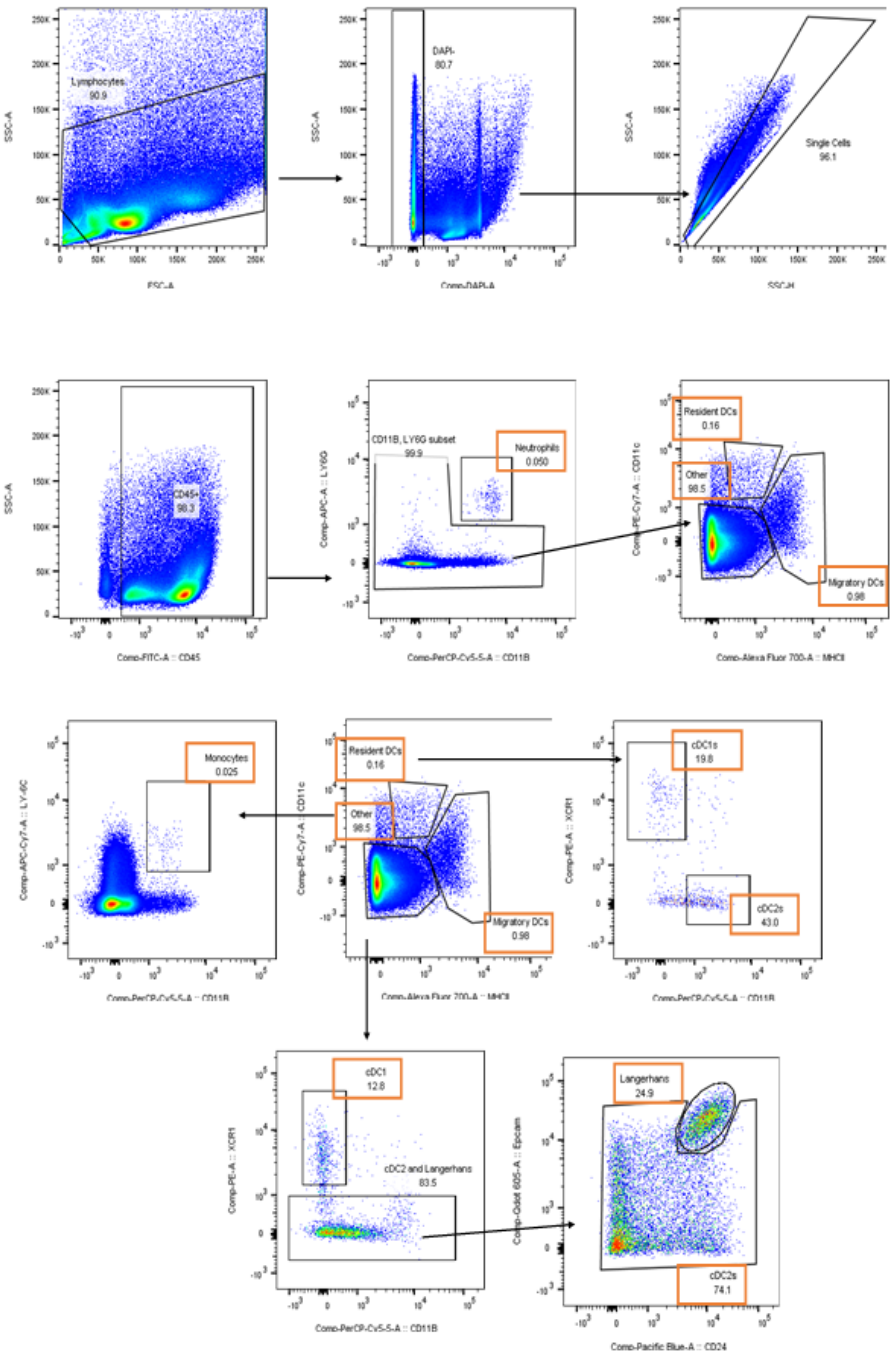


**Figure 5.8 Gating strategy for murine immune cells in inguinal lymph nodes**

Murine skin was excised from sacrificed mice and digested with collagenase and DNase I to release immune cells. Cells were stained with antibodies and analysed with FACS

| Immune cell | Gating | | | | | | | | | |
|---|---|---|---|---|---|---|---|---|---|---|
| **Neutrophils** | DAPI$^{-}$ | CD45$^{+}$ | CD11b$^{+}$ | Ly6G$^{+}$ | | | | | | |
| **Monocytes** | DAPI$^{-}$ | CD45$^{+}$ | CD11b$^{-/+}$ | Ly6G$^{-}$ | CD11c$^{-}$ | MHCII$^{-}$ | Ly6C$^{+}$ | CD11b$^{+}$ | | |
| **Residential cDC1s** | DAPI$^{-}$ | CD45$^{+}$ | CD11b$^{-/+}$ | Ly6G$^{-}$ | CD11c$^{+}$ | MHCII$^{-/+}$ | XCR1$^{+}$ | CD11b$^{-}$ | | |
| **Residential cDC2s** | DAPI$^{-}$ | CD45$^{+}$ | CD11b$^{-/+}$ | Ly6G$^{-}$ | CD11c$^{+}$ | MHCII$^{-/+}$ | XCR1$^{-}$ | CD11b$^{+}$ | | |
| **Langerhans** | DAPI$^{-}$ | CD45$^{+}$ | CD11b$^{-/+}$ | Ly6G$^{-}$ | CD11c$^{-/+}$ | MHCII$^{+}$ | XCR1$^{-}$ | CD11b$^{-/+}$ | EPCAM$^{+}$ | CD24$^{+}$ |
| **Migratory cDC1s** | DAPI$^{-}$ | CD45$^{+}$ | CD11b$^{-/+}$ | Ly6G$^{-}$ | CD11c$^{-/+}$ | MHCII$^{+}$ | XCR1$^{+}$ | CD11b$^{-}$ | | |
| **Migratory cDC2s** | DAPI$^{-}$ | CD45$^{+}$ | CD11b$^{-/+}$ | Ly6G$^{-}$ | CD11c$^{-/+}$ | MHCII$^{+}$ | XCR1$^{-}$ | CD11b$^{-/+}$ | EPCAM$^{-}$ | CD24$^{-/+}$ |

**Table 5.2 Flow cytometry gating strategy for murine immune cells in lymph nodes**

Following on from 5.2.3, we were also interested if the peptide treatment had negatively affected the immune cell migration away from infection towards the dLNs to prime a T cell response. For this, the harvested lymph nodes were enzymatically broken down into a single-cell suspension with an enzyme cocktail and then stained for analysis with flow cytometry, gating the cells for specific populations (Figure 5.8 and Table 5.2). Cells were first gated to remove cellular debris, then for living cells and then singlets before immune populations were determined by if the cells were MHC II positive or negative.

After 5 days of bacterial infection, we observed a significant decrease in residential cDC1s, migratory cDC2s and Langerhans (Figure 5.9). This was surprising as we did not expect the number of these cell types to decrease by day 5. We expected an increase as these cell types migrated from the skin and into the lymph nodes and increased in number to prime an adaptive immune response. These cells do not leave the lymph nodes upon arrival however, we hypothesise the decrease may be due to

the cells dying after T cell activation. We also hypothesise that this may be due to the lymph nodes also becoming infected with SH1000 which would also account for the increase in absolute cell numbers of neutrophils in the lymph nodes which we also did not anticipate. (Bogoslowski et al., 2018; Miller and Simon, 2018)

We observed a trend that migratory cDC1s decreased in absolute cell count. With no observed changes in the absolute cell numbers of neutrophils, monocytes and residential cDC2s.

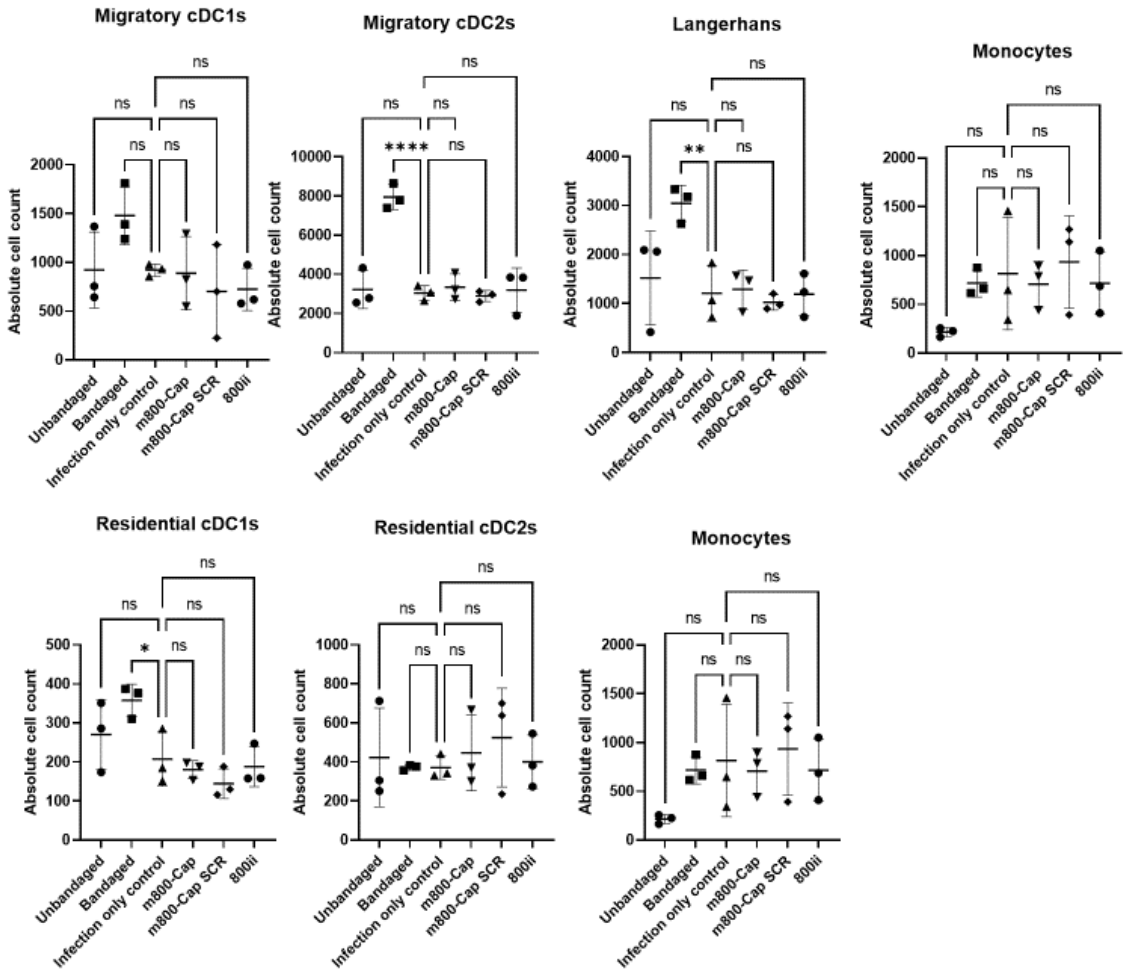


**Figure 5.9 Cell count of immune cells isolated from murine lymph nodes post-infection**

Absolute numbers of the main immune cell types in murine lymph nodes after the 5 days following cutaneous application of SH1000. Lymph nodes were harvested and broken down into a single-cell suspension for analysis with flow cytometry. Data are represented as mean ± SD. Data are normally distributed as determined by the Shapiro-Wilk Normality test. 3 biological replicates performed with 3 technical repeats.

Data analysed with One-way ANOVA with Šídák's multiple comparison test. *p≤0.05 **p≤0.01 ****p≤0.0001

## 5.3 Discussion

Given that we were unable to construct an immunocompetent human skin model in Chapter 4, and that current human skin models may only contain one immune cell type, we decided that it would be necessary to test the CD9-derived peptides on a living mouse model. We chose to do this because mice can support *S. aureus* infection and the mice at least 8 weeks old have a fully developed immune system and a functional vascular system. This is a significant advantage over the current human skin models because none of them have a vascular system and we would otherwise be unable to account for non-resident, migratory immune cells such as neutrophils that would migrate to the site of infection via the bloodstream.

We were able to reproduce the mouse model described by Liu et al. and perform experiments with a mouse model that mimicked epicutaneous *S. aureus* exposure with mild penetration of the skin barrier. We found the methodology of shaving the mice, applying hair removal cream, and applying bandages to the mice to be relatively straightforward. The bandaging was strong enough to maintain contact between the bacterial suspension and the skin, but not too rigid as to suffocate the mice. After the infection period of 5 days, we also saw the mice were more comfortable with the bandaging. The mice were moving without hindrance and did not exhibit stressed behaviour such as shivering or rigid tails. We found that bandaging was important not only for keeping the gauze pad in place, but also to replicate the same level of irritation and moisture on the uninfected, control mice. Application of the bacterial suspension and bandaging changed the immediate environment around the skin, so it was warmer and moister, as such it was necessary to replicate this environment for the control mice to reduce the number of variables.

CFU counts on the skin showed that the peptides reduced *S. aureus* infection of murine skin, much in line with the data shown in Chapter 3. This finding was similarly supported by the immunohistochemistry data that showed a decrease in macrophages

in mice treated with 800ii with a trend that neutrophils were lower in mice treated with m800-Cap or 800ii. This could be expected, with the decreased bacterial adhesion onto skin, there might be less inflammation and consequently less proinflammatory signalling and immune migration. However, we were surprised to not see this in the flow cytometry data. Whilst we saw a similar trend in macrophages and monocytes in that the absolute cell numbers increased with bandaging; we were surprised to not see this in neutrophils. This could perhaps indicate that the neutrophils only responded to *S. aureus* infection and not to possible irritation caused by the shaving and subsequent bandaging. This is in opposition to a publication that reported that tape-stripping the mouse induced enhanced neutrophil recruitment to the skin (Bitschar et al., 2020), this is a step we did not include in our model as the protocol published by Liu et al. demonstrated that tape-stripping was not necessary for *S. aureus* colonisation (Liu et al., 2017). However, this might have been a useful step for us as we were also interested in immune cell infiltration into the skin. Bitschar et al. reported that neutrophil infiltration was higher in tape-stripped versus non-tape-stripped mice after 24 hours. However, based on the previously mentioned study by Janela et al., the wave of neutrophils that infiltrated the skin would have begun to decline after 24 hours (Janela et al., 2019). Given that our protocol used a significantly longer period of infection, this prolonged infection could have also led to the enhanced neutrophil infiltration in the infected models by day 5 seen in our flow cytometry data. Overall, however, these findings support our conclusion that peptide treatment does not negatively affect immune cell migration.

Our mouse model supported the growth of *S. aureus*; however, it was not to the same extent as the same model used by Liu et al. As shown in Figure 5.1, $1x10^4$ CFU could be extracted from the murine skin, whereas Liu et al. yielded somewhere between $1x10^6$ and $1x10^7$ CFU (Liu et al, 2017). However, it is important to note that Liu's model challenged the skin with a bacterial infection for 7 days whereas our model only challenged for 5 days. Furthermore, Liu et al. used the USA300 strain of MRSA in their model. Whilst USA300 is a well-characterised strain of clinical significance, it has been known to cause persistent and aggressive SSTIs (Kreisel et al, 2011). Additionally, cell invasion assays performed by Strobel et al. on multiple strains of *S. aureus*, including USA300 and SH1000, showed that USA300 was the more aggressive of the two strains (Strobel et al., 2016). A similar epicutaneous bacterial infection model used

filter paper discs and Finn chambers rather than a gauze pad and bandages, respectively (Bitschar et al., 2020). In that study, the authors were able to epicutaneously infect the mice and take a CFU count from the skin afterwards. Combined, these studies suggest that our mouse model was an appropriate choice for studying peptide effects on *S. aureus* colonisation.

The flow cytometry data from the lymph nodes was unexpected as we had not expected a trend decrease of migratory and residential cDCs and Langerhans cells after infection. Based on the unbandaged, uninfected control, this indicates that cDCs and Langerhans had decreased in numbers in the lymph nodes due to bacterial infection. We did not check the harvested lymph nodes for the presence of *S. aureus*; however, it is possible that *S. aureus* that invaded the lymph nodes may have killed the dendritic cells present. The fate of dendritic cells after migrating to the lymph nodes is currently unknown, we also speculate that the dendritic cells may have already activated naive T cells by day 5 and died soon afterwards. Regarding the significant decrease observed in macrophages in the immunohistochemistry data and not in the flow cytometry, we believe that this might relate to the flow cytometry method having both positive and negative gating to specifically isolate macrophages whereas the immunohistochemistry only selected for CD68. Whilst CD68 is a macrophage marker, it is expressed by the monocyte lineage so this staining would be positive for macrophages and monocytes.

Analysis of the H&E staining revealed that the peptide treatment had not affected the gross morphology of the skin and, when removing the bandages from the mice, the skin did not appear significantly damaged or necrotic. Combined, the data in this chapter suggests that the peptides reduce *S. aureus* adherence to murine skin without negatively affecting the skin during inflammation.

This experiment was limited in that the skin was not further analysed for inflammation. This experiment could have been improved had the skin been homogenised and the homogenate analysed with an ELISA for proinflammatory cytokines. Our experiments showed a decrease in CFU of SH1000, which combined with our immunohistochemistry data indicates the possibility that the reduced infection also meant reduced inflammation, which resulted in fewer inflammatory immune cells being

recruited to the site of infection. However, the flow cytometry data showed no difference in absolute cell numbers of immune cells between peptide treatments, meaning there may not be reduced inflammation. This could possibly be due to artefacts of using different methods of analysis (flow cytometry versus immunohistochemistry). Given the spread of data in Figures 5.5 and 5.7, it is entirely possible that the experiments needed further repeats to draw a conclusion. Additionally, a further experiment could be added with ELISA. Cytokine analysis of the skin could shed light onto the processes occurring in the skin and as to how these two findings are related or if one of the experiments requires further repeats.

# Chapter 6 Conclusion

## 6.1 Summary

In this thesis, we developed and tested a variety of skin models to determine their suitability as models for bacterial infection, with the aim of testing tetraspanin-derived peptides as a potential therapeutic. We hypothesised that peptide treatment would be effective in reducing bacterial adhesion to wounded skin without negatively affecting the immune response.

*Staphylococcus aureus* is the leading cause of skin and soft tissue infections. It is directly involved with a range of clinical diseases such as cellulitis and abscesses. *S. aureus* is also associated with other skin diseases such as atopic dermatitis which affects 1-3% of all adults globally (Nutten, 2015), with patients suffering from issues ranging from an inability to bathe or sleep comfortably, decreased self-esteem and an overall decreased quality of life (Langan et al., 2020). Therefore, the development of skin models to study *S. aureus* colonisation and infection is essential for studying host-pathogen interactions and to serve as a platform for testing potential therapeutics.

The overuse of antibiotics has resulted in the emergence of antibiotic-resistant strains of *S. aureus*, namely MRSA. The emergence of resistant strains has led to previously treatable infections being harder to treat or even becoming untreatable resulting in higher medical costs, longer hospital stays and increased mortality. The development of antibiotics that can address the new resistant strains of pathogens has declined over the years due to the expensive investment needed and the high failure rate (Årdal et al., 2020). Therefore, there is an urgent demand for anti-bacterial therapeutics which are effective and not subject to the risk of the target pathogen developing resistance.

One approach to meet this demand is to target the adherence of the pathogen to the host at the start of infection, thereby reducing the burden of infection. As described by Cozens and Read, anti-adhesion therapy can be host-directed and not bactericidal, meaning a resistance to the therapeutic would evolve at a slower rate compared to pathogen-directed antibiotics (Cozens and Read, 2012).

The work undertaken here was inspired by prior work in the University of Sheffield by Green and Cozens, whose research highlights the potential tetraspanins have as therapeutic targets. Their research demonstrated that antibodies specific to tetraspanins and recombinant peptides derived from tetraspanins could reduce the adherence of multiple bacterial species on epithelial cells. Other researchers from the University of Sheffield have shown that the CD9-derived peptides can inhibit *P. aeruginosa* adherence to keratinocytes and other epithelial cells (Alrahimi et al., 2017), inhibit *B. pseudomallei*-induced multinucleated giant cell formation (Elgawidi et al., 2020, Sangsri et al., 2020) and most relevantly, reduce *S. aureus* adherence in skin models (Ventress et al., 2016). Ventress et al. demonstrated that peptides derived from the EC2 domain of tetraspanin CD9 were potent inhibitors of *S. aureus* adherence to keratinocytes. The authors were able to show this effect on a monolayer culture of keratinocytes as well as a 3D model of human skin, and that the expression of CD9 correlated with the efficacy of the peptide treatment on bacterial adhesion. However, they could not demonstrate that the peptide treatment would not negatively affect immune cells as they did not test the peptides on immune cells. Since then, we have developed a new generation of proteolytically-resistant stapled peptides. Thus, we were driven to find out if the new stapled peptides could still reduce bacterial adhesion on more complex, relevant skin models and if the peptides negatively affected immune cell function.

In **Chapter 3**, we explored and compared human skin models available to determine which models would be best suited as a platform for infection studies. We found that both collagen-based organotypics and tissue-engineered skin constructed with de-epidermised dermis could support a bacterial infection; however, we found the infection with tissue-engineered skin to be more consistent. We suspect this to be due to inconsistencies in wounding the collagen-based organotypics as they are delicate relative to tissue-engineered skin.

We were also able to demonstrate that a new generation of peptides, improved to be more proteolytically-resistant, had similar efficacy in reducing the adherence of *S. aureus.* This was demonstrated in 2D *in vitro* monolayer cultures, 3D tissue-engineered human skin models and *ex vivo* human skin explants, the most relevant model for human testing currently available. These results agreed with previous

studies, indicating the promise these peptides have as an antimicrobial therapeutic (Ventress et al., 2016). However, the treatment does not totally prevent bacterial adhesion. Peptide treatment consistently reduced bacterial adherence by roughly 50-60% across multiple human skin models, ranging from the 2D *in vitro*, to the 3D *ex vivo*. This indicates that other mechanisms of adhesion may be present which are unaffected by the treatment. As such, it is possible that the peptide alone would not be enough to be used as a therapeutic. Whilst no therapeutic can completely eradicate a bacterial infection, the advantages of a host-directed therapeutic remain promising, especially as they are less sensitive to a pathogen evolving resistance to the therapeutic. It would be interesting to see if the peptides could perhaps be part of a treatment in combination with other therapeutics. The tetraspanin-derived peptides could ease the initial burden of infection, reducing the remaining bacteria the other therapeutics must clear.

**Chapter 4** explored the effects of the peptides against isolated immune cells, namely neutrophils and macrophages. The peptide treatment did not affect the ability of the neutrophils or macrophages to phagocytose bacteria, nor did the treatment affect bacterial adhesion to immune cells. This is in alignment with prior studies that also showed that peptide treatment does not affect bacterial internalisation or adhesion to phagocytic cells, unlike epithelial cells (Sangsri et al., 2020, Elawadi et al., 2020). Combined, this indicates that the role of CD9, despite being highly expressed on macrophages, is not related to bacterial adhesion, or that phagocytosis is not a tetraspanin-dependent process.

Ultimately, we were unable to integrate MUTZ-3 cells into a human skin model for infection studies or peptide testing due to technical issues and time restraints and concluded that other immune cell types may be more appropriate for such studies. However, it is necessary to determine the impact these peptides may have on immune cell function, therefore a mouse model was used in Chapter 5 to investigate the possible effects peptide treatment may have on immune cell migration or population.

Finally, **Chapter 5** presented data on peptide treatment in an *in vivo* mouse model. Whilst the human skin models as used in this thesis can offer insight into the structure and interactions of peptides and the skin, it was unknown as to how the peptides affected immune cell migration as currently human skin models lack a vascular system.

We found that the peptide was able to successfully reduce the adherence of *S. aureus* on murine skin and flow cytometry showed that peptide treatment did not alter the migration or populations of various immune cells.

Whilst we found that peptide treatment did not affect human macrophage or neutrophil phagocytosis, this was in a 2D *in vitro* environment where the cells were studied in isolation. It was useful to study this further in a mouse model and see if the phagocytes responded differently in a 3D context. It was additionally advantageous to use a mouse model as it is a model available with a functional vasculature system and could give us insights as to how the peptides may affect cell migration and trafficking. Ultimately, we found that the peptide treatment did not affect immune cell migration at all which agrees with our initial hypothesis that the peptides would be both efficacious and safe. As there were no changes in immune cell migration between treatments, we speculate that the peptide treatment did not alter the net chemoattractant production, secretion, and effect. This is in line with Ventress et al. who found no change in cytokine production in skin models between treatments (Ventress et al., 2016).

Whilst we hypothesised that an infection would increase the number of immune cells in the skin and lymph nodes, we were surprised to see that the absolute number of cDC2s and Langerhans cells in the lymph nodes had decreased at day 5 rather than increased. There are multiple possible explanations for this: 1) these DCs had already activated T cells in the lymph nodes and died after their role had been fulfilled; 2) the DCs had died due to *S. aureus* infection that may have migrated to the lymph nodes and survived the immune response (Bogoslowski et al., 2018); 3) these unaccounted cells had migrated to another lymphoid tissue (Natsuaki et al., 2014). A possible lymphoid tissue is induced skin-associated lymphoid tissues (iSALTs), clusters of DCs and T cells located in the dermis. This could account for the decreased number of Langerhans cells and DCs, as they were not at the expected dLNs. To determine the fate of the DCs, future experiments could be repeated with multiple timepoints i.e., day 1, day 2 etc. to observe via flow cytometry at what point does the absolute number of immune cells peaks and begins to fall. Additionally, to determine the location of the DCs, an experiment performed similarly to Natsuaki et al. would shed light on this topic (Natsuaki et al., 2014). In brief, the authors imaged the migration of fluorophore-tagged DCs and T cells in mice with 2-photon microscopy. The authors were able to observe

the accumulation of DCs and T cells in the dermis that also required communication with macrophages. Alternatively, instead of tracking the immune cells, *S. aureus* could be the target. The strain of *S. aureus* used, SH1000, is tagged with GFP and a future experiment could include flow cytometry of lymph nodes to count the absolute number of SH1000.

**Future work**

Whilst this thesis has specifically focused on *S. aureus*, it would be useful to repeat experiments with clinical isolates of *S. aureus* such as strains of MRSA, but also other pathogenic bacteria such as *P. aeruginosa* or *E. coli* as these species of bacteria cause infections on epithelial surfaces such as the corneal or bladder, also pose a global threat regarding antibiotic resistance and skin infection.

It will be important to show that peptides do not affect commensal bacteria as commensal activity is critical in maintaining skin homeostasis (Byrd et al., 2018), and preventing the invasion of pathogenic or opportunistic bacteria e.g., *S. epidermidis* protects against *S. aureus*. This could be tested in future experiments by repeating the bacterial infection experiment on mice. Instead of using chloramphenicol in the agar plates, the antibiotic could be removed so all the bacterial species present on the skin could be observed. The colonies could then be analysed and sequenced to determine CFU as well as identifying the specific species of bacteria.

There is growing evidence that the peptides are also effective in reducing bacterial adhesion on the other epithelial surfaces such as the eyes or bladder (Monk et al., 2021). Research from the Monk lab using these peptides on corneal models have found the peptides to be even more effective in reducing bacterial adherence on corneas. This could lead to new avenues where the peptides could be used, for example, the integration of these peptides into eye drops for construction workers to reduce the prevalence of microbial keratitis which is one of the leading causes of blindness (O'Brien et al., 2015). Wannigama has also demonstrated the ability of the peptides to disrupt biofilms formed by clinical isolates of *P. aeruginosa* isolated from patients with chronic lung infections (Wannigama, 2018).

*In vivo* assays in mice corneas also show that the peptides may promote wound healing (Monk et al., 2021). It would be very interesting to test the capabilities of peptide treatment on wound healing in the human skin models.

The peptide's ability to hasten wound healing could also be further investigated with animal models. We were not initially looking into the peptide's ability to heal wounds; however, we were not expecting to see a wound with our methodology given how superficial the damage would be from shaving. This methodology is not necessarily a good wound model and an experiment that investigates the effects of wound healing would be better served by an established wounding method such as by incision. However, it would be necessary to consider the differences in wound healing between different animal species and humans. Certain cytokines and genes relating to wound healing in humans are not found in mice (Zomer and Trentin, 2018). Consequently, it may be important to investigate wound healing in a model that is similar to humans in terms of wound healing such as the Red Duroc pig (Sullivan et al., 2001; Zomer and Trentin, 2018).

As previously mentioned, one of the problems caused by pathogens such as *S. aureus* is the formation of biofilms that could grow on medical implants. Given the effectiveness of the peptides in reducing *S. aureus* adherence in its planktonic form, it would be of great interest to investigate if the peptides had any potential in aiding the removal of biofilms. An interesting experimental design to incorporate would be the protocol described by Bolle et al. Briefly, Bolle et al. established a model whereby a tissue-engineered human skin model was punctured with a tube to simulate an implant. The skin model was later challenged with *S. aureus* at the site where the implant was in contact with the skin model where the bacteria formed a biofilm (Bolle et al., 2020). This protocol appears as an ideal model upon which to test the peptides against biofilm development and attachment. Whilst the peptides will not have any effect on the abiotic implant as it will not express CD9, it could be useful to study how the biofilm interacts at the site where the skin model and implant meets.

**Concluding remarks**

To conclude, we have explored the potential of tetraspanin-derived peptides as a possible therapeutic against *Staphylococcus aureus* infection in skin and wound

infections. This treatment conferred a significant reduction in adherent bacteria to keratinocytes and reduced the bacterial load in various skin models. Whilst this treatment did not totally eliminate bacterial infection, it may be used in synergy with other therapeutics to lower the burden of infection. Additionally, we showed that peptide treatment did not negatively impact immune cell function, namely phagocytosis, nor did it appear to alter immune cell populations or migration in a mouse model of bacterial skin infection.

Whilst there is currently no antibacterial anti-adhesion therapeutic available, we believe that the CD9-derived peptides have serious potential, especially if combined with other treatments in treating wounds and bacterial infection on epithelial surfaces. However, it is also important to note that CD9 is ubiquitous throughout the body and its function varies on the cell. Thus, further research into CD9 and its interactions with these peptides is warranted.

# Bibliography


Al Kindi, A., Alkahtani, A. M., Nalubega, M., El-Chami, C., O'Neill, C., Arkwright, P. D., & Pennock, J. L. (2019). *Staphylococcus aureus*Internalized by Skin Keratinocytes Evade Antibiotic Killing. *Frontiers in microbiology*, *10*, 2242. https://doi.org/10.3389/fmicb.2019.02242

Alcayaga-Miranda, F., Cuenca, J., & Khoury, M. (2017). Antimicrobial activity of mesenchymal stem cells: Current status and new perspectives of antimicrobial peptide-based therapies. In *Frontiers in Immunology* (Vol. 8, Issue MAR). https://doi.org/10.3389/fimmu.2017.00339

Aleemardani, M., Trikić, M. Z., Green, N. H., & Claeyssens, F. (2021). The Importance of Mimicking Dermal-Epidermal Junction for Skin Tissue Engineering: A Review. In *Bioengineering* (Vol. 8, Issue 11). https://doi.org/10.3390/bioengineering8110148

Ali, A. M., Atmaj, J., Van Oosterwijk, N., Groves, M. R., & Dömling, A. (2019). Stapled Peptides Inhibitors: A New Window for Target Drug Discovery. *Computational and Structural Biotechnology Journal*, *17*, 263–281. https://doi.org/https://doi.org/10.1016/j.csbj.2019.01.012

Andreu, Z., & Yáñez-Mó, M. (2014). Tetraspanins in Extracellular Vesicle Formation and Function . In *Frontiers in Immunology* (Vol. 5). https://www.frontiersin.org/articles/10.3389/fimmu.2014.00442

Arango Duque, G., & Descoteaux, A. (2014). Macrophage Cytokines: Involvement in Immunity and Infectious Diseases . In *Frontiers in Immunology* (Vol. 5, p. 491). https://www.frontiersin.org/article/10.3389/fimmu.2014.00491

Archer, N. K., Mazaitis, M. J., Costerton, J. W., Leid, J. G., Powers, M. E., & Shirtliff, M. E. (2011). *Staphylococcus aureus* biofilms: properties, regulation, and roles in human disease. *Virulence*, *2*(5), 445–459. https://doi.org/10.4161/viru.2.5.17724

Årdal, C., Balasegaram, M., Laxminarayan, R., McAdams, D., Outterson, K., Rex, J. H., & Sumpradit, N. (2020). Antibiotic development — economic, regulatory and societal challenges. *Nature Reviews Microbiology*, *18*(5), 267–274. https://doi.org/10.1038/s41579-019-0293-3

Arnette, C., Koetsier, J. L., Hoover, P., Getsios, S., & Green, K. J. (2016). In Vitro Model of the Epidermis: Connecting Protein Function to 3D Structure. In *Methods in Enzymology* (Vol. 569). https://doi.org/10.1016/bs.mie.2015.07.015

Asadi, A., Razavi, S., Talebi, M., & Gholami, M. (2019). A review on anti-adhesion therapies of bacterial diseases. *Infection*, *47*(1), 13–23. https://doi.org/10.1007/s15010-018-1222-5

Asai, A., Tsuda, Y., Kobayashi, M., Hanafusa, T., Herndon, D. N., & Suzuki, F.

(2010). Pathogenic role of macrophages in intradermal infection of methicillin-resistant Staphylococcus aureus in thermally injured mice. *Infection and Immunity*, *78*(10), 4311–4319. https://doi.org/10.1128/IAI.00642-10

Aslam, B., Wang, W., Arshad, M. I., Khurshid, M., Muzammil, S., Rasool, M. H., Nisar, M. A., Alvi, R. F., Aslam, M. A., Qamar, M. U., Salamat, M. K. F., & Baloch, Z. (2018). Antibiotic resistance: a rundown of a global crisis. *Infection and Drug Resistance*, *11*, 1645–1658. https://doi.org/10.2147/IDR.S173867

Avci, P., Sadasivam, M., Gupta, A., De Melo, W. C., Huang, Y.-Y., Yin, R., Chandran, R., Kumar, R., Otufowora, A., Nyame, T., & Hamblin, M. R. (2013). Animal models of skin disease for drug discovery. *Expert Opinion on Drug Discovery*, *8*(3), 331–355. https://doi.org/10.1517/17460441.2013.761202

Avire, N. J., Whiley, H., & Ross, K. (2021). A Review of Streptococcus pyogenes: Public Health Risk Factors, Prevention and Control. *Pathogens (Basel, Switzerland)*, *10*(2). https://doi.org/10.3390/pathogens10020248

Baldwin, H. E., Bhatia, N. D., Friedman, A., Eng, R. M., & Seite, S. (2017). The Role of Cutaneous Microbiota Harmony in Maintaining a Functional Skin Barrier. *Journal of Drugs in Dermatology : JDD*, *16*(1), 12–18.

Bardhan, A., Bruckner-Tuderman, L., Chapple, I. L. C., Fine, J.-D., Harper, N., Has, C., Magin, T. M., Marinkovich, M. P., Marshall, J. F., McGrath, J. A., Mellerio, J. E., Polson, R., & Heagerty, A. H. (2020). Epidermolysis bullosa. *Nature Reviews Disease Primers*, *6*(1), 78. https://doi.org/10.1038/s41572-020-0210-0

Barrandon, Y., Grasset, N., Zaffalon, A., Gorostidi, F., Claudinot, S., Droz-Georget, S. L., Nanba, D., & Rochat, A. (2012). Capturing epidermal stemness for regenerative medicine. *Seminars in Cell & Developmental Biology*, *23*(8), 937–944. https://doi.org/https://doi.org/10.1016/j.semcdb.2012.09.011

Barreiro, O., Yáñez-Mó, M., Sala-Valdés, M., Gutiérrez-López, M. D., Ovalle, S., Higginbottom, A., Monk, P. N., Cabañas, C., & Sánchez-Madrid, F. (2005). Endothelial tetraspanin microdomains regulate leukocyte firm adhesion during extravasation. *Blood*, *105*(7), 2852–2861.
https://doi.org/https://doi.org/10.1182/blood-2004-09-3606

Bartelt, R. R., Cruz-Orcutt, N., Collins, M., & Houtman, J. C. D. (2009). Comparison of T cell receptor-induced proximal signaling and downstream functions in immortalized and primary T cells. *PloS One*, *4*(5), e5430. https://doi.org/10.1371/journal.pone.0005430

Beaven, E. P., & Cox, A. J. J. (1965). Organ Culture of human skin. *The Journal of Investigative Dermatology*, *44*, 151–156.

Bechetoille, N., Vachon, H., Gaydon, A., Boher, A., Fontaine, T., Schaeffer, E., Decossas, M., André-Frei, V., & Mueller, C. G. (2011). A new organotypic model

containing dermal-type macrophages. In *Experimental Dermatology*. https://doi.org/10.1111/j.1600-0625.2011.01383.x

Bestebroer, J., De Haas, C. J. C., & Van Strijp, J. A. G. (2010). How microorganisms avoid phagocyte attraction. In *FEMS Microbiology Reviews* (Vol. 34, Issue 3, pp. 395–414). https://doi.org/10.1111/j.1574-6976.2009.00202.x

Beura, L. K., Hamilton, S. E., Bi, K., Schenkel, J. M., Odumade, O. A., Casey, K. A., Thompson, E. A., Fraser, K. A., Rosato, P. C., Filali-Mouhim, A., Sekaly, R. P., Jenkins, M. K., Vezys, V., Haining, W. N., Jameson, S. C., & Masopust, D. (2016). Normalizing the environment recapitulates adult human immune traits in laboratory mice. *Nature*, *532*(7600), 512–516. https://doi.org/10.1038/nature17655

Bisson-Boutelliez, C., Miller, N., Demarch, D., & Bene, M. C. (2001). CD9 and HLA-DR expression by crevicular epithelial cells and polymorphonuclear neutrophils in periodontal disease. *Journal of Clinical Periodontology*, *28*(7), 650–656. https://doi.org/10.1034/j.1600-051x.2001.028007650.x

Bitschar, K., Staudenmaier, L., Klink, L., Focken, J., Sauer, B., Fehrenbacher, B., Herster, F., Bittner, Z., Bleul, L., Schaller, M., Wolz, C., Weber, A. N. R., Peschel, A., & Schittek, B. (2020). Staphylococcus aureus Skin Colonization Is Enhanced by the Interaction of Neutrophil Extracellular Traps with Keratinocytes. *The Journal of Investigative Dermatology*, *140*(5), 1054-1065.e4. https://doi.org/10.1016/j.jid.2019.10.017

Bhattacharya, M., Berends, E. T. M., Chan, R., Schwab, E., Roy, S., Sen, C. K., Torres, V. J., & Wozniak, D. J. (2018). *Staphylococcus aureus*biofilms release leukocidins to elicit extracellular trap formation and evade neutrophil-mediated killing. *Proceedings of the National Academy of Sciences of the United States of America*, *115*(28), 7416–7421. https://doi.org/10.1073/pnas.1721949115

Bock, S., Said, A., Müller, G., Schäfer-Korting, M., Zoschke, C., & Weindl, G. (2018). Characterization of reconstructed human skin containing Langerhans cells to monitor molecular events in skin sensitization. *Toxicology in Vitro*. https://doi.org/10.1016/j.tiv.2017.09.019

Bogoslowski, A., Butcher, E. C., & Kubes, P. (2018). Neutrophils recruited through high endothelial venules of the lymph nodes via PNAd intercept disseminating <em>Staphylococcus aureus</em> *Proceedings of the National Academy of Sciences*, *115*(10), 2449 LP – 2454. https://doi.org/10.1073/pnas.1715756115

Bolle, E. C. L., Verderosa, A. D., Dhouib, R., Parker, T. J., Fraser, J. F., Dargaville, T. R., & Totsika, M. (2020). An in vitro Reconstructed Human Skin Equivalent Model to Study the Role of Skin Integration Around Percutaneous Devices Against Bacterial Infection. *Frontiers in Microbiology*, *11*, 670. https://doi.org/10.3389/fmicb.2020.00670

Bonneville, M., O'Brien, R. L., & Born, W. K. (2010). Gammadelta T cell effector functions: a blend of innate programming and acquired plasticity. *Nature Reviews. Immunology*, *10*(7), 467–478. https://doi.org/10.1038/nri2781

Boucheix, C, & Rubinstein, E. (2001). Tetraspanins. *Cellular and Molecular Life Sciences : CMLS*, *58*(9), 1189–1205. https://doi.org/10.1007/PL00000933

Boucheix, Claude. (2000). Severely reduced female fertility in CD9-deficient mice. *Science*, *287*(5451), 319–321. https://doi.org/10.1126/science.287.5451.319

Boxberger, M., Cenizo, V., Cassir, N., & La Scola, B. (2021). Challenges in exploring and manipulating the human skin microbiome. *Microbiome*, *9*(1), 125. https://doi.org/10.1186/s40168-021-01062-5

Brann, K. R., Fullerton, M. S., Onyilagha, F. I., Prince, A. A., Kurten, R. C., Rom, J. S., Blevins, J. S., Smeltzer, M. S., & Voth, D. E. (2019). Infection of Primary Human Alveolar Macrophages Alters Staphylococcus aureus Toxin Production and Activity. *Infection and Immunity*, *87*(7). https://doi.org/10.1128/IAI.00167-19

Brosseau, C., Colas, L., Magnan, A., & Brouard, S. (2018). CD9 Tetraspanin: A New Pathway for the Regulation of Inflammation? *Frontiers in Immunology*, *9*, 2316. https://doi.org/10.3389/fimmu.2018.02316

Brown, C. L., Smith, K., McCaughey, L., & Walker, D. (2012). Colicin-like bacteriocins as novel therapeutic agents for the treatment of chronic biofilm-mediated infection. *Biochemical Society Transactions*, *40*(6), 1549–1552. https://doi.org/10.1042/BST20120241

Bucior, I., Pielage, J. F., & Engel, J. N. (2012). Pseudomonas aeruginosa pili and flagella mediate distinct binding and signaling events at the apical and basolateral surface of airway epithelium. *PLoS Pathogens*, *8*(4), e1002616. https://doi.org/10.1371/journal.ppat.1002616

Burian, M., Plange, J., Schmitt, L., Kaschke, A., Marquardt, Y., Huth, L., Baron, J. M., Hornef, M. W., Wolz, C., & Yazdi, A. S. (2021). Adaptation of *Staphylococcus aureus* to the Human Skin Environment Identified Using an *ex vivo* Tissue Model. *Frontiers in microbiology*, *12*, 728989. https://doi.org/10.3389/fmicb.2021.728989

Bush, K. A., & Pins, G. D. (2012). Development of microfabricated dermal epidermal regenerative matrices to evaluate the role of cellular microenvironments on epidermal morphogenesis. *Tissue Engineering. Part A*, *18*(21–22), 2343–2353. https://doi.org/10.1089/ten.TEA.2011.0479

Byrd, A. L., Belkaid, Y., & Segre, J. A. (2018). The human skin microbiome. In *Nature Reviews Microbiology* (Vol. 16, Issue 3). https://doi.org/10.1038/nrmicro.2017.157

Canton, J. (2014). Phagosome maturation in polarized macrophages. *Journal of Leukocyte Biology*, *96*(5), 729–738.

https://doi.org/https://doi.org/10.1189/jlb.1MR0114-021R

Carlson, M. W., Alt-Holland, A., Egles, C., & Garlick, J. A. (2008). Three-dimensional tissue models of normal and diseased skin. In *Current Protocols in Cell Biology* (Issue SUPPL. 41). https://doi.org/10.1002/0471143030.cb1909s41

Chakrabarty, K. H., Dawson, R. A., Harris, P., Layton, C., Babu, M., Gould, L., Phillips, J., Leigh, I., Green, C., Freedlander, E., & Mac Neil, S. (1999). Development of autologous human dermal-epidermal composites based on sterilized human allodermis for clinical use. *The British Journal of Dermatology*, *141*(5), 811–823. https://doi.org/10.1046/j.1365-2133.1999.03153.x

Chan, C.-C., Fan, S. M.-Y., Wang, W.-H., Mu, Y.-F., & Lin, S.-J. (2015). A Two-Stepped Culture Method for Efficient Production of Trichogenic Keratinocytes. *Tissue Engineering. Part C, Methods*, *21*(10), 1070–1079. https://doi.org/10.1089/ten.TEC.2015.0033

Chanput, W., Peters, V., & Wichers, H. (2015). *THP-1 and U937 Cells.* (K. Verhoeckx, P. Cotter, I. López-Expósito, C. Kleiveland, T. Lea, A. Mackie, T. Requena, D. Swiatecka, & H. Wichers (eds.); pp. 147–159). https://doi.org/10.1007/978-3-319-16104-4_14

Chapple, C., Osman, N., & MacNeil, S. (2013). Developing tissue-engineered solutions for the treatment of extensive urethral strictures. In *European Urology* (Vol. 63, Issue 3, pp. 539–541). https://doi.org/10.1016/j.eururo.2012.09.046

Chau, D. Y. S., Johnson, C., MacNeil, S., Haycock, J. W., & Ghaemmaghami, A. M. (2013). The development of a 3D immunocompetent model of human skin. *Biofabrication*, *5*(3), 035011. https://doi.org/10.1088/1758-5082/5/3/035011

Chiller, K., Selkin, B. A., & Murakawa, G. J. (2001). Skin microflora and bacterial infections of the skin. *The Journal of Investigative Dermatology. Symposium Proceedings*, *6*(3), 170–174. https://doi.org/10.1046/j.0022-202x.2001.00043.x

Cho, J. S., Pietras, E. M., Garcia, N. C., Ramos, R. I., Farzam, D. M., Monroe, H. R., Magorien, J. E., Blauvelt, A., Kolls, J. K., Cheung, A. L., Cheng, G., Modlin, R. L., & Miller, L. S. (2010). IL-17 is essential for host defense against cutaneous Staphylococcus aureus infection in mice. *Journal of Clinical Investigation*. https://doi.org/10.1172/JCI40891

Chovatiya, R., & Silverberg, J. I. (2019). Pathophysiology of Atopic Dermatitis and Psoriasis: Implications for Management in Children. *Children (Basel, Switzerland)*, *6*(10), 108. https://doi.org/10.3390/children6100108

Chu, C. Y. (2012). Skin as an immune organ. *Dermatologica Sinica*, *30*(4), 119–120. https://doi.org/10.1016/j.dsi.2012.11.001

Chung, E., Choi, H., Lim, J. E., & Son, Y. (2014). Development of skin inflammation test model by co-culture of reconstituted 3D skin and RAW264.7 cells. *Tissue Engineering and Regenerative Medicine*, *11*(1), 87–92. https://doi.org/10.1007/s13770-013-1113-x

Clayton, K., Vallejo, A. F., Davies, J., Sirvent, S., & Polak, M. E. (2017). Langerhans Cells-Programmed by the Epidermis. *Frontiers in Immunology*, *8*, 1676. https://doi.org/10.3389/fimmu.2017.01676

Cogen, A. L., Nizet, V., & Gallo, R. L. (2008). Skin microbiota: A source of disease or defence? *British Journal of Dermatology*, *158*(3), 442–455. https://doi.org/10.1111/j.1365-2133.2008.08437.x

Cogen, A. L., Yamasaki, K., Sanchez, K. M., Dorschner, R. A., Lai, Y., MacLeod, D. T., Torpey, J. W., Otto, M., Nizet, V., Kim, J. E., & Gallo, R. L. (2010). Selective antimicrobial action is provided by phenol-soluble modulins derived from Staphylococcus epidermidis, a normal resident of the skin. *The Journal of Investigative Dermatology*, *130*(1), 192–200. https://doi.org/10.1038/jid.2009.243

Colombo, I., Sangiovanni, E., Maggio, R., Mattozzi, C., Zava, S., Corbett, Y., Fumagalli, M., Carlino, C., Corsetto, P. A., Scaccabarozzi, D., Calvieri, S., Gismondi, A., Taramelli, D., & Dell'Agli, M. (2017). HaCaT Cells as a Reliable In Vitro Differentiation Model to Dissect the Inflammatory/Repair Response of Human Keratinocytes. *Mediators of Inflammation*, *2017*, 7435621. https://doi.org/10.1155/2017/7435621

Costerton, J. W., Geesey, G. G., & Cheng, K. J. (1978). How bacteria stick. *Scientific American*, *238*(1), 86–95. https://doi.org/10.1038/scientificamerican0178-86

Courtney, H. S., Hasty, D. L., & Dale, J. B. (2002). Molecular mechanisms of adhesion, colonization, and invasion of group A streptococci. *Annals of Medicine*, *34*(2), 77–87. https://doi.org/10.1080/07853890252953464

Cozens, D., & Read, R. C. (2012). Anti-adhesion methods as novel therapeutics for bacterial infections. In *Expert Review of Anti-Infective Therapy* (Vol. 10, Issue 12, pp. 1457–1468). https://doi.org/10.1586/eri.12.145

Crew, V. K., Burton, N., Kagan, A., Green, C. A., Levene, C., Flinter, F., Brady, R. L., Daniels, G., & Anstee, D. J. (2004). CD151, the first member of the tetraspanin (TM4) superfamily detected on erythrocytes, is essential for the correct assembly of human basement membranes in kidney and skin. *Blood*, *104*(8), 2217–2223. https://doi.org/10.1182/blood-2004-04-1512

Cue, D., Lam, H., & Cleary, P. P. (2001). Genetic dissection of the Streptococcus pyogenes M1 protein: regions involved in fibronectin binding and intracellular invasion. *Microbial Pathogenesis*, *31*(5), 231–242. https://doi.org/10.1006/mpat.2001.0467

Danso, M. O., Berkers, T., Mieremet, A., Hausil, F., & Bouwstra, J. A. (2015). An ex vivo human skin model for studying skin barrier repair. *Experimental Dermatology*, *24*(1). https://doi.org/10.1111/exd.12579

Davies, J., & Davies, D. (2010). Origins and Evolution of Antibiotic Resistance. *Microbiology and Molecular Biology Reviews*, *74*(3), 417–433. https://doi.org/10.1128/MMBR.00016-10

de Haas, C. J. C., Veldkamp, K. E., Peschel, A., Weerkamp, F., Van Wamel, W. J. B., Heezius, E. C. J. M., Poppelier, M. J. J. G., Van Kessel, K. P. M., & van Strijp, J. A. G. (2004). Chemotaxis inhibitory protein of Staphylococcus aureus, a bacterial antiinflammatory agent. *The Journal of Experimental Medicine*, *199*(5), 687–695. https://doi.org/10.1084/jem.20031636

Del Giudice, P. (2020). Skin Infections Caused by Staphylococcus aureus. *Acta Dermato-Venereologica*, *100*(9), adv00110. https://doi.org/10.2340/00015555-3466

del Pozo, J. L., & Patel, R. (2007). The Challenge of Treating Biofilm-associated Bacterial Infections. *Clinical Pharmacology & Therapeutics*, *82*(2), 204–209. https://doi.org/https://doi.org/10.1038/sj.clpt.6100247

Deshpande, P., Ralston, D. R., & Macneil, S. (2013). The use of allodermis prepared from Euro skin bank to prepare autologous tissue engineered skin for clinical use. *Burns*, *39*(6), 1170–1177. https://doi.org/10.1016/j.burns.2013.02.011

Dintakurti, A., Dauletbaev, N., Hamed, R., & Lands, L. C. (2017). *The Macrophage-Like Cell Lines THP-1 and U937 Are Differentially Inclined Towards M1 and M2 Phenotypes*.

Doke, S. K., & Dhawale, S. C. (2015). Alternatives to animal testing: A review. *Saudi Pharmaceutical Journal*, *23*(3), 223–229. https://doi.org/https://doi.org/10.1016/j.jsps.2013.11.002

Durai, V., & Murphy, K. M. (2016). Functions of Murine Dendritic Cells. *Immunity*, *45*(4), 719–736. https://doi.org/10.1016/j.immuni.2016.10.010

Earnest, J. T., Hantak, M. P., Li, K., McCray, P. B. J., Perlman, S., & Gallagher, T. (2017). The tetraspanin CD9 facilitates MERS-coronavirus entry by scaffolding host cell receptors and proteases. *PLoS Pathogens*, *13*(7), e1006546. https://doi.org/10.1371/journal.ppat.1006546

Elgawidi, A., Mohsin, M. I., Ali, F., Watts, A., Monk, P. N., Thomas, M. S., & Partridge, L. J. (2020). A role for tetraspanin proteins in regulating fusion induced by Burkholderia thailandensis. *Medical Microbiology and Immunology*, *209*(4), 473–487. https://doi.org/10.1007/s00430-020-00670-6

Elston, M. J., Dupaix, J. P., Opanova, M. I., & Atkinson, R. E. (2019). Cutibacterium acnes (formerly Proprionibacterium acnes) and Shoulder Surgery. *Hawai'i Journal of Health & Social Welfare*, *78*(11 Suppl 2), 3–5.

Eyerich, S., Eyerich, K., Traidl-Hoffmann, C., & Biedermann, T. (2018). Cutaneous Barriers and Skin Immunity: Differentiating A Connected Network. In *Trends in Immunology* (Vol. 39, Issue 4). https://doi.org/10.1016/j.it.2018.02.004

Fenner, J., & Clark, R. A. F. (2016). *Chapter 1 - Anatomy, Physiology, Histology, and Immunohistochemistry of Human Skin* (M. Z. Albanna & J. H. B. T.-S. T. E. and R. M. Holmes IV (eds.); pp. 1–17). Academic Press.

https://doi.org/https://doi.org/10.1016/B978-0-12-801654-1.00001-2

Fischer, K., Tschismarov, R., Pilz, A., Straubinger, S., Carotta, S., McDowell, A., & Decker, T. (2020). Cutibacterium acnes Infection Induces Type I Interferon Synthesis Through the cGAS-STING Pathway. *Frontiers in Immunology*, *11*, 571334. https://doi.org/10.3389/fimmu.2020.571334

Fischer, N., Mak, T. N., Shinohara, D. B., Sfanos, K. S., Meyer, T. F., & Brüggemann, H. (2013). Deciphering the intracellular fate of Propionibacterium acnes in macrophages. *BioMed Research International*, *2013*, 603046. https://doi.org/10.1155/2013/603046

Flannagan, R. S., Jaumouillé, V., & Grinstein, S. (2012). The cell biology of phagocytosis. *Annual Review of Pathology*, *7*, 61–98. https://doi.org/10.1146/annurev-pathol-011811-132445

Flemming, H. C., & Wingender, J. (2010). The biofilm matrix. *Nature reviews. Microbiology*, *8*(9), 623–633. https://doi.org/10.1038/nrmicro2415

Fluit, A. C. (2012). Livestock-associated Staphylococcus aureus. *Clinical Microbiology and Infection*, *18*(8), 735–744. https://doi.org/https://doi.org/10.1111/j.1469-0691.2012.03846.x

Frade, M. A. C., Andrade, T. A. M. de, Aguiar, A. F. C. L., Guedes, F. A., Leite, M. N., Passos, W. R., Coelho, E. B., & Das, P. K. (2015). Prolonged viability of human organotypic skin explant in culture method (hOSEC). *Anais Brasileiros de Dermatologia*, *90*(3), 347–350. https://doi.org/10.1590/abd1806-4841.20153645

Francolini, I., & Donelli, G. (2010). Prevention and control of biofilm-based medical-device-related infections. In *FEMS Immunology and Medical Microbiology* (Vol. 59, Issue 3, pp. 227–238). https://doi.org/10.1111/j.1574-695X.2010.00665.x

Frankart, A., Malaisse, J., De Vuyst, E., Minner, F., de Rouvroit, C. L., & Poumay, Y. (2012). Epidermal morphogenesis during progressive in vitro 3D reconstruction at the air–liquid interface. *Experimental Dermatology*, *21*(11), 871–875. https://doi.org/https://doi.org/10.1111/exd.12020

Fuchs, E., & Raghavan, S. (2002). Getting under the skin of epidermal morphogenesis. In *Nature Reviews Genetics* (Vol. 3, Issue 3, pp. 199–209). https://doi.org/10.1038/nrg758

Fux, C. A., Costerton, J. W., Stewart, P. S., & Stoodley, P. (2005). Survival strategies of infectious biofilms. *Trends in Microbiology*, *13*(1), 34–40. https://doi.org/10.1016/j.tim.2004.11.010

Garcia, M., Morello, E., Garnier, J., Barrault, C., Garnier, M., Burucoa, C., Lecron, J.-C., Si-Tahar, M., Bernard, F.-X., & Bodet, C. (2018). Pseudomonas aeruginosa flagellum is critical for invasion, cutaneous persistence and induction of

inflammatory response of skin epidermis. *Virulence*, *9*(1), 1163–1175. https://doi.org/10.1080/21505594.2018.1480830

Garrett, T.R., Bhakoo, M., & Zhang, Z. (2008) Bacterial adhesion and biofilms on surfaces. *Progress in Natural Science, 18 (9),* 1049-1056, https://doi.org/10.1016/j.pnsc.2008.04.001.

Gartlan, K. H., Wee, J. L., Demaria, M. C., Nastovska, R., Chang, T. M., Jones, E. L., Apostolopoulos, V., Pietersz, G. A., Hickey, M. J., van Spriel, A. B., & Wright, M. D. (2013). Tetraspanin CD37 contributes to the initiation of cellular immunity by promoting dendritic cell migration. *European journal of immunology*, *43*(5), 1208–1219. https://doi.org/10.1002/eji.201242730

Gebreyohannes, G., Nyerere, A., Bii, C., & Sbhatu, D. B. (2019). Challenges of intervention, treatment, and antibiotic resistance of biofilm-forming microorganisms. *Heliyon*, *5*(8), e02192–e02192. https://doi.org/10.1016/j.heliyon.2019.e02192

Goldmann, O., & Medina, E. (2017). Staphylococcus aureus strategies to evade the host acquired immune response. *International Journal of Medical Microbiology : IJMM*. https://doi.org/10.1016/j.ijmm.2017.09.013

Gould, I. M., Reilly, J., Bunyan, D., & Walker, A. (2010). Costs of healthcare-associated methicillin-resistant Staphylococcus aureus and its control. In *Clinical Microbiology and Infection* (Vol. 16, Issue 12, pp. 1721–1728). https://doi.org/10.1111/j.1469-0691.2010.03365.x

Gray, M. A., Choy, C. H., Dayam, R. M., Ospina-Escobar, E., Somerville, A., Xiao, X., Ferguson, S. M., & Botelho, R. J. (2016). Phagocytosis Enhances Lysosomal and Bactericidal Properties by Activating the Transcription Factor TFEB. *Current Biology*, *26*(15), 1955–1964. https://doi.org/10.1016/j.cub.2016.05.070

Green, L. R., Monk, P. N., Partridge, L. J., Morris, P., Gorringe, A. R., & Read, R. C. (2011). Cooperative role for tetraspanins in adhesin-mediated attachment of bacterial species to human epithelial cells. *Infection and Immunity*, *79*(6), 2241–2249. https://doi.org/10.1128/IAI.01354-10

Green, L. R., Issa, R., Albaldi, F., Urwin, L., Khalid, H., Turner, C. E., Ciani, B., Partridge, L. J., & Monk, P. N. (2023). CD9 co-operation with syndecan-1 is required for a major staphylococcal adhesion pathway. *BioRxiv*, 2023.01.17.524294. https://doi.org/10.1101/2023.01.17.524294

Grice, E. A., Kong, H. H., Conlan, S., Deming, C. B., Davis, J., Young, A. C., Bouffard, G. G., Blakesley, R. W., Murray, P. R., Green, E. D., Turner, M. L., & Segre, J. A. (2009). Topographical and temporal diversity of the human skin microbiome. *Science*, *324*(5931), 1190–1192. https://doi.org/10.1126/science.1171700

Gries, C. M., & Kielian, T. (2017). Staphylococcal Biofilms and Immune Polarization During Prosthetic Joint Infection. *The Journal of the American Academy of*

*Orthopaedic Surgeons*, *25 Suppl 1*(Suppl 1), S20–S24. https://doi.org/10.5435/JAAOS-D-16-00636

Haake, A., Scot, G. A., & Holbrook, K. A. (2001). Structure and function of the skin: overview of the epidermis and dermis. In *The Biology of the Skin* (pp. 19–45).

Haiko, J., & Westerlund-Wikström, B. (2013). The role of the bacterial flagellum in adhesion and virulence. *Biology*, *2*(4), 1242–1267. https://doi.org/10.3390/biology2041242

Hassuna, N., Monk, P. N., Moseley, G. W., & Partridge, L. J. (2009). Strategies for targeting tetraspanin proteins: Potential therapeutic applications in microbial infections. In *BioDrugs* (Vol. 23, Issue 6, pp. 341–359). https://doi.org/10.2165/11315650-000000000-00000

Hayashida, A., Amano, S., & Park, P. W. (2011). Syndecan-1 promotes Staphylococcus aureus corneal infection by counteracting neutrophil-mediated host defense. *The Journal of Biological Chemistry*, *286*(5), 3288–3297. https://doi.org/10.1074/jbc.M110.185165

Hemler, M. E. (2003). Tetraspanin Proteins Mediate Cellular Penetration, Invasion, and Fusion Events and Define a Novel Type of Membrane Microdomain. *Annual Review of Cell and Developmental Biology*, *19*(1), 397–422. https://doi.org/10.1146/annurev.cellbio.19.111301.153609

Higgins, C. A., Chen, J. C., Cerise, J. E., Jahoda, C. A. B., & Christiano, A. M. (2013). Microenvironmental reprogramming by three-dimensional culture enables dermal papilla cells to induce de novo human hair-follicle growth. *Proceedings of the National Academy of Sciences of the United States of America*, *110*(49), 19679–19688. https://doi.org/10.1073/pnas.1309970110

Honda, T., Egawa, G., & Kabashima, K. (2019). Antigen presentation and adaptive immune responses in skin. *International Immunology*, *31*(7), 423–429. https://doi.org/10.1093/intimm/dxz005

Huang, S., Yuan, S., Dong, M., Su, J., Yu, C., Shen, Y., Xie, X., Yu, Y., Yu, X., Chen, S., Zhang, S., Pontarotti, P., & Xu, A. (2005). The phylogenetic analysis of tetraspanins projects the evolution of cell-cell interactions from unicellular to multicellular organisms. *Genomics*, *86*(6), 674–684. https://doi.org/10.1016/j.ygeno.2005.08.004

Huet, F., Severino-Freire, M., Chéret, J., Gouin, O., Praneuf, J., Pierre, O., Misery, L., & Le Gall-Ianotto, C. (2018). Reconstructed human epidermis for in vitro studies on atopic dermatitis: A review. *Journal of Dermatological Science*, *89*(3), 213–218. https://doi.org/https://doi.org/10.1016/j.jdermsci.2017.11.015

Hutter, V., Kirton, S. B., & Chau, D. Y. S. (2017). Immunocompetent human in vitro skin models. In *Skin Tissue Models*. https://doi.org/10.1016/B978-0-12-810545-0.00015-2

Iwatsuki, K., Yamasaki, O., Morizane, S., & Oono, T. (2006). Staphylococcal cutaneous infections: invasion, evasion and aggression. In *Journal of dermatological science* (Vol. 42, Issue 3, pp. 203–214). https://doi.org/10.1016/j.jdermsci.2006.03.011

Jacobs, J. J. L., Lehé, C. L., Hasegawa, H., Elliott, G. R., & Das, P. K. (2006). Skin irritants and contact sensitizers induce Langerhans cell migration and maturation at irritant concentration. *Experimental Dermatology*, *15*(6), 432–440. https://doi.org/10.1111/j.0906-6705.2006.00420.x

Janela, B., Patel, A. A., Lau, M. C., Goh, C. C., Msallam, R., Kong, W. T., Fehlings, M., Hubert, S., Lum, J., Simoni, Y., Malleret, B., Zolezzi, F., Chen, J., Poidinger, M., Satpathy, A. T., Briseno, C., Wohn, C., Malissen, B., Murphy, K. M., … Ginhoux, F. (2019). A Subset of Type I Conventional Dendritic Cells Controls Cutaneous Bacterial Infections through VEGFα-Mediated Recruitment of Neutrophils. *Immunity*. https://doi.org/10.1016/j.immuni.2019.03.001

Jin, H., He, R., Oyoshi, M., & Geha, R. S. (2009). Animal Models of Atopic Dermatitis. *Journal of Investigative Dermatology*, *129*(1), 31–40. https://doi.org/https://doi.org/10.1038/jid.2008.106

Jockers, J. J., & Novak, N. (2006). Different expression of adhesion molecules and tetraspanins of monocytes of patients with atopic eczema. *Allergy*, *61*(12), 1419–1422. https://doi.org/10.1111/j.1398-9995.2006.01191.x

Joh, D., Wann, E. R., Kreikemeyer, B., Speziale, P., & Höök, M. (1999). Role of fibronectin-binding MSCRAMMs in bacterial adherence and entry into mammalian cells. In *Matrix Biology* (Vol. 18, Issue 3, pp. 211–223). https://doi.org/10.1016/S0945-053X(99)00025-6

Johansson, L., Thulin, P., Low, D. E., & Norrby-Teglund, A. (2010). Getting under the skin: the immunopathogenesis of Streptococcus pyogenes deep tissue infections. *Clinical Infectious Diseases : An Official Publication of the Infectious Diseases Society of America*, *51*(1), 58–65. https://doi.org/10.1086/653116

Josse, J., Laurent, F., & Diot, A. (2017). Staphylococcal Adhesion and Host Cell Invasion: Fibronectin-Binding and Other Mechanisms . In *Frontiers in Microbiology* (Vol. 8, p. 2433). https://www.frontiersin.org/article/10.3389/fmicb.2017.02433

Jubrail, J., Morris, P., Bewley, M. A., Stoneham, S., Johnston, S. A., Foster, S. J., Peden, A. A., Read, R. C., Marriott, H. M., & Dockrell, D. H. (2016). Inability to sustain intraphagolysosomal killing of Staphylococcus aureus predisposes to bacterial persistence in macrophages. *Cellular Microbiology*, *18*(1), 80–96. https://doi.org/https://doi.org/10.1111/cmi.12485

Jung, E. C., & Maibach, H. I. (2015). Animal models for percutaneous absorption. *Journal of Applied Toxicology : JAT*, *35*(1), 1–10. https://doi.org/10.1002/jat.3004

Kaneko, J., & Kamio, Y. (2004). Bacterial Two-component and Hetero-heptameric

Pore-forming Cytolytic Toxins: Structures, Pore-forming Mechanism, and Organization of the Genes. *Bioscience, Biotechnology, and Biochemistry*, *68*(5), 981–1003. https://doi.org/10.1271/bbb.68.981

Kaplan, M. J., & Radic, M. (2012). Neutrophil extracellular traps (NETs): Double-edged swords of innate immunity. *Journal of Immunology (Baltimore, Md. : 1950)*, *189*(6), 2689–2695. https://doi.org/10.4049/jimmunol.1201719

Karauzum, H., & Datta, S. K. (2017). Adaptive Immunity Against Staphylococcus aureus. *Current Topics in Microbiology and Immunology*, *409*, 419–439. https://doi.org/10.1007/82_2016_1

Kew, R. R. (2014). *The Complement System* (L. M. McManus & R. N. B. T.-P. of H. D. Mitchell, Eds.; pp. 231–243). Academic Press. https://doi.org/https://doi.org/10.1016/B978-0-12-386456-7.01802-5

Khatoon, Z., McTiernan, C. D., Suuronen, E. J., Mah, T.-F., & Alarcon, E. I. (2018). Bacterial biofilm formation on implantable devices and approaches to its treatment and prevention. *Heliyon*, *4*(12), e01067. https://doi.org/10.1016/j.heliyon.2018.e01067

Kim, H. K., Missiakas, D., & Schneewind, O. (2014). Mouse models for infectious diseases caused by Staphylococcus aureus. *Journal of Immunological Methods*, *410*, 88–99. https://doi.org/10.1016/j.jim.2014.04.007

Kinnebrew, M. A., Buffie, C. G., Diehl, G. E., Zenewicz, L. A., Leiner, I., Hohl, T. M., Flavell, R. A., Littman, D. R., & Pamer, E. G. (2012). Interleukin 23 production by intestinal CD103(+)CD11b(+) dendritic cells in response to bacterial flagellin enhances mucosal innate immune defense. *Immunity*, *36*(2), 276–287. https://doi.org/10.1016/j.immuni.2011.12.011

Kintarak, S., Whawell, S. A., Speight, P. M., Packer, S., & Nair, S. P. (2004). Internalization of Staphylococcus aureus by human keratinocytes. *Infection and Immunity*, *72*(10), 5668–5675. https://doi.org/10.1128/IAI.72.10.5668-5675.2004

Kondělková, K., Vokurková, D., Krejsek, J., Borská, L., Fiala, Z., & Ctirad, A. (2010). Regulatory T cells (TREG) and their roles in immune system with respect to immunopathological disorders. *Acta Medica (Hradec Kralove)*, *53*(2), 73–77. https://doi.org/10.14712/18059694.2016.63

Kosten, I. J., Spiekstra, S. W., de Gruijl, T. D., & Gibbs, S. (2015). MUTZ-3 derived Langerhans cells in human skin equivalents show differential migration and phenotypic plasticity after allergen or irritant exposure. *Toxicology and Applied Pharmacology*, *287*(1), 35–42. https://doi.org/10.1016/j.taap.2015.05.017

Kotzerke, K., Mempel, M., Aung, T., Wulf, G. G., Urlaub, H., Wenzel, D., Schön, M. P., & Braun, A. (2013). Immunostimulatory activity of murine keratinocyte-derived exosomes. *Experimental dermatology*, *22*(10), 650–655. https://doi.org/10.1111/exd.12230

Krachler, A. M., & Orth, K. (2013). Targeting the bacteria-host interface strategies in anti-adhesion therapy. In *Virulence* (Vol. 4, Issue 4, pp. 284–294). https://doi.org/10.4161/viru.24606

Kraft, S., Jouvin, M. H., Kulkarni, N., Kissing, S., Morgan, E. S., Dvorak, A. M., Schröder, B., Saftig, P., & Kinet, J. P. (2013). The tetraspanin CD63 is required for efficient IgE-mediated mast cell degranulation and anaphylaxis. Journal of immunology (Baltimore, Md. : 1950), 191(6), 2871–2878. https://doi.org/10.4049/jimmunol.1202323

Krasowska, A., & Sigler, K. (2014). How microorganisms use hydrophobicity and what does this mean for human needs? *Frontiers in Cellular and Infection Microbiology*, *4*. https://doi.org/10.3389/fcimb.2014.00112

Kreisel, K. M., Stine, O. C., Johnson, J. K., Perencevich, E. N., Shardell, M. D., Lesse, A. J., Gordin, F. M., Climo, M. W., & Roghmann, M.-C. (2011). USA300 methicillin-resistant Staphylococcus aureus bacteremia and the risk of severe sepsis: is USA300 methicillin-resistant Staphylococcus aureus associated with more severe infections? *Diagnostic Microbiology and Infectious Disease*, *70*(3), 285–290. https://doi.org/10.1016/j.diagmicrobio.2011.03.010

Krishna, S., & Miller, L. S. (2012a). Host-pathogen interactions between the skin and Staphylococcus aureus. In *Current Opinion in Microbiology*. https://doi.org/10.1016/j.mib.2011.11.003

Krishna, S., & Miller, L. S. (2012b). Innate and adaptive immune responses against Staphylococcus aureus skin infections. In *Seminars in Immunopathology* (Vol. 34, Issue 2, pp. 261–280). https://doi.org/10.1007/s00281-011-0292-6

Kühbacher, A., Henkel, H., Stevens, P., Grumaz, C., Finkelmeier, D., Burger-Kentischer, A., Sohn, K., & Rupp, SteKühbacher, A., Henkel, H., Stevens, P., Grumaz, C., Finkelmeier, D., Burger-Kentischer, A., Sohn, K., & Rupp, S. (2017). Central role for dermal fibroblasts in skin model protection against candida albicans. Journal of Infectious Diseases, 215(11, 1742–1752. https://doi.org/10.1093/infdis/jix153ffen. (2017). Central role for dermal fibroblasts in skin model protection against candida albicans. *Journal of Infectious Diseases*, *215*(11), 1742–1752. https://doi.org/10.1093/infdis/jix153

Kühbacher, A., Sohn, K., Burger-Kentischer, A., & Rupp, S. (2017). Immune cell-supplemented human skin model for studying fungal infections. In *Methods in Molecular Biology*. https://doi.org/10.1007/978-1-4939-6515-1_25

Kumar, S., Jeong, Y., Ashraf, M. U., & Bae, Y.-S. (2019). Dendritic Cell-Mediated Th2 Immunity and Immune Disorders. *International Journal of Molecular Sciences*, *20*(9), 2159. https://doi.org/10.3390/ijms20092159

Kwiecinski, J. M., Jacobsson, G., Horswill, A. R., Josefsson, E., & Jin, T. (2019). Biofilm formation by Staphylococcus aureus clinical isolates correlates with the infection type. *Infectious diseases*, *51*(6), 446–451. https://doi.org/10.1080/23744235.2019.1593499

Kwiecinski, J. M., Kratofil, R. M., Parlet, C. P., Surewaard, B. G. J., Kubes, P., & Horswill, A. R. (2021). Staphylococcus aureus uses the ArlRS and MgrA cascade to regulate immune evasion during skin infection. *Cell reports*, *36*(4), 109462. https://doi.org/10.1016/j.celrep.2021.109462

Laabei, M., & Ermert, D. (2019). Catch Me if You Can: Streptococcus pyogenes Complement Evasion Strategies. *Journal of Innate Immunity*, *11*(1), 3–12. https://doi.org/10.1159/000492944

Laborel-Préneron, E., Bianchi, P., Boralevi, F., Lehours, P., Fraysse, F., Morice-Picard, F., Sugai, M., Sato'O, Y., Badiou, C., Lina, G., Schmitt, A. M., Redoulès, D., Casas, C., & Davrinche, C. (2015). Effects of the staphylococcus aureus and staphylococcus epidermidis secretomes isolated from the skin microbiota of atopic children on CD4+ T cell activation. *PLoS ONE*, *10*(10). https://doi.org/10.1371/journal.pone.0141067

Lai, Y., Di Nardo, A., Nakatsuji, T., Leichtle, A., Yang, Y., Cogen, A. L., Wu, Z.-R., Hooper, L. V, Schmidt, R. R., von Aulock, S., Radek, K. A., Huang, C.-M., Ryan, A. F., & Gallo, R. L. (2009). Commensal bacteria regulate Toll-like receptor 3-dependent inflammation after skin injury. *Nature Medicine*, *15*(12), 1377–1382. https://doi.org/10.1038/nm.2062

Langan, S. M., Irvine, A. D., & Weidinger, S. (2020). Atopic dermatitis. *The Lancet*, *396*(10247), 345–360. https://doi.org/10.1016/S0140-6736(20)31286-1

Laubach, V., Zöller, N., Rossberg, M., Görg, K., Kippenberger, S., Bereiter-Hahn, J., Kaufmann, R., & Bernd, A. (2011). Integration of Langerhans-like cells into a human skin equivalent. *Archives of Dermatological Research*, *303*(2), 135–139. https://doi.org/10.1007/s00403-010-1092-x

Le, K. Y., & Otto, M. (2015). Quorum-sensing regulation in staphylococci-an overview. *Frontiers in microbiology*, *6*, 1174. https://doi.org/10.3389/fmicb.2015.01174

Ledger, E. V. K., Pader, V., & Edwards, A. M. (2017). Enterococcus faecalis and pathogenic streptococci inactivate daptomycin by releasing phospholipids. *Microbiology (United Kingdom)*, *163*(10), 1502–1508. https://doi.org/10.1099/mic.0.000529

Ley, K., Laudanna, C., Cybulsky, M. I., & Nourshargh, S. (2007). Getting to the site of inflammation: the leukocyte adhesion cascade updated. *Nature Reviews Immunology*, *7*(9), 678–689. https://doi.org/10.1038/nri2156

Li, Q., Yang, X. H., Xu, F., Sharma, C., Wang, H. X., Knoblich, K., Rabinovitz, I., Granter, S. R., & Hemler, M. E. (2013). Tetraspanin CD151 plays a key role in skin squamous cell carcinoma. *Oncogene*, *32*(14), 1772–1783. https://doi.org/10.1038/onc.2012.205

Liu, H., Archer, N. K., Dillen, C. A., Wang, Y., Ashbaugh, A. G., Ortines, R. V., Kao,

T., Lee, S. K., Cai, S. S., Miller, R. J., Marchitto, M. C., Zhang, E., Riggins, D. P., Plaut, R. D., Stibitz, S., Geha, R. S., & Miller, L. S. (2017). Staphylococcus aureus Epicutaneous Exposure Drives Skin Inflammation via IL-36-Mediated T Cell Responses. *Cell Host and Microbe*. https://doi.org/10.1016/j.chom.2017.10.006

Liu, X., Zhu, R., Luo, Y., Wang, S., Zhao, Y., Qiu, Z., Zhang, Y., Liu, X., Yao, X., Li, X., & Li, W. (2021). Distinct human Langerhans cell subsets orchestrate reciprocal functions and require different developmental regulation. *Immunity*, *54*(10), 2305–2320.e11. https://doi.org/10.1016/j.immuni.2021.08.012

Llarrull, L. I., Fisher, J. F., & Mobashery, S. (2009). Molecular basis and phenotype of methicillin resistance in Staphylococcus aureus and insights into new ??-lactams that meet the challenge. In *Antimicrobial Agents and Chemotherapy* (Vol. 53, Issue 10, pp. 4051–4063). https://doi.org/10.1128/AAC.00084-09

Losquadro, W. D. (2017). Anatomy of the Skin and the Pathogenesis of Nonmelanoma Skin Cancer. In *Facial Plastic Surgery Clinics of North America* (Vol. 25, Issue 3, pp. 283–289). https://doi.org/10.1016/j.fsc.2017.03.001

Lu, L., Hu, W., Tian, Z., Yuan, D., Yi, G., Zhou, Y., Cheng, Q., Zhu, J., & Li, M. (2019). Developing natural products as potential anti-biofilm agents. *Chinese medicine*, *14*, 11. https://doi.org/10.1186/s13020-019-0232-2

MacNeil, S. (2007). Progress and opportunities for tissue-engineered skin. *Nature*, *445*(7130), 874–880. https://doi.org/10.1038/nature05664

Madhvi, A., Mishra, H., Leisching, G. R., Mahlobo, P. Z., & Baker, B. (2019). Comparison of human monocyte derived macrophages and THP1-like macrophages as in vitro models for M. tuberculosis infection. *Comparative Immunology, Microbiology and Infectious Diseases*, *67*, 101355. https://doi.org/https://doi.org/10.1016/j.cimid.2019.101355

Madison, K. C. (2003). Barrier Function of the Skin: ‘‘La Raison d’Etre" of the Epidermis. *Journal of Investigative Dermatology*, *121*(2), 231–241. https://doi.org/10.1046/j.1523-1747.2003.12359.x

Malara, M. M., Blackstone, B. N., Baumann, M. E., Bailey, J. K., Supp, D. M., & Powell, H. M. (2020). Cultured Epithelial Autograft Combined with Micropatterned Dermal Template Forms Rete Ridges In Vivo. *Tissue Engineering. Part A*, *26*(21–22), 1138–1146. https://doi.org/10.1089/ten.TEA.2020.0090

Malissen, B., Tamoutounour, S., & Henri, S. (2014). The origins and functions of dendritic cells and macrophages in the skin. In *Nature Reviews Immunology* (Vol. 14, Issue 6, pp. 417–428). https://doi.org/10.1038/nri3683

Manning, D. D., Reed, N. D., & Shaffer, C. F. (1973). Maintenance of skin xenografts of widely divergent phylogenetic origin of congenitally athymic (nude) mice. *The Journal of Experimental Medicine*, *138*(2), 488–494.

https://doi.org/10.1084/jem.138.2.488

Mantegazza, A. R., Barrio, M. M., Moutel, S., Bover, L., Weck, M., Brossart, P., Teillaud, J. L., & Mordoh, J. (2004). CD63 tetraspanin slows down cell migration and translocates to the endosomal-lysosomal-MIICs route after extracellular stimuli in human immature dendritic cells. *Blood*, *104*(4), 1183–1190. https://doi.org/10.1182/blood-2004-01-0104

Marbach, H., Vizcay-Barrena, G., Memarzadeh, K., Otter, J. A., Pathak, S., Allaker, R. P., Harvey, R. D., & Edgeworth, J. D. (2019). Tolerance of MRSA ST239-TW to chlorhexidine-based decolonization: Evidence for keratinocyte invasion as a mechanism of biocide evasion. *The Journal of infection*, *78*(2), 119–126. https://doi.org/10.1016/j.jinf.2018.10.007

Martín, C., Ordiales, H., Vázquez, F., Pevida, M., Rodríguez, D., Merayo, J., Vázquez, F., García, B., & Quirós, L. M. (2022). Bacteria associated with acne use glycosaminoglycans as cell adhesion receptors and promote changes in the expression of the genes involved in their biosynthesis. *BMC Microbiology*, *22*(1), 65. https://doi.org/10.1186/s12866-022-02477-2

Martin, V., Dorte, F., Hanne, I., A., F. V., P., N. R., J., F. J., A., P. D., Miriam, B., & I., R. J. (2019). Antibiotic Resistance and the MRSA Problem. *Microbiology Spectrum*, *7*(2), 7.2.18. https://doi.org/10.1128/microbiolspec.GPP3-0057-2018

Masterson, A. J., Sombroek, C. C., De Gruijl, T. D., Graus, Y. M. F., van der Vliet, H. J. J., Lougheed, S. M., van den Eertwegh, A. J. M., Pinedo, H. M., & Scheper, R. J. (2002). MUTZ-3, a human cell line model for the cytokine-induced differentiation of dendritic cells from CD34+ precursors. *Blood*, *100*(2), 701–703. https://doi.org/10.1182/blood.v100.2.701

Mendoza-Coronel, E., & Castañón-Arreola, M. (2016). Comparative evaluation of in vitro human macrophage models for mycobacterial infection study. *Pathogens and Disease*, *74*(6). https://doi.org/10.1093/femspd/ftw052

Merad, M., Ginhoux, F., & Collin, M. (2008). Origin, homeostasis and function of Langerhans cells and other langerin-expressing dendritic cells. In *Nature Reviews Immunology* (Vol. 8, Issue 12, pp. 935–947). https://doi.org/10.1038/nri2455

Merad, M., Sathe, P., Helft, J., Miller, J., & Mortha, A. (2013). The dendritic cell lineage: ontogeny and function of dendritic cells and their subsets in the steady state and the inflamed setting. *Annual Review of Immunology*, *31*, 563–604. https://doi.org/10.1146/annurev-immunol-020711-074950

Mestas, J., & Hughes, C. C. W. (2004). Of Mice and Not Men: Differences between Mouse and Human Immunology. *The Journal of Immunology*, *172*(5), 2731–2738. https://doi.org/10.4049/jimmunol.172.5.2731

Miller, L. S., & Cho, J. S. (2011). Immunity against Staphylococcus aureus cutaneous infections. In *Nature Reviews Immunology*. https://doi.org/10.1038/nri3010

Miller, L. S., Fowler Jr, V. G., Shukla, S. K., Rose, W. E., & Proctor, R. A. (2020). Development of a vaccine against Staphylococcus aureus invasive infections: Evidence based on human immunity, genetics and bacterial evasion mechanisms. *FEMS Microbiology Reviews*, *44*(1), 123–153. https://doi.org/10.1093/femsre/fuz030

Miller, L. S., & Simon, S. I. (2018). Neutrophils in hot pursuit of MRSA in the lymph nodes. *Proceedings of the National Academy of Sciences*, *115*(10), 2272 LP – 2274. https://doi.org/10.1073/pnas.1800448115

Moniz, T., Costa Lima, S. A., & Reis, S. (2020). Human skin models: From healthy to disease-mimetic systems; characteristics and applications. *British Journal of Pharmacology*, *177*(19), 4314–4329. https://doi.org/10.1111/bph.15184

Monk, P. N., & Partridge, L. J. (2012). Tetraspanins: gateways for infection. *Infect Disord Drug Targets*, *12*(1), 4–17. https://doi.org/10.2174/187152612798994957

Monk P, R. I. and B. C. (2021). *PCT/EP2021/055109, "Antimicrobial target"* (Patent No. PCT/EP2021/055109).

Moriwaki, M., Iwamoto, K., Niitsu, Y., Matsushima, A., Yanase, Y., Hisatsune, J., Sugai, M., & Hide, M. (2019). Staphylococcus aureus from atopic dermatitis skin accumulates in the lysosomes of keratinocytes with induction of IL-1α secretion via TLR9. *Allergy*, *74*(3), 560–571. https://doi.org/10.1111/all.13622

Muszer, M., Noszczyńska, M., Kasperkiewicz, K., & Skurnik, M. (2015). Human Microbiome: When a Friend Becomes an Enemy. In *Archivum Immunologiae et Therapiae Experimentalis* (Vol. 63, Issue 4, pp. 287–298). https://doi.org/10.1007/s00005-015-0332-3

Naik, S., Bouladoux, N., Wilhelm, C., Molloy, M. J., Salcedo, R., Kastenmuller, W., Deming, C., Quinones, M., Koo, L., Conlan, S., Spencer, S., Hall, J. A., Dzutsev, A., Kong, H., Campbell, D. J., Trinchieri, G., Segre, J. A., & Belkaid, Y. (2012). Compartmentalized control of skin immunity by resident commensals. *Science (New York, N.Y.)*, *337*(6098), 1115–1119. https://doi.org/10.1126/science.1225152

Nakajima, S., Nomura, T., Common, J., & Kabashima, K. (2019). Insights into atopic dermatitis gained from genetically defined mouse models. In *Journal of Allergy and Clinical Immunology*. https://doi.org/10.1016/j.jaci.2018.11.014

Nakamura, K, Williams, I. R., & Kupper, T. S. (1995). Keratinocyte-derived monocyte chemoattractant protein 1 (MCP-1): analysis in a transgenic model demonstrates MCP-1 can recruit dendritic and Langerhans cells to skin. *The Journal of Investigative Dermatology*, *105*(5), 635–643. https://doi.org/10.1111/1523-1747.ep12324061

Nakamura, Kuniaki, Mitamura, T., Takahashi, T., Kobayashi, T., & Mekada, E. (2000). Importance of the major extracellular domain of CD9 and the epidermal growth factor (EGF)-like domain of heparin-binding EGF-like growth factor for

up-regulation of binding and activity. *Journal of Biological Chemistry*, *275*(24), 18284–18290. https://doi.org/10.1074/jbc.M907971199

Nakatsuji, T., Chen, T. H., Narala, S., Chun, K. A., Two, A. M., Yun, T., Shafiq, F., Kotol, P. F., Bouslimani, A., Melnik, A. V., Latif, H., Kim, J. N., Lockhart, A., Artis, K., David, G., Taylor, P., Streib, J., Dorrestein, P. C., Grier, A., … Gallo, R. L. (2017). Antimicrobials from human skin commensal bacteria protect against Staphylococcus aureus and are deficient in atopic dermatitis. *Science Translational Medicine*, *9*(378). https://doi.org/10.1126/scitranslmed.aah4680

Nakatsuji, T., Chen, T. H., Two, A. M., Chun, K. A., Narala, S., Geha, R. S., Hata, T. R., & Gallo, R. L. (2016). Staphylococcus aureus Exploits Epidermal Barrier Defects in Atopic Dermatitis to Trigger Cytokine Expression. *Journal of Investigative Dermatology*, *136*(11). https://doi.org/10.1016/j.jid.2016.05.127

Nasiri, G., Azarpira, N., Alizadeh, A., Goshtasbi, S., & Tayebi, L. (2020). Shedding light on the role of keratinocyte-derived extracellular vesicles on skin-homing cells. *Stem cell research & therapy*, *11*(1), 421. https://doi.org/10.1186/s13287-020-01929-8

Natsuaki, Y., Egawa, G., Nakamizo, S., Ono, S., Hanakawa, S., Okada, T., Kusuba, N., Otsuka, A., Kitoh, A., Honda, T., Nakajima, S., Tsuchiya, S., Sugimoto, Y., Ishii, K. J., Tsutsui, H., Yagita, H., Iwakura, Y., Kubo, M., Ng, L. G., … Kabashima, K. (2014). Perivascular leukocyte clusters are essential for efficient activation of effector T cells in the skin. *Nature Immunology*. https://doi.org/10.1038/ni.2992

Neil, J. E., Brown, M. B., & Williams, A. C. (2020). Human skin explant model for the investigation of topical therapeutics. *Scientific Reports*, *10*(1), 21192. https://doi.org/10.1038/s41598-020-78292-4

Nestle, F. O., Di Meglio, P., Qin, J.-Z., & Nickoloff, B. J. (2009). Skin immune sentinels in health and disease. *Nature Reviews Immunology*. https://doi.org/10.1038/nri2622

Nguyen, L. T., Haney, E. F., & Vogel, H. J. (2011). The expanding scope of antimicrobial peptide structures and their modes of action. In *Trends in Biotechnology* (Vol. 29, Issue 9, pp. 464–472). https://doi.org/10.1016/j.tibtech.2011.05.001

Nippe, N., Varga, G., Holzinger, D., Löffler, B., Medina, E., Becker, K., Roth, J., Ehrchen, J. M., & Sunderkötter, C. (2011). Subcutaneous infection with S. aureus in mice reveals association of resistance with influx of neutrophils and Th2 response. *The Journal of Investigative Dermatology*, *131*(1), 125–132. https://doi.org/10.1038/jid.2010.282

Novak, N., Valenta, R., Bohle, B., Laffer, S., Haberstok, J., Kraft, S., & Bieber, T. (2004). FcepsilonRI engagement of Langerhans cell-like dendritic cells and inflammatory dendritic epidermal cell-like dendritic cells induces chemotactic signals and different T-cell phenotypes in vitro. *The Journal of allergy and clinical immunology*, *113*(5), 949–957. https://doi.org/10.1016/j.jaci.2004.02.005

Nutten, S. (2015). Atopic Dermatitis: Global Epidemiology and Risk Factors. *Annals of Nutrition and Metabolism*, *66(suppl 1*(Suppl. 1), 8–16. https://doi.org/10.1159/000370220

O'Brien, K. S., Lietman, T. M., Keenan, J. D., & Whitcher, J. P. (2015). Microbial keratitis: a community eye health approach. *Community Eye Health*, *28*(89), 1–2. https://pubmed.ncbi.nlm.nih.gov/26435582

Ogston, A. (1881). Report upon Micro-Organisms in Surgical Diseases. *British Medical Journal*, *1*(1054), 369.b2-369.b375. https://doi.org/10.1136/bmj.1.1054.369

Oh, J. W., Hsi, T.-C., Guerrero-Juarez, C. F., Ramos, R., & Plikus, M. V. (2013). Organotypic skin culture. *The Journal of Investigative Dermatology*, *133*(11), 1–4. https://doi.org/10.1038/jid.2013.387

Okabe, Y., & Medzhitov, R. (2014). Tissue-Specific Signals Control Reversible Program of Localization and Functional Polarization of Macrophages. *Cell*, *157*(4), 832–844. https://doi.org/10.1016/j.cell.2014.04.016

Olsen I. (2015). Biofilm-specific antibiotic tolerance and resistance. *European journal of clinical microbiology & infectious diseases : official publication of the European Society of Clinical Microbiology*, *34*(5), 877–886. https://doi.org/10.1007/s10096-015-2323-z

Ong, P. Y., Ohtake, T., Brandt, C., Strickland, I., Boguniewicz, M., Ganz, T., Gallo, R. L., & Leung, D. Y. M. (2002). Endogenous Antimicrobial Peptides and Skin Infections in Atopic Dermatitis. *New England Journal of Medicine*, *347*(15), 1151–1160. https://doi.org/10.1056/NEJMoa021481

Ono, S., & Kabashima, K. (2015). Novel insights into the role of immune cells in skin and inducible skin-associated lymphoid tissue (iSALT). *Allergo Journal International*, *24*, 170–179. https://doi.org/10.1007/s40629-015-0065-1

Pader, V., Hakim, S., Painter, K. L., Wigneshweraraj, S., Clarke, T. B., & Edwards, A. M. (2016). Staphylococcus aureus inactivates daptomycin by releasing membrane phospholipids. *Nature Microbiology*, *2*. https://doi.org/10.1038/nmicrobiol.2016.194

Painter, K. L., Hall, A., Ha, K. P., & Edwards, A. M. (2017). The electron transport chain sensitizes Staphylococcus aureus and Enterococcus faecalis to the oxidative burst. *Infection and Immunity*, *85*(12). https://doi.org/10.1128/IAI.00659-17

Painter, K. L., Strange, E., Parkhill, J., Bamford, K. B., Armstrong-James, D., & Edwards, A. M. (2015). Staphylococcus aureus adapts to oxidative stress by producing H<inf>2</inf>O<inf>2</inf>-resistant small-colony variants via the SOS response. *Infection and Immunity*, *83*(5), 1830–1844. https://doi.org/10.1128/IAI.03016-14

Papayannakos, C. J., DeVoti, J. A., Israr, M., Alsudani, H., Bonagura, V., &

Steinberg, B. M. (2021). Extracellular vesicles produced by primary human keratinocytes in response to TLR agonists induce stimulus-specific responses in antigen-presenting cells. *Cellular signalling*, *83*, 109994. https://doi.org/10.1016/j.cellsig.2021.109994

Parthasarathy, V., Martin, F., Higginbottom, A., Murray, H., Moseley, G. W., Read, R. C., Mal, G., Hulme, R., Monk, P. N., & Partridge, L. J. (2009). Distinct roles for tetraspanins CD9, CD63 and CD81 in the formation of multinucleated giant cells. *Immunology*, *127*(2), 237–248. https://doi.org/10.1111/j.1365-2567.2008.02945.x

Pasparakis, M., Haase, I., & Nestle, F. O. (2014). Mechanisms regulating skin immunity and inflammation. *Nature Reviews Immunology*, *14*(5), 289–301. https://doi.org/10.1038/nri3646

Peacock, S. J., & Paterson, G. K. (2015). Mechanisms of Methicillin Resistance in Staphylococcus aureus. *Annual Review of Biochemistry*, *84*, 577–601. https://doi.org/10.1146/annurev-biochem-060614-034516

Perlman, R. L. (2016). Mouse models of human disease: An evolutionary perspective. *Evolution, Medicine, and Public Health*, *2016*(1), 170–176. https://doi.org/10.1093/emph/eow014

Peng, Q., Tang, X., Dong, W., Sun, N., & Yuan, W. (2022). A Review of Biofilm Formation of *Staphylococcus aureus* and Its Regulation Mechanism. *Antibiotics (Basel, Switzerland)*, *12*(1), 12. https://doi.org/10.3390/antibiotics12010012

Peng, W. M., Yu, C. F., Kolanus, W., Mazzocca, A., Bieber, T., Kraft, S., & Novak, N. (2011). Tetraspanins CD9 and CD81 are molecular partners of trimeric FcεRI on human antigen-presenting cells. *Allergy*, *66*(5), 605–611. https://doi.org/10.1111/j.1398-9995.2010.02524.x

Pidwill, G. R., Gibson, J. F., Cole, J., Renshaw, S. A., & Foster, S. J. (2021). The Role of Macrophages in Staphylococcus aureus Infection . In *Frontiers in Immunology* (Vol. 11, p. 3506). https://www.frontiersin.org/article/10.3389/fimmu.2020.620339

Plantinga, M., de Haar, C., & Nierkens, S. (2015). *Dendritic Cells.* (K. Verhoeckx, P. Cotter, I. López-Expósito, C. Kleiveland, T. Lea, A. Mackie, T. Requena, D. Swiatecka, & H. Wichers (eds.); pp. 181–196). https://doi.org/10.1007/978-3-319-16104-4_17

Poh, S. E., Goh, J. P. Z., Fan, C., Chua, W., Gan, S. Q., Lim, P. L. K., Sharma, B., Leavesley, D. I., Dawson Jr, T. L., & Li, H. (2020). Identification of Malassezia furfur Secreted Aspartyl Protease 1 (MfSAP1) and Its Role in Extracellular Matrix Degradation. *Frontiers in Cellular and Infection Microbiology*, *10*, 148. https://doi.org/10.3389/fcimb.2020.00148

Pouliot-Bérubé, C., Zaniolo, K., Guérin, S. L., & Pouliot, R. (2016). Tissue-engineered human psoriatic skin supplemented with cytokines as an

in vitro model to study plaque psoriasis. *Regenerative Medicine*, *11*(6), 545–557. https://doi.org/10.2217/rme-2016-0037

Pupovac, A., Senturk, B., Griffoni, C., Maniura-Weber, K., Rottmar, M., & McArthur, S. L. (2018). Toward Immunocompetent 3D Skin Models. *Advanced Healthcare Materials*. https://doi.org/10.1002/adhm.201701405

Qi, J. C., Wang, J., Mandadi, S., Tanaka, K., Roufogalis, B. D., Madigan, M. C., Lai, K., Yan, F., Chong, B. H., Stevens, R. L., & Krilis, S. A. (2006). Human and mouse mast cells use the tetraspanin CD9 as an alternate interleukin-16 receptor. *Blood*, *107*(1), 135–142. https://doi.org/10.1182/blood-2005-03-1312

Rajesh, A., Wise, L., & Hibma, M. (2019). The role of Langerhans cells in pathologies of the skin. *Immunology & Cell Biology*, *97*(8), 700–713. https://doi.org/https://doi.org/10.1111/imcb.12253

Ramadan, Q., & Ting, F. C. W. (2016). In vitro micro-physiological immune-competent model of the human skin. *Lab on a Chip*, *16*(10), 1899–1908. https://doi.org/10.1039/c6lc00229c

Ratushny, V., Gober, M. D., Hick, R., Ridky, T. W., & Seykora, J. T. (2012). From keratinocyte to cancer: the pathogenesis and modeling of cutaneous squamous cell carcinoma. *The Journal of Clinical Investigation*, *122*(2), 464–472. https://doi.org/10.1172/JCI57415

Read, A. F., & Woods, R. J. (2014). Antibiotic resistance management. In *Evolution, medicine, and public health* (Vol. 2014, Issue 1, p. 147). https://doi.org/10.1093/emph/eou024

Reddersen, K., Wiegand, C., Elsner, P., & Hipler, U.-C. (2019). Three-dimensional human skin model infected with Staphylococcus aureus as a tool for evaluation of bioactivity and biocompatibility of antiseptics. *International Journal of Antimicrobial Agents*, *54*(3), 283–291. https://doi.org/https://doi.org/10.1016/j.ijantimicag.2019.06.022

Reyes, R., Cardeñes, B., Machado-Pineda, Y., & Cabañas, C. (2018). Tetraspanin CD9: A Key Regulator of Cell Adhesion in the Immune System. *Frontiers in Immunology*, *9*, 863. https://doi.org/10.3389/fimmu.2018.00863

Rheinwald, J. G., & Green, H. (1975). Serial Cultivation of Strains of Human Epidermal Keratinocytes: the Formation of Keratinizing Colonies from Single Cells. *Cell*, *6*, 331–344. https://doi.org/10.1016/S0092-8674(75)80001-8

Ribet, D., & Cossart, P. (2015). How bacterial pathogens colonize their hosts and invade deeper tissues. In *Microbes and Infection* (Vol. 17, Issue 3, pp. 173–183). https://doi.org/10.1016/j.micinf.2015.01.004

Ribot, J. C., Lopes, N., & Silva-Santos, B. (2021). γδ T cells in tissue physiology and surveillance. *Nature Reviews. Immunology*, *21*(4), 221–232.

https://doi.org/10.1038/s41577-020-00452-4

Ricciardi, B. F., Muthukrishnan, G., Masters, E., Ninomiya, M., Lee, C. C., & Schwarz, E. M. (2018). Staphylococcus aureus Evasion of Host Immunity in the Setting of Prosthetic Joint Infection: Biofilm and Beyond. *Current reviews in musculoskeletal medicine*, *11*(3), 389–400. https://doi.org/10.1007/s12178-018-9501-4

Rigby, K. M., & DeLeo, F. R. (2012). Neutrophils in innate host defense against Staphylococcus aureus infections. *Seminars in Immunopathology*, *34*(2), 237–259. https://doi.org/10.1007/s00281-011-0295-3

Rindler, K., Krausgruber, T., Thaler, F. M., Alkon, N., Bangert, C., Kurz, H., Fortelny, N., Rojahn, T. B., Jonak, C., Griss, J., Bock, C., & Brunner, P. M. (2021). Spontaneously Resolved Atopic Dermatitis Shows Melanocyte and Immune Cell Activation Distinct From Healthy Control Skin. *Frontiers in immunology*, *12*, 630892. https://doi.org/10.3389/fimmu.2021.630892

Rocha-Perugini, V., Sánchez-Madrid, F., & Martínez Del Hoyo, G. (2016). Function and Dynamics of Tetraspanins during Antigen Recognition and Immunological Synapse Formation. *Frontiers in immunology*, *6*, 653. https://doi.org/10.3389/fimmu.2015.00653

Roger, M., Fullard, N., Costello, L., Bradbury, S., Markiewicz, E., O'Reilly, S., Darling, N., Ritchie, P., Määttä, A., Karakesisoglou, I., Nelson, G., von Zglinicki, T., Dicolandrea, T., Isfort, R., Bascom, C., & Przyborski, S. (2019). Bioengineering the microanatomy of human skin. *Journal of Anatomy*, *234*(4), 438–455. https://doi.org/https://doi.org/10.1111/joa.12942

Rutherford, S. T., & Bassler, B. L. (2012). Bacterial quorum sensing: its role in virulence and possibilities for its control. *Cold Spring Harbor perspectives in medicine*, *2*(11), a012427. https://doi.org/10.1101/cshperspect.a012427

Rygaard, J. (1974). Skin grafts in nude mice. 3. Fate of grafts from man and donors of other taxonomic classes. *Acta Pathologica et Microbiologica Scandinavica. Section A, Pathology*, *82*(1), 105–112.

Sachs, N., Kreft, M., van den Bergh Weerman, M. A., Beynon, A. J., Peters, T. A., Weening, J. J., & Sonnenberg, A. (2006). Kidney failure in mice lacking the tetraspanin CD151. *The Journal of Cell Biology*, *175*(1), 33–39. https://doi.org/10.1083/jcb.200603073

Saiz, M. L., Cibrian, D., Ramírez-Huesca, M., Torralba, D., Moreno-Gonzalo, O., & Sánchez-Madrid, F. (2017). Tetraspanin CD9 Limits Mucosal Healing in Experimental Colitis. *Frontiers in Immunology*, *8*, 1854. https://doi.org/10.3389/fimmu.2017.01854

Salgado, G., Ng, Y. Z., Koh, L. F., Goh, C. S. M., & Common, J. E. (2017). Human reconstructed skin xenografts on mice to model skin physiology. In *Differentiation* (Vol. 98, pp. 14–24). https://doi.org/10.1016/j.diff.2017.09.004

Salmon, J. K., Armstrong, C. A., & Ansel, J. C. (1994). The skin as an immune organ. *Western Journal of Medicine*, *160*(2), 146–152. http://www.ncbi.nlm.nih.gov/pmc/articles/PMC1022320/

Sangsri, T., Saiprom, N., Tubsuwan, A., Monk, P., Partridge, L. J., & Chantratita, N. (2020). Tetraspanins are involved in Burkholderia pseudomallei-induced cell-to-cell fusion of phagocytic and non-phagocytic cells. *Scientific Reports*, *10*(1), 17972. https://doi.org/10.1038/s41598-020-74737-y

Santegoets, S. J. A. M., Schreurs, M. W. J., Masterson, A. J., Liu, Y. P., Goletz, S., Baumeister, H., Kueter, E. W. M., Lougheed, S. M., van den Eertwegh, A. J. M., Scheper, R. J., Hooijberg, E., & de Gruijl, T. D. (2006). In vitro priming of tumor-specific cytotoxic T lymphocytes using allogeneic dendritic cells derived from the human MUTZ-3 cell line. *Cancer Immunology, Immunotherapy : CII*, *55*(12), 1480–1490. https://doi.org/10.1007/s00262-006-0142-x

Santegoets, S. J. A. M., van den Eertwegh, A. J. M., van de Loosdrecht, A. A., Scheper, R. J., & de Gruijl, T. D. (2008). Human dendritic cell line models for DC differentiation and clinical DC vaccination studies. *Journal of Leukocyte Biology*, *84*(6), 1364–1373. https://doi.org/https://doi.org/10.1189/jlb.0208092

Secor, P. R., James, G. A., Fleckman, P., Olerud, P., McInnerney, K. & Stewart, P. S. (2011). *Staphylococcus aureus* Biofilm and Planktonic cultures differentially impact gene expression, mapk phosphorylation, and cytokine production in human keratinocytes. BMC Microbiology, 11(143). https://doi.org/10.1186/1471-2180-11-143

Schulz, A., Jiang, L., de Vor, L., Ehrström, M., Wermeling, F., Eidsmo, L., & Melican, K. (2019). Neutrophil Recruitment to Noninvasive MRSA at the Stratum Corneum of Human Skin Mediates Transient Colonization. *Cell Reports*, *29*(5). https://doi.org/10.1016/j.celrep.2019.09.055

Schulze, A., Mitterer, F., Pombo, J. P., & Schild, S. (2021). Biofilms by bacterial human pathogens: Clinical relevance - development, composition and regulation - therapeutical strategies. *Microbial cell (Graz, Austria)*, *8*(2), 28–56. https://doi.org/10.15698/mic2021.02.741

Shepherd, J., Douglas, I., Rimmer, S., Swanson, L., & MacNeil, S. (2009). Development of three-dimensional tissue-engineered models of bacterial infected human skin wounds. *Tissue Engineering. Part C, Methods*, *15*(3), 475–484. https://doi.org/10.1089/ten.tec.2008.0614

Shin, J. S., & Greer, A. M. (2015). The role of FcεRI expressed in dendritic cells and monocytes. *Cellular and molecular life sciences : CMLS*, *72*(12), 2349–2360. https://doi.org/10.1007/s00018-015-1870-x

Sinha, B., Francois, P. P., Nusse, O., Foti, M., Hartford, O. M., Vaudaux, P., Foster, T. J., Lew, D. P., Herrmann, M., & Krause, K.-H. (1999). Fibronectin-binding protein acts as Staphylococcus aureus invasin via fibronectin bridging to integrin alpha5beta1. *Cellular Microbiology*, *1*(2), 101–117.

https://doi.org/10.1046/j.1462-5822.1999.00011.x

Slade, E. A., Thorn, R. M. S., Young, A., & Reynolds, D. M. (2019). An in vitro collagen perfusion wound biofilm model; with applications for antimicrobial studies and microbial metabolomics. *BMC Microbiology*, *19*(1), 310. https://doi.org/10.1186/s12866-019-1682-5

Smeekens, S. P., Huttenhower, C., Riza, A., van de Veerdonk, F. L., Zeeuwen, P. L. J. M., Schalkwijk, J., van der Meer, J. W. M., Xavier, R. J., Netea, M. G., & Gevers, D. (2014). Skin microbiome imbalance in patients with STAT1/STAT3 defects impairs innate host defense responses. *Journal of Innate Immunity*, *6*(3), 253–262. https://doi.org/10.1159/000351912

Soell, M., Diab, M., Haan-Archipoff, G., Beretz, A., Herbelin, C., Poutrel, B., & Klein, J. P. (1995). Capsular polysaccharide types 5 and 8 of Staphylococcus aureus bind specifically to human epithelial (KB) cells, endothelial cells, and monocytes and induce release of cytokines. *Infection and Immunity*, *63*(4), 1380–1386. https://doi.org/10.1128/iai.63.4.1380-1386.1995

Spoor, L. E., McAdam, P. R., Weinert, L. A., Rambaut, A., Hasman, H., Aarestrup, F. M., Kearns, A. M., Larsen, A. R., Skov, R. L., & Fitzgerald, J. R. (2013). Livestock origin for a human pandemic clone of community-associated methicillin-resistant Staphylococcus aureus. *MBio*, *4*(4). https://doi.org/10.1128/mBio.00356-13

Stoitzner, P. (2010). The Langerhans cell controversy: are they immunostimulatory or immunoregulatory cells of the skin immune system? *Immunology and Cell Biology*, *88*(4), 348–350. https://doi.org/10.1038/icb.2010.46

Stojadinovic, O., Yin, N., Lehmann, J., Pastar, I., Kirsner, R. S., & Tomic-Canic, M. (2013). Increased number of Langerhans cells in the epidermis of diabetic foot ulcers correlates with healing outcome. *Immunologic Research*, *57*(1–3), 222–228. https://doi.org/10.1007/s12026-013-8474-z

Streilein, J. W. (1983). Skin-associated lymphoid tissues (SALT): origins and functions. *The Journal of Investigative Dermatology*, *80 Suppl*, 12s-16s. https://doi.org/10.1111/1523-1747.ep12536743

Strobel, M., Pförtner, H., Tuchscherr, L., Völker, U., Schmidt, F., Kramko, N., Schnittler, H.-J., Fraunholz, M. J., Löffler, B., Peters, G., & Niemann, S. (2016). Post-invasion events after infection with Staphylococcus aureus are strongly dependent on both the host cell type and the infecting S. aureus strain. *Clinical Microbiology and Infection : The Official Publication of the European Society of Clinical Microbiology and Infectious Diseases*, *22*(9), 799–809. https://doi.org/10.1016/j.cmi.2016.06.020

Strömberg, N., Ahlfors, S., Borén, T., Bratt, P., Hallberg, K., Hammarström, K. J., Holm, C., Johansson, I., Järvholm, M., Kihlberg, J., Li, T., Ryberg, M., & Zand, G. (1996). Anti-adhesion and diagnostic strategies for oro-intestinal bacterial pathogens. *Advances in Experimental Medicine and Biology*, *408*, 9–24.

https://doi.org/10.1007/978-1-4613-0415-9_2

Sullivan, T. P., Eaglstein, W. H., Davis, S. C., & Mertz, P. (2001). The pig as a model for human wound healing. *Wound Repair and Regeneration : Official Publication of the Wound Healing Society [and] the European Tissue Repair Society*, *9*(2), 66–76. https://doi.org/10.1046/j.1524-475x.2001.00066.x

Summerfield, A., Meurens, F., & Ricklin, M. E. (2015). The immunology of the porcine skin and its value as a model for human skin. *Molecular Immunology*, *66*(1), 14–21. https://doi.org/https://doi.org/10.1016/j.molimm.2014.10.023

Sundberg, J. P., Nanney, L. B., Fleckman, P., & King, L. E. (2012). *23 - Skin and Adnexa* (P. M. Treuting & S. M. B. T.-C. A. and H. Dintzis (eds.); pp. 433–455). Academic Press. https://doi.org/https://doi.org/10.1016/B978-0-12-381361-9.00023-8

Sukumaran, V., & Senanayake, S. (2016). Bacterial skin and soft tissue infections. *Australian Prescriber*, *39*(5), 159–163. https://doi.org/10.18773/austprescr.2016.058

Surewaard, B. G. J., Deniset, J. F., Zemp, F. J., Amrein, M., Otto, M., Conly, J., Omri, A., Yates, R. M., & Kubes, P. (2016). Identification and treatment of the Staphylococcus aureus reservoir in vivo. *The Journal of Experimental Medicine*, *213*(7), 1141–1151. https://doi.org/10.1084/jem.20160334

Tai, Y., Wang, Q., Korner, H., Zhang, L., & Wei, W. (2018). Molecular Mechanisms of T Cells Activation by Dendritic Cells in Autoimmune Diseases. *Frontiers in Pharmacology*, *9*, 642. https://doi.org/10.3389/fphar.2018.00642

Tao, L., & Reese, T. A. (2017). Making Mouse Models That Reflect Human Immune Responses. *Trends in Immunology*, *38*(3), 181–193. https://doi.org/10.1016/j.it.2016.12.007

Teunissen, M. B. M., Haniffa, M., & Collin, M. P. (2012). Insight into the immunobiology of human skin and functional specialization of skin dendritic cell subsets to innovate intradermal vaccination design. *Current Topics in Microbiology and Immunology*, *351*, 25–76. https://doi.org/10.1007/82_2011_169

Thi, M. T. T., Wibowo, D., & Rehm, B. H. A. (2020). Pseudomonas aeruginosa Biofilms. *International Journal of Molecular Sciences*, *21*(22). https://doi.org/10.3390/ijms21228671

Thomer, L., Schneewind, O., & Missiakas, D. (2016). Pathogenesis of Staphylococcus aureus Bloodstream Infections. *Annual Review of Pathology: Mechanisms of Disease*, *11*(1), annurev-pathol-012615-044351. https://doi.org/10.1146/annurev-pathol-012615-044351

Thurlow, L. R., Hanke, M. L., Fritz, T., Angle, A., Aldrich, A., Williams, S. H., Engebretsen, I. L., Bayles, K. W., Horswill, A. R. & Kielian, T. (2011*). Staphylococcus aureus* biofilms prevent macrophage phagocytosis and

attenuate inflammation in vivo. *Journal of Immunology*, 186(11): 6585–6596. https://doi.org/10.4049/jimmunol.1002794

Tippett, E., Cameron, P. U., Marsh, M., & Crowe, S. M. (2013). Characterization of tetraspanins CD9, CD53, CD63, and CD81 in monocytes and macrophages in HIV-1 infection. *Journal of Leukocyte Biology*, *93*(6), 913–920. https://doi.org/10.1189/jlb.0812391

Tong, S. Y. C., Davis, J. S., Eichenberger, E., Holland, T. L., & Fowler, V. G. (2015). Staphylococcus aureus infections: Epidemiology, pathophysiology, clinical manifestations, and management. *Clinical Microbiology Reviews*, *28*(3), 603–661. https://doi.org/10.1128/CMR.00134-14

Tranchemontagne, Z. R., Camire, R. B., O'Donnell, V. J., Baugh, J., & Burkholder, K. M. (2015). Staphylococcus aureus Strain USA300 Perturbs Acquisition of Lysosomal Enzymes and Requires Phagosomal Acidification for Survival inside Macrophages. *Infection and Immunity*, *84*(1), 241–253. https://doi.org/10.1128/IAI.00704-15

Tsuchiya, S., Yamabe, M., Yamaguchi, Y., Kobayashi, Y., Konno, T., & Tada, K. (1980). Establishment and characterization of a human acute monocytic leukemia cell line (THP-1). *International Journal of Cancer*, *26*(2), 171–176. https://doi.org/10.1002/ijc.2910260208

Uribe-Querol, E., & Rosales, C. (2020). Phagocytosis: Our Current Understanding of a Universal Biological Process . In *Frontiers in Immunology* (Vol. 11, p. 1066). https://www.frontiersin.org/article/10.3389/fimmu.2020.01066

van Dalen, R., De La Cruz Diaz, J. S., Rumpret, M., Fuchsberger, F. F., van Teijlingen, N. H., Hanske, J., Rademacher, C., Geijtenbeek, T. B. H., van Strijp, J. A. G., Weidenmaier, C., Peschel, A., Kaplan, D. H., & van Sorge, N. M. (2019). Langerhans Cells Sense Staphylococcus aureus Wall Teichoic Acid through Langerin To Induce Inflammatory Responses . *MBio*, *10*(3). https://doi.org/10.1128/mbio.00330-19

van den Bogaard, E. H., Tjabringa, G. S., Joosten, I., Vonk-Bergers, M., van Rijssen, E., Tijssen, H. J., Erkens, M., Schalkwijk, J., & Koenen, H. J. P. M. (2014). Crosstalk between Keratinocytes and T Cells in a 3D Microenvironment: A Model to Study Inflammatory Skin Diseases. *Journal of Investigative Dermatology*, *134*(3), 719–727. https://doi.org/10.1038/jid.2013.417

van der Aar, A. M. G., Picavet, D. I., Muller, F. J., de Boer, L., van Capel, T. M. M., Zaat, S. A. J., Bos, J. D., Janssen, H., George, T. C., Kapsenberg, M. L., van Ham, S. M., Teunissen, M. B. M., & de Jong, E. C. (2013). Langerhans Cells Favor Skin Flora Tolerance through Limited Presentation of Bacterial Antigens and Induction of Regulatory T Cells. *Journal of Investigative Dermatology*, *133*(5), 1240–1249. https://doi.org/https://doi.org/10.1038/jid.2012.500

van der Aar, A. M. G., Sylva-Steenland, R. M. R., Bos, J. D., Kapsenberg, M. L., de Jong, E. C., & Teunissen, M. B. M. (2007). Cutting Edge: Loss of TLR2, TLR4,

and TLR5 on Langerhans Cells Abolishes Bacterial Recognition. *The Journal of Immunology*, *178*(4), 1986 LP – 1990. https://doi.org/10.4049/jimmunol.178.4.1986

Ventress, J. K., Partridge, L. J., Read, R. C., Cozens, D., MacNeil, S., & Monk, P. N. (2016). Peptides from tetraspanin CD9 are potent inhibitors of Staphylococcus aureus adherence to keratinocytes. *PLoS ONE*, *11*(7). https://doi.org/10.1371/journal.pone.0160387

Ventola, C. L. (2015). The antibiotic resistance crisis: part 1: causes and threats. *P & T : A Peer-Reviewed Journal for Formulary Management*, *40*(4), 277–283.

von Wintersdorff, C. J. H., Penders, J., van Niekerk, J. M., Mills, N. D., Majumder, S., van Alphen, L. B., Savelkoul, P. H. M., & Wolffs, P. F. G. (2016). Dissemination of Antimicrobial Resistance in Microbial Ecosystems through Horizontal Gene Transfer. *Frontiers in Microbiology*, *7*, 173. https://doi.org/10.3389/fmicb.2016.00173

Wannigama, D. (2018). OVERCOMING BIOFILM MEDIATED RESPIRATORY INFECTIONS THROUGH EXPLOITATION OF PATHOGEN AND HOST-DIRECTED NOVEL PEPTIDES. *Respirology*, *23*(S2), 67–68. https://doi.org/https://doi.org/10.1111/resp.13419_164

West, H. C., & Bennett, C. L. (2018). Redefining the Role of Langerhans Cells As Immune Regulators within the Skin . In *Frontiers in Immunology* (Vol. 8, p. 1941). https://www.frontiersin.org/article/10.3389/fimmu.2017.01941

Viswanathan, P., Guvendiren, M., Chua, W., Telerman, S. B., Liakath-Ali, K., Burdick, J. A., & Watt, F. M. (2016). Mimicking the topography of the epidermal-dermal interface with elastomer substrates. *Integrative Biology : Quantitative Biosciences from Nano to Macro*, *8*(1), 21–29. https://doi.org/10.1039/c5ib00238a

Walker, M. J., Barnett, T. C., McArthur, J. D., Cole, J. N., Gillen, C. M., Henningham, A., Sriprakash, K. S., Sanderson-Smith, M. L., & Nizet, V. (2014). Disease manifestations and pathogenic mechanisms of Group A Streptococcus. *Clinical Microbiology Reviews*, *27*(2), 264–301. https://doi.org/10.1128/CMR.00101-13

WHO. (2005). *The Current Evidence for the Burden of Group A Streptococcal Diseases*.

Wilhelm, I., Levit-Zerdoun, E., Jakob, J., Villringer, S., Frensch, M., Übelhart, R., Landi, A., Müller, P., Imberty, A., Thuenauer, R., Claudinon, J., Jumaa, H., Reth, M., Eibel, H., Hobeika, E., & Römer, W. (2019). Carbohydrate-dependent B cell activation by fucose-binding bacterial lectins. *Science Signaling*, *12*(571). https://doi.org/10.1126/scisignal.aao7194

Williams, M. R., Costa, S. K., Zaramela, L. S., Khalil, S., Todd, D. A., Winter, H. L., Sanford, J. A., O'Neill, A. M., Liggins, M. C., Nakatsuji, T., Cech, N. B., Cheung, A. L., Zengler, K., Horswill, A. R., & Gallo, R. L. (2019). Quorum sensing between bacterial species on the skin protects against epidermal injury in atopic dermatitis. *Science Translational Medicine*, *11*(490). https://doi.org/10.1126/scitranslmed.aat8329

Wong, V. W., Sorkin, M., Glotzbach, J. P., Longaker, M. T., & Gurtner, G. C. (2011). Surgical Approaches to Create Murine Models of Human Wound Healing. *Journal of Biomedicine and Biotechnology*, *2011*, 969618. https://doi.org/10.1155/2011/969618

Xie, Y., Rizzi, S. C., Dawson, R., Lynam, E., Richards, S., Leavesley, D. I., & Upton, Z. (2010). Development of a Three-Dimensional Human Skin Equivalent Wound Model for Investigating Novel Wound Healing Therapies. *Tissue Engineering Part C: Methods*, *16*(5), 1111–1123. https://doi.org/10.1089/ten.tec.2009.0725

Yamamoto, K., Uchida, K., Furukawa, A., Tamura, T., Ishige, Y., Negi, M., Kobayashi, D., Ito, T., Kakegawa, T., Hebisawa, A., Awano, N., Takemura, T., Amano, T., Akashi, T., & Eishi, Y. (2019). Catalase expression of Propionibacterium acnes may contribute to intracellular persistence of the bacterium in sinus macrophages of lymph nodes affected by sarcoidosis. *Immunologic Research*, *67*(2–3), 182–193. https://doi.org/10.1007/s12026-019-09077-9

Yáñez-Mó, M., Barreiro, O., Gordon-Alonso, M., Sala-Valdés, M., & Sánchez-Madrid, F. (2009). Tetraspanin-enriched microdomains: a functional unit in cell plasma membranes. In *Trends in Cell Biology* (Vol. 19, Issue 9, pp. 434–446). https://doi.org/10.1016/j.tcb.2009.06.004

Yilmaz, G., & Granger, D. N. (2010). Leukocyte recruitment and ischemic brain injury. *Neuromolecular Medicine*, *12*(2), 193–204. https://doi.org/10.1007/s12017-009-8074-1

Young, A. (2013). *NHS STANDARD CONTRACT FOR SPECIALISED BURNS CARE (ALL AGES)*. https://www.england.nhs.uk/wp-content/uploads/2014/04/d06-spec-burn-care-0414.pdf

Yousef, H., & Sharma, S. (2017). *Anatomy, Skin (Integument), Epidermis*.

Zhang, J., Dong, J., Gu, H., Yu, S., Zhang, X., Gou, Y., Xu, W., Burd, A., Huang, L., Miyado, K., Huang, Y., & Chan, H. C. (2012). CD9 is critical for cutaneous wound healing through JNK signaling. *The Journal of investigative dermatology*, *132*(1), 226–236. https://doi.org/10.1038/jid.2011.268

Zhang, Quanri, Lee, W.-B., Kang, J.-S., Kim, L. K., & Kim, Y.-J. (2018). Integrin CD11b negatively regulates Mincle-induced signaling via the Lyn-SIRPα-SHP1 complex. *Experimental & Molecular Medicine*, *50*(2), e439–e439.

https://doi.org/10.1038/emm.2017.256

Zhang, Qun, Wen, J., Liu, C., Ma, C., Bai, F., Leng, X., Chen, Z., Xie, Z., Mi, J., & Wu, X. (2020). Early-stage bilayer tissue-engineered skin substitute formed by adult skin progenitor cells produces an improved skin structure in vivo. *Stem Cell Research & Therapy*, *11*(1), 407. https://doi.org/10.1186/s13287-020-01924-z

Zhao, G., Usui, M. L., Lippman, S. I., James, G. A., Stewart, P. S., Fleckman, P., & Olerud, J. E. (2013). Biofilms and Inflammation in Chronic Wounds. *Advances in Wound Care*, *2*(7), 389–399. https://doi.org/10.1089/wound.2012.0381

Zheng, Y., He L., Asiamah T. K. & Otto M. (2018). Colonization of Medical Devices by Staphylococci. *Environmental microbiology*, 20(9): 3141-3153. https://doi.org/10.1111/1462-2920.14129

Zomer, H. D., & Trentin, A. G. (2018). Skin wound healing in humans and mice: Challenges in translational research. *Journal of Dermatological Science*, *90*(1), 3–12. https://doi.org/10.1016/j.jdermsci.2017.12.009

Zoschke, C., Ulrich, M., Sochorová, M., Wolff, C., Vávrová, K., Ma, N., Ulrich, C., Brandner, J. M., & Schäfer-Korting, M. (2016). The barrier function of organotypic non-melanoma skin cancer models. *Journal of Controlled Release : Official Journal of the Controlled Release Society*, *233*, 10–18. https://doi.org/10.1016/j.jconrel.2016.04.037